AD NUMBER

AD-506 871

CLASSIFICATION CHANGES

TO **UNCLASSIFIED**

FROM **CONFIDENTIAL**

AUTHORITY

AFAL Ltr; Apr 11, 1978

AD NUMBER

AD-506 871

NEW LIMITATION CHANGE

TO

DISTRIBUTION STATEMENT: A

Approved for public release; Distribution is unlimited.

LIMITATION CODE: 1

FROM **No Prior DoD Distr Scty Cntrl St'mt Assgn'd**

AUTHORITY

AFAL Ltr; Apr 11, 1978

[redacted]

AFAPL-TR-69-92
VOLUME III

(UNCLASSIFIED TITLE)
INVESTIGATION OF
A HIGHLY LOADED
TWO-STAGE FAN-DRIVE TURBINE

VOLUME III. Phase II, Part 2. Experimental Baseline Airfoil Evaluation

H. Welna, D. E. Dahlberg and W. H. Heiser
Pratt & Whitney Aircraft
Division of United Aircraft Corporation

Technical Report
AFAPL-TR-69-92 Volume III
December 1969

AIR FORCE AERO PROPULSION LABORATORY (APTC)
AIR FORCE SYSTEMS COMMAND
WRIGHT-PATTERSON AIR FORCE BASE, OHIO. 45433

AFLC–WPAFB–JAN 70 33

[redacted]

SECURITY MARKING

The classified or limited status of this report applies to each page, unless otherwise marked.
Separate page printouts MUST be marked accordingly.

THIS DOCUMENT CONTAINS INFORMATION AFFECTING THE NATIONAL DEFENSE OF THE UNITED STATES WITHIN THE MEANING OF THE ESPIONAGE LAWS, TITLE 18, U.S.C., SECTIONS 793 AND 794. THE TRANSMISSION OR THE REVELATION OF ITS CONTENTS IN ANY MANNER TO AN UNAUTHORIZED PERSON IS PROHIBITED BY LAW.

NOTICE: When government or other drawings, specifications or other data are used for any purpose other than in connection with a definitely related government procurement operation, the U.S. Government thereby incurs no responsibility, nor any obligation whatsoever; and the fact that the Government may have formulated, furnished, or in any way supplied the said drawings, specifications, or other data is not to be regarded by implication or otherwise as in any manner licensing the holder or any other person or corporation, or conveying any rights or permission to manufacture, use or sell any patented invention that may in any way be related thereto.

[redacted]

NOTICE

When Government drawings, specifications, or other data are used for any purpose other than in connection with a definitely related Government procurement operation, the United States Government thereby incurs no responsibility nor any obligation whatsoever; and the fact that the Government may have formulated, furnished, or in any way supplied the said drawings, specifications, or other data, is not to be regarded by implication or otherwise as in any manner licensing the holder or any other person or corporation, or conveying any rights or permission to manufacture, use, or sell any patented invention that may in any way be related thereto.

Copies of this report should not be returned unless return is required by security considerations, contractual obligations, or notice on a specific document.

[redacted]

[redacted]

(UNCLASSIFIED TITLE)
INVESTIGATION OF
A HIGHLY LOADED
TWO-STAGE FAN-DRIVE TURBINE

VOLUME III. Phase II, Part 2. Experimental Baseline Airfoil Evaluation

H. Welna, D. E. Dahlberg and W. H. Heiser

[redacted]

FOREWORD

(U) This Iterim Technical Status Report (Contractors Reference No. PWA 3717) was prepared by Pratt & Whitney Aircraft, Division of United Aircraft Corportion, East Hartford, Connecticut, as the third Semiannual Report under Unites States Air Force Contract F33615-68-C-1208, Project No. 3066, Task No. 306606. This report was submitted by the Contractor on 30 June 1969, and covers the report period from 1 January 1969 to 30 June 1969.

(U) The findings and conclusions of this report are not deemed as final by the Contractor. They are subject to verification or revision in the Final Report to be published upon the completion of this Contract.

(U) The Air Force Program Monitor is Mr. Wayne Tall, APTC, Air Force Aero Propulsion Laboratory, Wright-Patterson Air Force Base, Ohio, 45433.

(U) This report contains no Classified information extracted from other Classified documents.

(U) Publication of this report does not constitute Air Force approval of the report's findings or conclusions. It is published only for the exchange and stimulation of ideas.

Wayne Tall
Project Engineer
Air Force Aero Propulsion Laboratory

UNCLASSIFIED ABSTRACT

(U) An extensive, four-phase, three-year program is in progress to investigate methods of improving the performance of fan-drive turbines. The goals of this program are to develop turbine design procedures and aerodynamic techniques for high work, efficient, low-pressure turbines. The first phase effort defining the preliminary turbine design has been completed, and the results were reported. The second phase consists of an experimental evaluation which includes establishment of both two-dimensional loss levels and three-dimensional flow behavior for the baseline airfoils and for airfoils utilizing boundary layer control devices. The design of the cascade hardware and baseline airfoils was previously reported. The test results of baseline airfoil performance in the annular cascade and the status of the other tasks are presented in this report.

Distribution of this abstract is unlimited.

(The reverse of this page is blank)

TABLE OF CONTENTS

TABLE OF CONTENTS (Cont'd)

LIST OF ILLUSTRATIONS

LIST OF ILLUSTRATIONS (Cont'd)

LIST OF ILLUSTRATIONS (Cont'd)

LIST OF ILLUSTRATIONS (Cont'd)

LIST OF ILLUSTRATIONS (Cont'd)

LIST OF ILLUSTRATIONS (Cont'd)

LIST OF ILLUSTRATIONS (Cont'd)

LIST OF ILLUSTRATIONS (Cont'd)

LIST OF ILLUSTRATIONS (Cont'd)

LIST OF ILLUSTRATIONS (Cont'd)

LIST OF ILLUSTRATIONS (Cont'd)

LIST OF TABLES

LIST OF TABLES (Cont'd)

LIST OF SYMBOLS

A	- area, square inches
B	- axial chord, inches
C	- absolute gas velocity, feet per second
C_F	- drag coefficient
C_L	- Zwiefel load coefficient
C_L*	- load coefficient, $\Delta Cu/U$
E	- diffusion parameter
H	- boundary layer shape factor
ΔH	- work, Btu per pound
M	- Mach number
P	- pressure, psia
ΔP	- pressure rise from minimum to exit value on suction surface
Q	- exit dynamic head
R	- fillet radius, inches
R_C	- radius of curvature, inches
Re_θ	- Reynolds number based on boundary layer momentum thickness
S	- distance along airfoil surface, inches
T	- temperature, °R
u	- tangential velocity, feet per second
W	- relative gas velocity, feet per second
Wg	- gas flow, pounds per second
X	- axial distance, inches
Y	- tangential distance, inches
Z	- number of airfoils
α	- absolute gas angle, degrees
β	- relative gas angle degrees
δ	- boundary layer thickness, inches
δ*	- boundary layer displacement thickness
θ	- boundary layer momentum thickness, inches
θ_b	- blade camber, degrees
θ_v	- vane camber, degrees
τ	- gap, inches
η	- efficiency, percent

Subscripts

0	inlet to first vane
1	inlet to first blade
2	exit from stage or airfoil section

LIST OF SYMBOLS (Cont'd)

G	gage point
ws	wetted surface
ms	mainstream surface
S	static
T	total

(The reverse of this page is blank)

SECTION I

INTRODUCTION

(U) The bypass turbofan engine has seen increased use in recent military aircraft applications, and future mission studies indicate continued interest in this type of jet engine. A characteristic of the bypass turbofan is that the fuel economy increases with the bypass ratio. However, increased bypass ratios require increased fan power which must be supplied by the fan-drive or low-pressure turbine. It is imperative that the turbine meet these increased turbine loading requirements without a turbine efficiency penalty.

(U) The efficiency of a turbine is the result of optimization studies based on trade-offs between turbine diameter, rotational speed number of stages and airfoil loading. The fan-drive turbine design is constrained by further requirements. The rotational speed of the turbine must be limited in order that the fan tip Mach number does not exceed the limit for reasonable losses. At high bypass ratios, where larger fan diameters are required, this problem is further aggravated. Applying conventional aerodynamics, at fixed rotational speed, increased work can only be realized by a further increase in the number of stages and/or the turbine diameter. Reduction of the turbine diameter or airfoil solidity results in a lighter turbine, but with a sacrifice in efficiency due to losses associated with increased airfoil loading. If the turbine diameter and solidity can be reduced without a penalty in turbine efficiency, considerable gains can be realized by the engine. Therefore, present turbine technology must be improved in order to provide the desired level of performance for future turbofan engines.

(U) The objective of the work done under this contract is to analyze and test concepts which will increase the low pressure turbine loading and maintain or increase current turbine efficiency levels. The goals of this program are to develop design procedures and turbine aerodynamic techniques for efficient high-work, low-pressure turbines by means of analytical studies and cascade testing, and to demonstrate the effectiveness of the techniques by designing and testing a two-stage turbine that meets or exceeds the contract stage work and efficiency goals.

(U) The complete program is being conducted in four phases over a three year period which began on 1 January 1968. Phase I defined the basic turbine design and an analysis of promising increased loading concepts was completed. The results of the Phase I study are reported in Reference 1. Phases II and III consist of experimental testing to verify and extend the turbine aerodynamic techniques and design procedures for high loading levels. As part of the Phase II effort, the design details of the baseline cascade test airfoils for both the annular and plane cascade rig were reported in Reference 2. Phase IV will subject the aerodynamic techniques and design procedure to a two-stage rotating rig test.

(U) Work on this contract during the report period proceeded on Phase II, with a design effort initiated on Phase III. The annular cascade testing of the four baseline airfoils was completed and the results are described in this report. The status of the other Phase II tasks is also presented.

(The reverse of this page is blank)

SECTION II

BACKGROUND

(U) The Phase I analysis of this program has been completed and the results are described in Reference 1. The objective of the Phase I study was to select a preliminary turbine design that is capable of meeting the performance requirements of this Contract (see Table I).

TABLE I

TURBINE DESIGN PARAMETERS

Number of Stages		2
Average Load Coefficient, C_2*		2.2
First Blade Tip Wheel Speed		1000 fps
First Blade Inlet Hub-Tip Diameter Ratio	$\leq$	0.8
Exit Swirl Angle Without Exit Guide Vane		20°
With Exit Guide Vane		0°
Turbine Inlet Temperature		1450°F
Airflow	$\geq$	50 lb/sec
Average Stage Efficiency		91%
Life		10,000 hr.

The final choice of the preliminary turbine configuration was based on analyses formed during Phase I. These analyses included consideration of the flowpath, reaction level, load coefficient level, and variations in work distribution for which velocity triangles were generated. Furthermore, as part of Phase I, preliminary airfoil contours were defined for the same velocity triangles for three levels of reaction and three levels of solidity for equal work-split stages.

(U) The selected airfoils for Phases II and III baseline evaluation were the medium-reaction normal solidity airfoils. After the airfoil sections were subjected to additional refinement, the selection was based on the resulting two-dimensional suction surface pressure coefficients and diffusion parameters, and on two-dimensional boundary layer calculations. These baseline airfoil contours, for the first and second vane and the first and second blade, were described in Reference 2. All of the baseline airfoils were fabricated for evaluation in the annular segment cascade and plane cascade rigs.

(The reverse of this page is blank)

SECTION III

TWO-DIMENSIONAL DESIGN VERIFICATION (Task IIa)

1. RFP OBJECTIVE

(U) Provide an experimental verification of the two-dimensional design characteristics.

2. TASK OBJECTIVE

(U) The purpose of this Task is to conduct plane cascade tests in order to verify the aerodynamic concepts applied to the turbine design during the Phase I program, and to establish the two-dimensional loss levels for the chosen turbine airfoil profiles at design conditions.

(U) The plane cascade tests will serve two, equally important, purposes. First the measured profile losses will be compared with those contained in the computer programs to verify the existing design procedures. Second, the total pressure and flow angle profiles at the exit plane will indicate whether or not the surface boundary layer has separated. Each airfoil has been designed so that such two-dimensional separation should not occur, and these tests will constitute a verification of the entire airfoil section design procedure.

3. AIRFOIL SECTION AND FACILITY DESIGN

(U) Under this task, the six medium reaction normal-solidity airfoil sections are to be tested. These are the mean sections of each airfoil row as well as the second vane and blade root sections. These sections will be manufactured as plane cascade packs consisting of constant sections. The design details of the airfoil sections, including the airfoil coordinates and the fabrication details of the cascade test packs, were presented in Reference 2.

(U) The design of the plane cascade rig was also presented in Reference 2, where all important features of the rig were described and illustrated.

4. STATUS

(U) The fabrication of the plane cascade test packs has been completed. The surface static pressure taps were installed in one airfoil of each pack as indicated in Reference 2. One of the completed packs, the first vane mean cascade pack, is shown in Figures 1 and 2.

(U) The rig was also fabricated and has been installed in the Aerodynamic Cascade Facility. The first test pack has been placed into the rig, and check-out runs were being made at the time of this report.

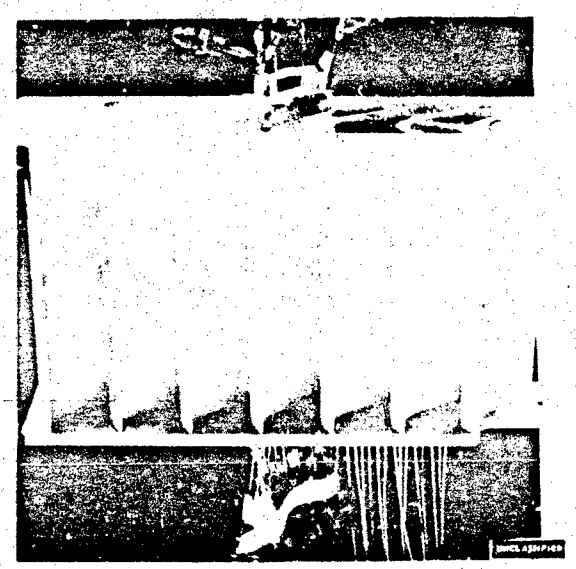

Figure 1 First Vane Mean Plane Cascade Pack-Leading Edge (XP-97607)

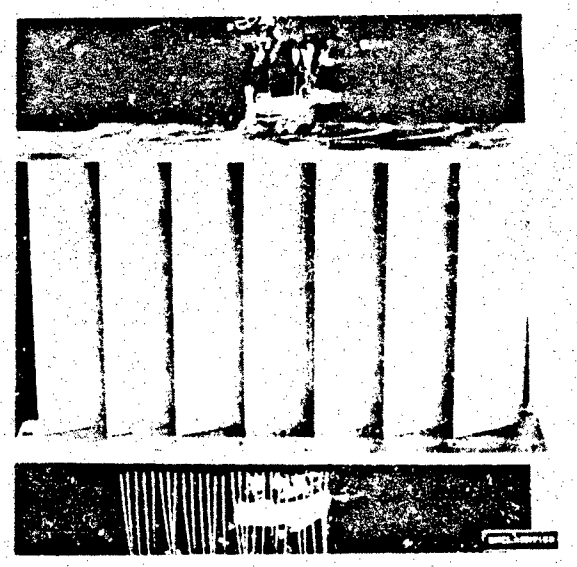

Figure 2 First Vane Mean Plane Cascade Pack-Trailing Edge (XP-97608)

SECTION IV

BASELINE AIRFOIL EVALUATION (Task IIb)

1. RFP OBJECTIVE

(U) Determine the design point performance of the baseline turbine airfoils and the need for corner boundary layer control.

2. TASK OBJECTIVE

(U) Each of the baseline airfoil designs, as determined by the Phase I portion of this Contract, will be evaluated in an annular segment cascade. Turning vanes will be located ahead of the test airfoil cascade to provide the correct incidence angle over the airfoil span. The central test airfoil in each of the four cascade packs will be instrumented with a row of surface pressure taps at the root, mean and tip portions to obtain the surface pressure profiles. Each airfoil design will be separately tested at the design incidence angle and Reynolds number, and three Mach numbers near the design point. Exit surveys will be made over the entire central passage containing the test airfoil to obtain local and circumferentially mass averaged profile loss coefficients and exit angle deviations. The exit plane data will indicate the high and low loss regions of the passage and, specifically, will indicate boundary layer separation if it occurs. The mass-averaged flow characteristics will indicate the cumulative effect of the local losses over the passage width. The airfoil surface pressure measurements will be compared with predicted pressure profiles and will also provide an indication of flow separation. During these tests simple flow visualization techniques will be employed to determine the approximate chordwise location of any separated regions, if they occur. If the results of these tests indicate that corner separation does not occur, or is not pending, the baseline airfoil designs will not require boundary layer control. On the other hand, if corner separation occurs, as is often the case for highly loaded airfoils, the results of these tests will serve as a guide for the application of boundary layer control methods. At this point, the vane and blade showing the highest tendency for corner separation will be selected for testing the most promising boundary layer control methods (Task IIc).

(U) These task objectives were met by the following steps:

- Measurement of all important aerodynamic properties at the cascade inlet and exit planes
- Reconstruction of the entire exit plane loss distribution
- Reconstruction of the entire exit plane flow pattern
- Flow visualization of the airfoil and end-wall flow patterns
- Measurement of the airfoil surface static pressure distributions at three radial locations

- Careful analysis of all data and visual clues
- Selection of appropriate end-wall boundary layer control techniques.

3. BASELINE AIRFOIL AND TEST PACK DESIGN

(U) The design of the baseline airfoil, medium-reaction normal-solidity cascade packs was described in Reference 2; sketches of the cascade flowpaths for each of the four baseline airfoils were also shown. The inlet to each cascade consists of a bellmouth transition section followed by turning vanes which provide the proper radial flow distributions. The test airfoils are placed behind the turning vanes and these are followed by exit wall extensions.

(U) The required exit angles, vane elevations, coordinates and all design details of the inlet turning vanes were shown in Reference 2. As previously indicated, two long chord turning vanes-per-pack were used.

(U) The design details of the first and second stage vane and blade airfoils were also presented in Reference 2. These details include the airfoil elevations, profiles and their coordinates, design values of the airfoil angles, gaging distances, axial chords, gaps and uncovered turnings.

(U) Airfoil surface static pressure taps were distributed around each cascade test airfoil at root, mean and tip sections. Location of these taps for the first vane were shown in Reference 2. A close-up view of a pressure tap installation is shown in Figure 3. Static pressure taps were drilled into small bore tubing installed in spanwise grooves machined into the airfoil surfaces. A finished airfoil surface with taps installed is shown in Figure 4. A view of a completed cascade test pack indicating the method of bringing out the airfoil surface static pressure tap connections is shown in Figure 5. These taps can also be seen on the airfoil surfaces in the flow visualization photographs which will be discussed later in this report.

(U) A single cone probe was designed for measuring exit plane total and static pressures simultaneously, and exit gas flow angles. A sketch of the probe design was shown in Reference 2. The probe was calibrated to determine total and static pressure errors due to the pitch angle over the test Mach number range. Based on the calibration, corrections for the theoretical pitch angle were added to the data reduction program.

(U) A total pressure traverse probe was also installed just upstream of the test airfoils in order to measure the losses due to the turning vanes. The total pressure loss measured for the inlet turning vane was used to determine the local inlet total pressure profile upstream of the test airfoils. Turning vane losses are accounted for in the data reduction program used to calculate the test airfoil performance.

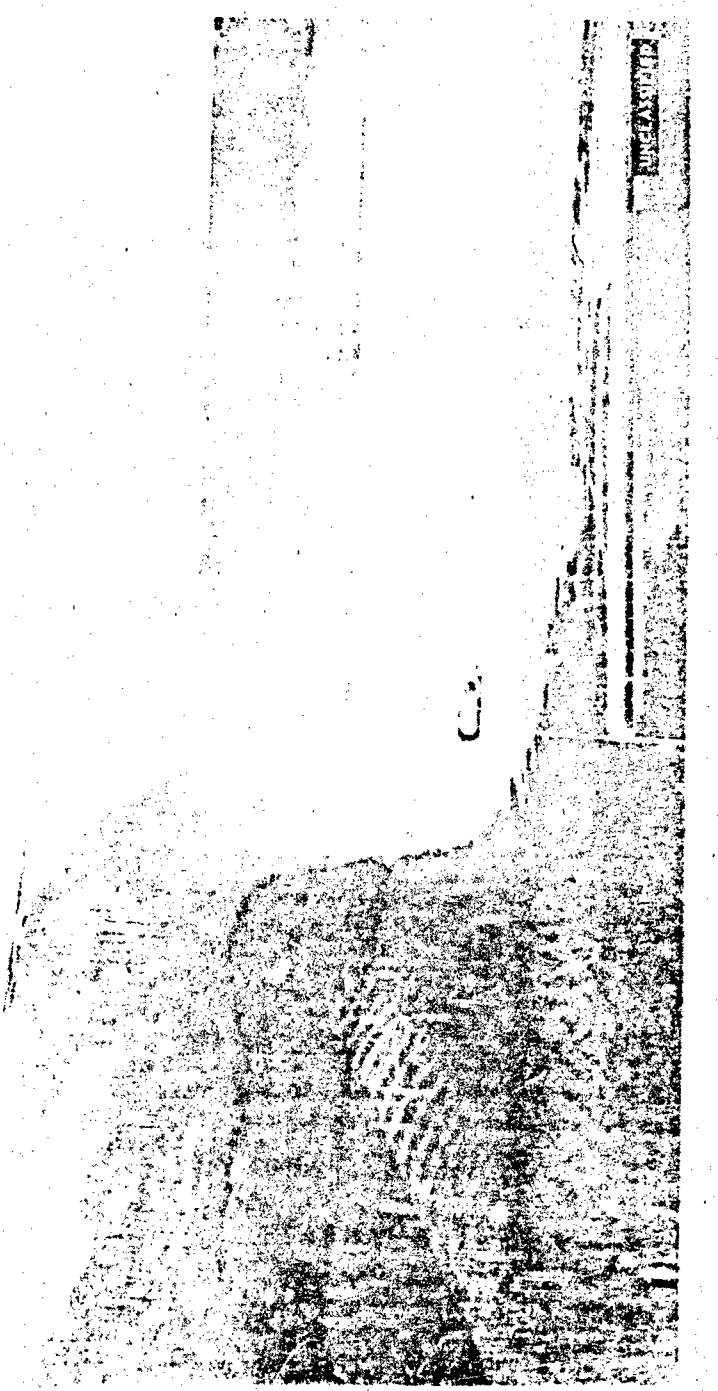

Figure 3 Static Pressure Tap Installation Method
(E-82483)

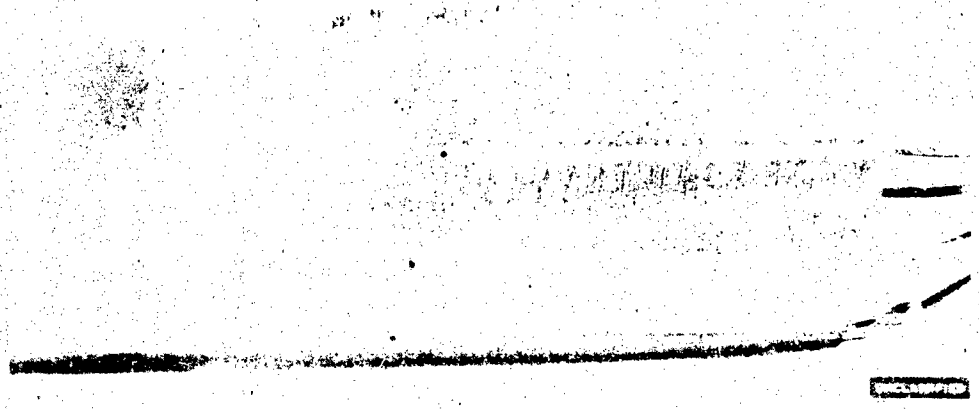

Figure 4 Static Pressure Taps After Brazing and Surface Smoothing (FE-82831)

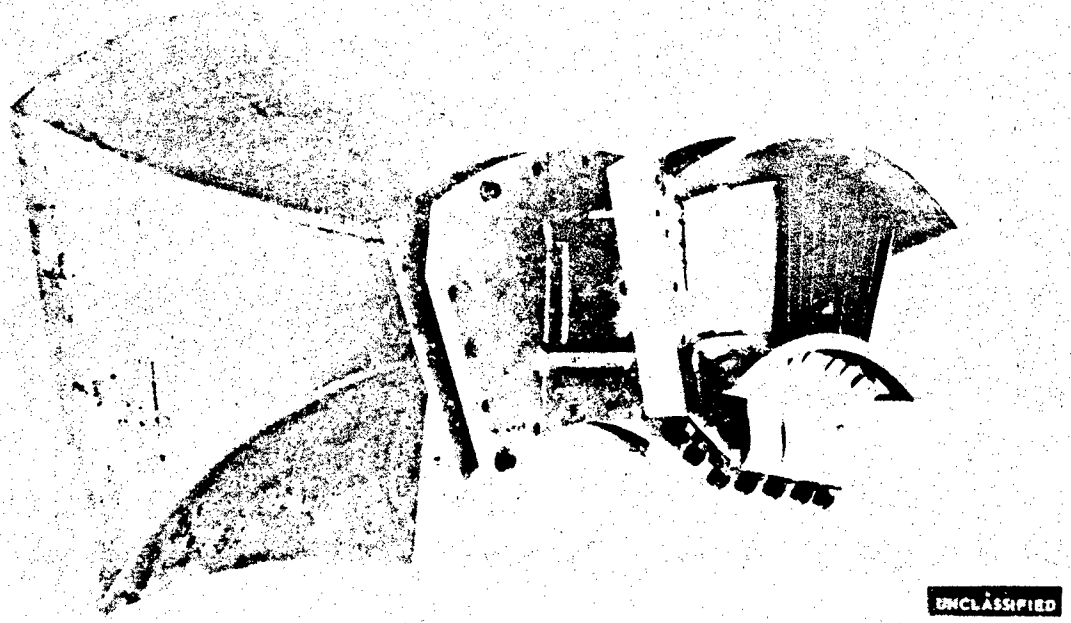

Figure 5 First Blade Cascade Assembly With Static Pressure Connections (FE-82744)

4. DISCUSSION

(U) The four baseline airfoils, namely the medium-reaction, normal-solidity first vane, first blade, second vane and second blade were tested in the annular segment cascade. The entire collection of data points that were taken during these tests is tabulated in Table II. The design values indicated in this table are placed next to the nearest experimental data point. The most useful data (at the nearest to design test value) is presented herein, including photographs of the flow visualization tests. Analysis of this data and the visual information indicated that the four baseline airfoils behaved similarly in all important respects. Therefore, the results of all four airfoils will be discussed in each aerodynamic performance category. The behavior of these airfoils will be discussed, in the following paragraphs, in the order of the listing of steps taken to meet Task Objectives (See paragraph 2 of this section).

TABLE II

SUMMARY OF PHASE IIb DATA

	Midspan Turbine Design M_2	Midspan Test M_2	Midspan Turbine Design Re	Midspan Test Re
First Vane – No Screen		0.717		3.22×10^5
		0.794		3.72
	0.852	0.858	4.38×10^5	4.18
		0.907		4.44
First Vane – With Screen		0.704		3.10×10^5
		0.779		3.60
	0.852	0.884	4.38×10^5	4.18
First Blade – No Screen		0.734		2.03×10^5
	0.788	0.816	2.26×10^5	2.33
		0.912		2.73
Second Vane – No Screen		0.823		2.76×10^5
	0.870	0.883	2.95×10^5	3.00
		1.019		3.61
Second Vane – With Screen		0.784		2.53
	0.870	0.837	2.95×10^5	2.80
		0.981		3.38
Second Blade – No Screen		0.836		1.60×10^5
	0.904	0.946	1.07×10^5	1.80
		1.046		2.04

UNCLASSIFIED

(U) The inlet guide vane total pressure loss for each cascade was determined by traversing the inlet to the test airfoils. The measured spanwise total pressure distributions are shown in Figures 6 through 11. For both the first and second vanes, two sets of data are shown: with and without turbulence screen. In order to determine if the loss levels could be significantly affected by an increase in cascade turbulence levels, a screen with a 0.009 inch diameter wire (with a 0.063 inch center-to-center spacing) was mounted at the cascade inlet flange approximately one inch upstream of the leading edge. The screen was designed in order to produce 6% turbulence intensity, which is representative of turbine levels. Photographs of the screen are shown in Figures 12 and 13.

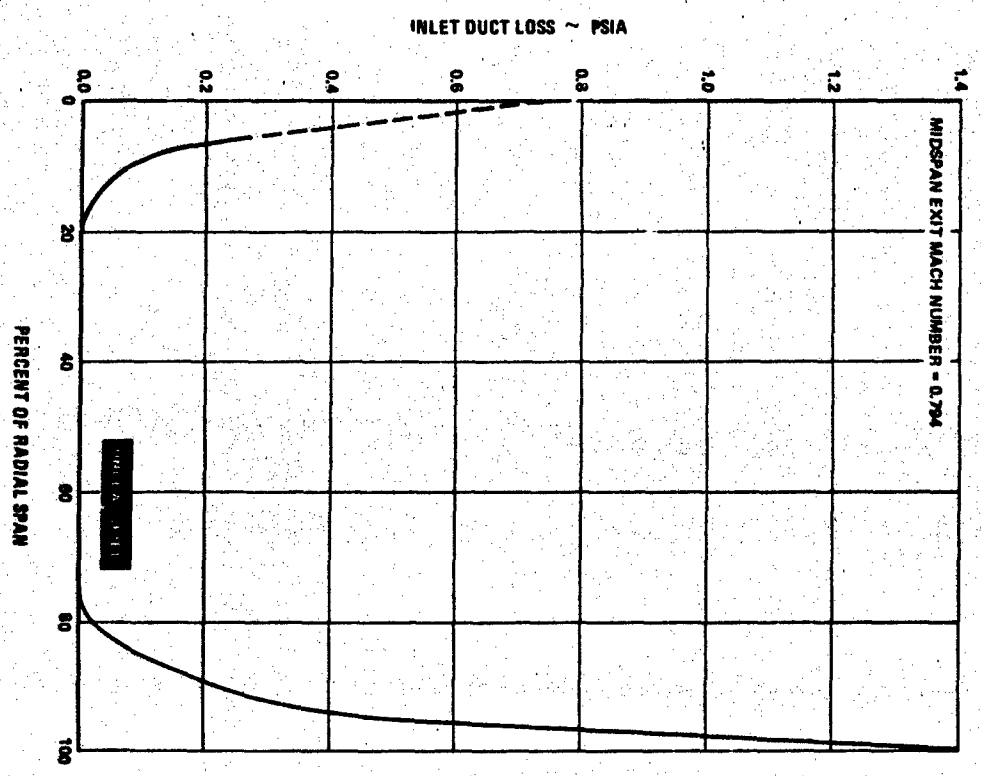

Figure 6 Inlet Duct Loss vs. Percent Radial Span – First Vane Cascade

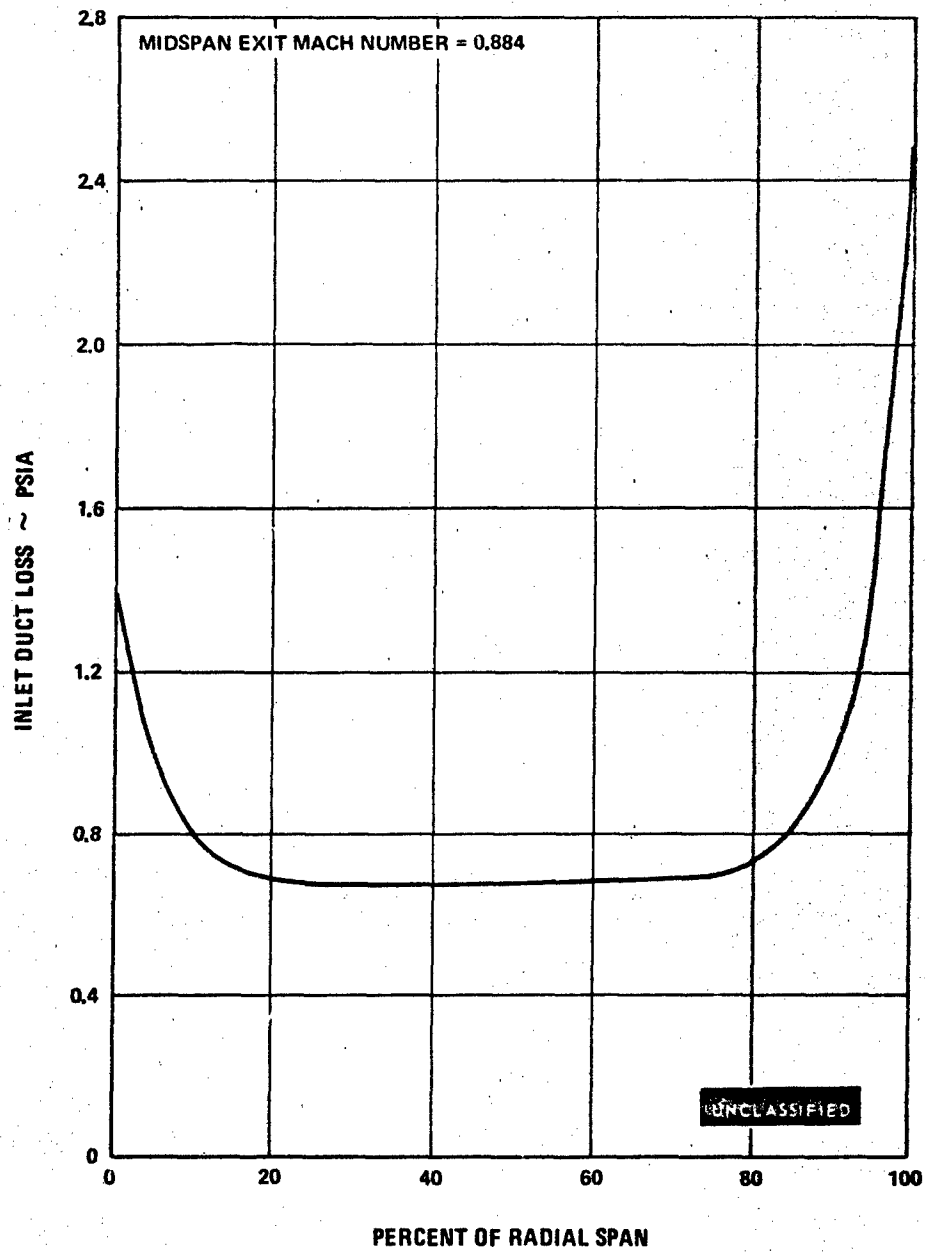

Figure 7 Inlet Duct Loss vs. Percent Radial Span – First Vane Cascade, Inlet Screen Installed

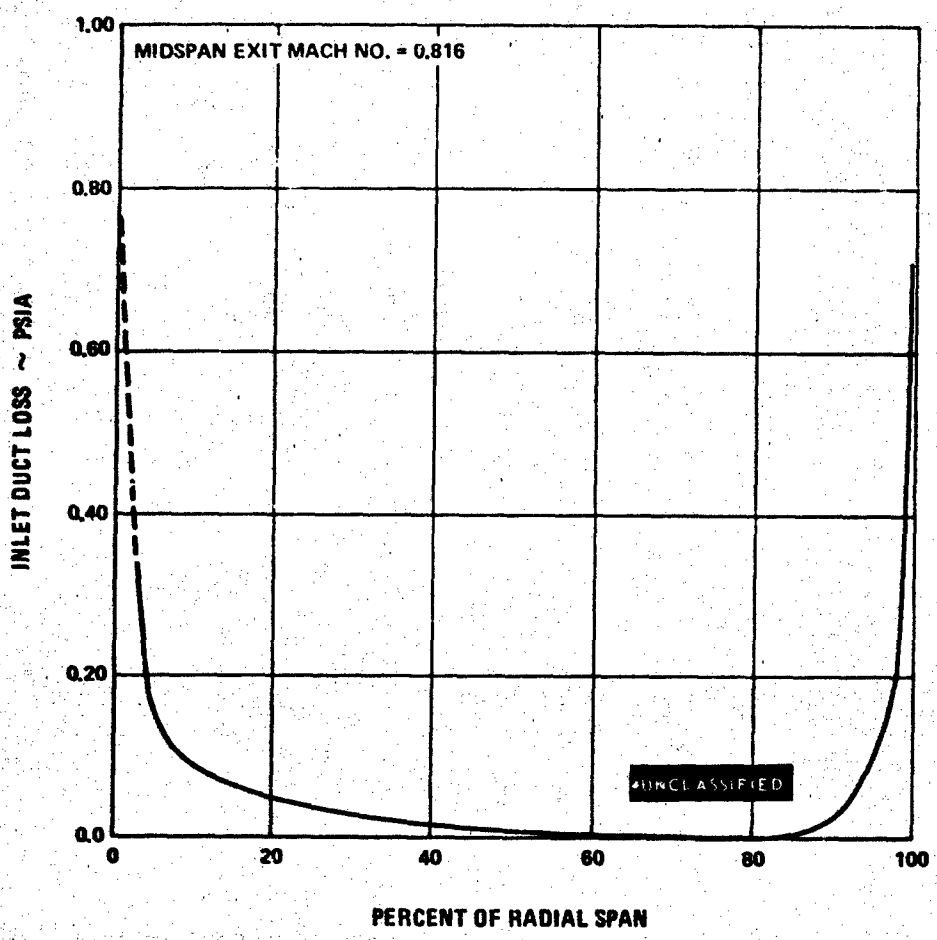

Figure 8 Inlet Duct Loss vs. Percent Radial Span – First Blade Cascade

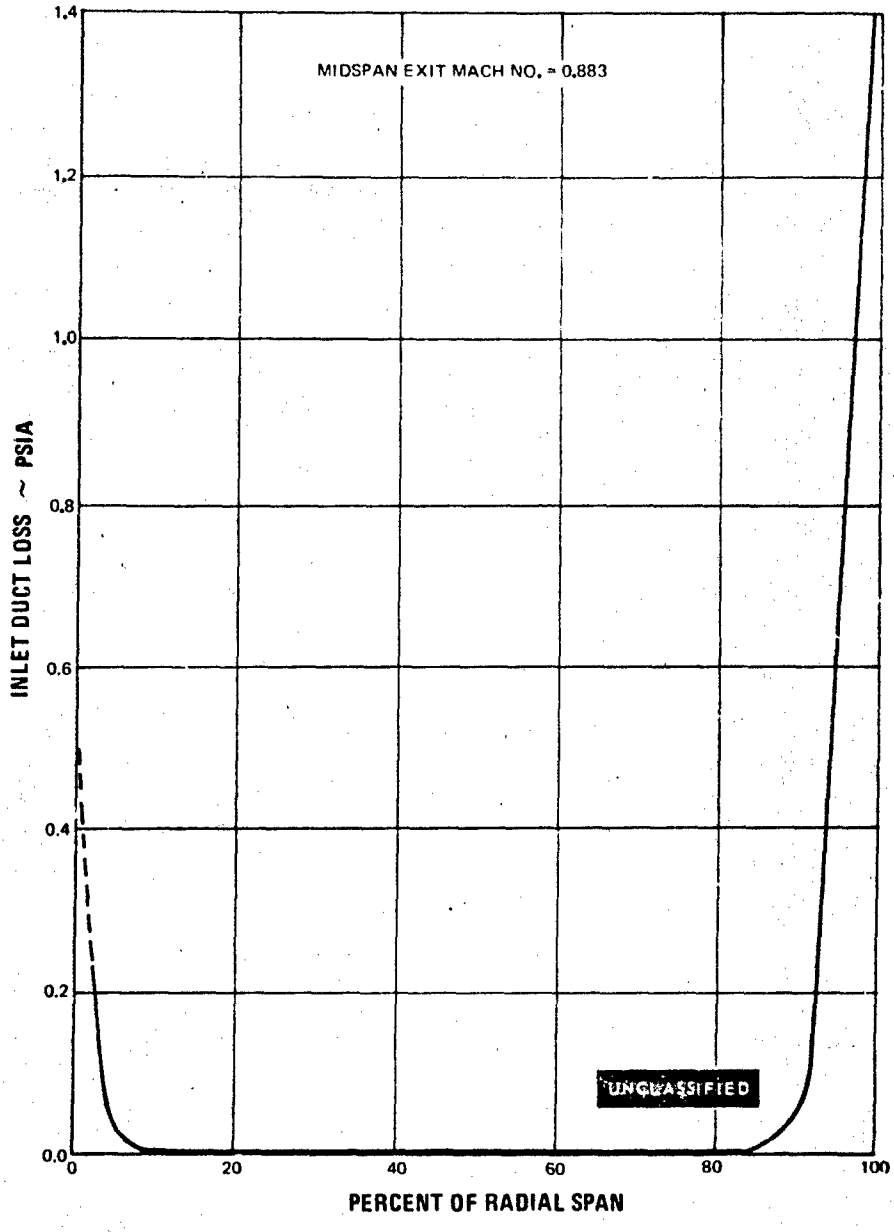

Figure 9 Inlet Duct Loss vs. Percent Radial Span – Second Vane Cascade, Inlet Screen Removed

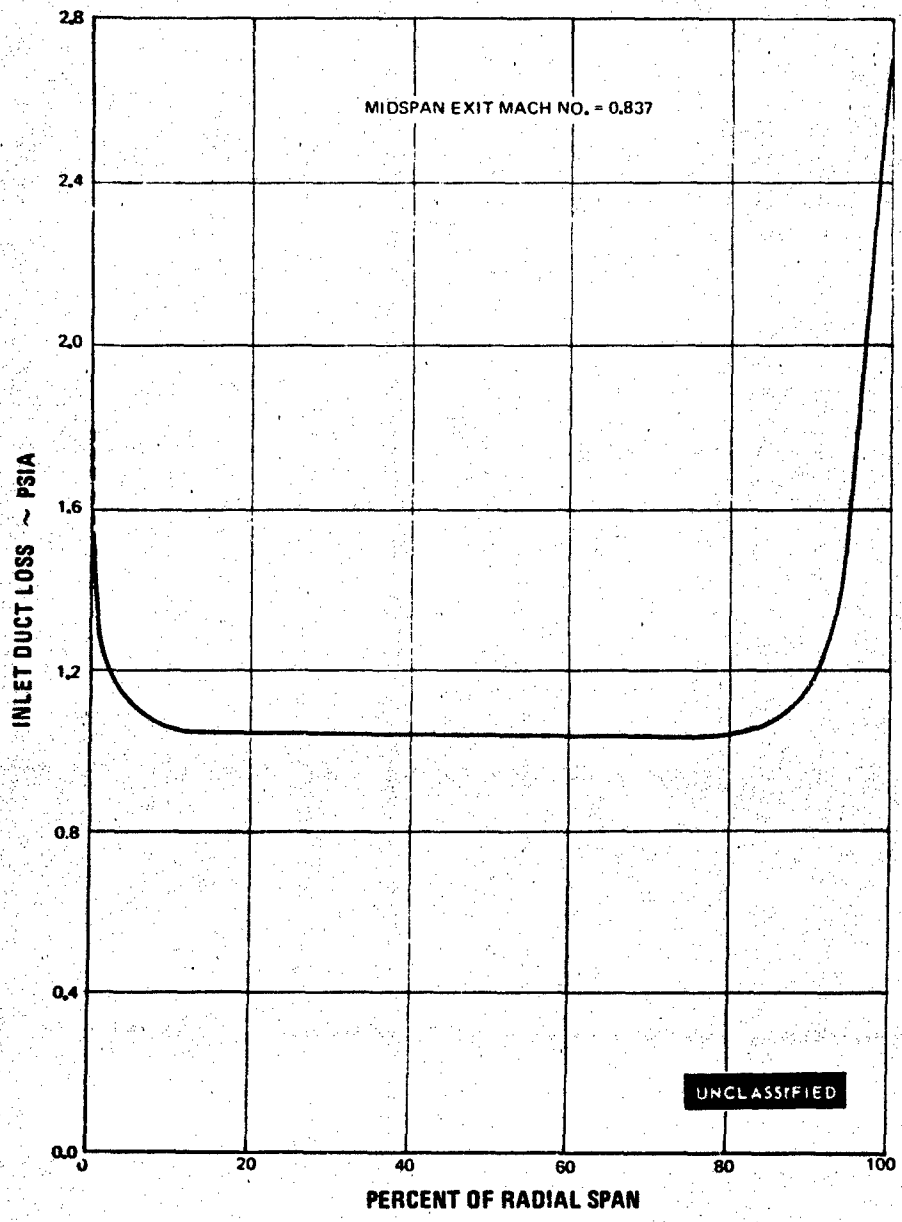

Figure 10 Inlet Duct Loss vs. Percent Radial Span – Second Vane Cascade, Inlet Screen Installed

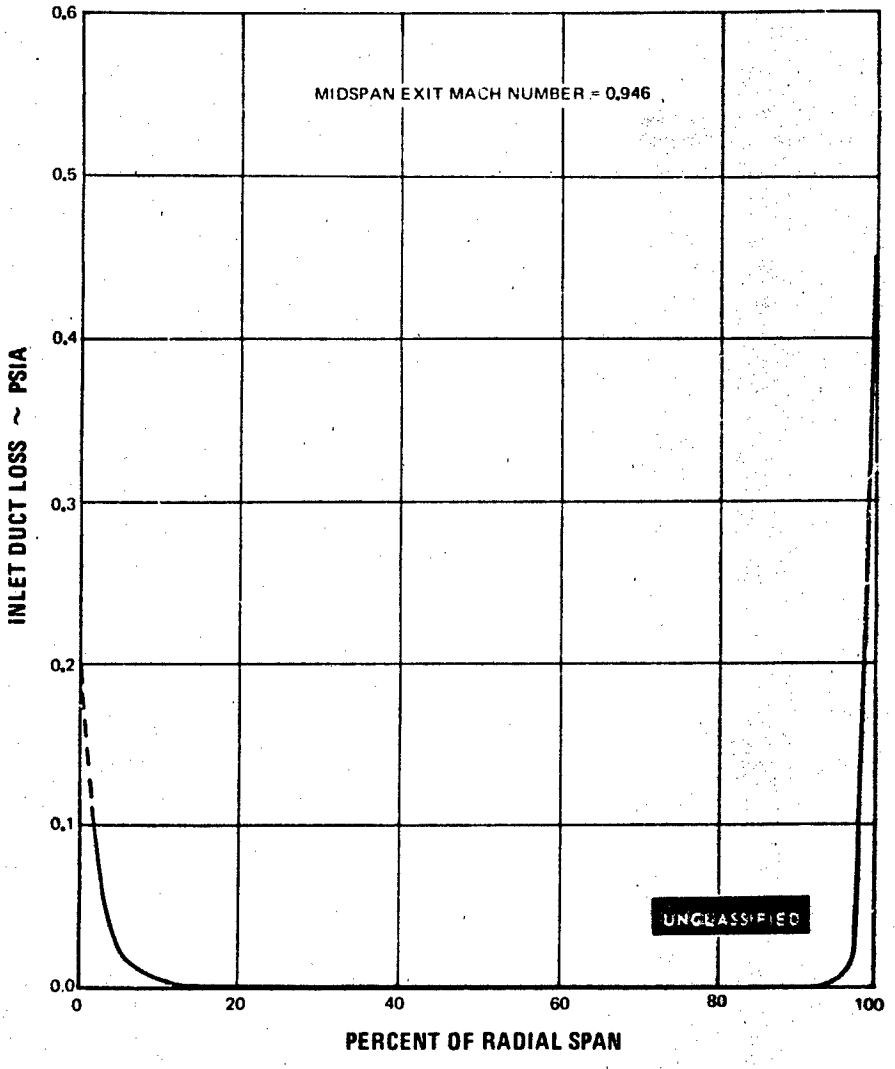

Figure 11 Inlet Duct Loss vs. Percent Radial Span – Second Blade Cascade

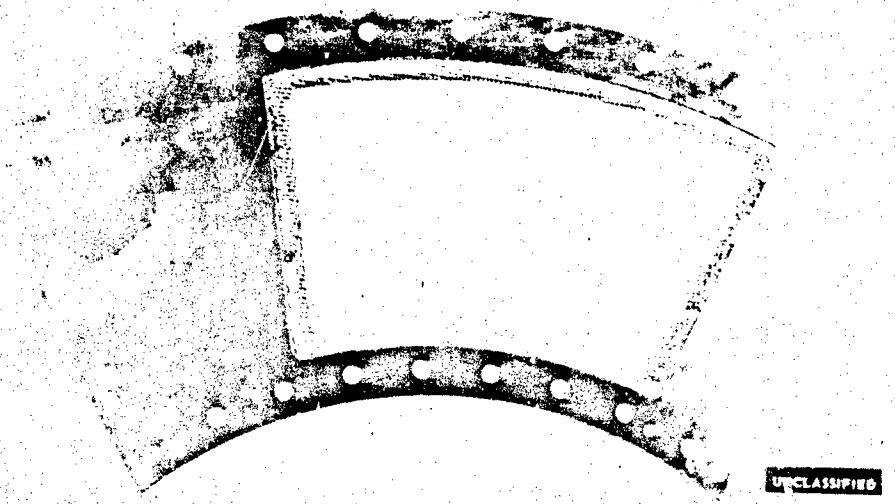

Figure 12 Turbulence Screen Upstream Side
(FE-82742)

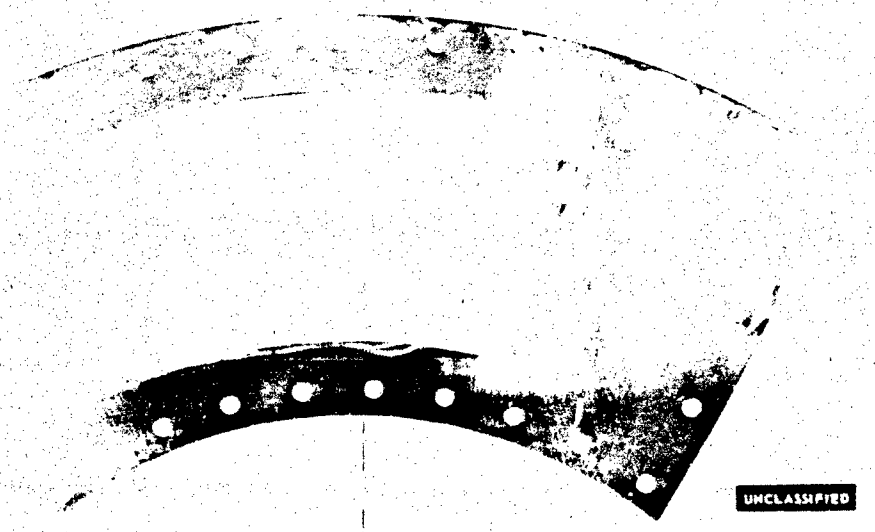

Figure 13 Turbulence Screen Downstream Side
(FE-82741)

(U) The inlet flow angle approaching the test foils was also measured for each cascade. The design of the inlet guide vanes was acceptable, since the flow angles were within approximately 4 degrees of the design value. A typical trace of the inlet flow angle variation is shown in Figures 14 through 16 for the first stage vane cascade.

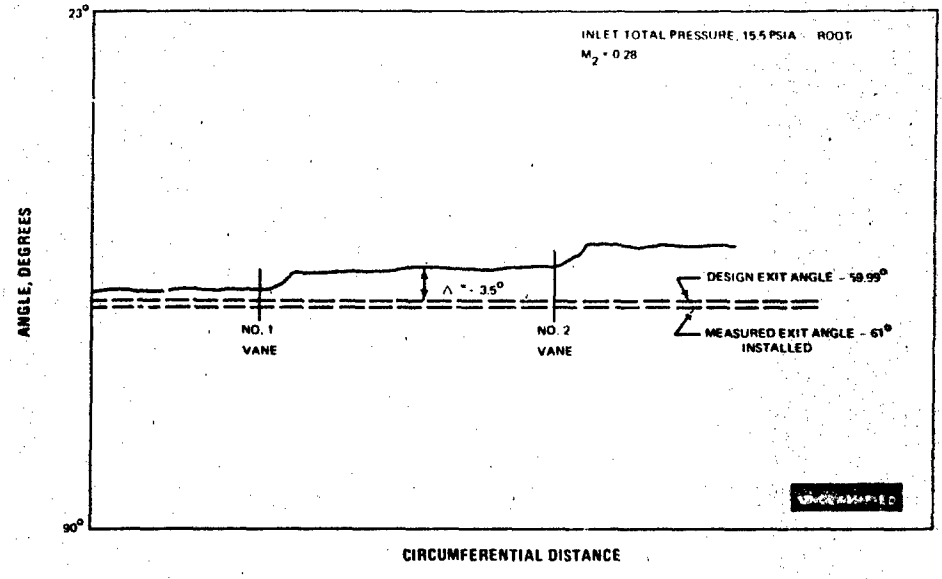

Figure 14 First Stage Turning Vane Exit Angle Measurement

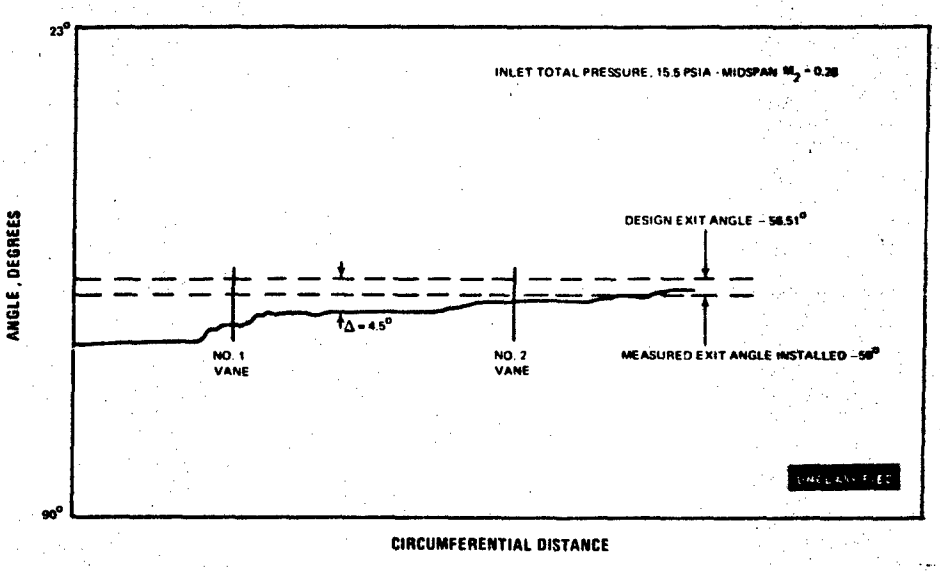

Figure 15 First Stage Turning Vane Exit Angle Measurement

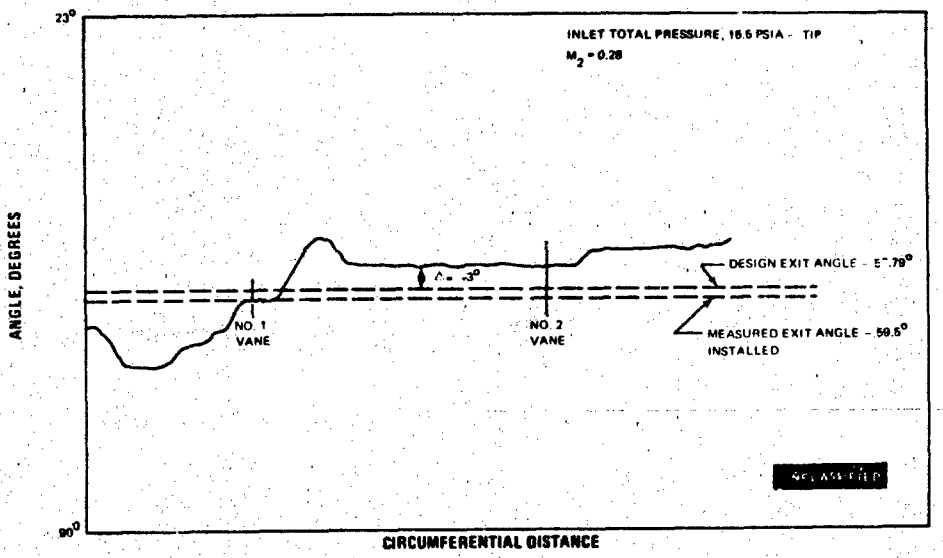

Figure 16 First Stage Turning Vane Exit Angle Measurement

(U) The plots of the important aerodynamic quantities based on the inlet and exit plane measurements for the four baseline airfoils are shown in Figures 17 through 52 at exit flow Mach numbers nearest to the design value. These plots include the total pressure loss and exit gas flow angle contours over three passages. Further, the average spanwise distribution of the total pressure loss, loss coefficient, exit flow angle and exit Mach number are presented.

(U) The contour plots for both the total pressure loss and exit gas flow angle for each airfoil show wakes from the inlet guide vanes which are readily distinguishable from the loss patterns of the test foils themselves. The diagonal orientation of these wakes with respect to the cascade passages requires loss calculations in different passages over the span in order to avoid wake losses which should not be charged to the test airfoils. Therefore, the data reduction program was modified to calculate the average spanwise distribution of any flow parameter over selected passage intervals. It is felt that this yields the fairest measure of the test foil performance. Future tests (Task IIc) will avoid this problem since the inlet guide vanes for the second vane cascade were restacked with the trailing edges approximately parallel to the leading edges of the test airfoils. This change is indicated in Figure 53. A baseline second vane retest will be made when fabrication of the new hardware is completed and those results will be compared with the results presented here, based on the selected passage interval data reduction procedure.

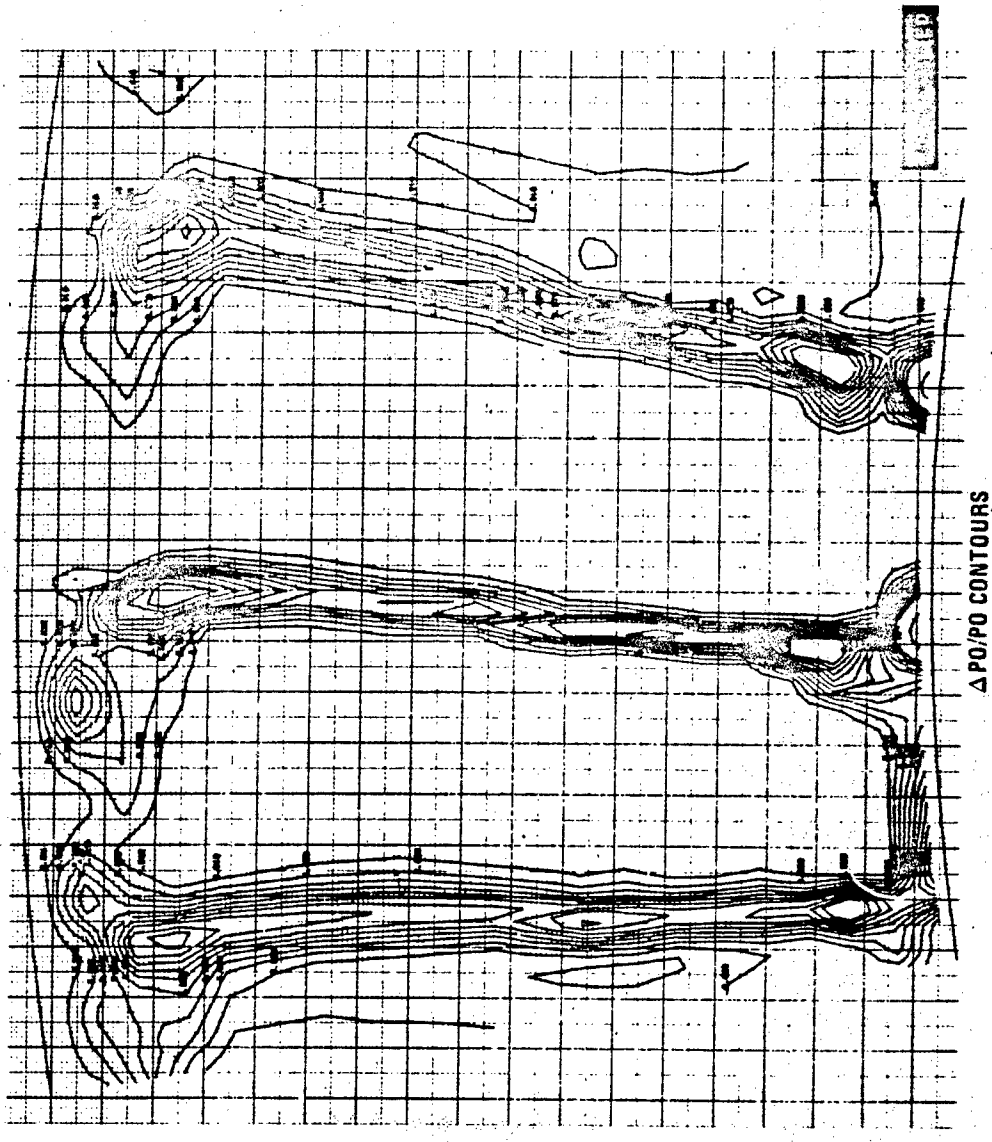

Figure 17 Pressure Loss Contours, First Vane Screen Removed. Three Flow Passages, Midspan Exit Mach No. = 0.858

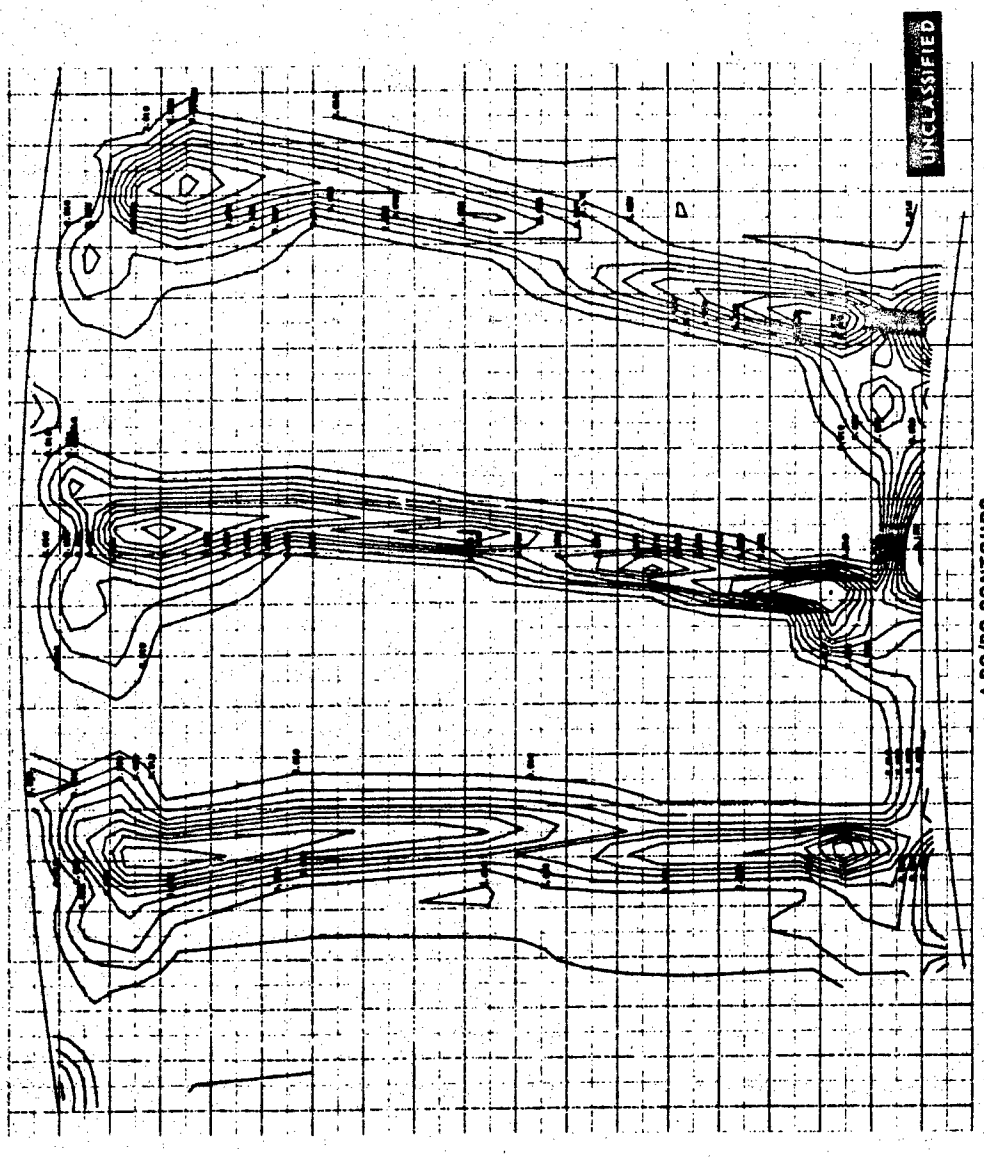

Figure 18 Pressure Loss Contours, First Vane – Screen Installed, Three Flow Passages, Midspan Exit Mach No. = 0.884

Figure 19 Pressure Loss Contours, First Blade Screen Removed, Three Flow Passages, Midspan Exit Mach No. = 0.816

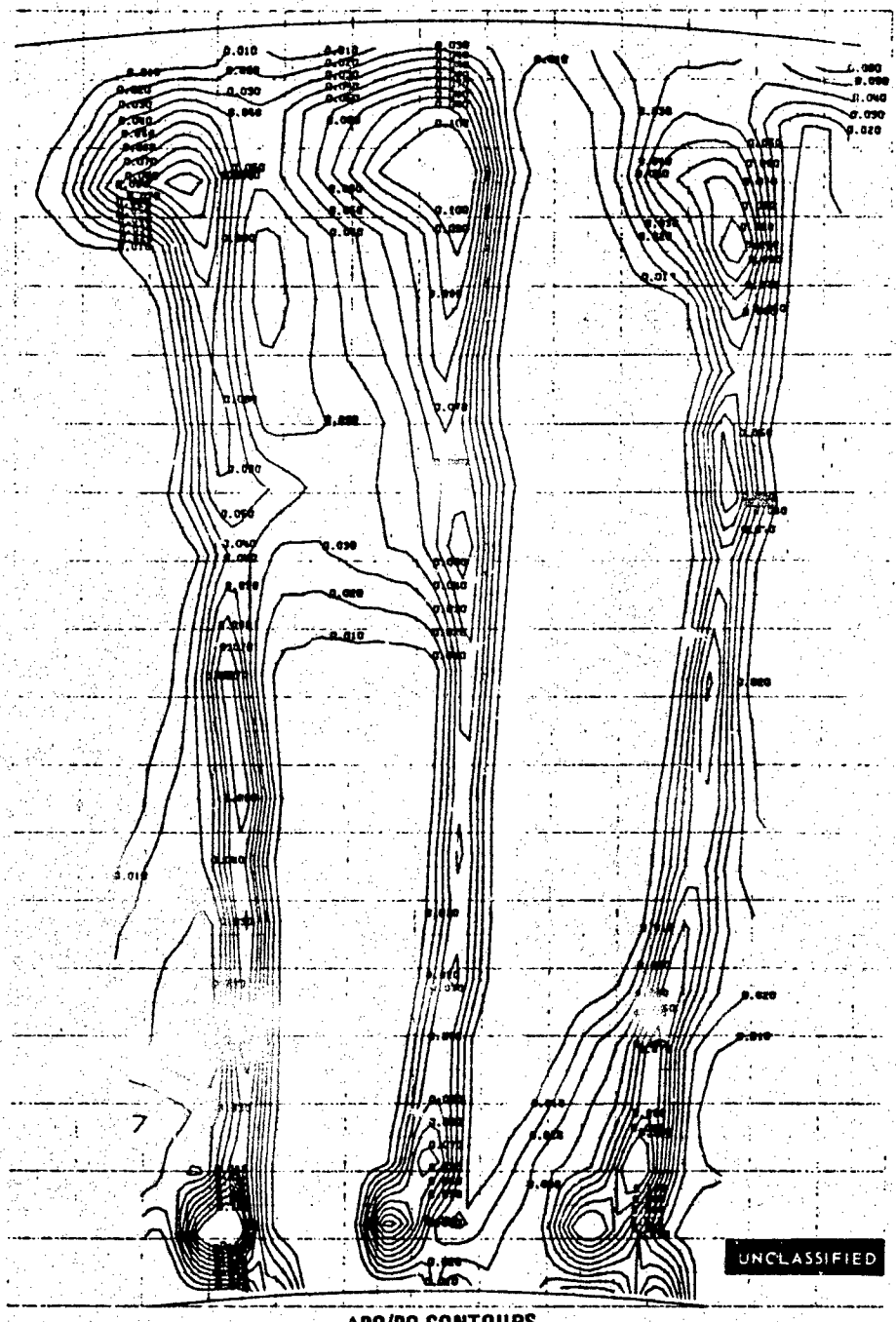

ΔPO/PO CONTOURS

Figure 20 Pressure Loss Contours, Second Vane – Screen Removed, Three Flow Passages, Midspan Exit Mach No. = 0.883

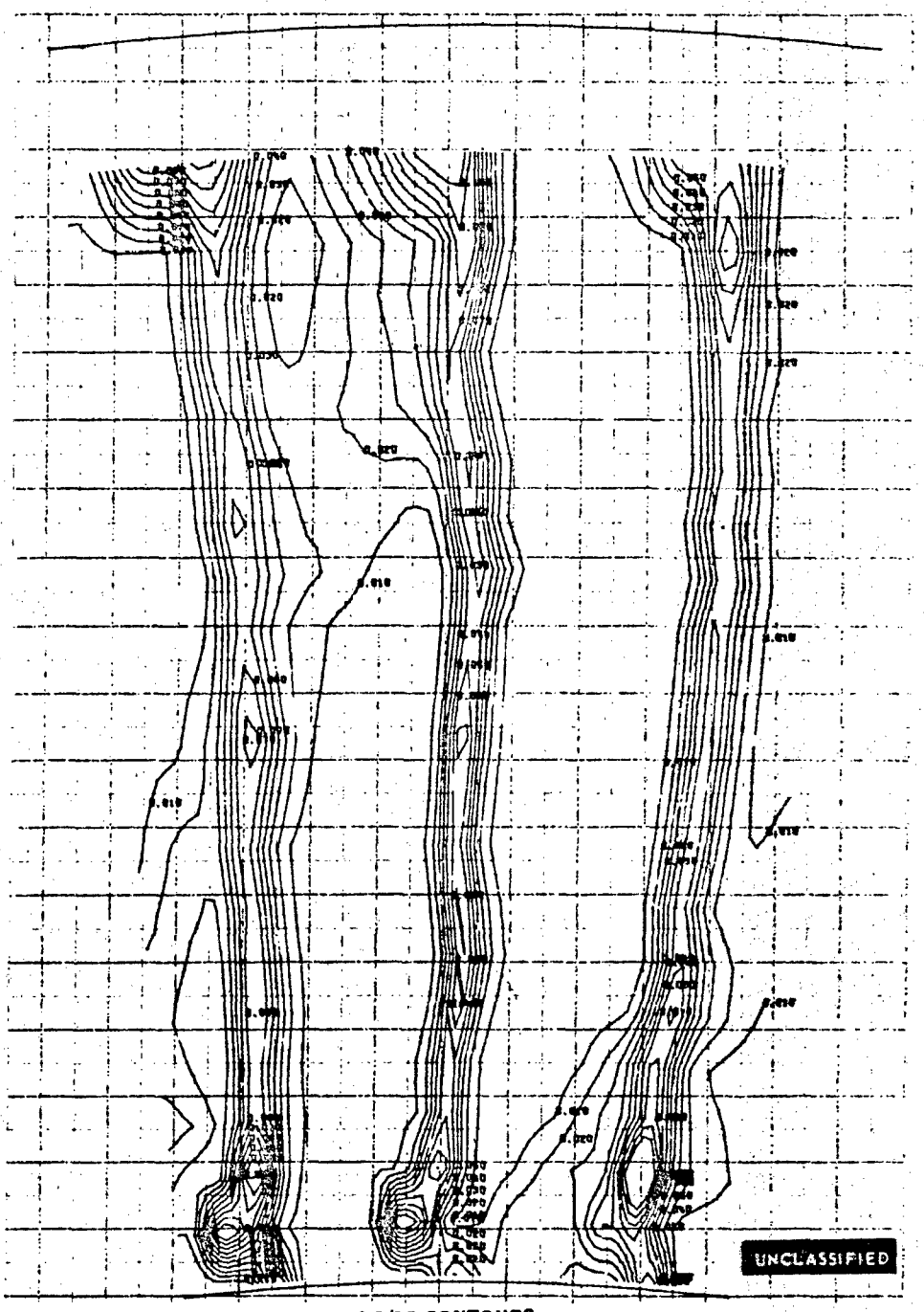

ΔPO/PO CONTOURS

Figure 21 Pressure Loss Contours, Second Vane Screen Installed, Three Flow Passages, Midspan Exit Mach No. = 0.837

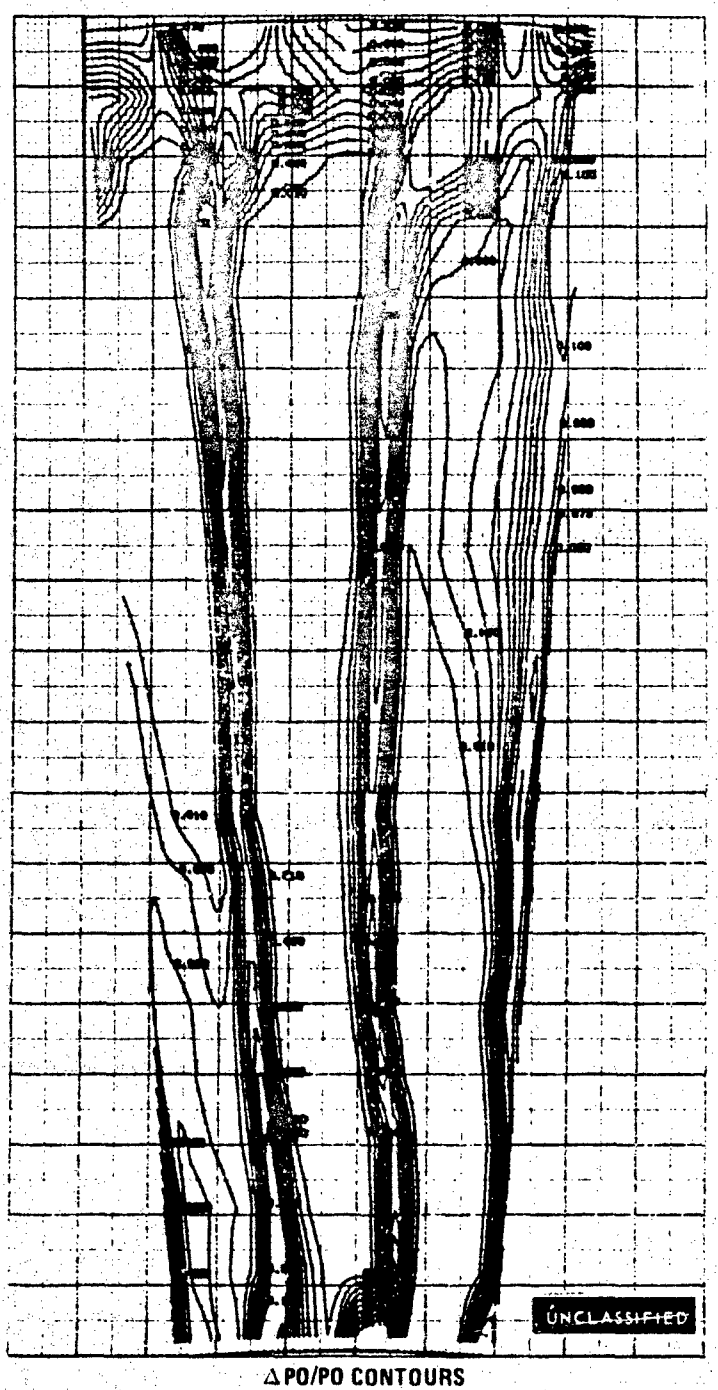

Figure 22 Pressure Loss Contours, Second Blade Screen Removed, Three Flow Passages, Midspan Exit Mach No. = 0.946

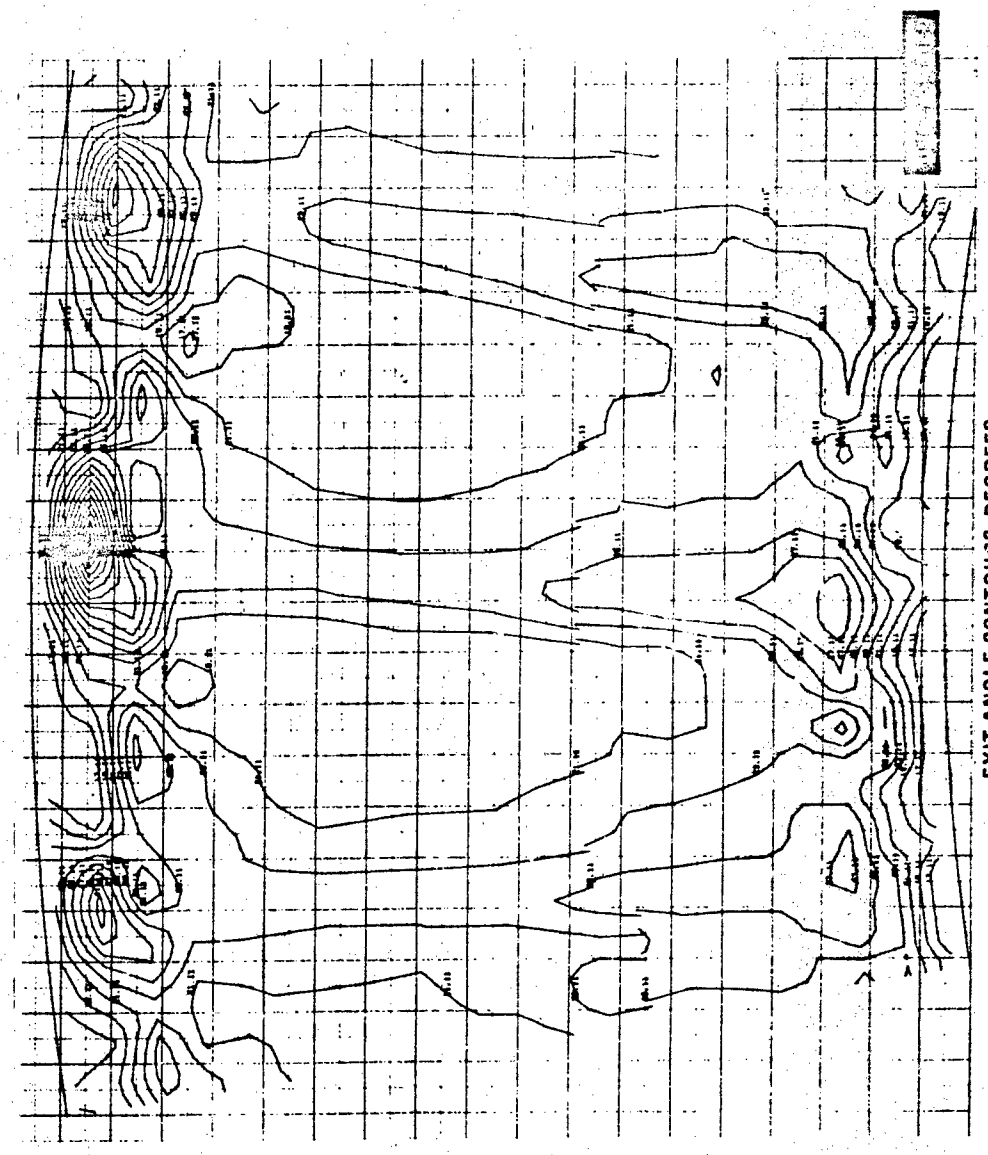

Figure 23 Exit Gas Angle Contours, First Vane Screen Removed, Three Flow Passages, Midspan Exit Mach No. = 0.858

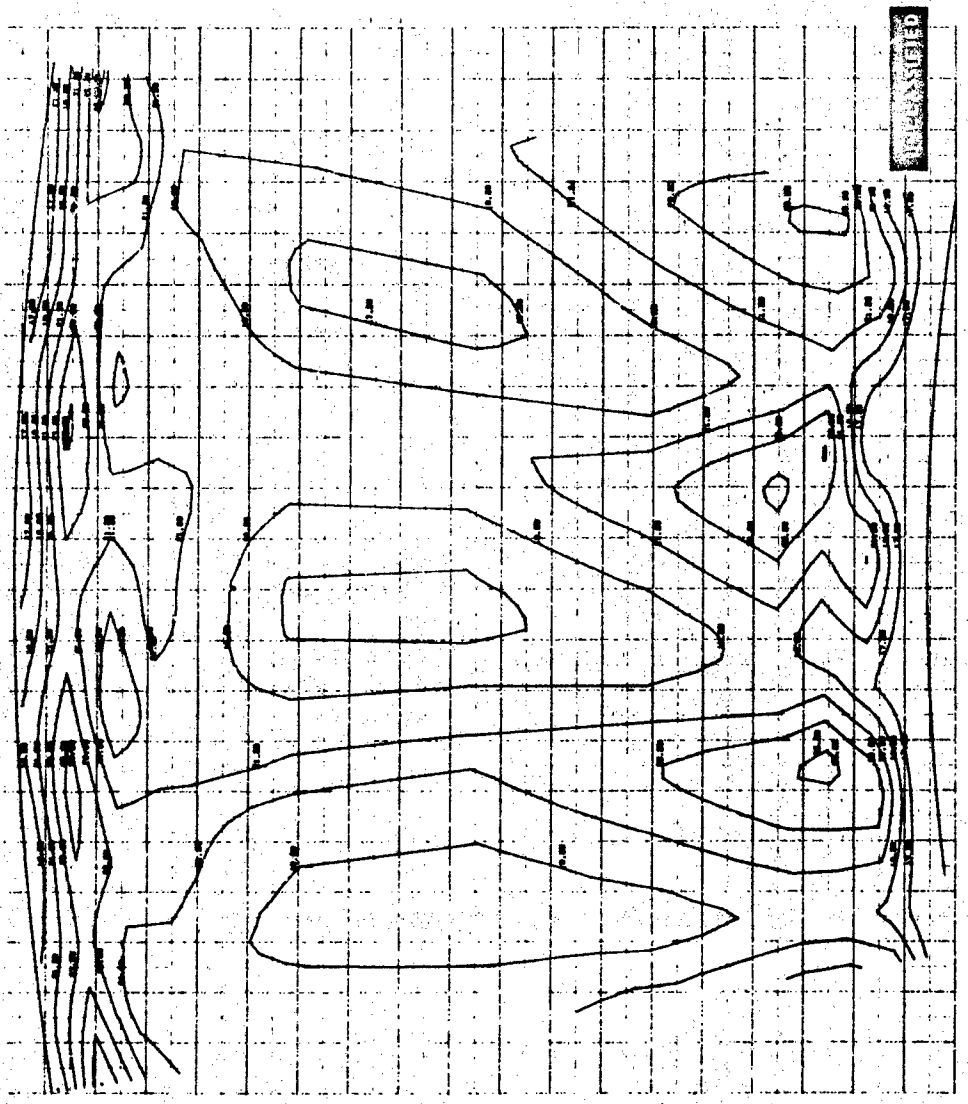

Figure 24 Exit Gas Angle Contours, First Vane – Screen Installed, Three Flow Passages, Midspan Exit Mach No. = 0.884

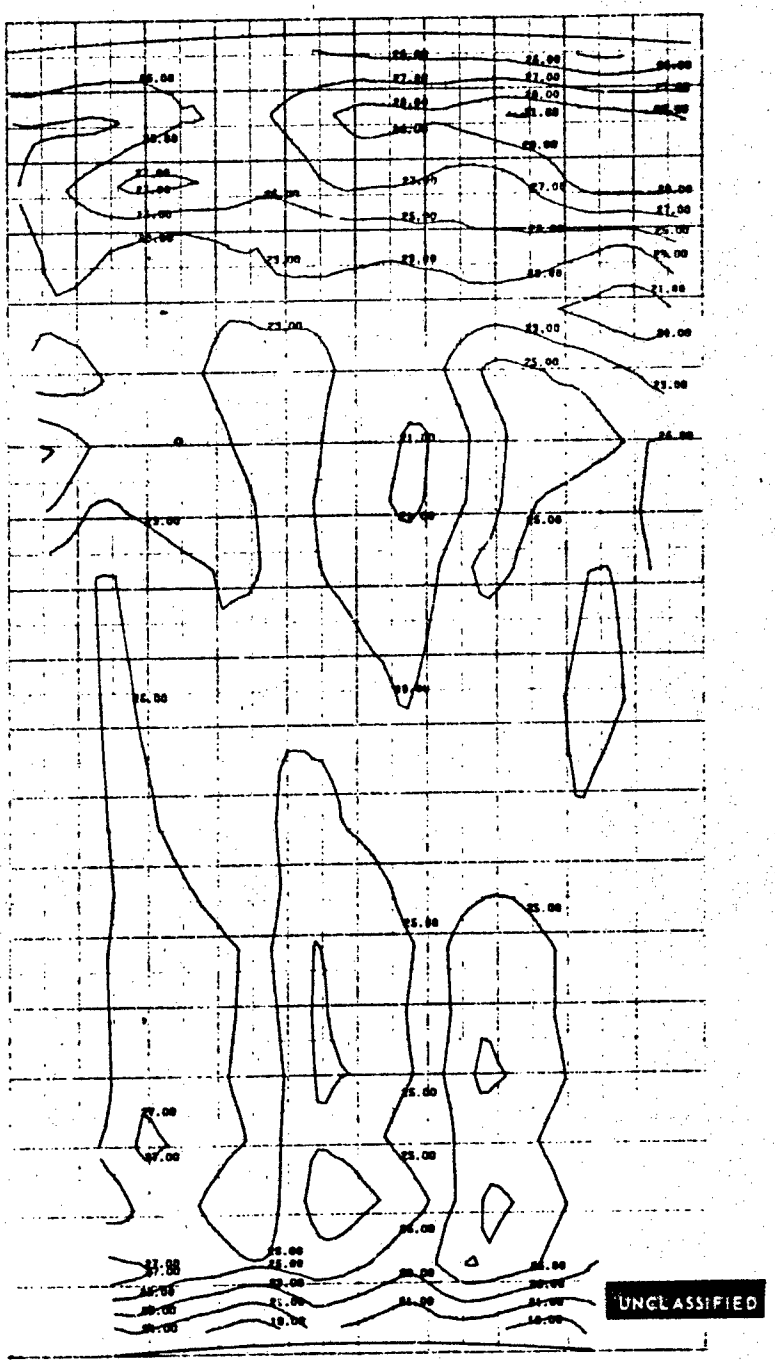

EXIT GAS ANGLE CONTOURS, DEGREES

Figure 25 Exit Gas Angle Contours, First Blade Screen Removed, Three Flow Passages, Midspan Exit Mach No. = 0.816

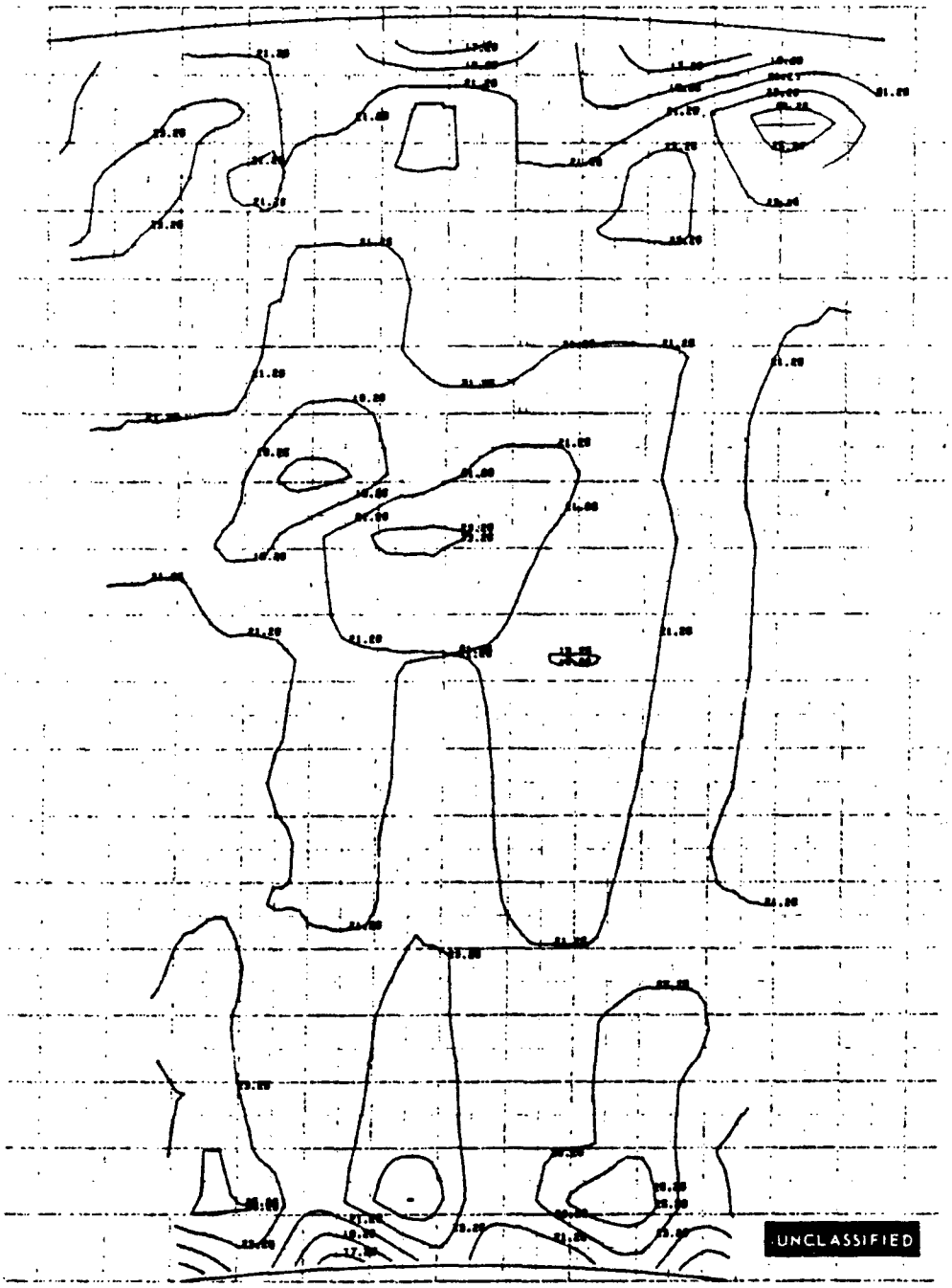

EXIT GAS ANGLE CONTOURS, DEGREES

Figure 26 Exit Gas Angle Contours, Second Vane -- Screen Removed, Three Flow Passages, Midspan Exit Mach No. = 0.883

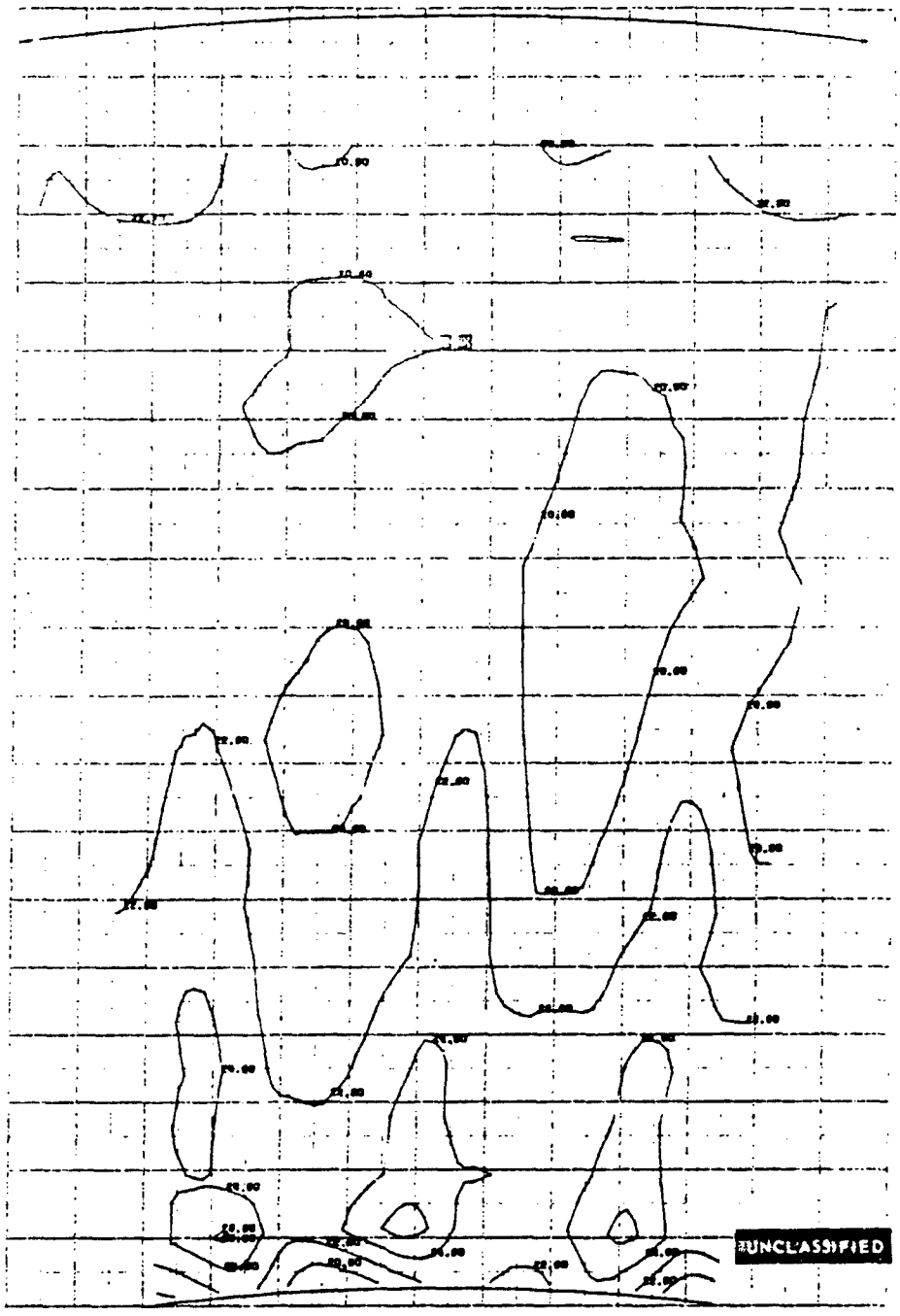

EXIT GAS ANGLE CONTOURS, DEGREES

Figure 27 Exit Gas Angle Contours, Second Vane – Screen Installed. Three Flow Passages, Midspan Exit Mach No. = 0.837

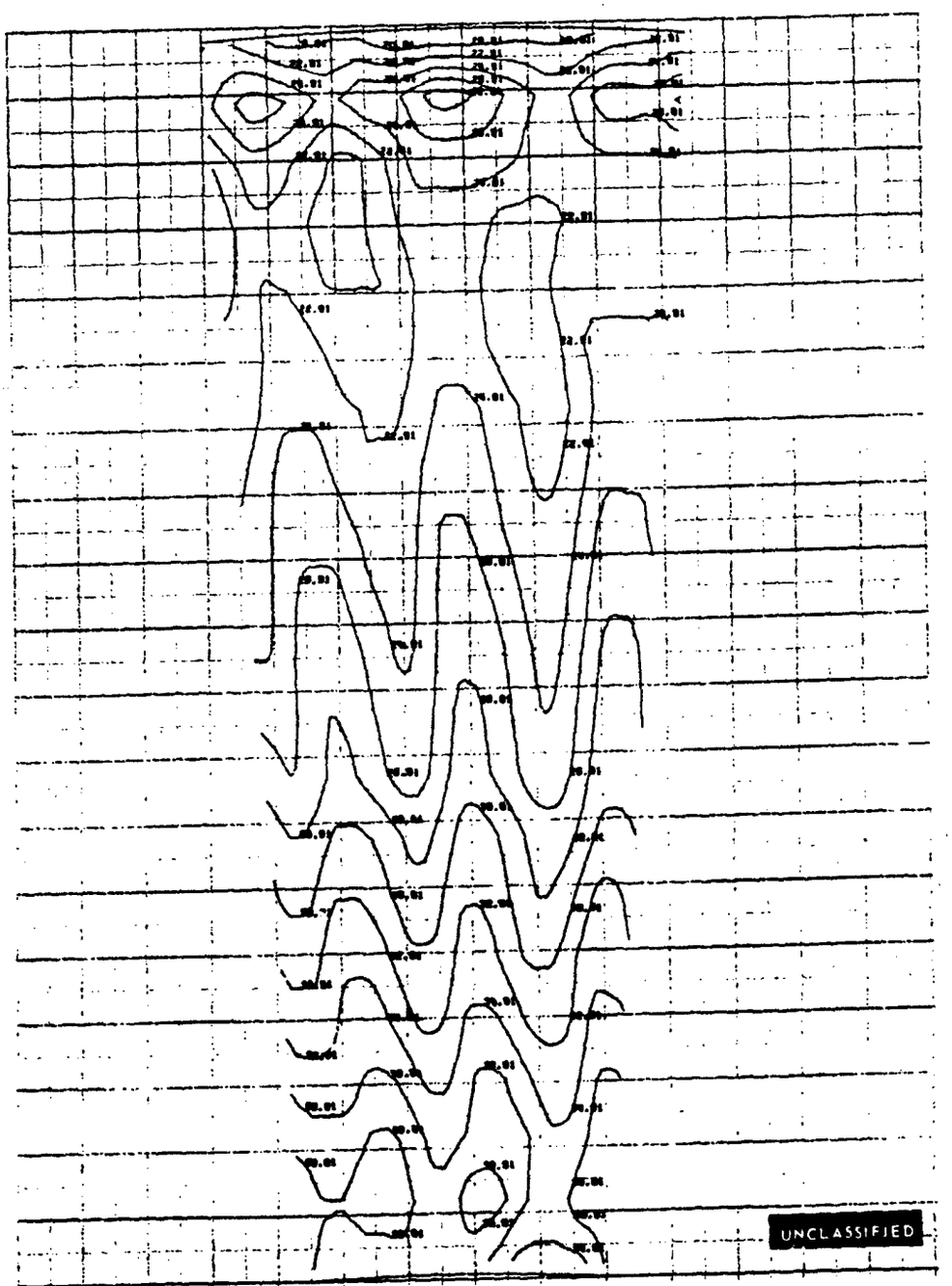

EXIT GAS ANGLE CONTOURS, DEGREES

Figure 28 Exit Gas Angle Contours, Second Blade – Screen Removed, Three Flow Passages, Midspan Exit Mach No. = 0.946

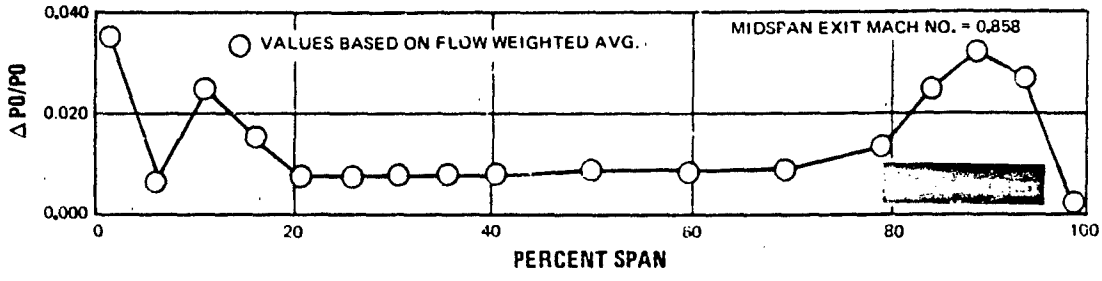

Figure 29 Spanwise Pressure Loss Distribution, First Vane - Screen Removed, Computed at Specified Intervals, Midspan Exit Mach No. 0.858

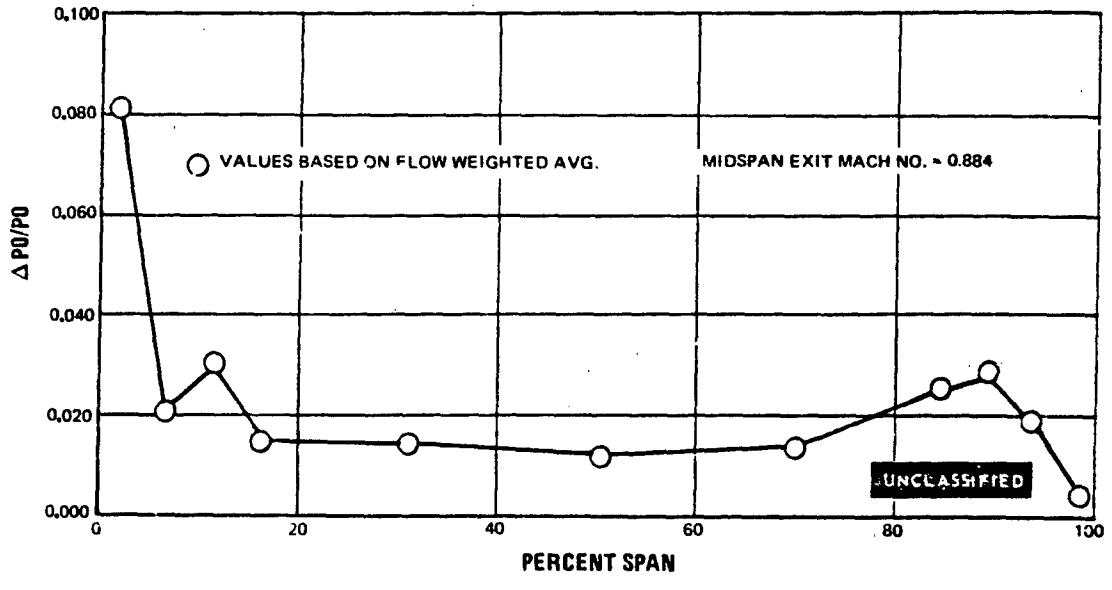

Figure 30 Spanwise Pressure Loss Distribution, First Vane – Screen Installed, Computed at Specified Intervals, Midspan Exit Mach No. = 0.884

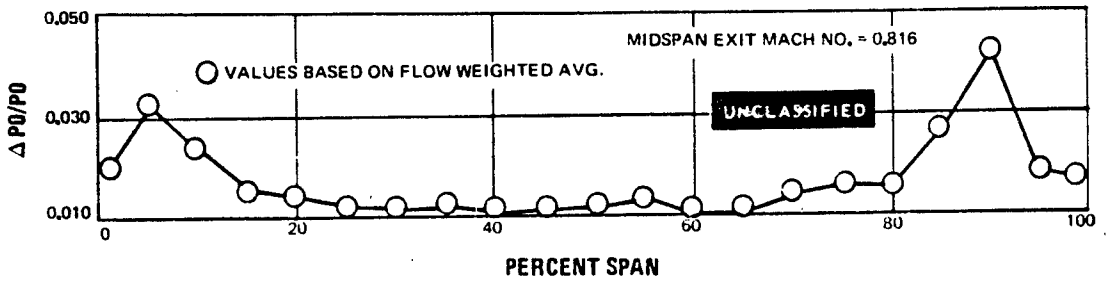

Figure 31 Spanwise Pressure Loss Distribution, First Blade – Screen Removed, Computed at Specified Intervals, Midspan Exit Mach No. = 0.816

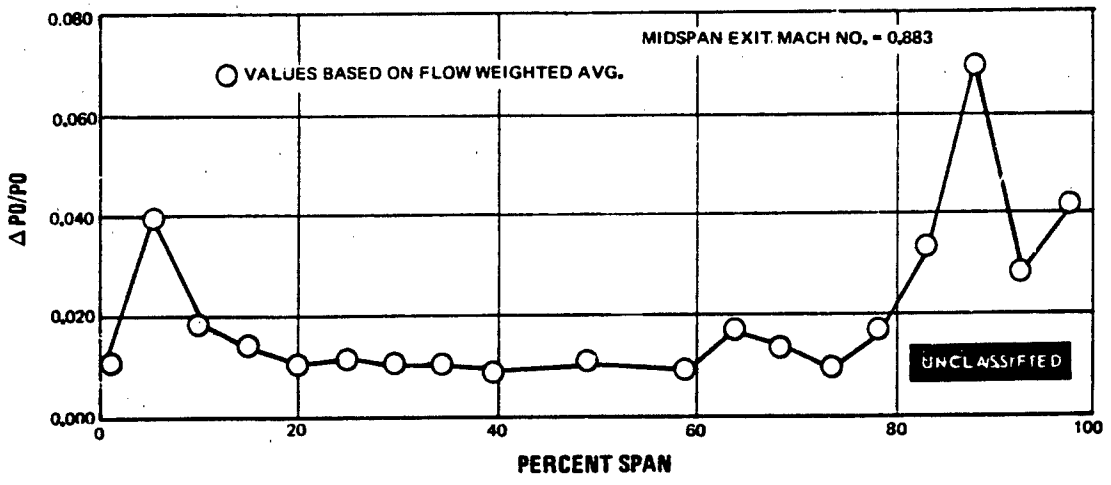

Figure 32 Spanwise Pressure Loss Distribtuion, Second Vane – Screen Removed, Computed at Specified Intervals, Midspan Exit Mach No. = 0.883

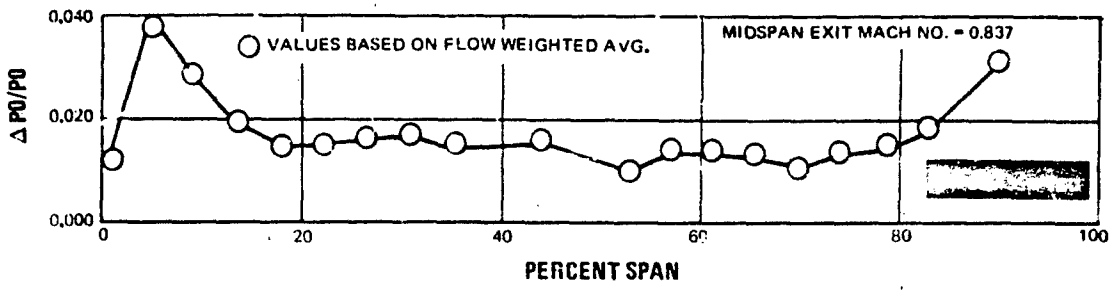

Figure 33 Spanwise Pressure Loss Distribtuion Second Vane – Screen Installed, Computed at Specified Intervals, Midspan Exit Mach No. = 0.837

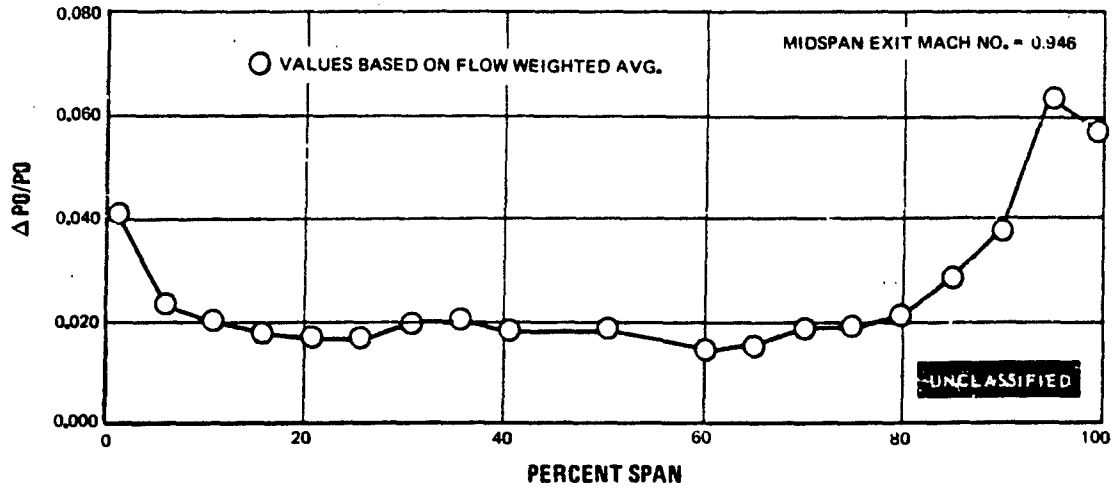

Figure 34 Spanwise Pressure Loss Distribution, Second Blade – Screen Removed, Computed at Specified Intervals, Midspan Exit Mach No. = 0.946

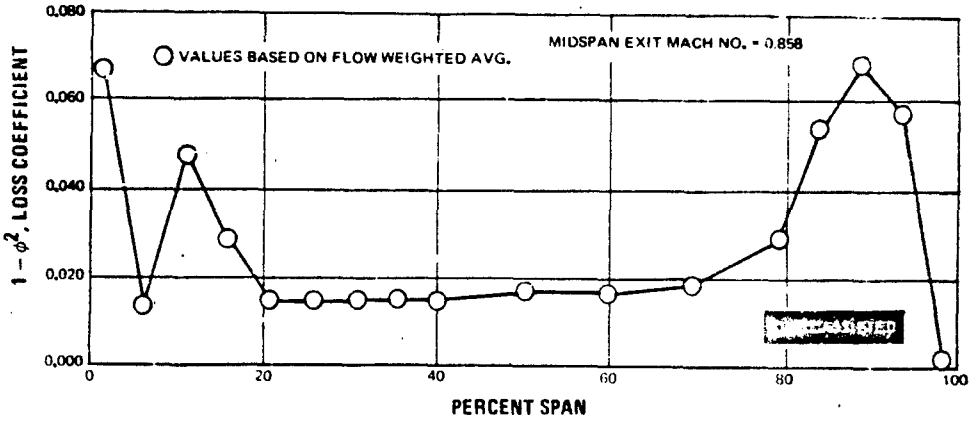

Figure 35 Spanwise Loss Coefficient Distribution, First Vane – Screen Removed, Computed at Specified Intervals, Midspan Exit Mach No. = 0.858

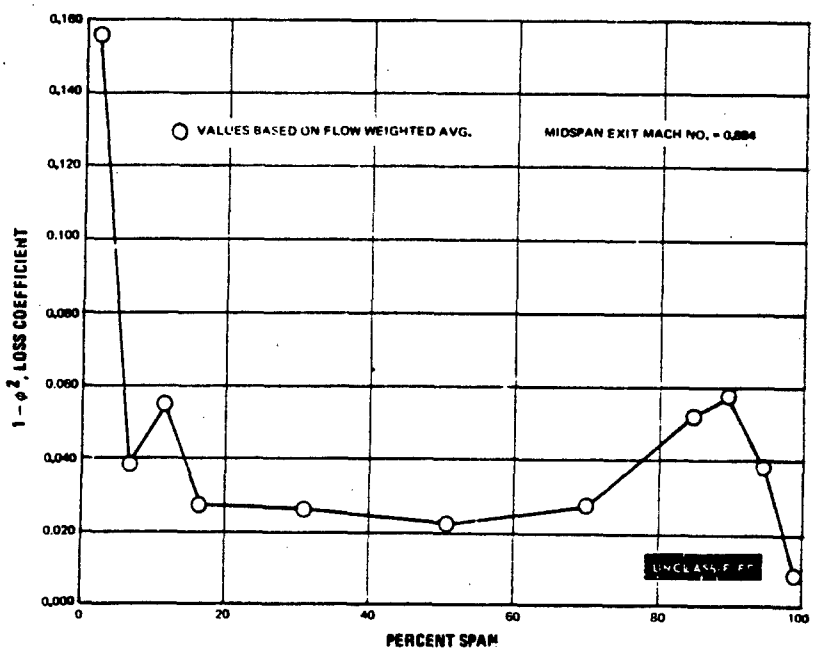

Figure 36 Spanwise Loss Coefficient Distribution, First Vane – Screen Installed, Computed at Specified Intervals, Midspan Exit Mach No. = 0.884

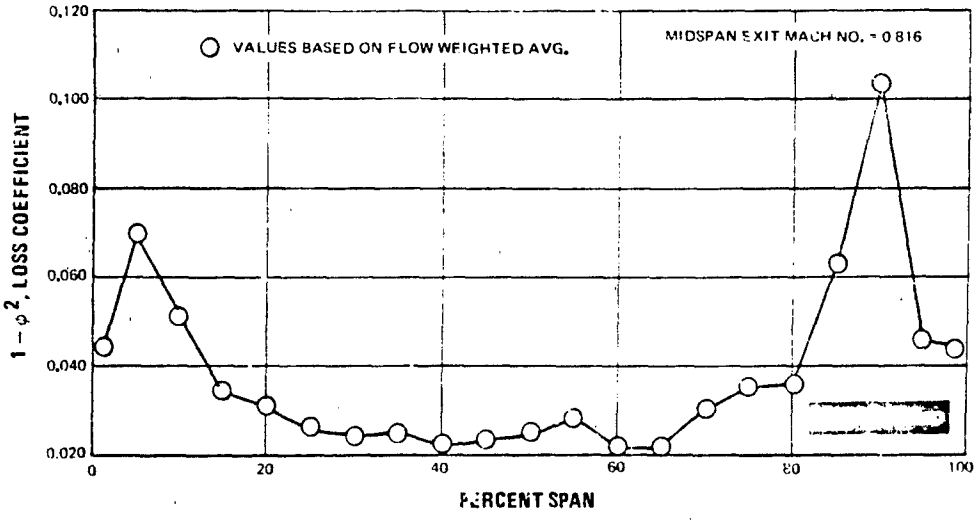

Figure 37 Spanwise Loss Coefficient Distribution First Blade – Screen Removed, Computed at Specified Intervals, Midspan Exit Mach No. = 0.816

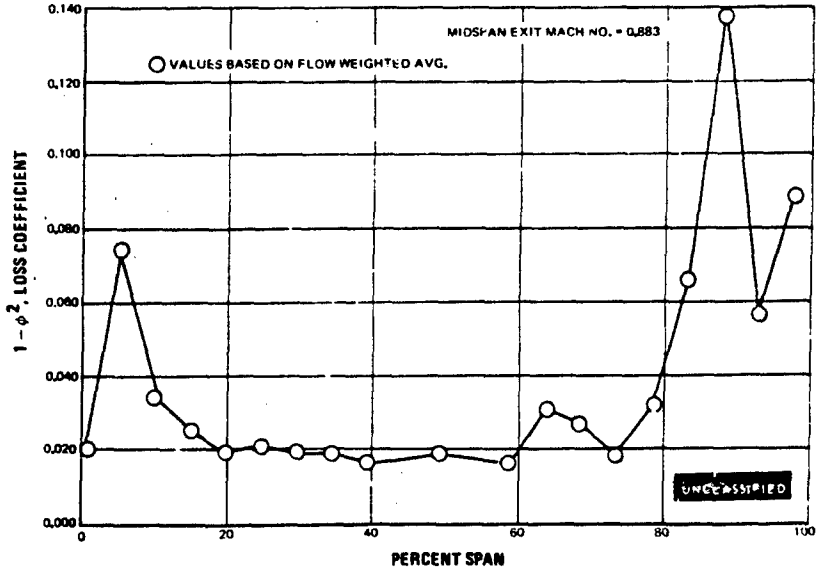

Figure 38 Spanwise Loss Coefficient Distribution, Second Vane – Screen Removed, Computed at Specified Intervals, Midspan Exit Mach No. = 0.883

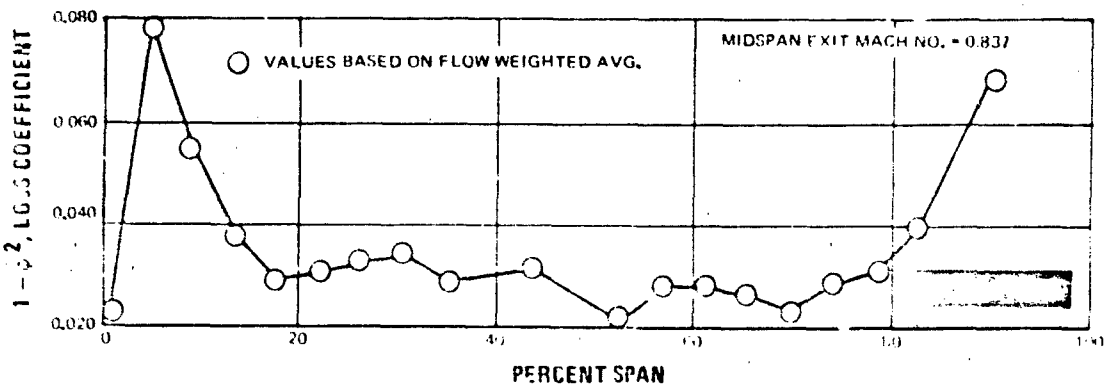

Figure 39 Spanwise Loss Coefficient Distribution, Second Vane – Screen Installed, Computed at Specified Intervals, Midspan Exit Mach No. = 0.837

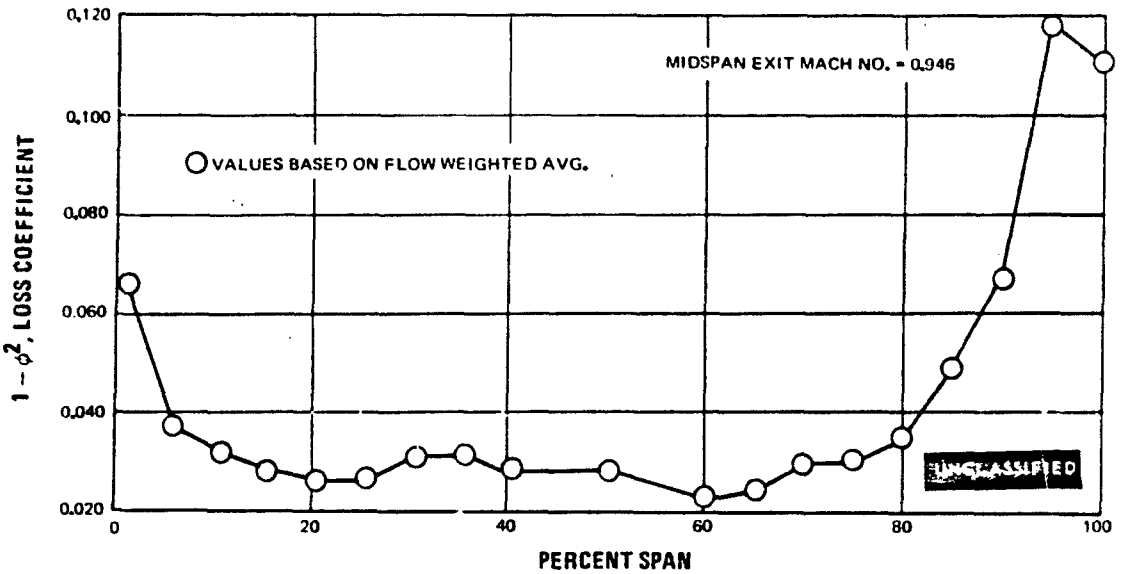

Figure 40 Spanwise Loss Coefficient Distribution, Second Blade – Screen Removed, Computed at Specified Intervals, Midspan Exit Mach No. = 0.946

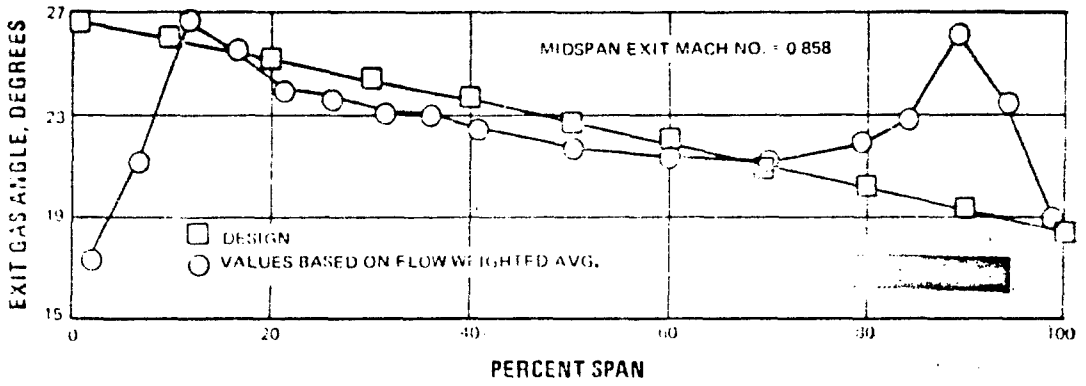

Figure 41 Spanwise Exit Gas Angle Distribution, First Vane – Screen Removed, Computed at Specified Intervals. Midspan Exit Mach No. = 0.858

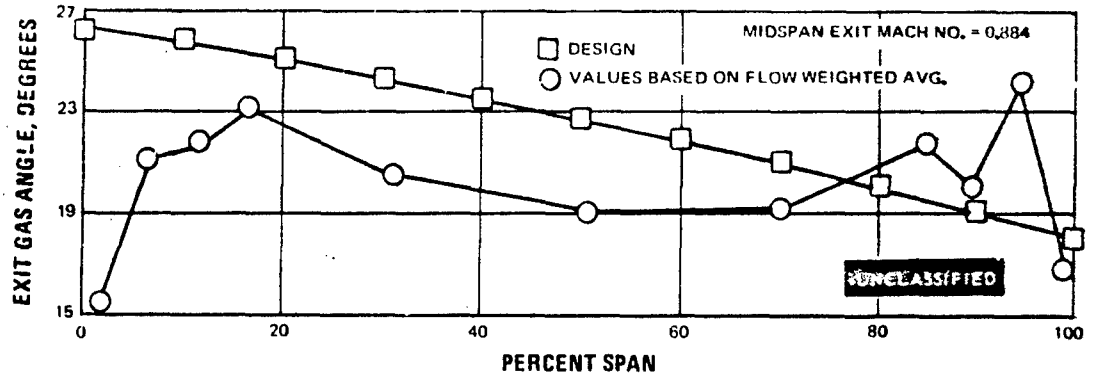

Figure 42 Spanwise Exit Gas Angle Distribution, First Vane Screen Installed, Computed at Specified Intervals. Midspan Exit Mach No. = 0.884

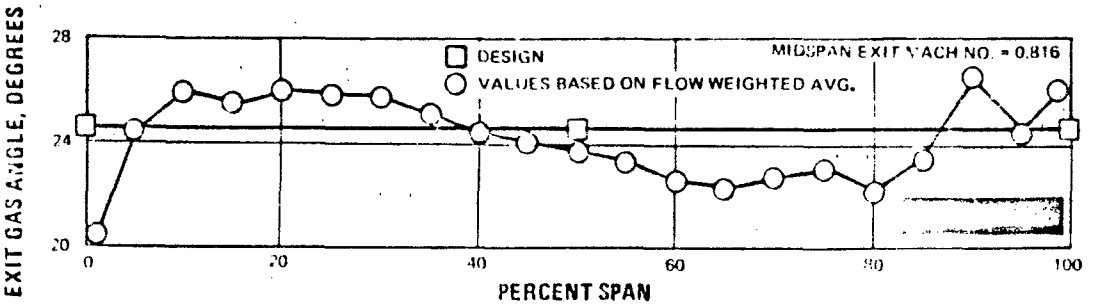

Figure 43 Spanwise Exit Gas Angle Distribution, First Blade – Screen Removed, Computed at Specified Intervals, Midspan Exit Mach No. = 0.816

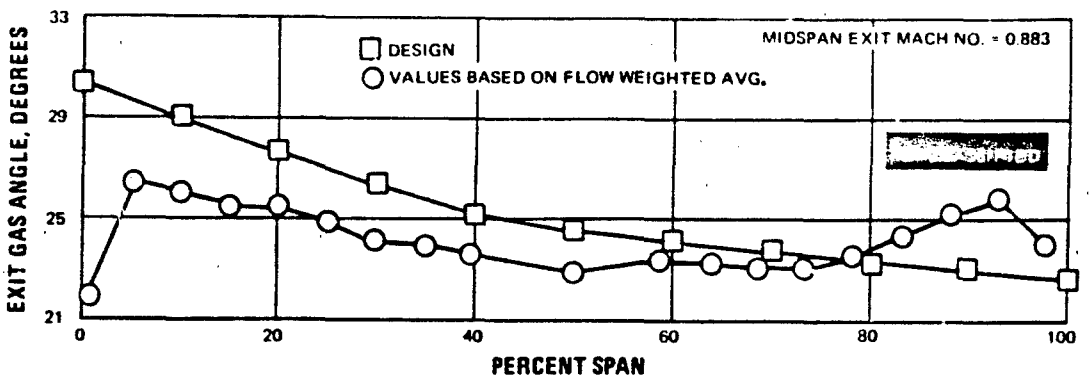

Figure 44 Spanwise Exit Gas Angle Distribution, Second Vane – Screen Removed, Computed at Specified Intervals, Midspan Exit Mach No. = 0.883

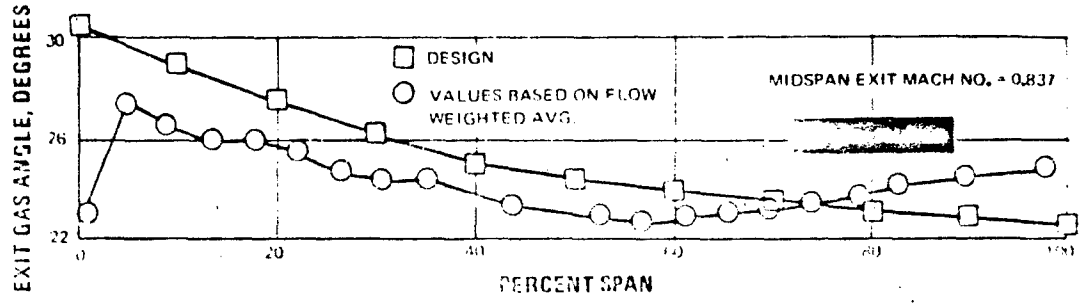

Figure 45 Spanwise Exit Gas Angle Distribution, Second Vane – Screen Installed, Computed at Specified Intervals, Midspan Exit Mach No. = 0.837

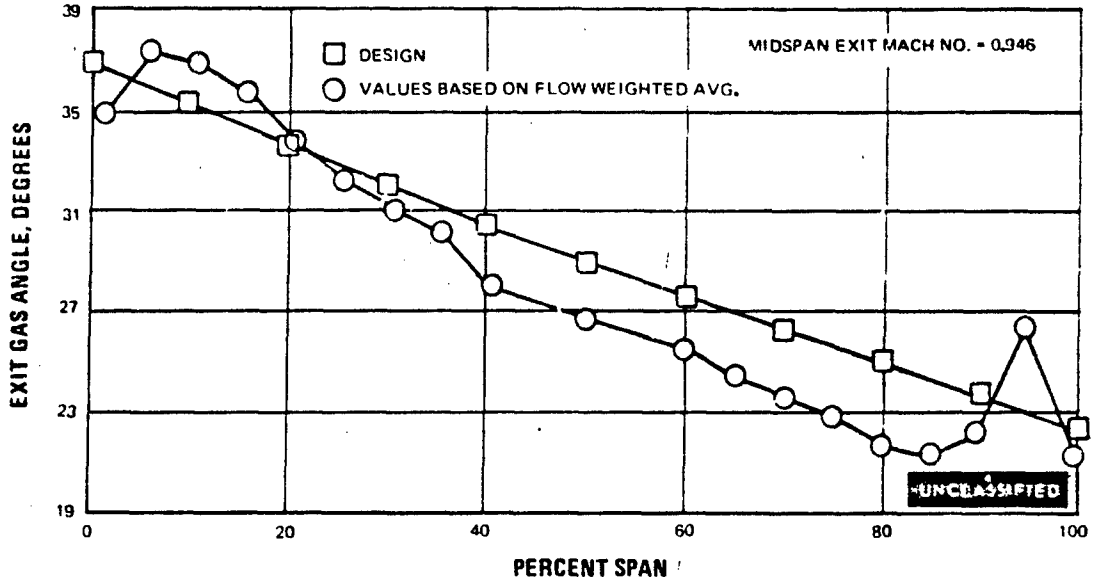

Figure 46 Spanwise Exit Gas Angle Distribution, Second Blade – Screen Removed, Computed at Specified Intervals, Midspan Exit Mach No. = 0.946

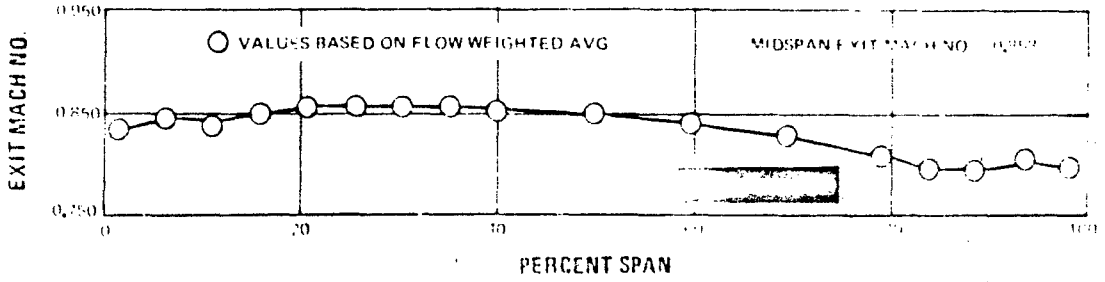

Figure 47 Spanwise Exit Mach Number Distribution, First Vane Screen Removed, Computed at Specified Intervals, Midspan Exit Mach No. = 0.858

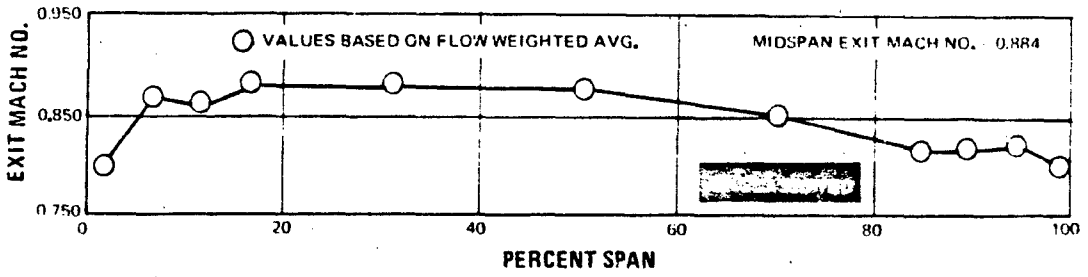

Figure 48 Spanwise Exit Mach Number Distribution, First Vane Screen Installed, Computed at Specified Intervals, Midspan Exit Mach No. = 0.884

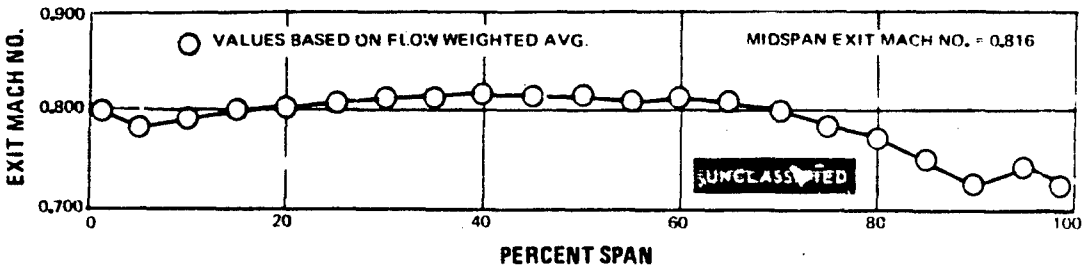

Figure 49 Spanwise Exit Mach Number Distribution, First Blade Screen Removed, Computed at Specified Intervals, Midspan Exit Mach No. = 0.816

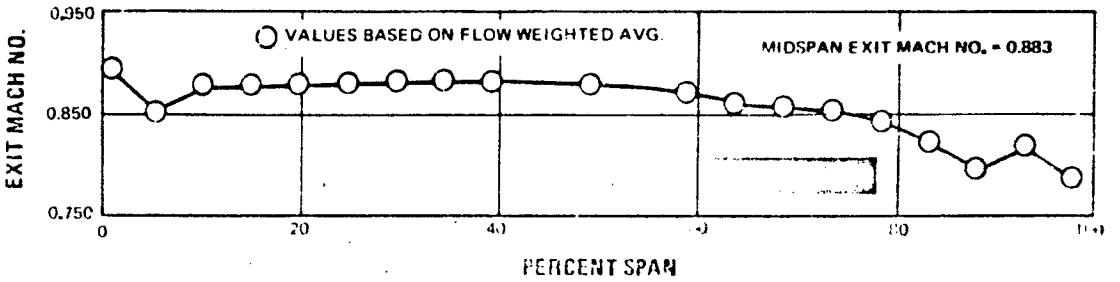

Figure 50 Spanwise Exit Mach Number Distribution, Second Vane Screen Removed, Computed at Specified Interals, Midspan Exit Mach No. = 0.883

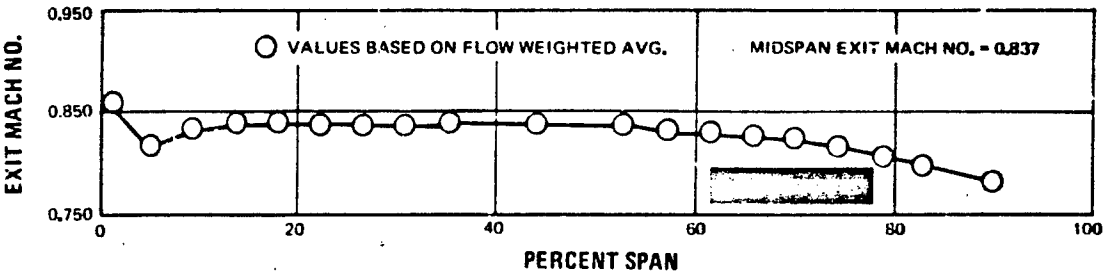

Figure 51 Spanwise Exit Mach Number Distribtuion, Second Vane Screen Installed, Computed at Specified Intervals, Midspan Exit Mach No. = 0.837

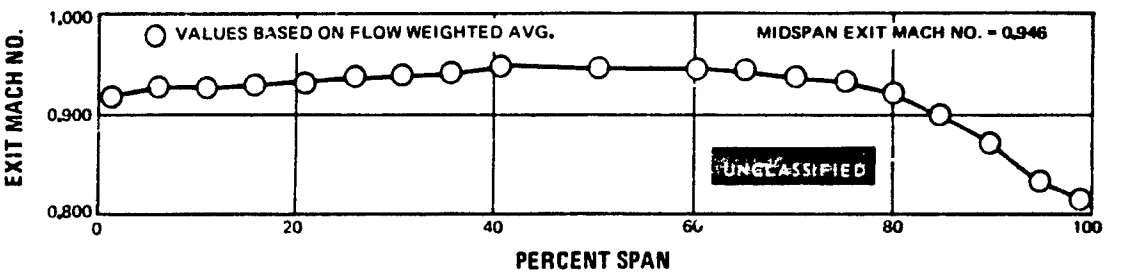

Figure 52 Spanwise Exit Mach Number Distribution, Second Blade Screen Removed, Computed at Specified Intervals, Midspan Exit Mach No. = 0.946

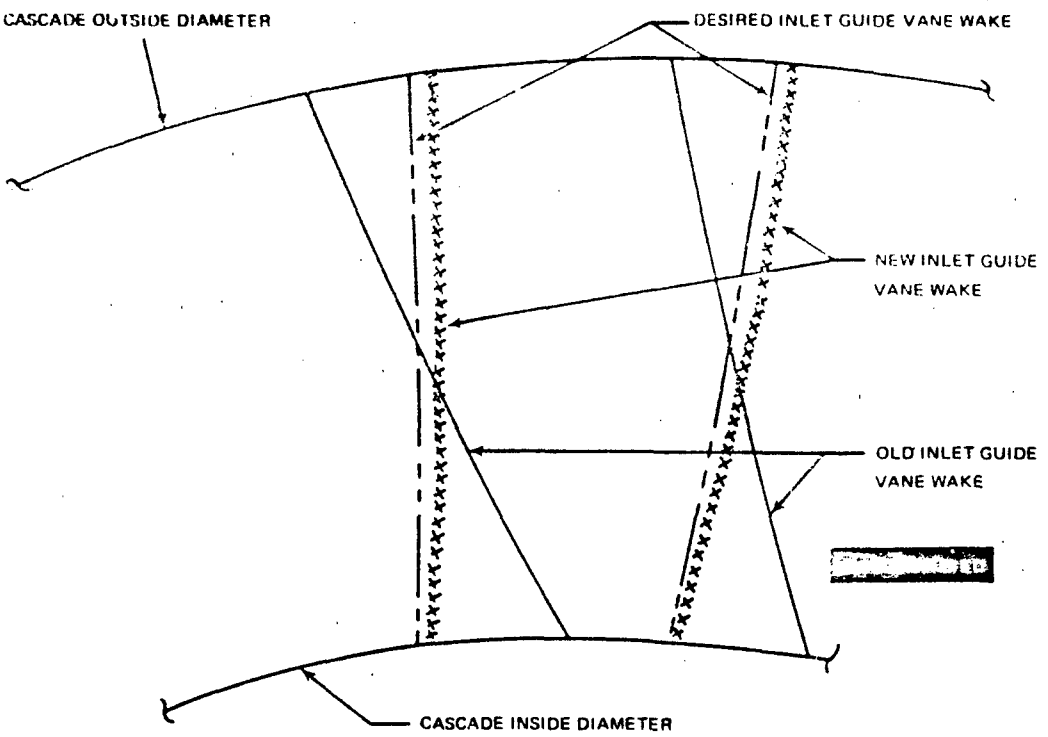

Figure 53 New Inlet Guide Vane Design, Second Stage Vane Cascade Plane at Leading Edges of Test Airfoil Looking Downstream

(U) The performance of a turbine depends directly on the sum of the total pressure losses through the machine. The measure of the total pressure drop through each turbine airfoil row is, therefore, the most useful indication of a successful turbine design. The loss coefficient ($1-\phi^2$), which is a monotonically increasing function of the total pressure loss, is also presented since it is widely used in industry as a measure of turbine efficiency.

(U) Contours of the total pressure loss for all of the tested airfoils indicate similar results. Low loss pockets are evident over the midspan areas with high loss regions in the suction surface corners. These losses probably originate at the end-wall but migrate from the pressure surface to the suction surface and

accumulate in the corners. Such a collection of end-wall losses in the channel passages at the inside and outside diameters is reflected in the plots of the average spanwise variations of the total pressure loss and loss coefficients. This is indicated by peak loss values in the 5-10% and 90-95% radial span regions, which obviously is a separate phenomenon at both the root and tip. The minimum losses occur at the midspan, which represent essentially the two dimensional airfoil profile drag only. There is no evidence of large boundary layer thicknesses at the cascade walls, since the accumulated waste at the end walls was swept into the cascade corners. There is also no evidence of flow separation in the pressure loss and loss coefficient data.

(U) A summary plot of the average spanwise loss variation for the four baseline airfoils is presented in Figure 54. This plot indicates very small differences in the behavior of these airfoils. The turbulence screen that was installed ahead of the first and second vane cascade does not appear to have significantly affected cascade losses. Figures 55 and 56 compare the change in spanwise distribution of the loss coefficient for both airfoils. Although there is some difference in Mach numbers at which the data were taken, there is very little difference in loss profiles. This difference in Mach number is not significant since, as shown in Figure 57, there was a very small effect of Mach number variation on loss for these airfoils. Any small variation may be attributed to the fact that, during the tests, the Reynolds number increased slightly with Mach number. Since airfoil losses decrease with increasing Reynolds number, some decrease in losses may be charged to this effect. It can also be concluded that none of the airfoils exhibited a transonic drag rise over the Mach number range tested.

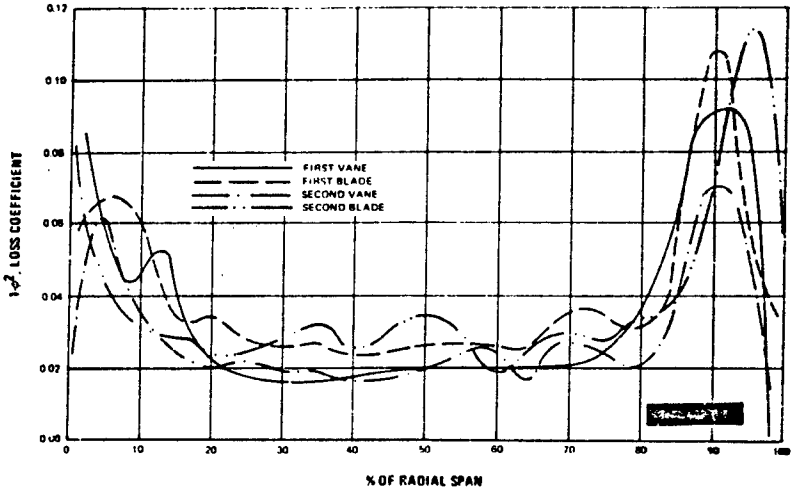

Figure 54 Loss Coefficient vs. Span – Baseline Airfoils

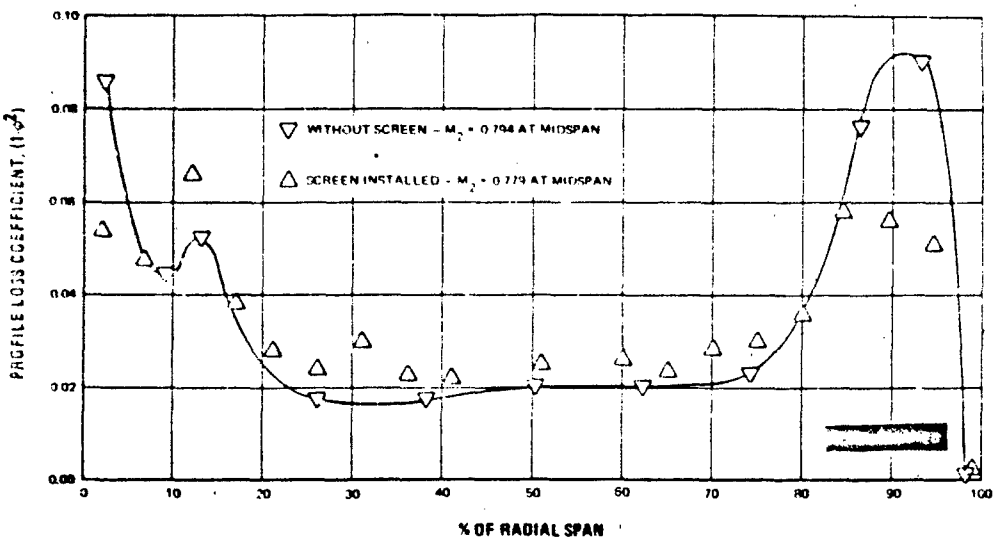

Figure 55 Effect of Turbulence Screen on First Vane Loss

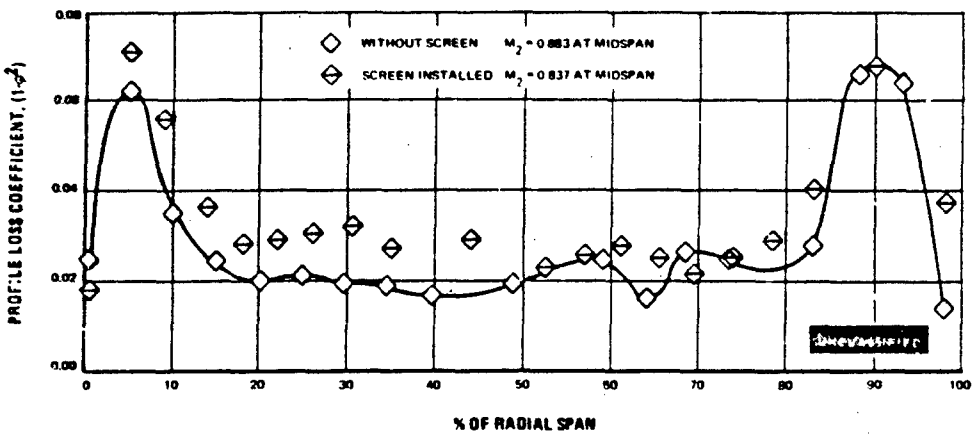

Figure 56 Effect of Turbulence Screen on Second Vane Loss

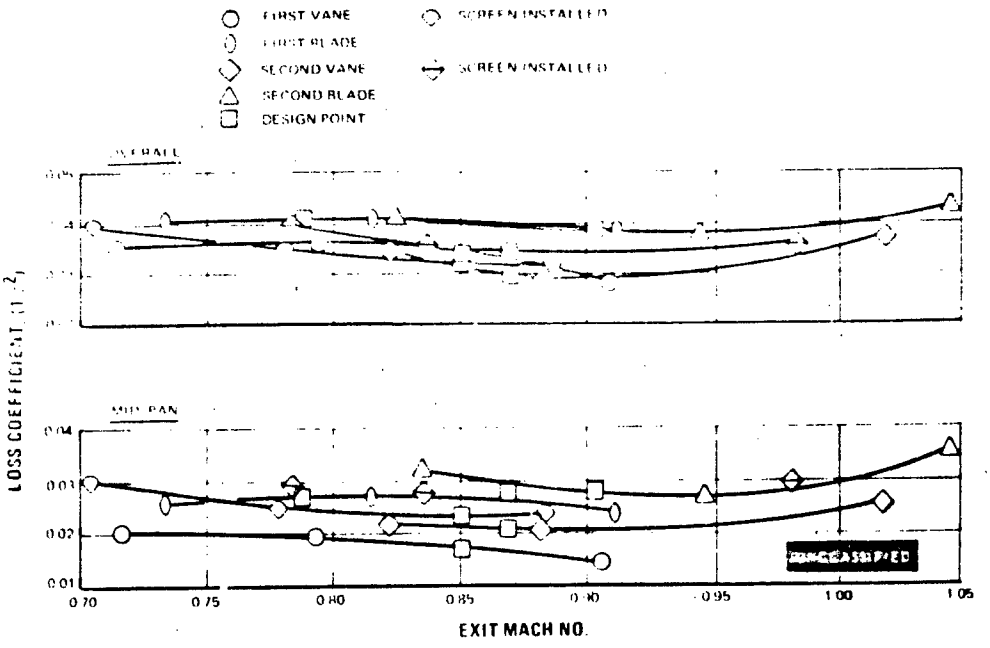

Figure 57 Effect of Mach Number on Loss

(U) A comparison of the predicted and measured loss coefficients is shown in Table III. Two prediction methods were used to determine midspan or profile losses. One method used the Ainley and Mathieson correlation based or global airfoil design parameters, as the amount of turning, gap-to-chord ratio, airfoil thickness, convergence ratio, etc. The other method was based on boundary layer parameters computed by the Airfoil Boundary Layer Deck. The airfoil surface static pressure and velocity distributions were calculated from predicted values. The overall predicted value was based on the global profile loss correlation with a correlated end loss value added. For all four airfoils, the midspan measured profile losses are well below the predicted values, indicating that the normal solidity airfoil profiles were well designed. The measured overall losses were also below predicted overall values, leading to the conclusion that the baseline design can meet the turbine design requirements.

TABLE III

MEASURED LOSS VS PREDICTED - BASELINE AIRFOILS

	Turbine Design Midspan Exit Mach. No.	Midspan			Overall	
		Test	Predicted Correlation	Predicted Boundary Layer	Test	Pred.
First Vane	0.854	0.017 0.023*	0.031	0.032	0.034 0.032*	0.049
First Blade	0.780	0.0266	0.036	0.049	0.040	0.054
Second Vane	0.869	0.021 0.028*	0.036	0.046	0.030 0.034*	0.050
Second Blade	0.904	0.028	0.030	0.044	0.038	0.042

UNCLASSIFIED

*With inlet turbulence screen

(U) The exit plane flow patterns were reconstructed and these results are presented as the exit gas flow angle contours over three flow passages, average spanwise exit gas flow angle and Mach number distributions at the nearest-to-design test conditions. The exit gas angle contours indicate close to design angles for the midspan portion of each airfoil, with some overturning at the roots and underturning at the tips. This is more clearly shown on the exit angle spanwise plots on which the design exit angles are also plotted. There was no evidence of flow separation. The turbulence screen that was installed ahead of the first and second vane cascades does not appear to have significantly affected the gas exit flow angles. A comparison of these angles, with and without screens, is shown in Figure 58.

(U) To provide additional clues as to the behavior of the flow in these cascades, a mixture of oil and graphite was painted on two airfoils (one on either side of the test airfoil) for each airfoil cascade test pack. Movies and still photographs were taken of the flow patterns at various test conditions. Selected photographs for each test pack are shown in Figures 59 through 70. The location of the surface static pressure taps are also shown on these photographs.

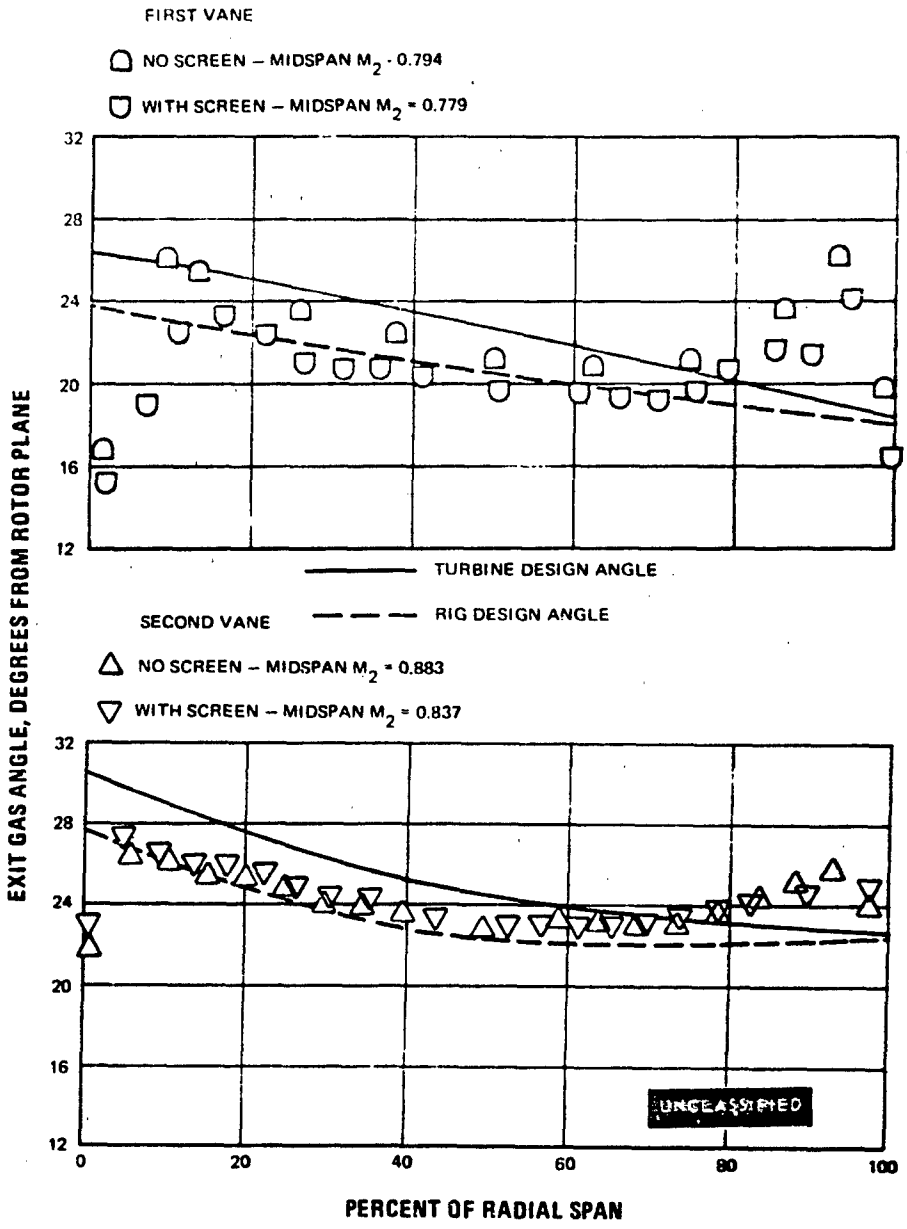

Figure 58 Effect of Turbulence Screen on Exit Gas Angle

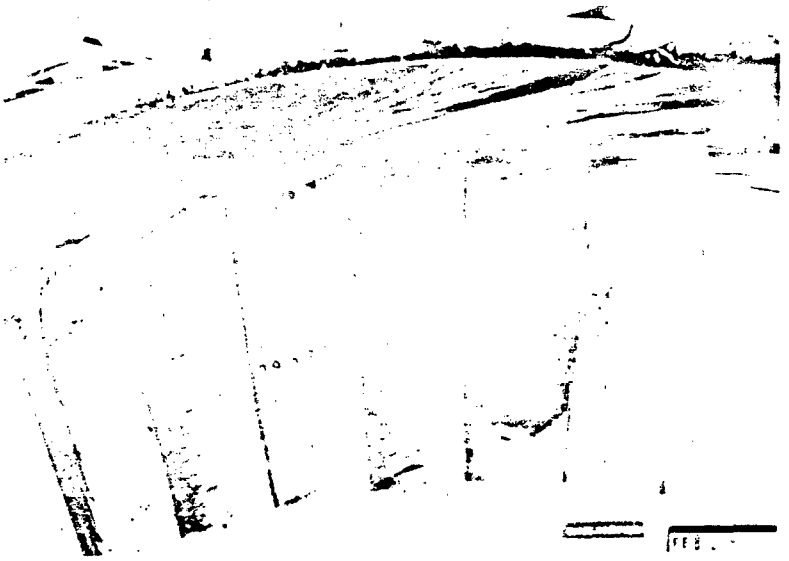

Figure 59 Oil and Graphite Flow Patterns, Airfoil Static Taps Circled, First Vane, Mach No. = 0.85, Screen Removed

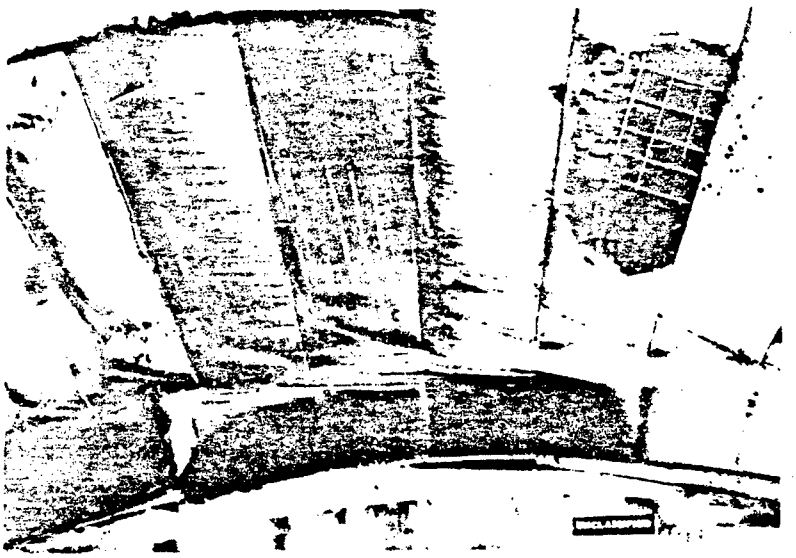

Figure 60 Oil and Graphite Flow Patterns, Airfoil Static Taps Circled, First Vane, Mach No. = 0.85, Screen Removed

Figure 61 Oil and Graphite Flow Patterns, Airfoil Static Taps Circled, First Vane, Mach No. = 0.85, Screen Installed

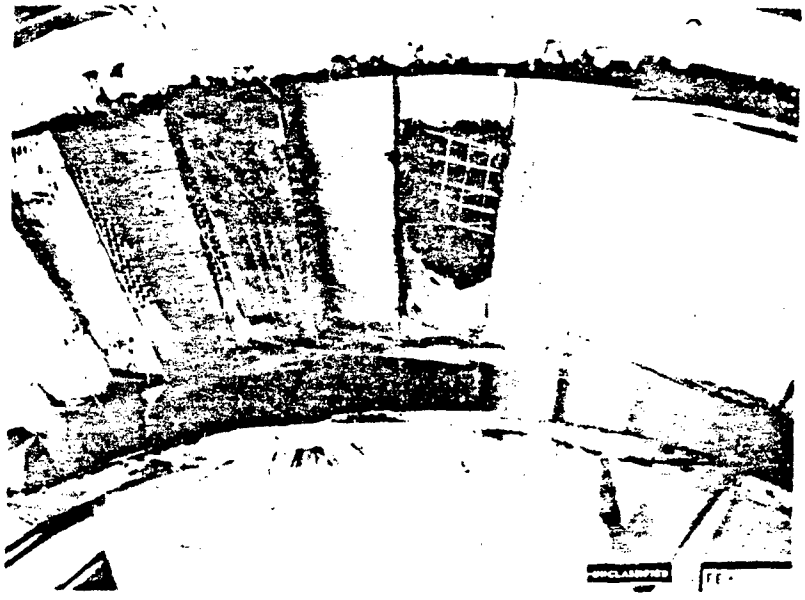

Figure 62 Oil and Graphite Flow Patterns, Airfoil Static Taps Circled, First Vane, Mach No. = 0.85, Screen Installed

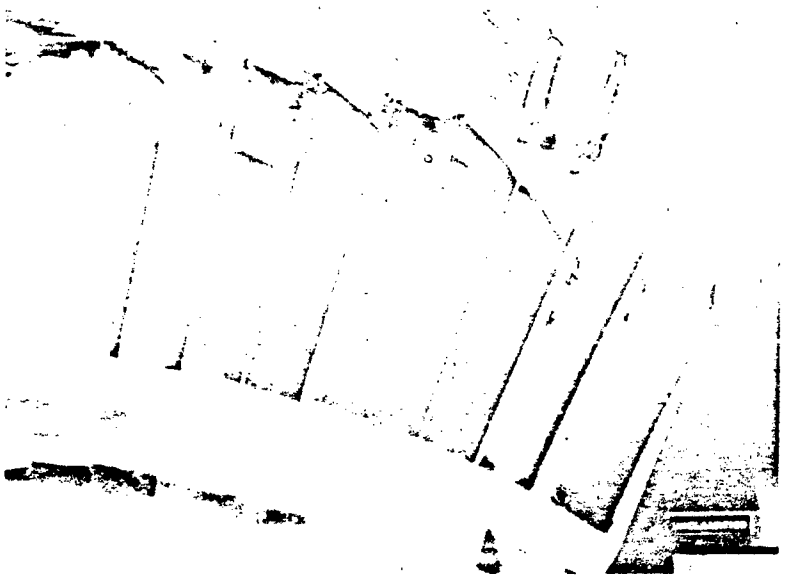

Figure 63 Oil and Graphite Flow Patterns, Airfoil Static Taps Circled, First Blade, Mach No. = 0.79

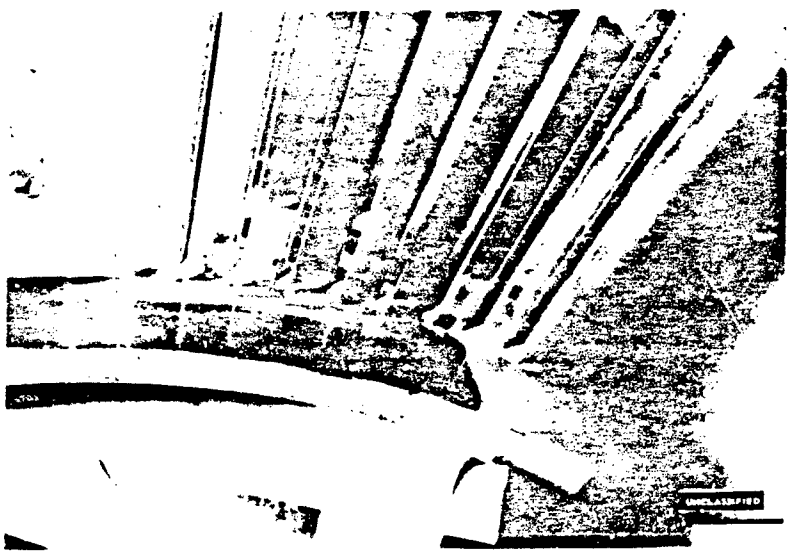

Figure 64 Oil and Graphite Flow Patterns, Airfoil Static Taps Circled, First Blade, Mach No. = 0.79

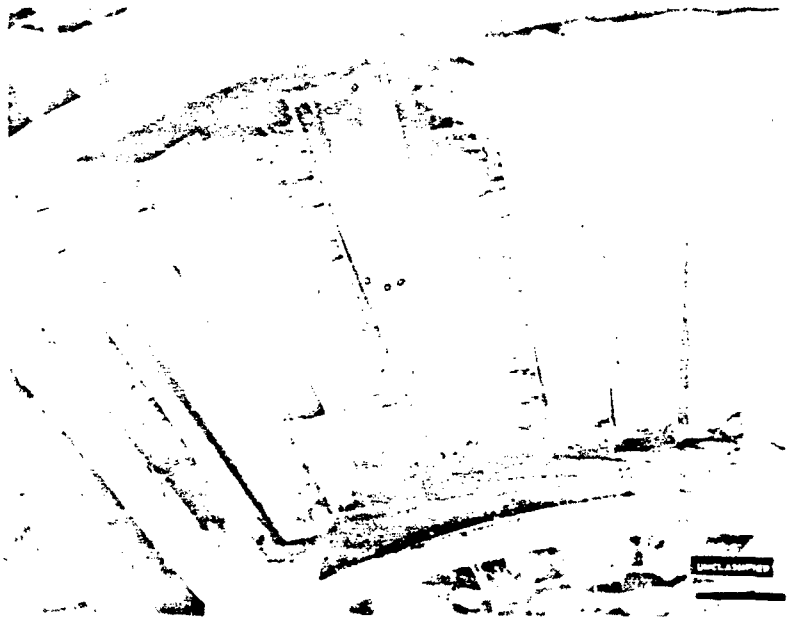

Figure 65 Oil and Graphite Flow Patterns, Airfoil Static Taps Circled, Second Vane, Mach No. = 0.87, Screen Removed

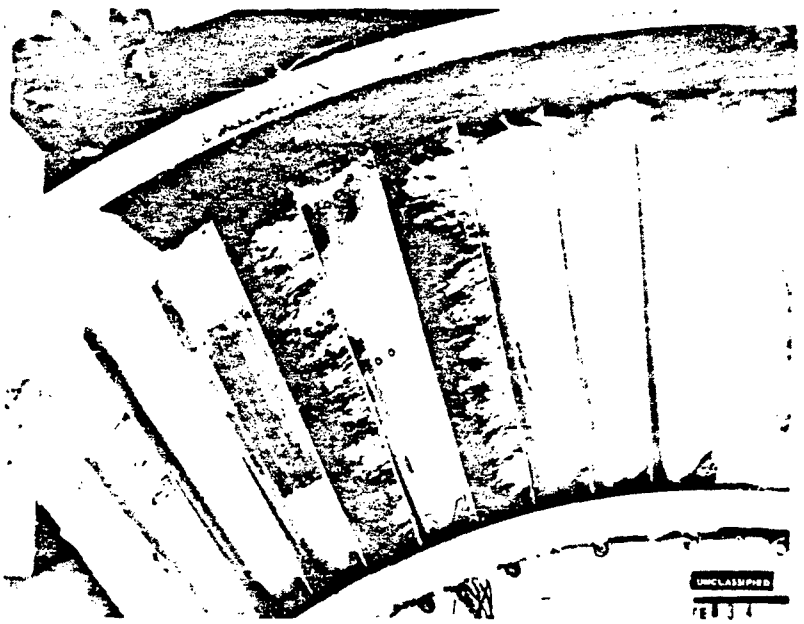

Figure 66 Oil and Graphite Flow Patterns, Airfoil Static Taps Circled, Second Vane, Mach No. = 0.87, Screen Removed

Figure 67 Oil and Graphite Flow Patterns, Airfoil Static Taps Circled, Second Vane, Mach No. = 0.87, Screen Installed

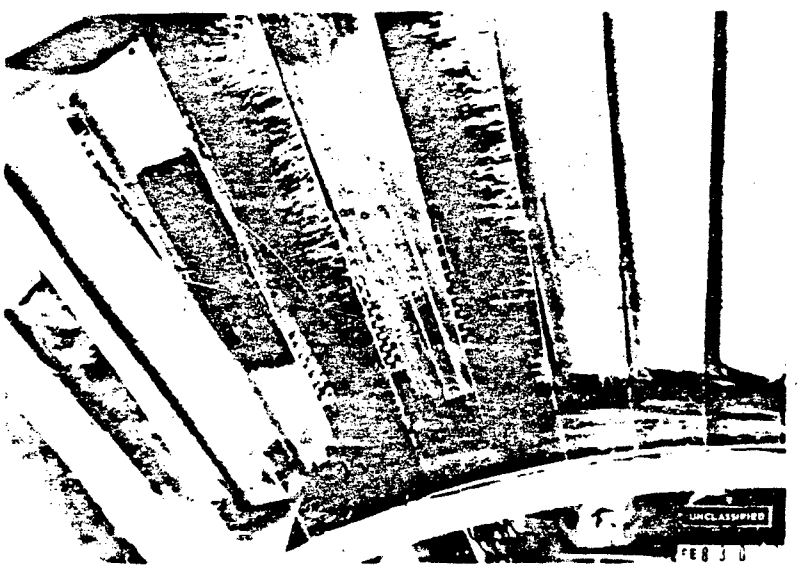

Figure 68 Oil and Graphite Flow Patters, Airfoil Static Taps Circled, Second Vane, Mach No. = 0.87, Screen Installed

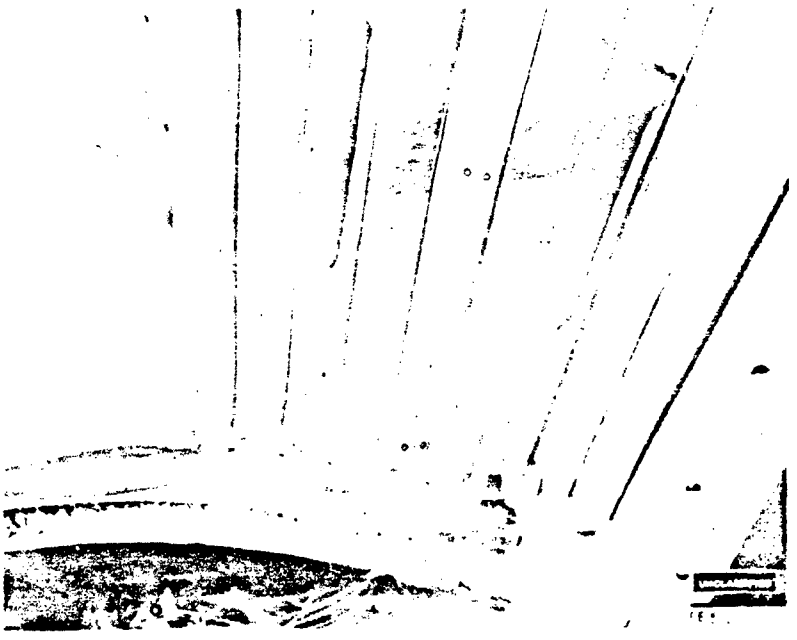

Figure 69 Oil and Graphite Flow Patterns. Airfoil Static Taps Circled. Second Blade, Mach No. = 0.90

Figure 70 Oil and Graphite Flow Patterns. Airfoil Static Taps Circled. Second Blade, Mach. No. = 0.90

(U) The patterns indicate that the corner flow remains attached, although the end-wall losses are high. Studies of the movies indicate that separation and reattachment of the airfoil suction surface boundary layer frequently occurs to some extent in all of the cascades, caused by shocks on portions of the airfoil surface where local supersonic flow exists. It is slight on the first vane but indicates a significant separated strip on the first blade over approximately 70% of the span. The losses for these airfoils, even with local separation and reattachment, were low, as previously indicated. Strong cross-flow patterns can be observed from these photographs at the walls but no separation on these walls in the vicinity of the airfoils was detected. The first vane and first blade inside diameter wall extensions have a slight axisymmetric separation. (The cause of this effect will be explained later.) This resulted in the elimination of these cascades from being chosen for the Task IIc effort. It can also be noted on these figures that the airfoil surface static taps are well within the corner vortex. Furthermore, comparisons of the photographs taken with and without the turbulence screens for the two vane packs indicated only slight differences in local airfoil surface separation patterns.

(U) Since the annular segment cascade does not perfectly reproduce the exit conditions that the airfoils would have in the complete turbine, we cannot expect that the resulting flow patterns will exactly duplicate what would be found in the rotating machine. Nonetheless, the important systematic differences in the flow patterns caused by slight experimental imperfections can be readily understood and identified. Correct interpretation of the data becomes possible when the systematic differences are anticipated and are not attributed to the cascade airfoils. It should be noted in advance that it is possible to conclude that the annular segment cascade actually provided a very realistic environment for the aerodynamic tests, and that the experimental data is very consistent and reliable.

(U) Figure 71 is a sketch which indicates the important features of the Task IIb cascade. The fundamental difference between the annular segment cascade and rotating rig is that finite extension of the inside and outside diameter walls tends to make the exit plane static pressure uniform and atmospheric, rather than reproducing the radially increasing static pressure of the axisymmetric rotating flow. The allowable extension of the inside and outside diameter walls is determined by the length of a practical cantilevered measuring probe. Since the cascade flow field is almost entirely subsonic, the effect of the altered exit plane static pressure distribution can be far-reaching, even though it is not especially strong. The following discussion focuses on the two dimensional effects of these changes.

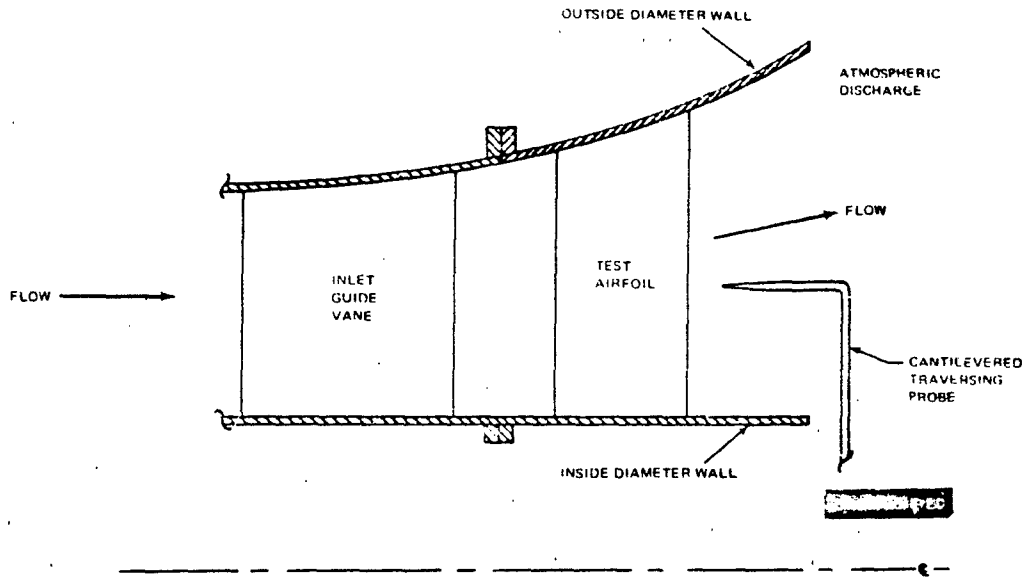

Figure 71 Annular Segment Cascade – Flowpath Cross-Section

(U) The altered, more uniform exit-plane static pressure distribution is clearly seen in Figure 72, which contains theoretical and measured spanwise distributions of circumferentially area-averaged static pressures. The same trend is also evident in a similar exit-plane Mach number distribution, shown in Figure 73. The gentle droop of the measured Mach number near the inside and outside diameter walls is due to the lower total pressures there, which are caused by end losses. The turbine design procedure distributes end losses uniformly across the airfoil span and does not, therefore, exhibit such inside and outside diameter droops.

(U) There are two direct and observable consequences of the exit-plane effect. First, the airfoil roots are slightly less loaded and the airfoil tips are slightly more loaded than the complete turbine required. However, the differences between the desired loading and the measured loading never exceed a few percent at any spanwise location. Furthermore, the measured loading in the midspan region was almost identical to the desired value for all airfoil cascades. Consequently, the experiments provided a suitable test for each section of each airfoil. Second, the inside diameter wall boundary layer must overcome a static pressure increase in order to reach atmospheric pressure and can, therefore, possibly separate. Such separation can be clearly seen in Figures 60 and 64. Since the cascades were designed with this possibility in mind, the separation always occurred downstream of the measuring probe. The outside diameter boundary is subject to a favorable pressure gradient and always remained attached. Once again, it is unlikely that this effect had an important influence on aerodynamic performance.

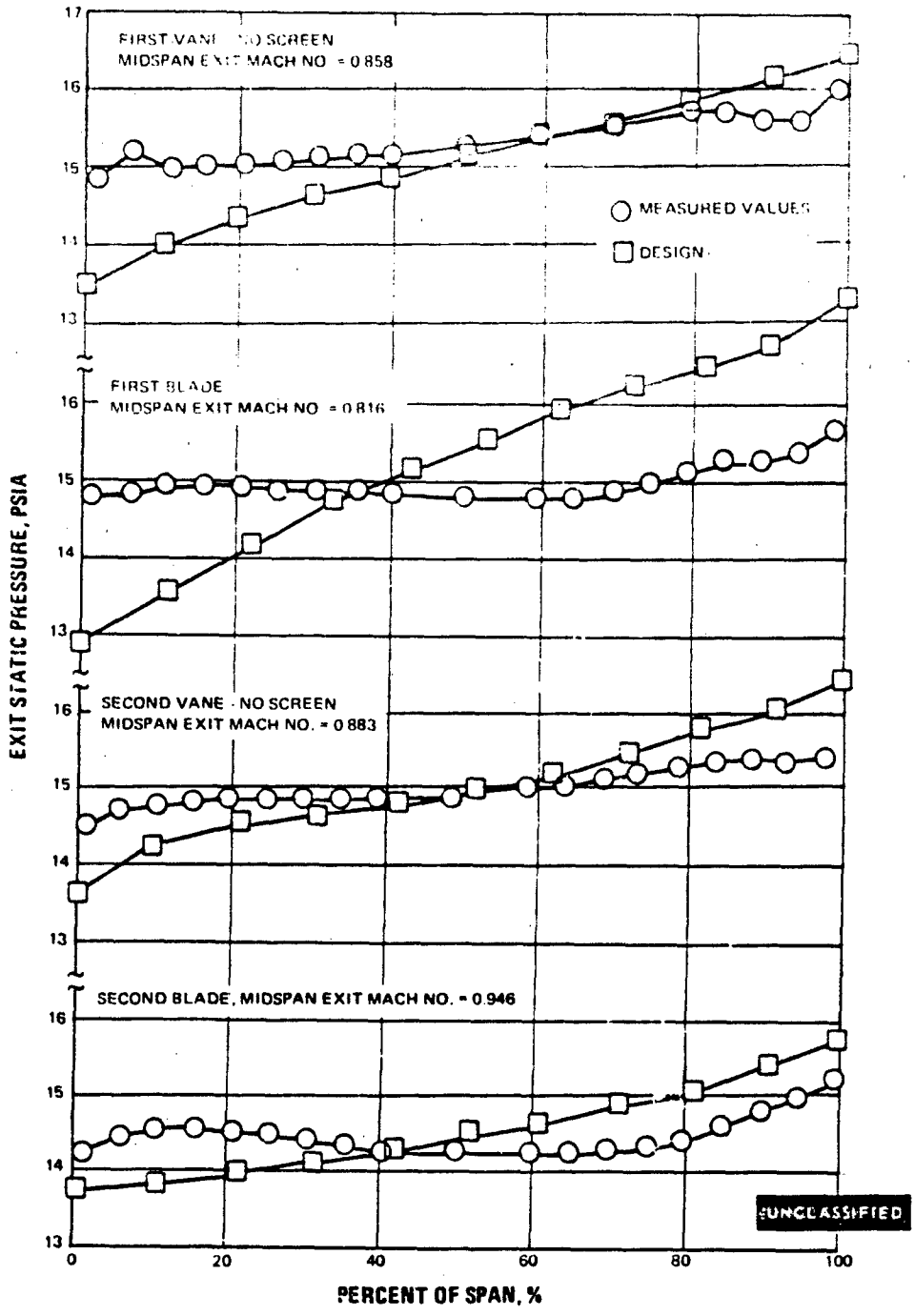

Figure 72 Comparison of Measured and Theoretical Radial Exit Static Pressure Variations

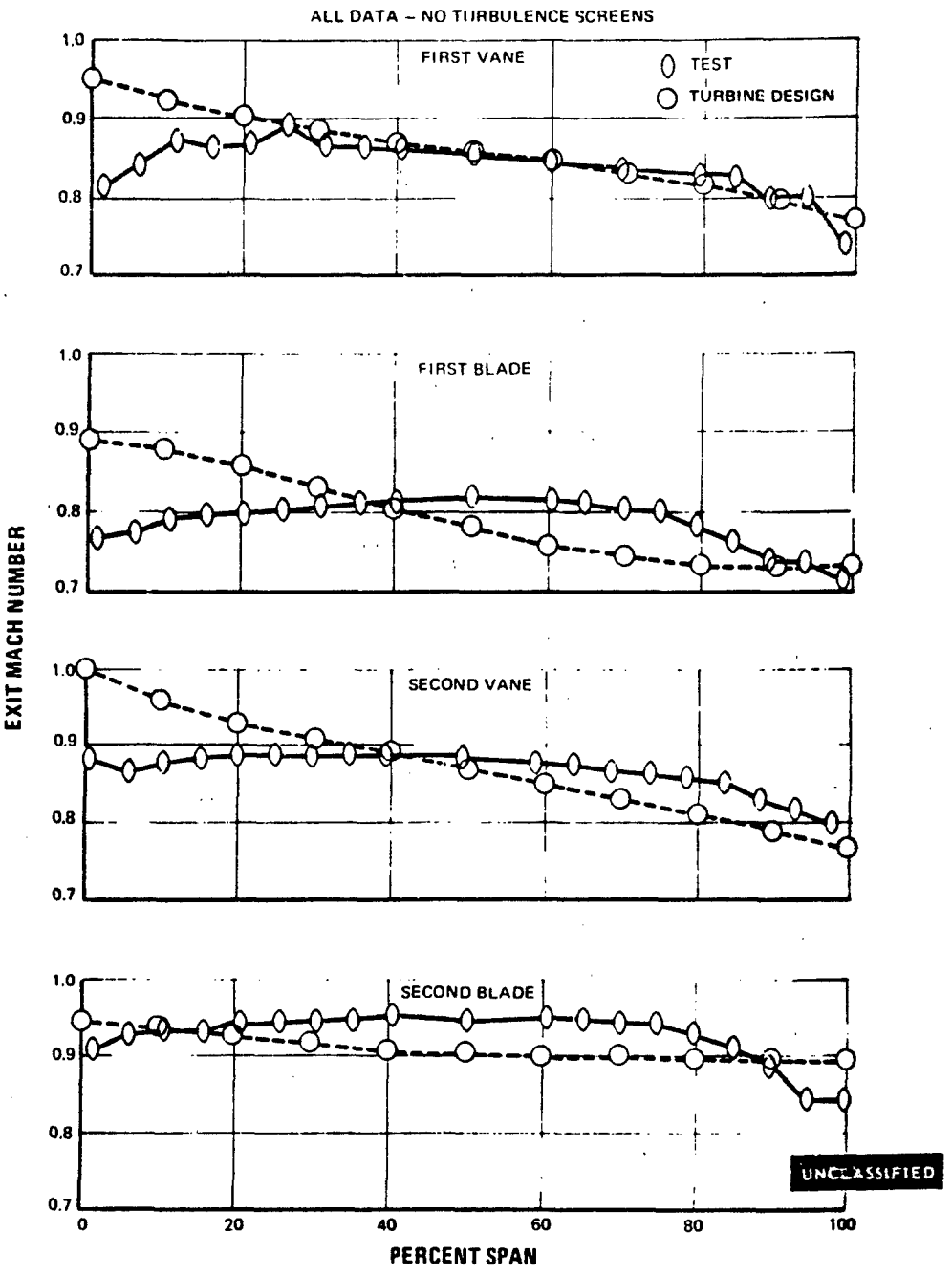

Figure 73 Spanwise Variation of Exit Mach Number

(U) The previously discussed inability of the annular segment cascade to exactly reproduce the desired exit-plane condition for the airfoils must also be reflected in the airfoil pressure distributions. The pressure distributions are shown for the four airfoils in Figures 74 through 91. This is so because the area enclosed by the pressure-axial distance curve equals the airfoil section loading, which has already been shown to be affected by altering the static pressure spanwise distribution.

(U) Since the midspan loading was found to be almost identical to the design value, it is not surprising to find that the static pressure distribution at all midspan sections was almost identical to the prediction. The previous discussion indicated that the root loading would tend to be reduced, and the tip loading increased in the annular segment cascade. No separation is evident from the airfoil surface pressure distributions and this verifies the pressure distribution design technique.

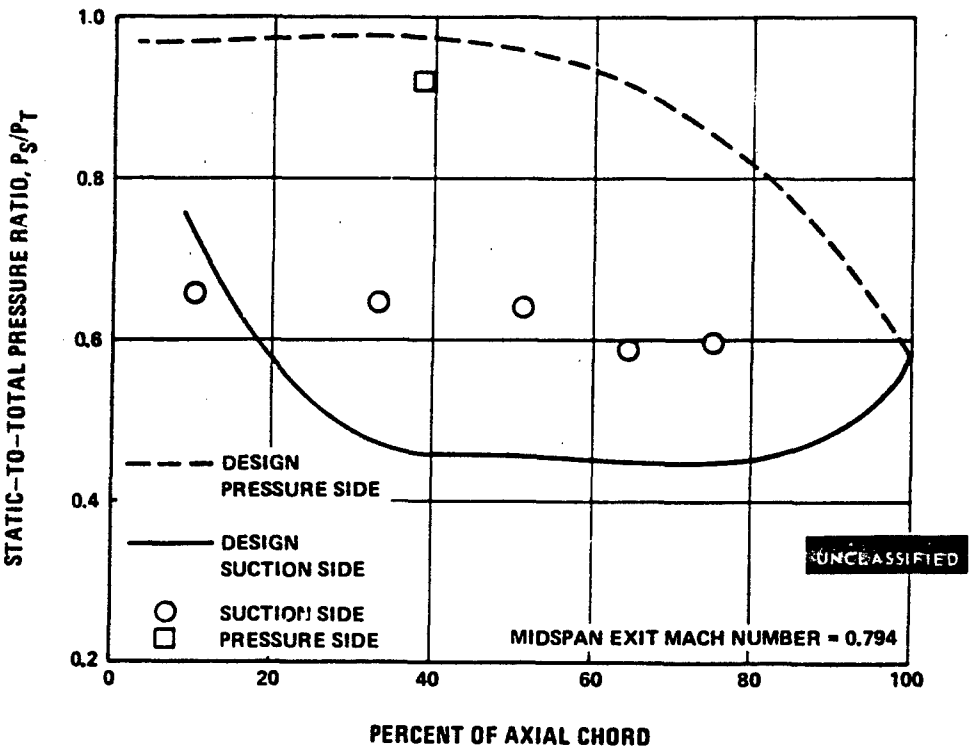

Figure 74 Static-to-Total Pressure Ratio vs. Percent of Axial Chord, First Vane Cascade – Root Section, Inlet Screen Removed

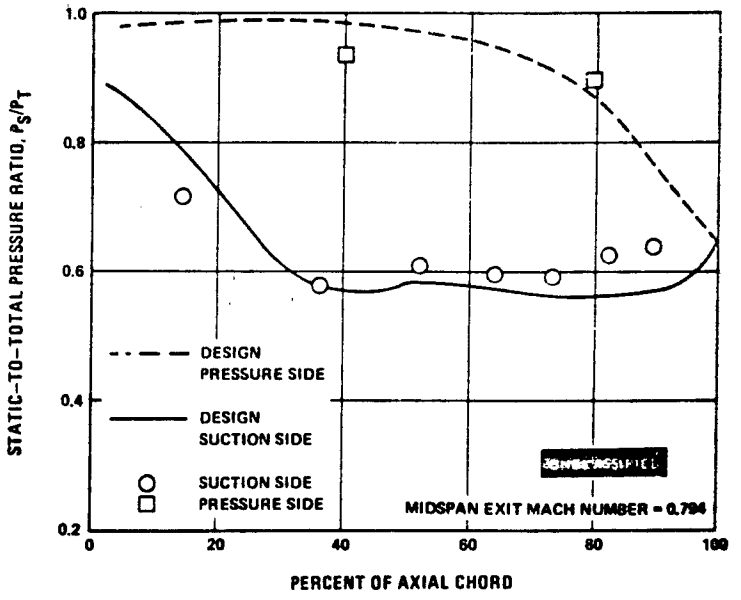

Figure 75 Static-to-Total Pressure Ratio vs. Percent of Axial Chord, First Vane Cascade – Mean Section, Inlet Screen Removed

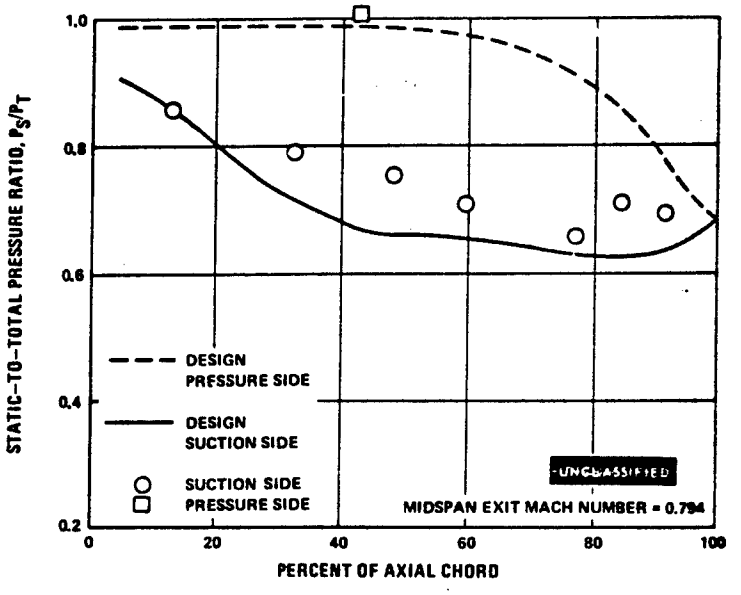

Figure 76 Static-to-Total Pressure Ratio vs. Percent of Axial Chord, First Vane Cascade – Tip Section, Inlet Screen Removed

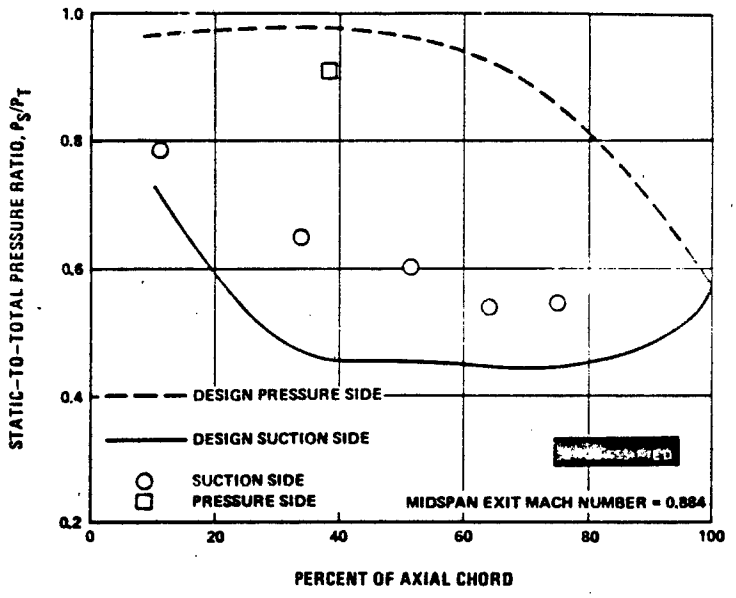

Figure 77 Static-to-Total Pressure Ratio vs. Percent of Axial Chord, First Vane Cascade – Root Section, Inlet Screen Installed

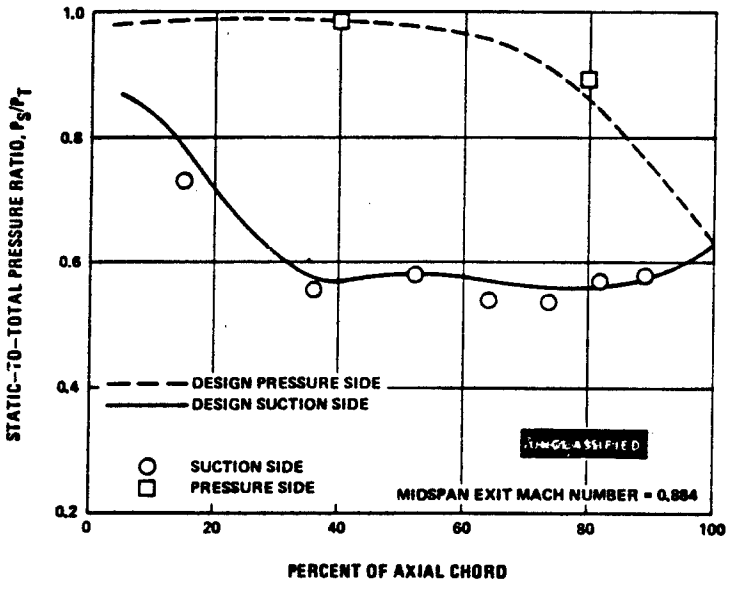

Figure 78 Static-to-Total Pressure Ratio vs. Percent of Axial Chord, First Vane Cascade – Mean Section, Inlet Screen Installed

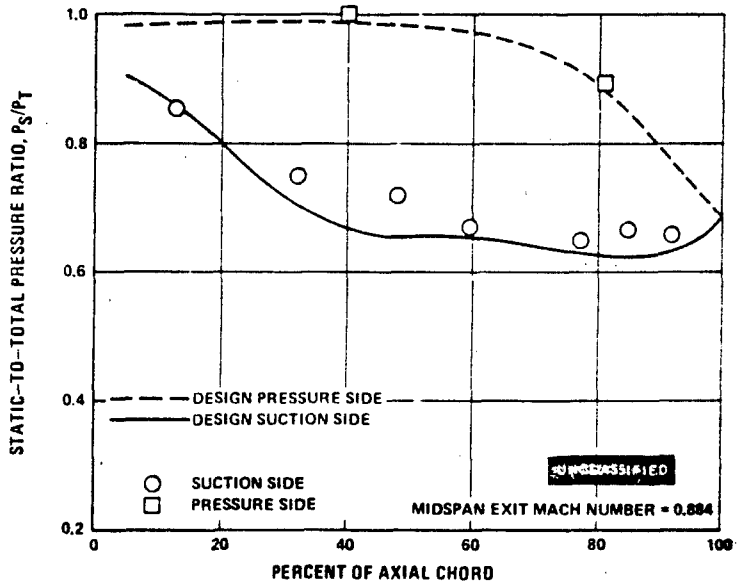

Figure 79 Static-to-Total Pressure Ratio vs. Percent of Axial Chord, First Vane Cascade – Tip Section, Inlet Screen Installed

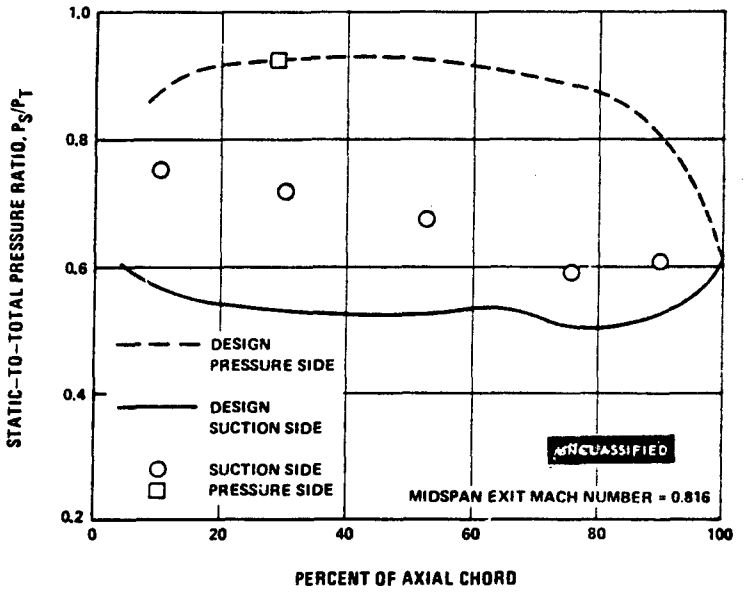

Figure 80 Static-to-Total Pressure Ratio vs. Percent of Axial Chord, First Blade Cascade -- Root Section

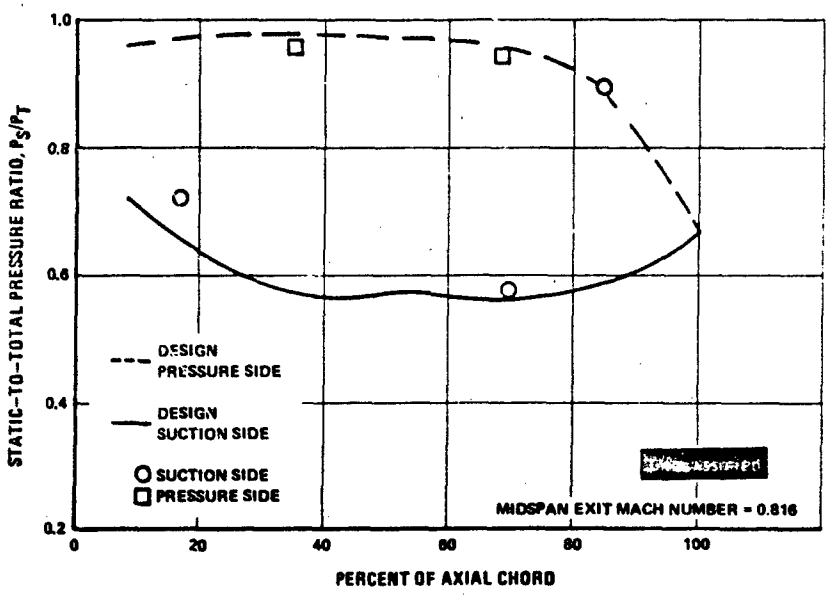

Figure 81 Static-to-Total Pressure Ratio vs. Percent of Axial Chord, First Blade Cascade – Mean Section

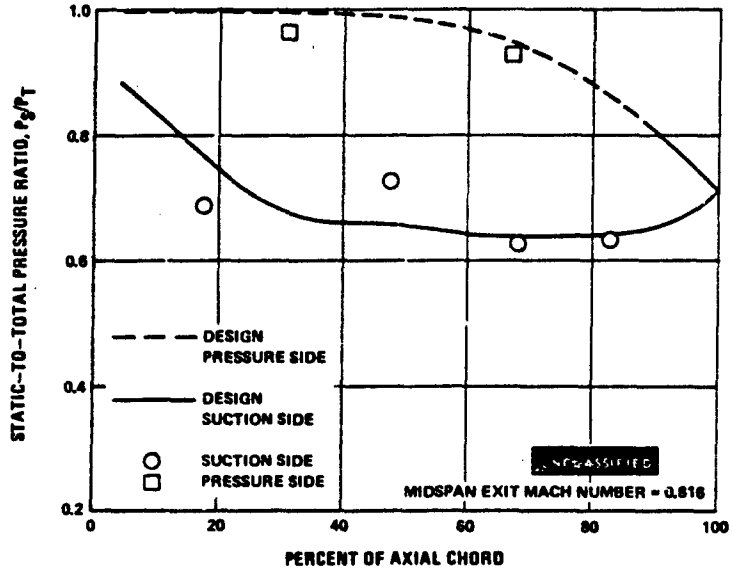

Figure 82 Static-to-Total Pressure Ratio vs. Percent of Axial Chord, First Blade Cascade – Tip Section

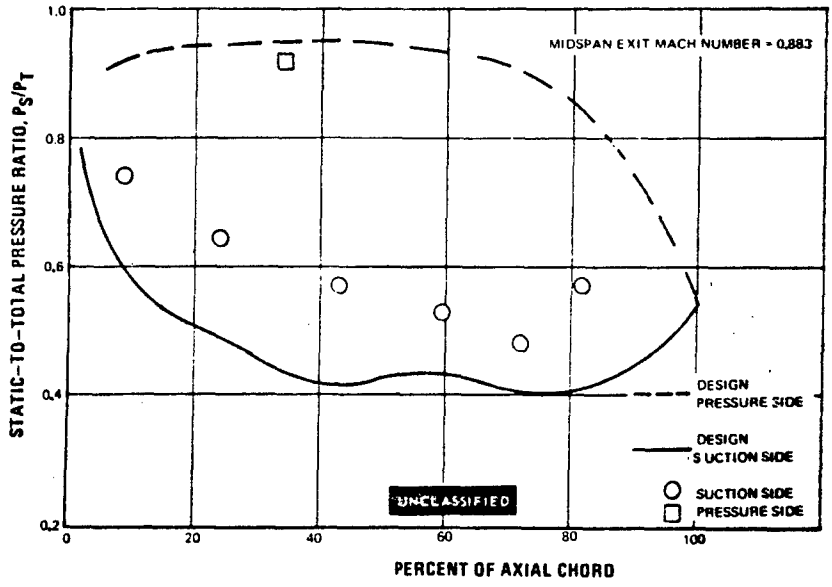

Figure 83 Static-to-Total Pressure Ratio vs. Percent of Axial Chord, Second Vane Cascade - Root Section, Inlet Screen Removed

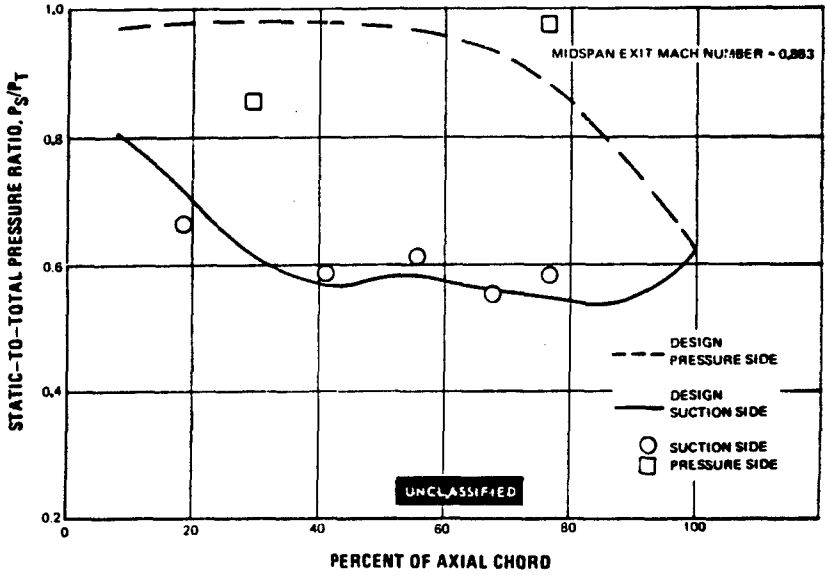

Figure 84 Static-to-Total Pressure Ratio vs. Percent of Axial Chord, Second Vane Cascade - Mean Section, Inlet Screen Removed

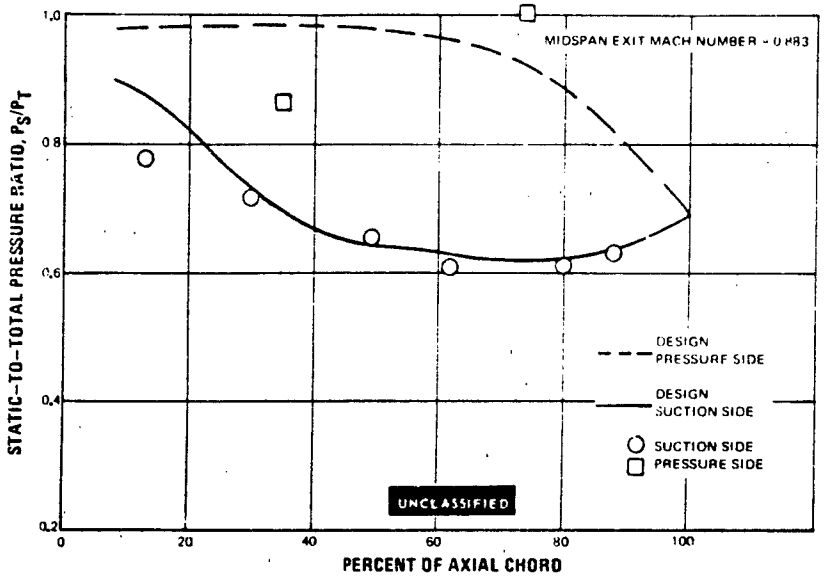

Figure 85 Static-to-Total Pressure Ratio vs. Percent of Axial Chord, Second Vane Cascade - Tip Section, Inlet Screen Removed

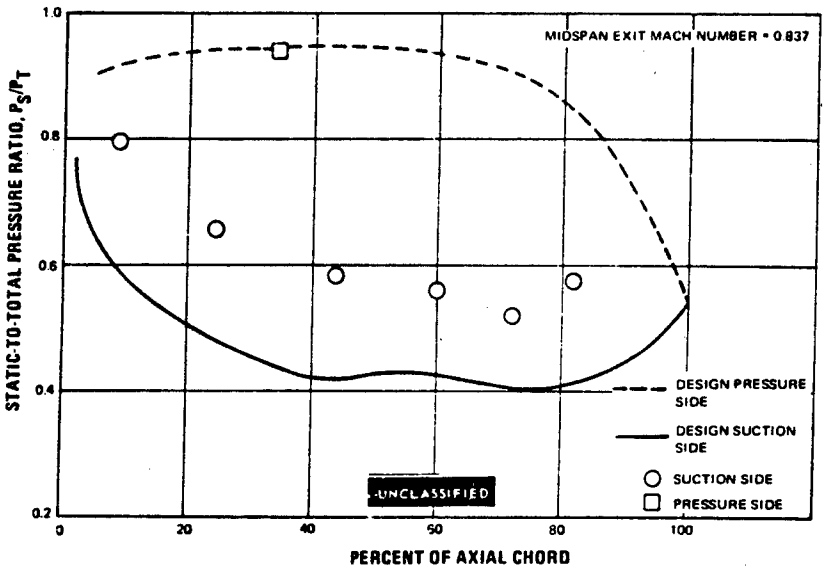

Figure 86 Static-to-Total Pressure Ratio vs. Percent of Axial Chord, Second Vane Cascade - Root Section, Inlet Screen Installed

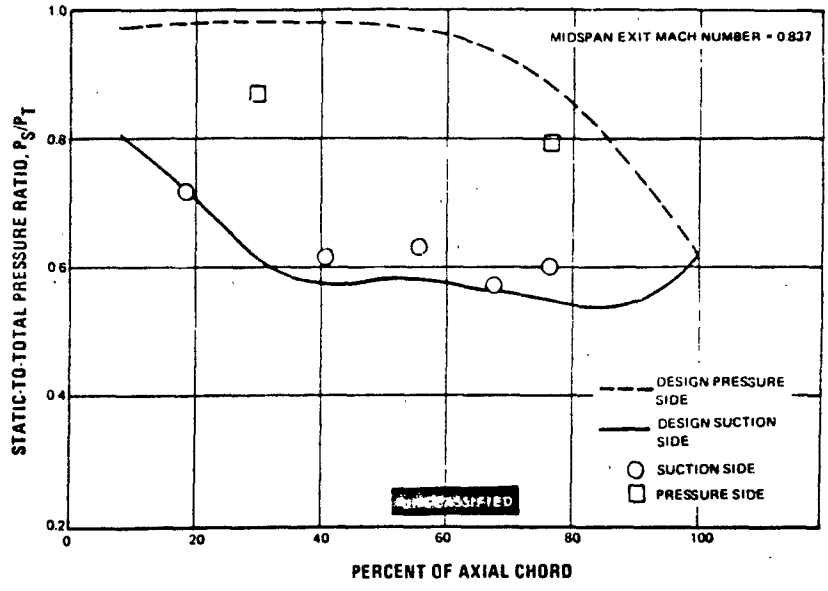

Figure 87 Static-to-Total Pressure Ratio vs. Percent of Axial Chord, Second Vane Cascade – Mean Section, Inlet Screen Installed

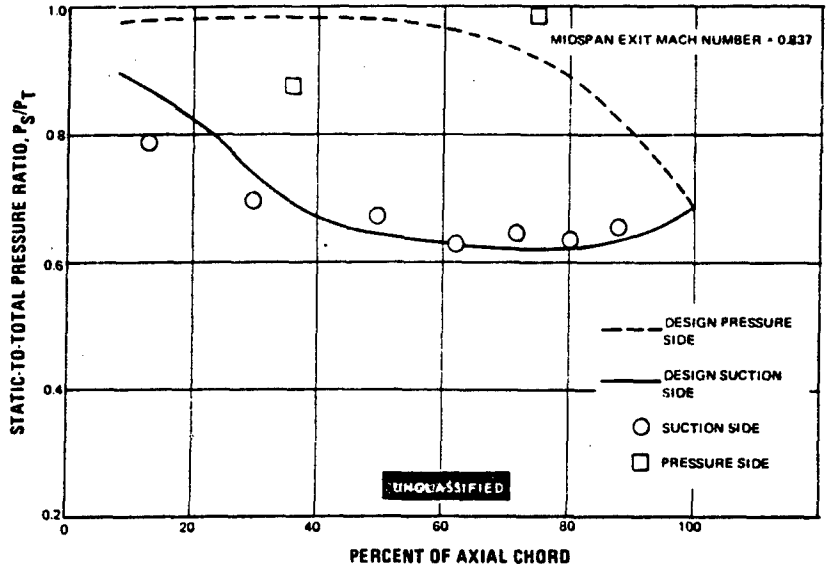

Figure 88 Static-to-Total Pressure Ratio vs. Percent of Axial Chord, Second Vane Cascade – Tip Section, Inlet Screen Installed

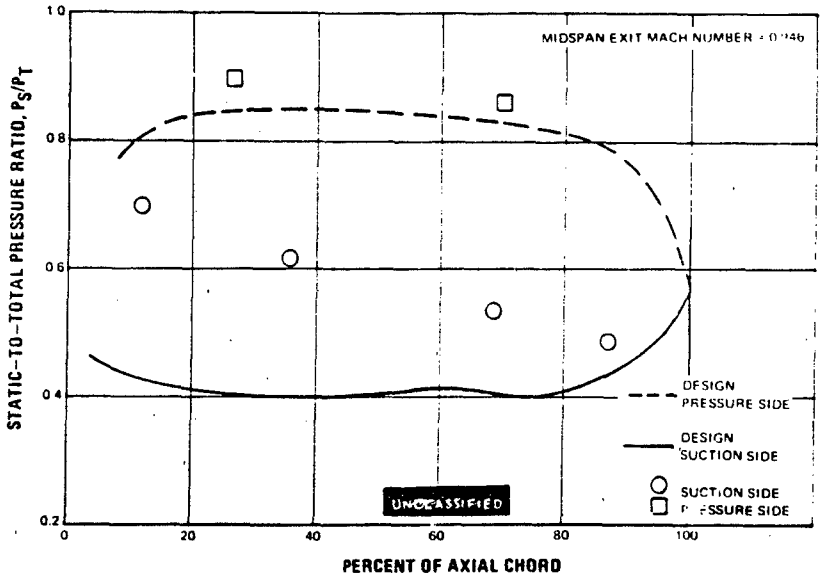

Figure 89 Static-to-Total Pressure Ratio vs. Percent of Axial Chord, Second Blade Cascade Root Section

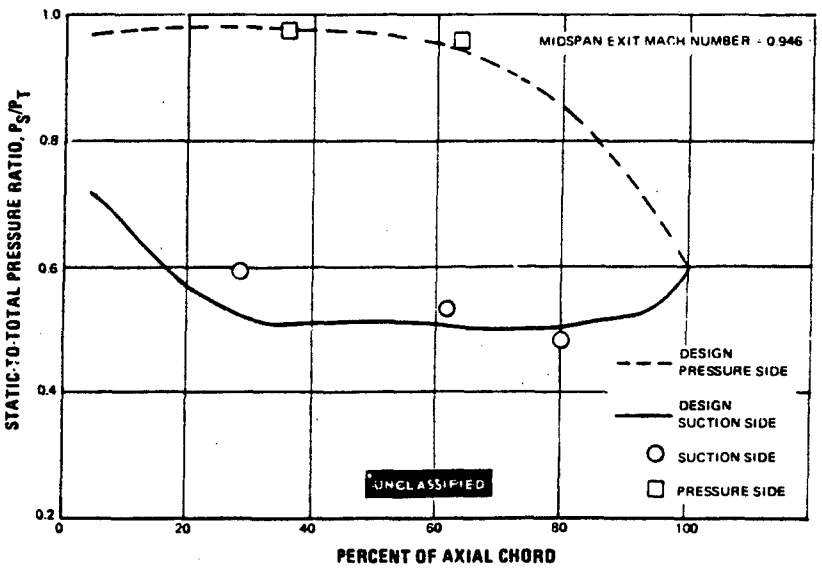

Figure 90 Static-to-Total Pressure Ratio vs. Percent of Axial Chord, Second Blade Cascade Mean Section

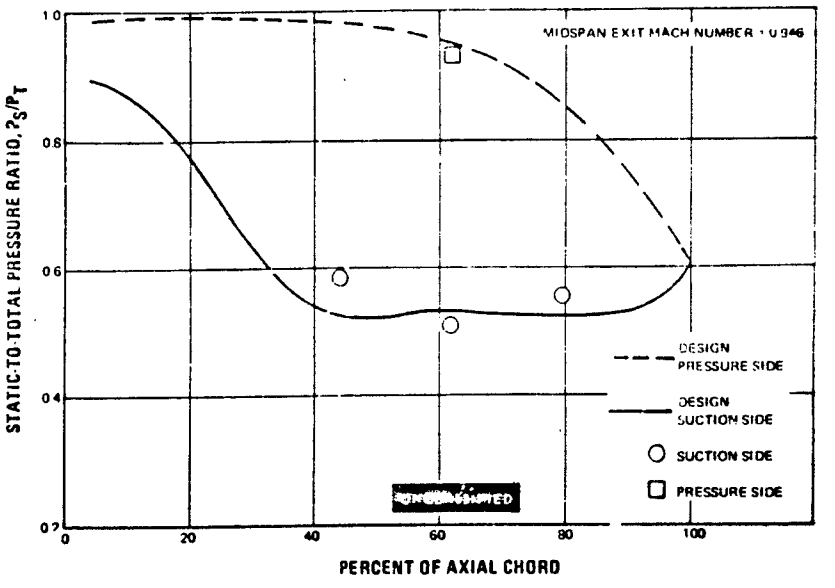

Figure 91 Static-to-Total Pressure Ratio vs. Percent of Axial Chord, Second Blade Cascade – Tip Section

(U) However, in addition to these effects, it is evident that the loading at the root and tip will both be reduced because they are required to turn the low total pressure end-wall fluid through essentially the same turning angle as the remainder of the airfoil. As a result, the root loading is reduced by both effects, while the tip loading has an indeterminate outcome. There is no doubt that these qualitative observations explain the differences between experimental and theoretical pressure distributions.

5. CONCLUSIONS

- The results of the baseline tests entirely verified the soundness of the two-dimensional airfoil design procedures and the ability of the annular segment cascade to simulate turbine conditions realistically. The data taken in these tests was sufficiently comprehensive and detailed that a clear, thorough understanding of the aerodynamic behavior was obtained.

- The performance of each of the four medium-reaction, normal-solidity baseline airfoils was very similar and no distinguishing characteristics for any particular airfoil warrants selection over another for applying boundary layer control techniques.

- The normal solidity second vane was chosen for further study by the process of elimination. The first stage vane and blade inside diameter end-wall extensions indicated some separation beyond the test cascade, which could influence probe readings near this wall in future tests if it became more severe. The short second stage blade chord makes the fabrication of end-wall boundary layer control techniques difficult.

- The results of the baseline data analysis indicate that reduction of secondary flow, rather than corner separation, is required. The applicable boundary layer control techniques that were chosen are local contouring, local recambering, end wall contouring, addition of flow fences and increased surface roughness. These will be applied to the second vane under the Task IIc effort.

- Since four boundary layer control techniques will now be applied to one airfoil under Task IIc, rather than two techniques to two different airfoils as initially planned, the need for Task IId was eliminated. It was recommended, therefore, that the Task IIb tests should be repeated by a test of a lower solidity design as a substitute for the original Task IId. Analysis of the data for the normal-solidity airfoils shows that the limit of airfoil loading has not been reached, and further gains may be achieved by increasing the airfoil load coefficient.

6. TEST PROCEDURE

(U) The test procedure which was followed during the Task IIb annular segment cascade evaluation of the baseline airfoils is outlined below.

- The cascade test pack was installed on the stand and all of the instrumentation was connected

- The exit plane traversing probe was installed and the circumferential tracking along the outside diameter shroud was checked and adjusted as necessary by lateral positioning of traverse probe mount assembly

- The exit traversing probe was positioned at midspan and set at the airfoil exit metal angle. This was done by sighting along the probe head and shank

- Then, the radial tracking was checked by traversing the probe from the inside to outside diameter. Shims were placed under the actuator to achieve constant distance from trailing edge to the probe tip

- The probe distance aft of the trailing edges along the projection of the airfoil exit metal angle was set at 0.50 inches with a scale. Adjustment screws were incorporated into the traverse actuator assembly for this purpose

- The inside and outside diameter limits were set with the probe at the minimum angle. The minimum angle of 15^{O} was set with a sheet metal template placed between the test airfoil trailing edges and the probe shank.

- The exit probe calibration was made through the data recording system, with the calibrated lowest angle of 15^{O} and the maximum angle of 62^{O}. The actuator was preset in the laboratory for a 47^{O} total travel

- The data recording system calibration was made for radial travel of both the exit and inlet traverse probes

- Secondary calibrations were completed for all transducers

- The J-75 slave engine was started and air was bypassed around the rig in order to remove moisture that may have been present during the initial start-up. Air was bled through the bypass until operating temperature was reached and the moisture cloud had disappeared

- The bypass was then closed and air was directed through the rig. A pressure check was then made with a soap solution. No leaks were permitted on instrumentation lines. Small, fuzzy leaks around rig flanges were allowed

- The inlet pressure and temperature were set to achieve the desired Mach number and Reynolds number

- The inlet traverse probe was traversed from the inside to the outside diameter

- The exit traverse probe was traversed from left to right (looking upstream) and from the inside to the outside diameter

- The inlet traverse was repeated

- The static pressures were recorded manually from U-tubes

- The next test point was set and the last four steps were repeated.

(The reverse of this page is blank)

SECTION V

BOUNDARY LAYER CONTROL EVALUATION (Task IIc)

1. RFP OBJECTIVE

(U) Determine the effects of the most promising boundary layer control techniques on corner flow separation.

2. TASK OBJECTIVE

(U) Initially, two methods of boundary layer control indicating the best potential for reducing end-wall losses were to be applied to two airfoils selected in Task IIb. For the reasons given in Section IV, four boundary layer control methods were selected and these are only to be applied to one airfoil, for which the second vane was chosen.

(U) The RFP Objective indicates that methods to eliminate flow separation will be considered. Since the baseline tests indicated that the end-wall problem for these airfoils was that of high loss without corner boundary layer separation, the apparent source of the high end-region loss is secondary flow of the end wall boundary layer across the channel. This is reflected in the baseline tests as high loss regions in suction surface corners. These regions probably originate at the end wall but migrate from pressure surface to suction surface and accumulate in the corners. Therefore, the boundary layer control methods that are applicable to the baseline airfoils involve those that have a tendency to reduce the secondary flow at the end-walls.

(U) The selected techniques that will be experimentally evaluated are (1) local recontouring (2) local recambering (3) end wall contouring and (4) use of flow fences and application of increased surface roughening.

3. DESCRIPTION OF BOUNDARY LAYER CONTROL METHODS

(a) Locally Recontoured Second Vane

(U) The local recontourings of the second vane root and tip sections are shown in Figures 92 and 93. The airfoil surface static pressure gradient at the leading portion was reduced in order to decrease the loading toward the airfoil leading edge, while keeping the overall loading constant. This change is intended to delay the onset of strong secondary flow in the upstream portion of the channel and to reduce the total accumulation of losses near the airfoil suction surface corners. These recontoured sections were faired into the existing midspan contour at approximately the 25%- and 75%-span locations.

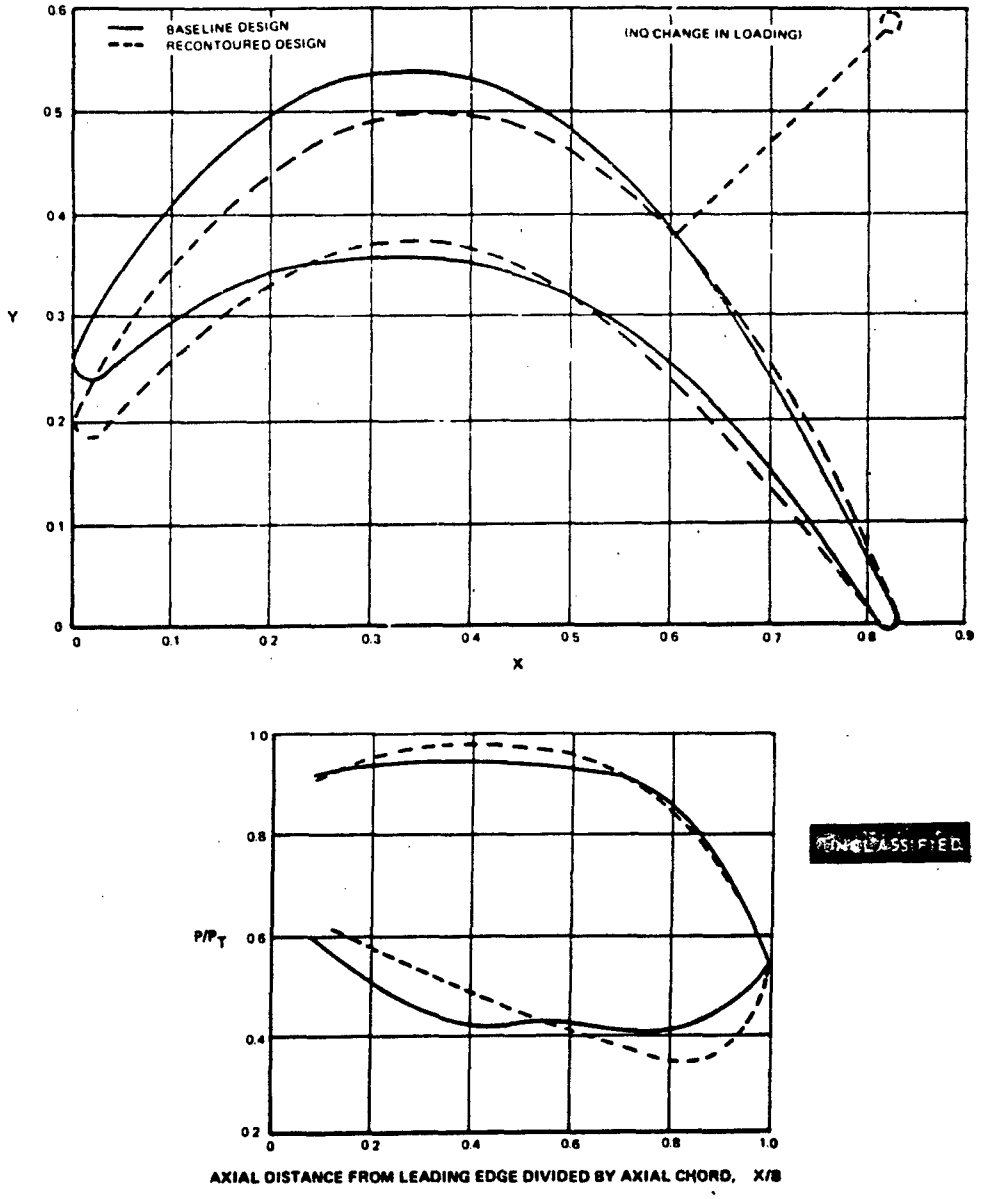

Figure 92 Second Vane Baseline Airfoil Recontouring, Root Section Static Pressure Redistribution

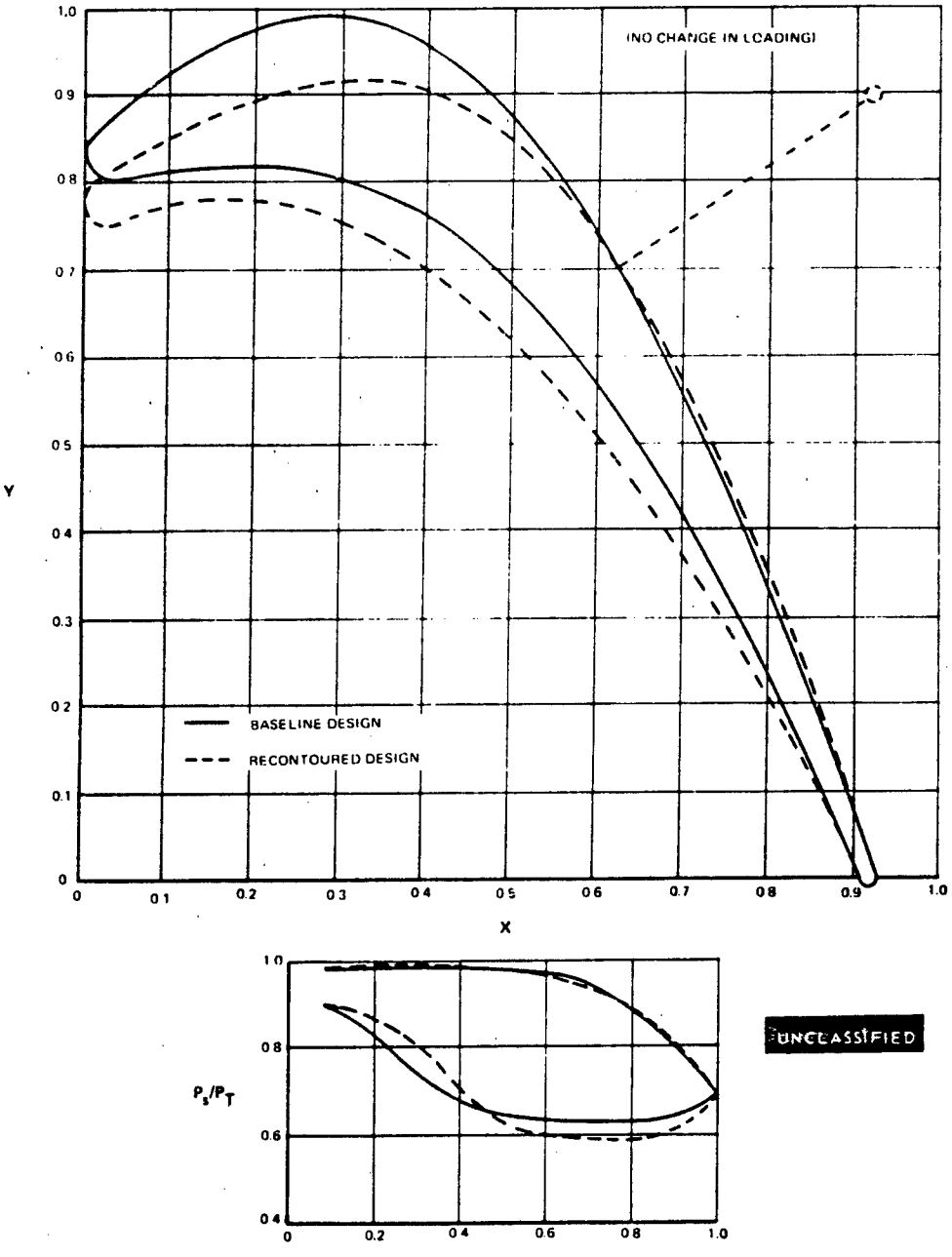

Figure 93 Second Vane Baseline Airfoil Recontouring, Tip Section Static Pressure Redistribution

(b) Locally Recambered Second Vane

(U) The application of the local recambering to reduce secondary flow at the root and tip sections of the second vane required streamline analysis of the entire study turbine. Inlet angles were held constan to allow the use of the same inlet bellmouth and inlet guide vane rig sections. The tip exit angle was reduced (or closed) by 5 degrees, while the root exit angle was increased (or opened) by 5 . degrees. These camber changes were then curved-line faired into the original camber at the 25%– and 75% - span sections as shown in Figure 94 The streamline analysis indicated that, in order to maintain the same turbine stage work and reaction level, the second stage blade had to be opened by increasing the exit angle by 0.5 degrees.

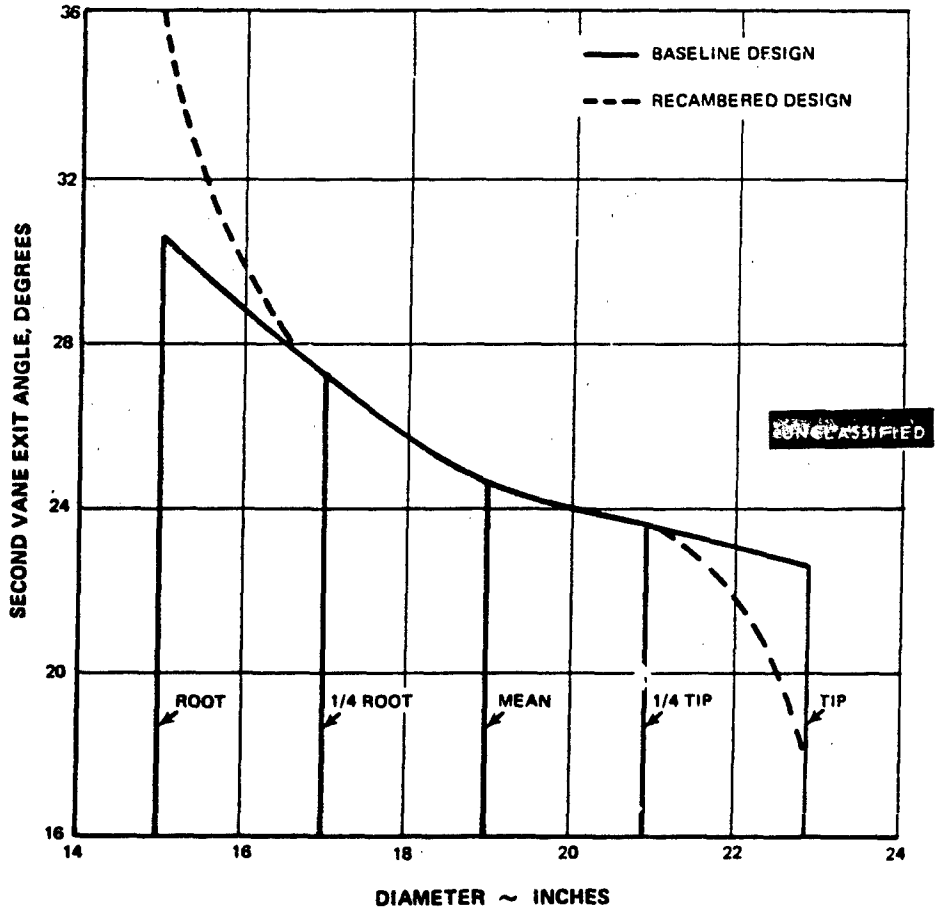

Figure 94 Second Vane Recambering, Exit Angle Distribution

(U) Figures 95 and 96 show the recambered second vane root and tip sections. These changes will have the tendency to reduce the root overturning and the tip underturning as was observed in the baseline tests. The tip airfoil surface static pressure distribution indicates that with the high turning, the overall loading is increased, but the increase in passage convergence shifts the loading toward the trailing edge. This reduces the pressure difference between the suction and pressure sides of the channel at the forward end and will tend to delay the onset of strong secondary flow. The reduction in camber at the root will result in a lower overall airfoil loading. This reduction should occur more or less uniformly over the chord length. The effects of the airfoil recambering are summarized in Table IV.

TABLE IV

SUMMARY OF LOCAL RECAMBERING EFFECTS

Parameter	Tip	Root
Exit Angle	Closed	Opened
Tangential Force	Increased	Decreased
Zweifel Load Coefficient	Decreased (0.85 to 0.65)	Increased (1.1 to 1.3)
Channel Convergence	Increased	Decreased
Suction Pressure Distribution	Descending	Flat
Crossflow Potential	Increased but shifted toward trailing edge	Decreased overall

(c) End Wall Contouring

(U) Another boundary layer control method is the application of end wall contouring. This method holds the promise of reducing the local airfoil loading, and consequently the secondary flow losses, without causing any appreciable disturbance to the flow at other sections of the airfoil or downstream of the airfoil row. Secondary flows occur when the momentum of the fluid near an end-wall has been reduced to a point where it can no longer withstand the circumferential pressure gradient impressed by the potential flow. One way to achieve a reduction in strength of the secondary flow field is to reduce the tangential pressure difference near the end-wall.

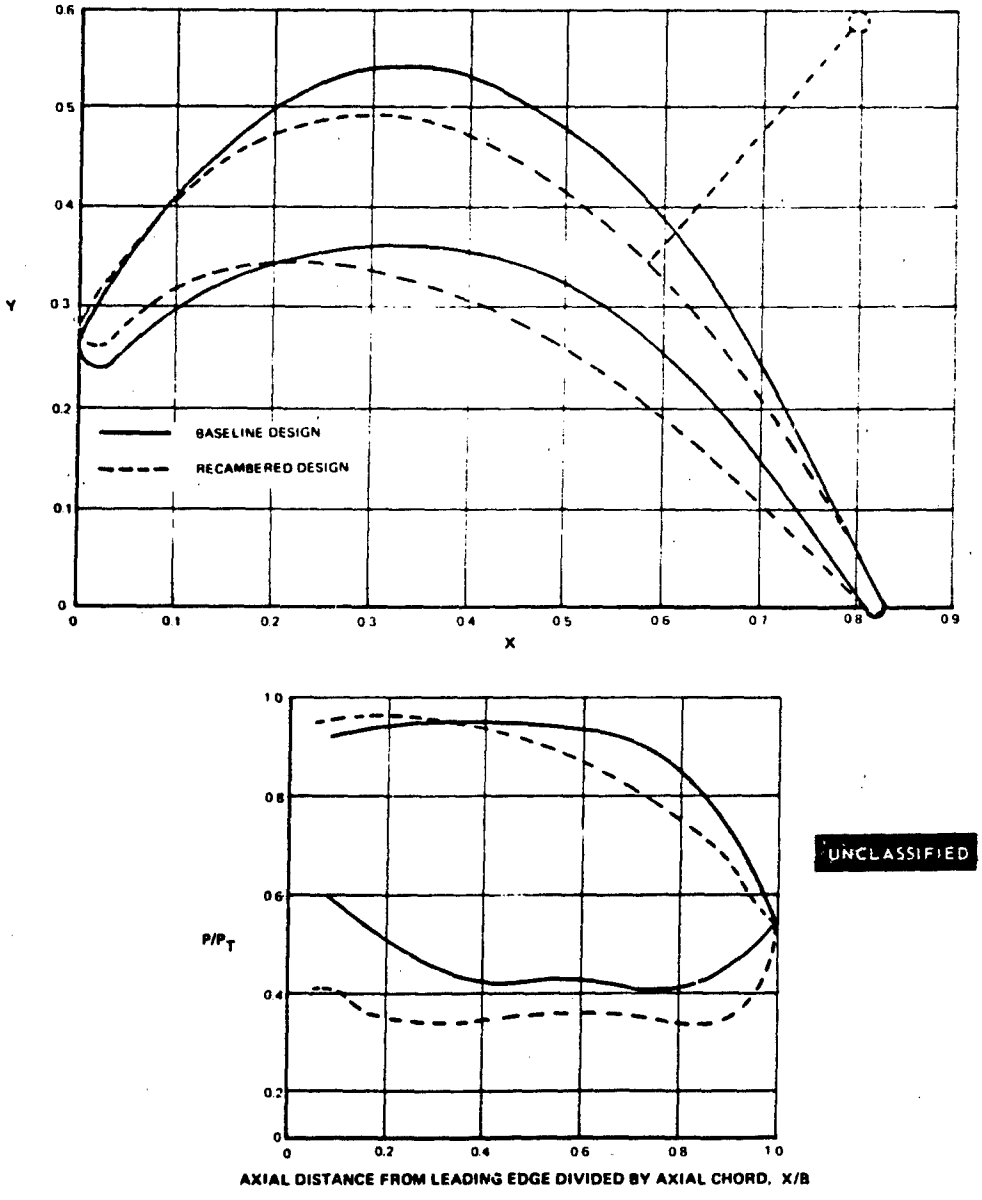

Figure 95 Second Vane Root Section Recambering

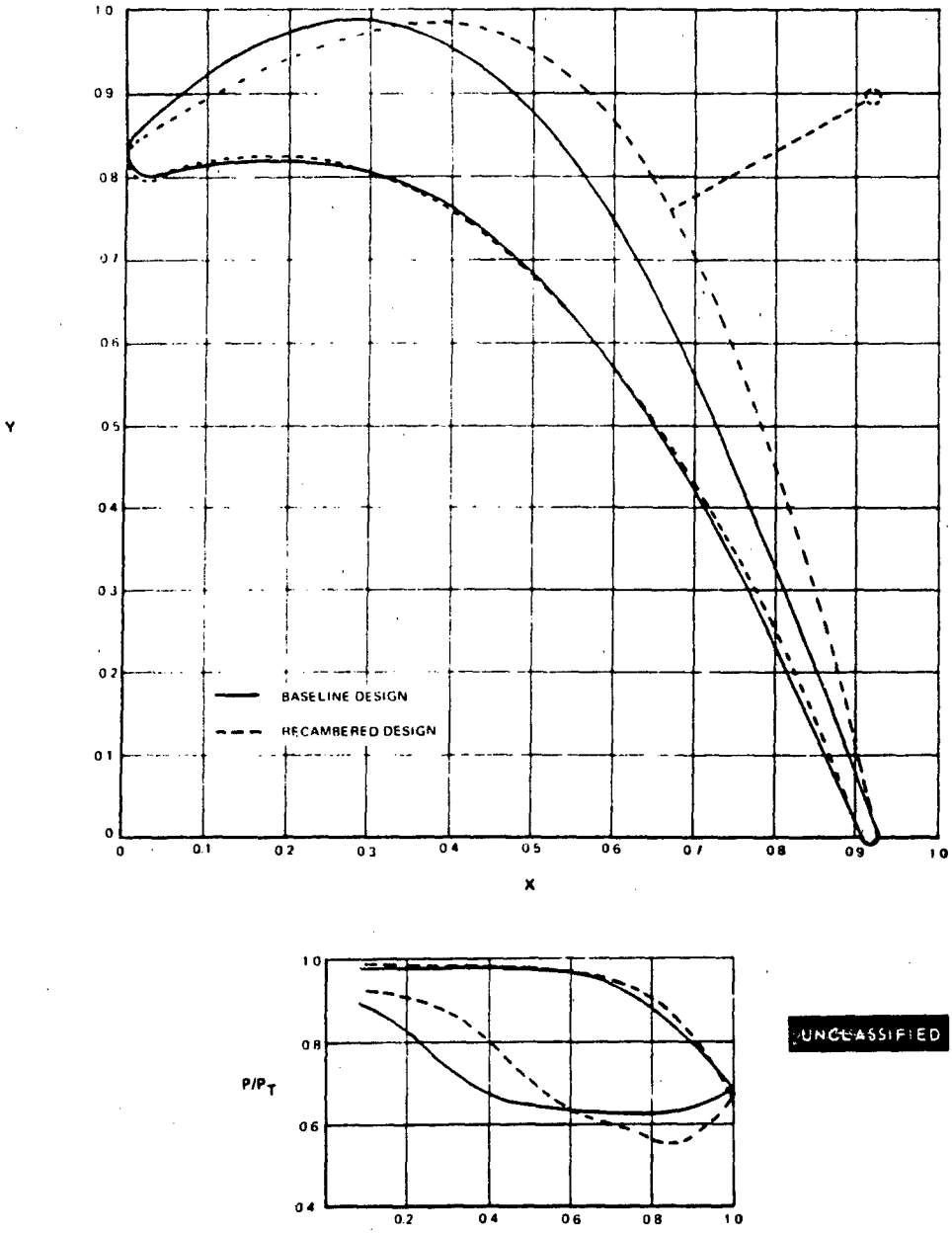

Figure 96 Second Vane Tip Section Recambering

(U) Two computer programs were used to design the final wall contours. The first calculated the pressure distribution around an airfoil of the desired profile on a cylindrical surface. This program allows streamtube height variations but can not account for radial pressure gradients. The second deck performs axisymmetric intrablade calculations. The basic requirements that were set for a good wall contouring design are:

- The contour must decrease the local airfoil loading
- The contour must not cause flow separation on the end wall
- The increase in positive incidence caused by the contour must be less than 5°
- The contour must not increase the adverse pressure gradient on the uncovered portion of the suction surface.

(U) Contours were designed for both the inner and outer walls of the airfoil. Airfoil pressure distribution studies established that end-wall contouring using depths large enough to produce a significant reduction in the tangential pressure difference should not be accomplished by contours completely within the airfoil row. More acceptable was a contour designed to relieve the airfoil blockage effects by increasing the annulus area in the leading edge region.

(U) After a study was made of many wall contours, the final contour which was judged to be the best design was one with sinusoidal inlet and exit sections, having the leading and trailing edges intersecting at the inflection points. The final design is shown in Figure 97. The inlet and exit sections were connected by a constant area section starting at approximately 24% of axial chord and ending at approximately 76% of axial chord. The static-to-total pressure distribution computed along the mean streamline at the airfoil root section is shown in Figure 98. This design met all the conditions which were established as requirements for wall contouring.

(d) Flow Fences and Surface Roughness

(U) Exploratory methods of boundary layer control which were deemed useful of some consideration were the use of flow fences and increased surface roughness. The flow fences are intended to block or impede channel cross flows at the passage walls, while increased surface roughness would force the boundary layer to an early transition from laminar to turbulent flow. Much promise was not held for the effectiveness of these two methods. They were simple to test, since as add-ons to the existing rig they could be run while hardware was manufactured for the more promising methods.

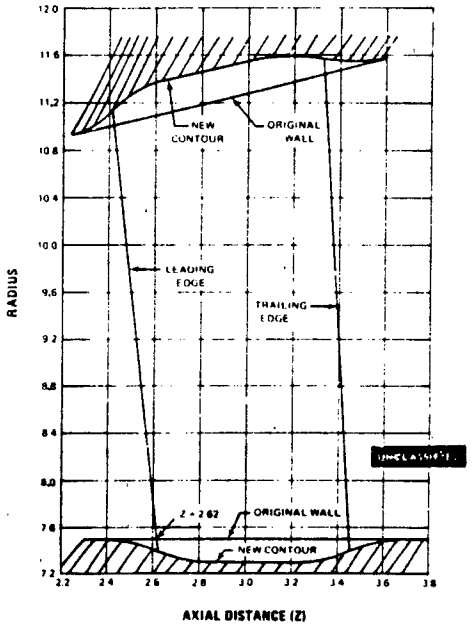

Figure 97 End-Wall Contouring, Second Stage Vane

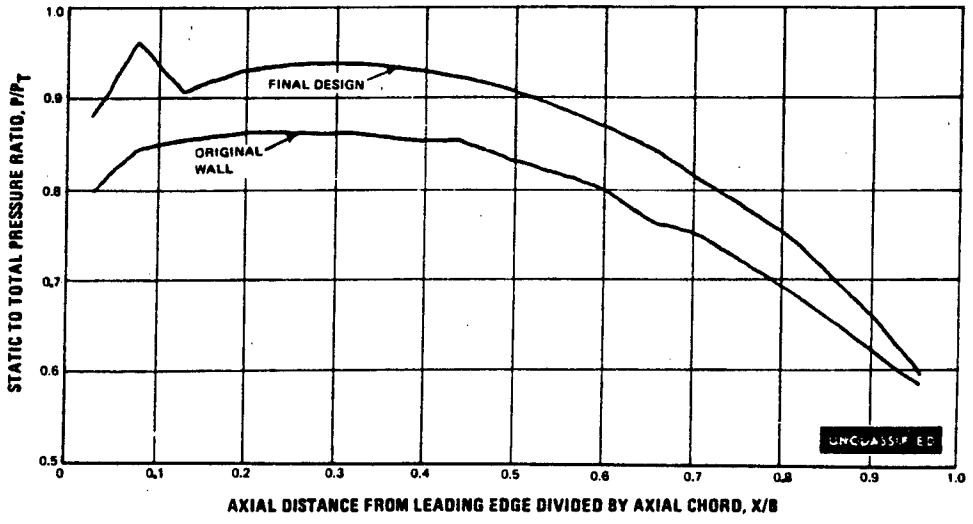

Figure 98 Wall Contoured Mean Streamline Root Section

(U) The design of the flow fences is shown in Figure 99. These are to be applied to the second vane outside diameter wall and their height was obtained from the suction surface secondary flow patterns that were observed in the baseline tests described in Section IV. The flow lines, indicating a radially inward boundary layer movement, at the airfoil trailing edge, extended to approximately 0.5 inch from the wall surface. Allowing for the growth in corner vortex size from inside the passage to the exit plane, the fence height required to significantly reduce the end wall crossflow was estimated to be one-half the trailing edge size indication, or 6.3% of the span height. The fences were mounted in four passages midway between airfoil surfaces and extended the full passage length from leading edge to trailing edge.

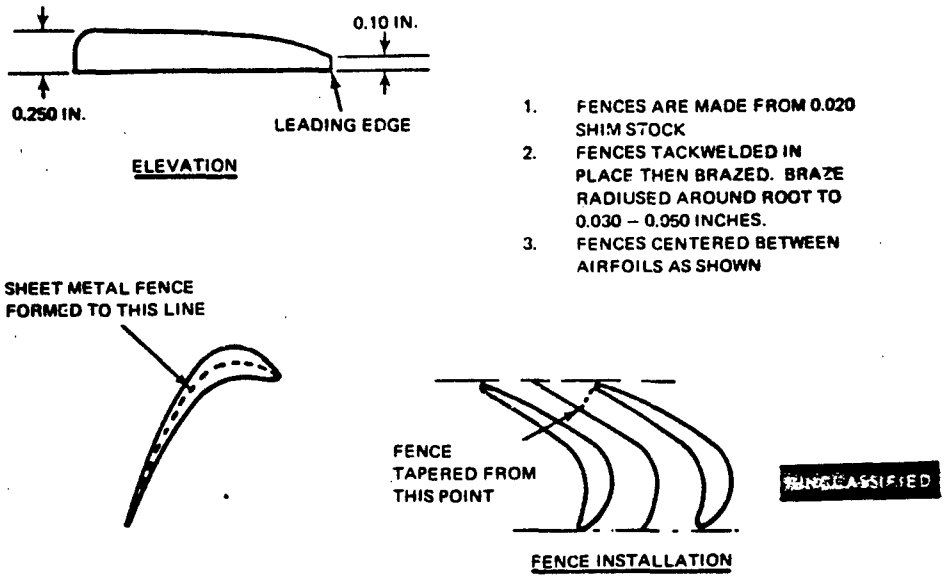

Figure 99 Second Vane OD Shroud Fence Installation

(U) Roughening of the inside diameter end wall was accomplished by attaching emery cloth to the end wall region in four passages. Calculations of the wall boundary layer indicated that the boundary layer would be transitional in the region between the inlet guide vanes and the test airfoils. Since this calculation involved approximations to the pressure gradient through the rig, it was decided to try the increased surface roughening in case the boundary layer had not actually transitioned. The calculated boundary layer thickness prior to transition was 0.020 inch. The coarsest emery cloth available was No. 50 grit which has an average roughness height of 0.013 inch. This value is above the computed critical value for boundary layer transition. This was cemented to the inside diameter end-wall and to the leading edges of the airfoils adjacent to the inside diameter wall.

4. STATUS

(U) The locally recontoured airfoil design and fabrication was completed and the airfoils were inspected. Fabrication of the annular cascade pack is in process.

(U) The locally recambered airfoil design was completed and the airfoils were fabricated. The airfoils will be installed into the annular cascade pack after inspection.

(U) Extended airfoils for the wall contoured second vane tests were designed and fabrication of the airfoils was completed. The contoured walls are being fabricated.

(U) Tests of the flow fences and increased surface roughness were completed. These tests were run simultaneously with the flow fences mounted on the outside wall and the roughness additions to the inside wall. The data from these tests is being analyzed.

(The reverse of this page is blank)

SECTION VI

MEDIUM SOLIDITY AIRFOIL EVALUATION (Task IId)

1. OBJECTIVE

(U) The initial objective of Task IId was to investigate two additional boundary layer control methods, other than the two methods that were investigated under Task IIc, on two different airfoils. Since the performance of the four baseline airfoils (Section IV) were very similar, Task IIc was modified so that four boundary layer control methods were applied to only one airfoil, eliminating the need for Task IId as originally conceived. By mutual agreement with the Air Force, the work substituted for the original Task IId will now include the evaluation of the performance of higher load coefficient airfoils designed for the same velocity triangles as the baseline airfoils of Task IIb. The performance of these lower solidity airfoils will be compared to the performance of the nominal solidity airfoils reported in Section IV.

2. TASK OBJECTIVE

(U) Each of the four medium solidity airfoils will be evaluated in an annular segment cascade. The entire testing program run previously for Task IIb will be reproduced for these airfoils.

3. AIRFOIL SECTION AND FACILITY DESIGN

(U) The medium-reaction, medium-solidity airfoils were designed to the same turbine velocity diagrams as the normal solidity airfoils. A summary of the pertinent design values is presented in Table V. The elevations, gaging distribution, airfoil section, predicted surface pressure distribution, and airfoil radius of curvature distribution for each of the four airfoils is presented at five spanwise locations in Appendix I. The four airfoils are the first and second vanes and first and second blades. The fabrication coordinates of each of the airfoils are tabulated in Tables VI through XXXVI of Appendix II. The airfoil angles, airfoil areas, axial chords and uncovered turnings are also tabulated.

(U) The test section design for each of the four medium-solidity airfoils is the same as those for the normal solidity airfoils. The inlet guide vane designs will be identical to those for the already completed normal solidity evaluation. The designs of the normal solidity cascades and inlet guide vanes were presented in Reference 2.

TABLE V

MEDIUM-REACTION MEDIUM-SOLIDITY AIRFOIL SUMMARY

First Stage Vane	No. of Foils	Exit Mach Number, M_2	$\Delta P/Q$	Max. Surface Mach Number
Root	54	0.949	0.393	1.218
¼ Root	54	0.891	0.335	1.113
Mean	54	0.853	0.330	1.043
¼ Tip	54	0.820	0.3087	0.991
Tip	54	0.770	0.291	0.915
First Stage Blade				
Root	100	0.890	0.376	1.128
¼ Root	100	0.849	0.370	1.077
Mean	100	0.788	0.372	0.994
¼ Tip	100	0.738	0.3648	0.931
[illegible]	100	0.730	0.362	0.915
Second Stage V				
Root	70	0.991	0.432	1.310
¼ Root	70	0.920	[illegible]54	1.150
Mean	[illegible]	0.873	[illegible]	1.094
¼ Tip	[illegible]	0.821	0.3	1.001
Tip	70	0.765	0.3	0.926
Second Stage Blade				
Root	110	[illegible]	[illegible]	
¼ Root	110	0.92[illegible]	0.420	1.210
Mean	110	0.904	0.39	1.160
¼ Tip	110	0.897	0.324	1.102
Tip	110	0.892	0.371	1.128

[illegible]ASSIFIED

(U) The instrumentation that will be installed for these tests will be essentially identical to that used for the normal solidity tests. The method of installation of surface static pressure taps, as shown for the normal solidity airfoils in Reference 2, was varied in that all the grooves for laying in the airfoil surface static pressure tubes were made on the pressure side, and holes were drilled through from the suction surface for those taps required on the suction surface. This method improved the suction surface finish since back filling of the grooves on the suction surface was not required. A radial traversing probe which can be positioned at different circumferential stations will be used to measure exit plane conditions.

(U) A sketch of the test stand is shown in Figure 100. This stand is located in the Willgoos Laboratory, East Hartford.

4. STATUS

(U) The design and fabrication of the test stand has been completed. Reoperation of the test stand has been completed. The cascade packs are being fabricated and the first vane cascade pack, shown in Figures 101, 102 and 103, has been completed. This pack has been installed into the rig and testing has been initiated.

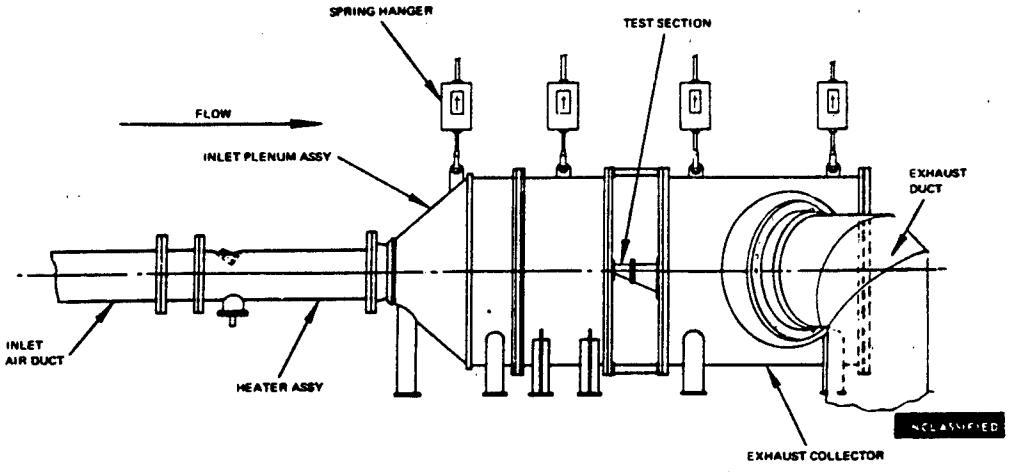

Figure 100 Annular Cascade Rig Installation

Figure 101 First Vane High Load Annular Cascade Rig, Pre-Swirl Pack (X-31697)

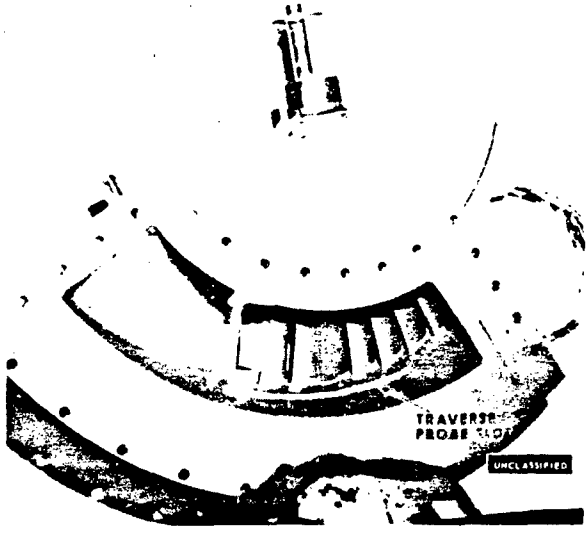

Figure 102 First Vane High Load Annular Cascade Rig, Rear View (X-31695)

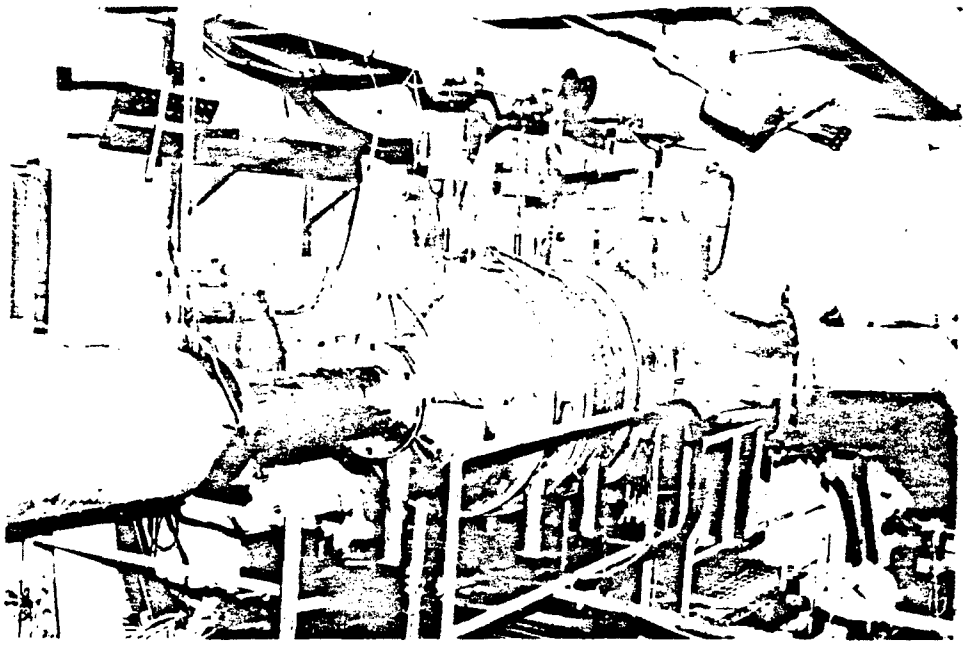

Figure 103 First Vane High Load Annular Cascade Rig, Side View (X-31699)

(The reverse of this page is blank)

SECTION VII

PRELIMINARY DESIGN MANUAL PREPARATION (TASK IIe)

1. RFP OBJECTIVE

(U) Prepare the preliminary draft of the Turbine Design Procedure Manual.

2. TASK OBJECTIVE

(U) The purpose of this task is to prepare and deliver a complete Turbine Design Procedures Manual. This manual will contain the following information for each computer program used to design the contract turbine: a flow diagram; a listing for all input and output items and their definitions; a list of definitions for each term used in the computer code; a write-up of the pertinent engineering equations; a listing of the computer code in Fortran IV; a copy of the computer program decks in Fortran IV; any necessary test cases for deck check-out.

3. STATUS

(U) Work is in process on the following computer programs:

- Turbine Meanline Design Program
- Turbine Stage-Off Design Program
- Turbine Streamline Analysis Program
- Airfoil Pressure Distribution Program
- Airfoil Boundary Layer Program
- Turbine Airfoil Design and Section Properties Program
- Airfoil Curved Line Fairing Program
- Airfoil Straight Line Fairing Program

(U) All of the decks have been converted to Fortran IV, and these were checked out on an IBM 7094. Flow diagrams for all decks have been completed. Listings have been made for all variables and for the input and output items of these decks. Engineering writeup of these decks has been initiated.

(The reverse of this page is blank)

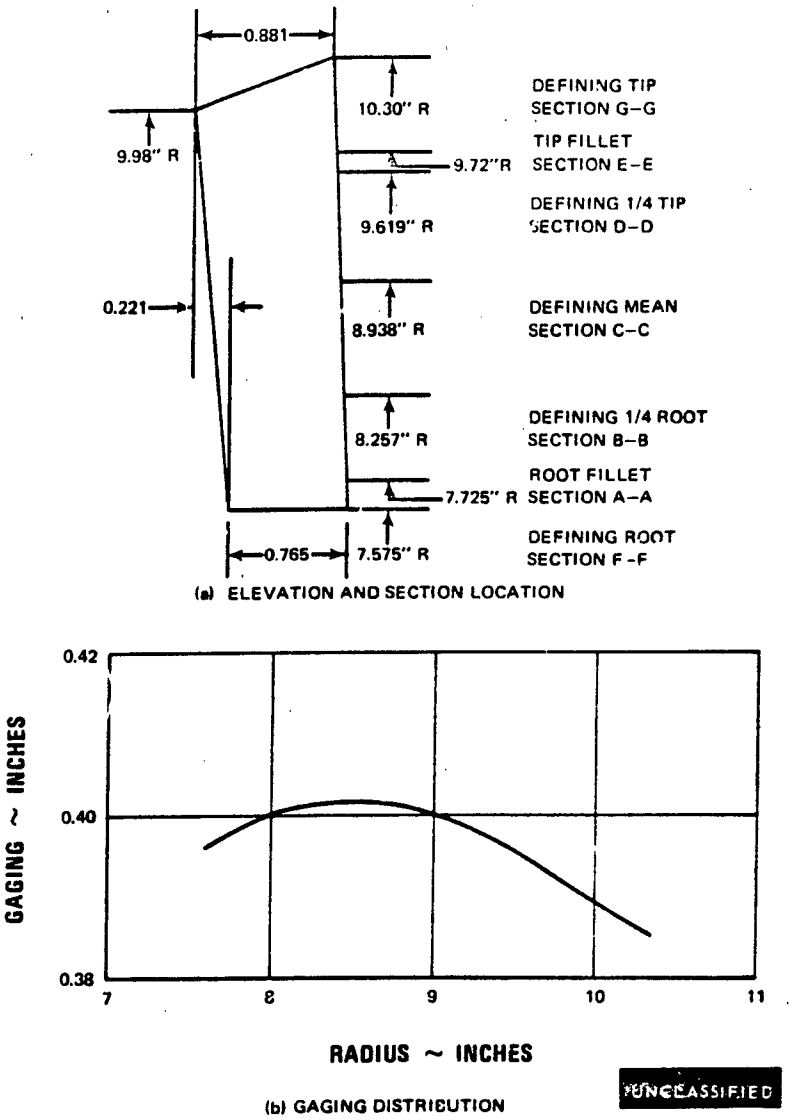

Figure 104 Medium Reaction, Medium Solidity, First Stage Vane

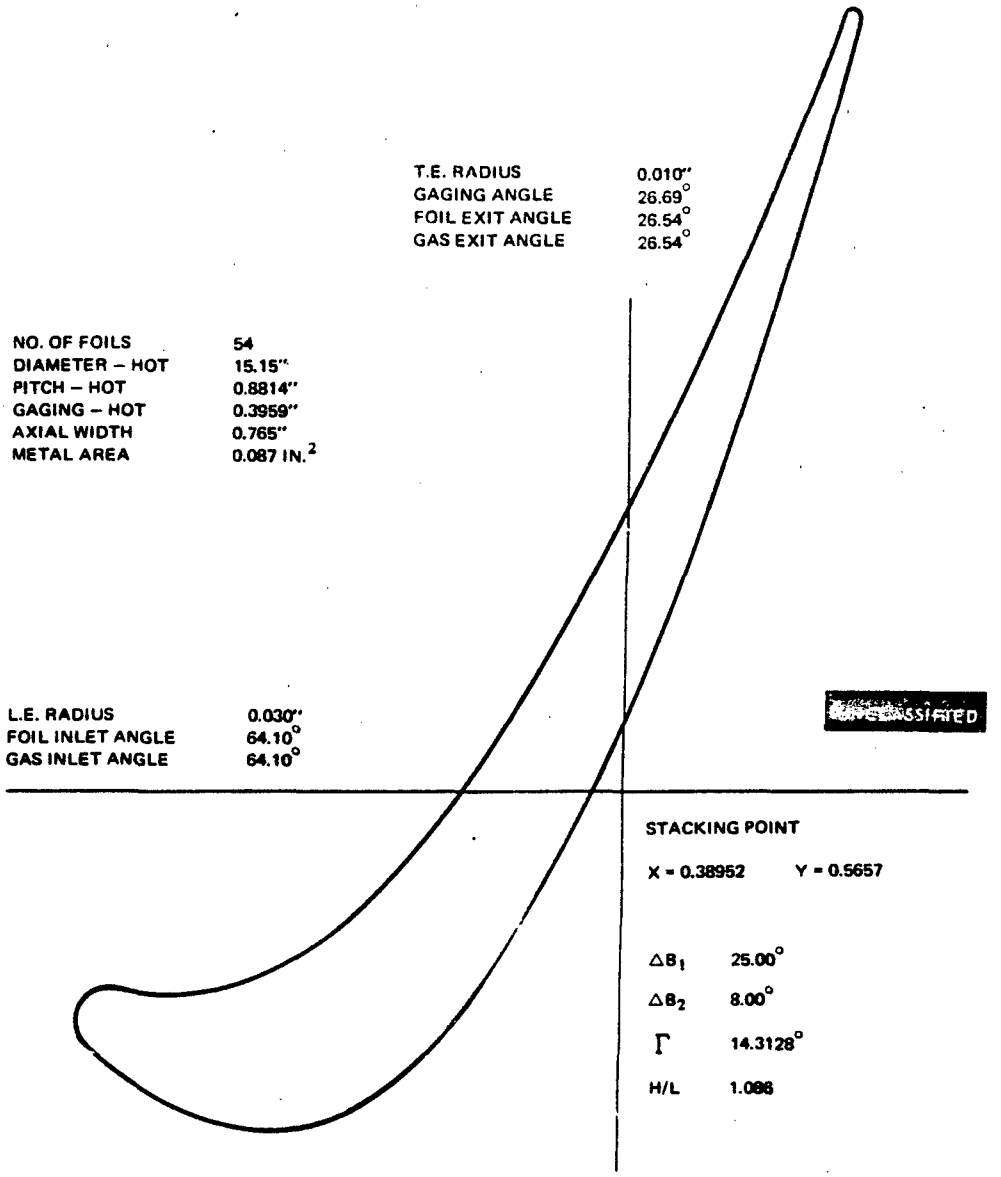

Figure 105 Medium Reaction, Medium Solidity, First Stage Vane, Root (F-F) Section

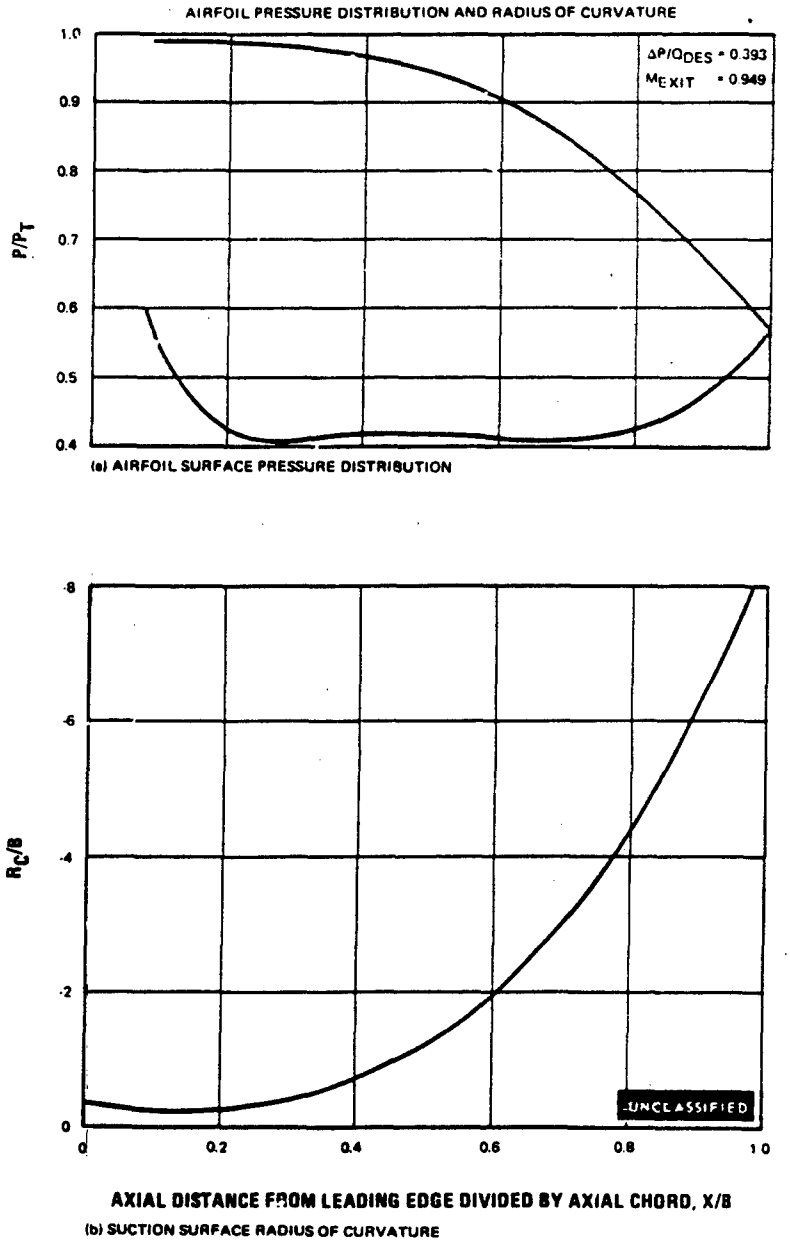

Figure 106 Medium Reaction, Medium Solidity, First Stage Vane Root

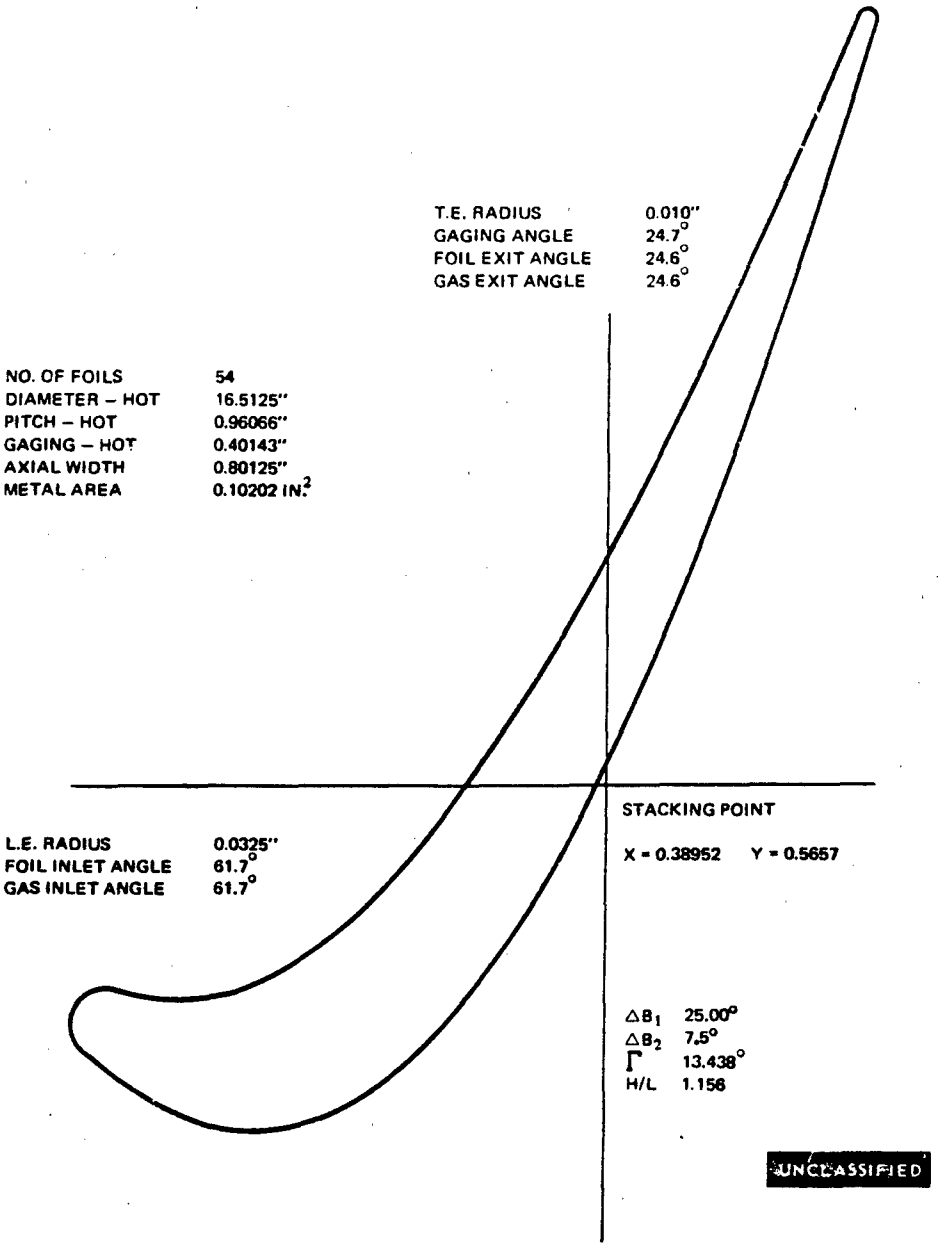

Figure 107 Medium Reaction, Medium Solidity, First Stage Vane, 1/4 Root (B-B) Section

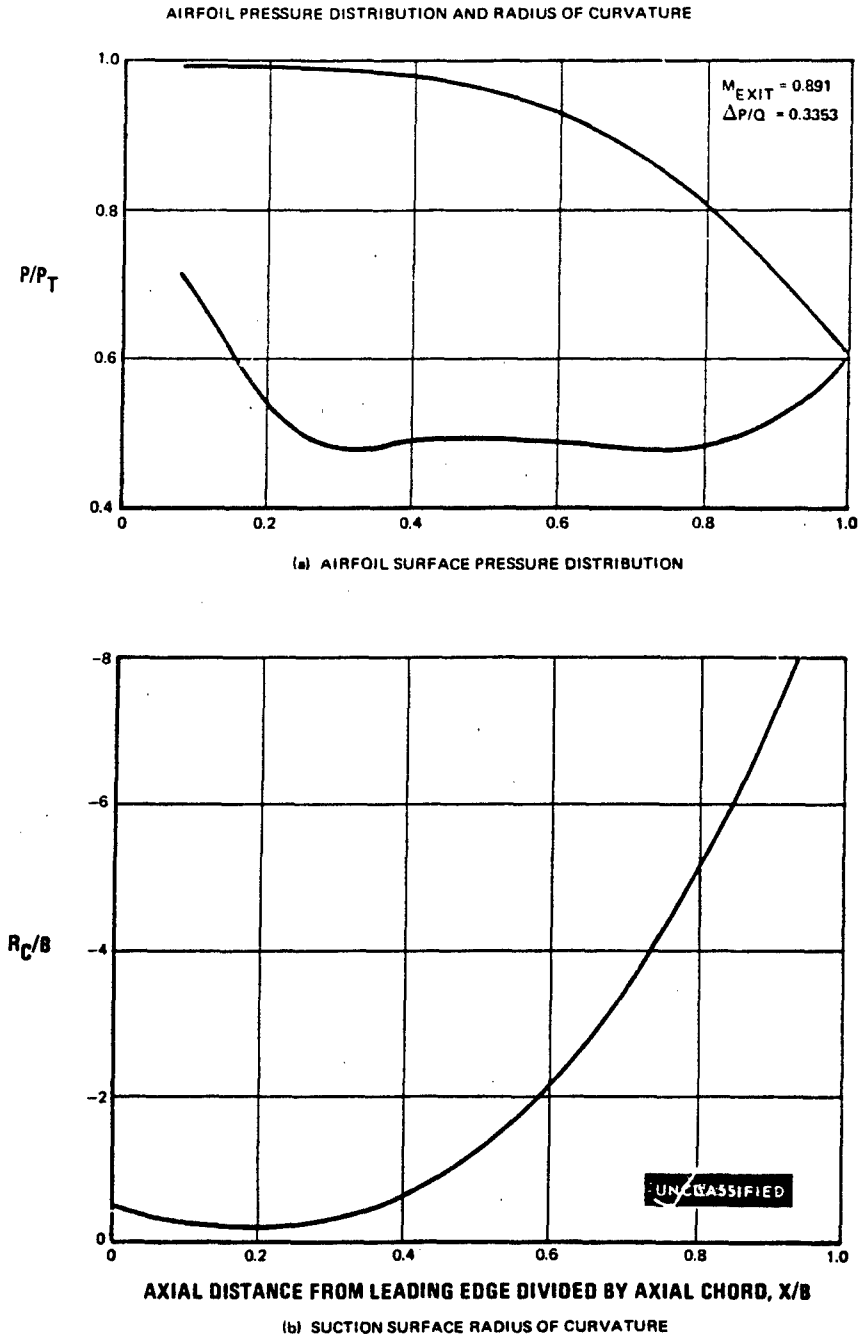

Figure 108 Medium Reaction, Medium Solidity, First Stage Vane, 1/4 Root Section

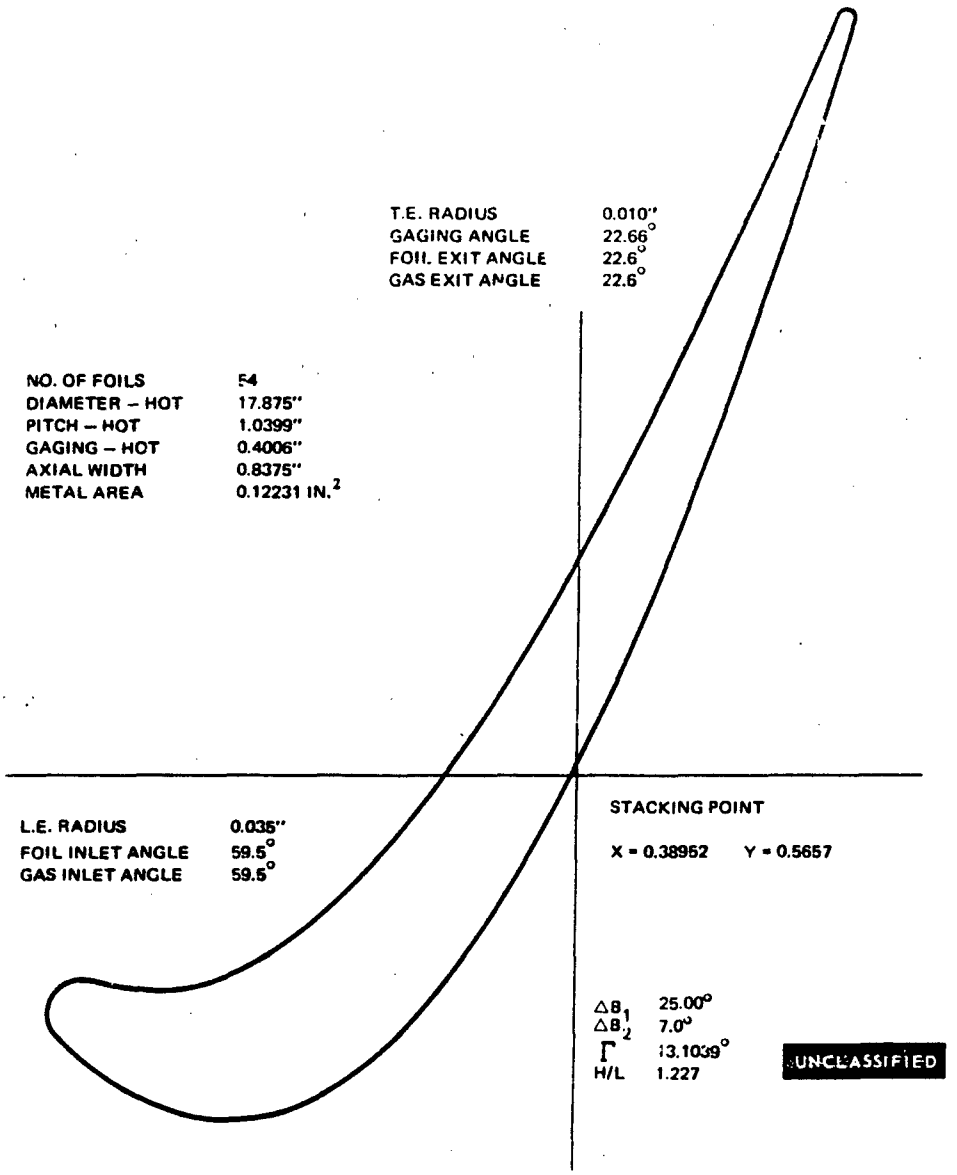

Figure 109 Medium Reaction, Medium Solidity, First Stage Vane, Mean (C-C) Section

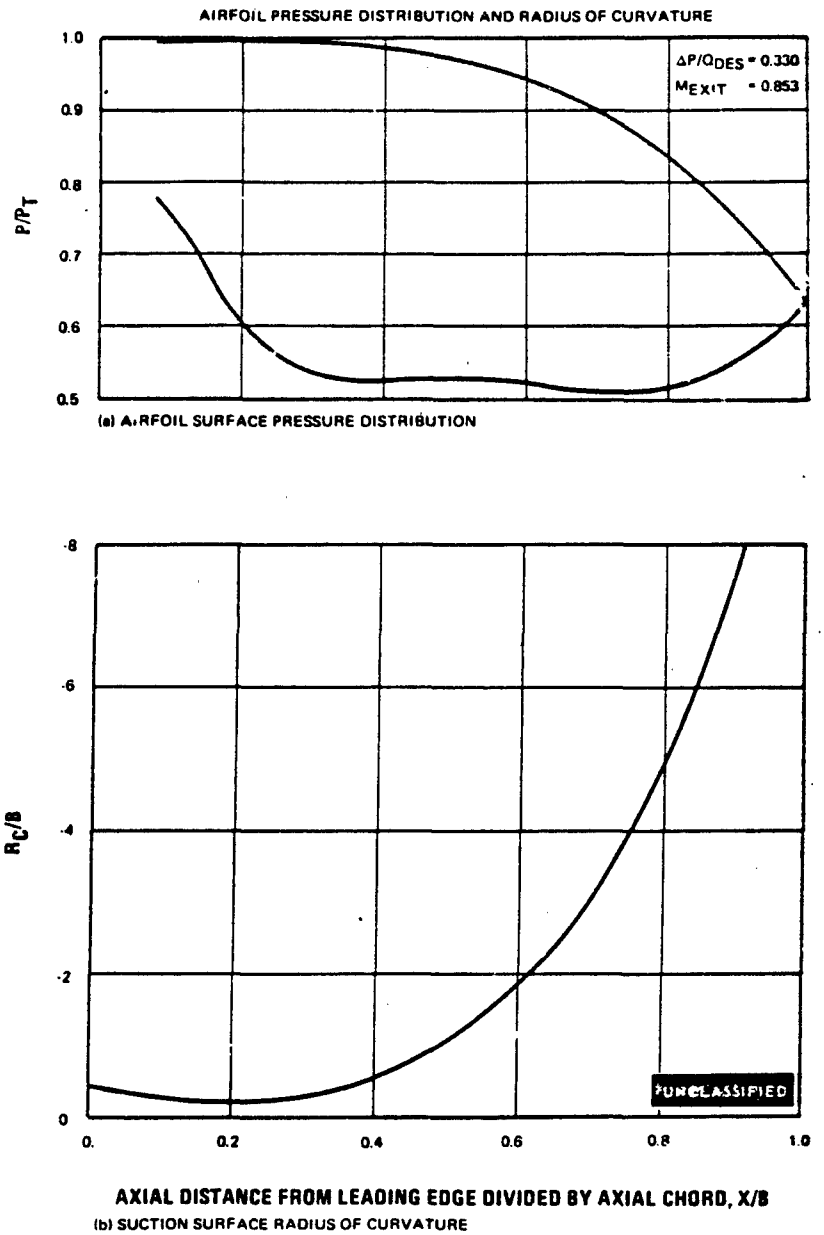

Figure 110 Medium Reaction, Medium Solidity, First Stage Vane, Mean Section

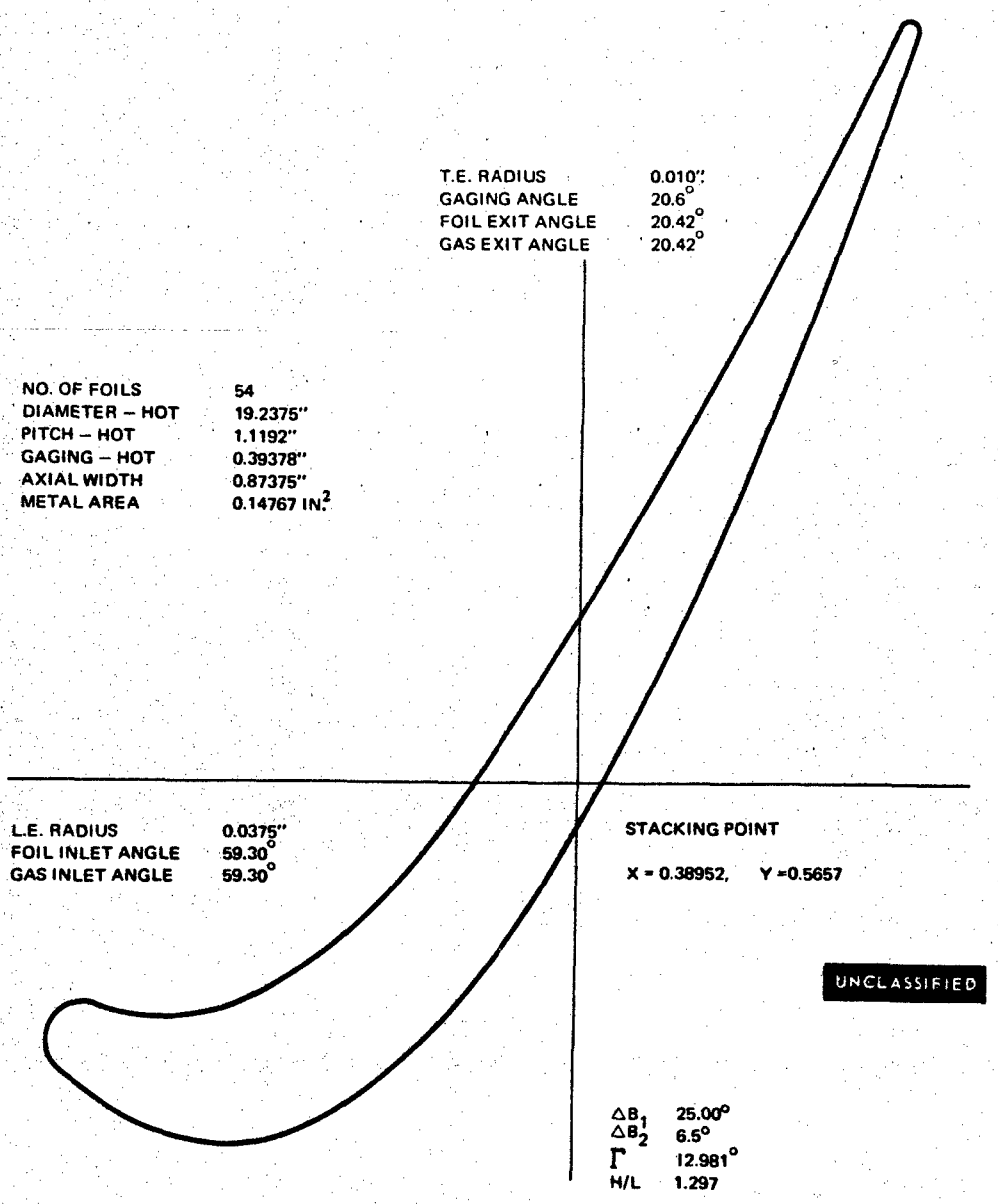

Figure 111 Medium Reaction, Medium Solidity, First Stage Vane, 1/4 Tip (D–D) Section

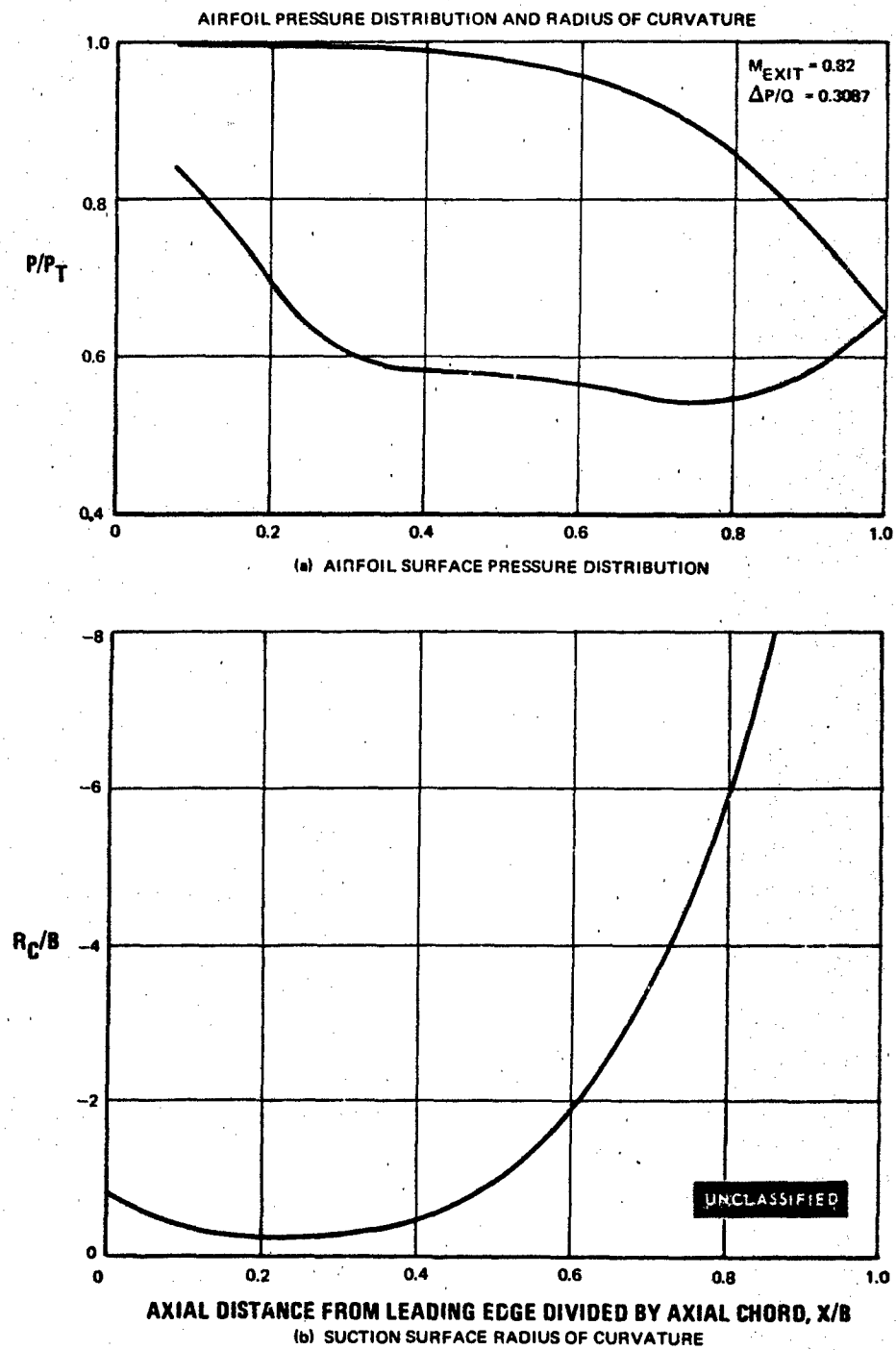

Figure 112 Medium Reaction, Medium Solidity, First Stage Vane, 1/4 Tip Section

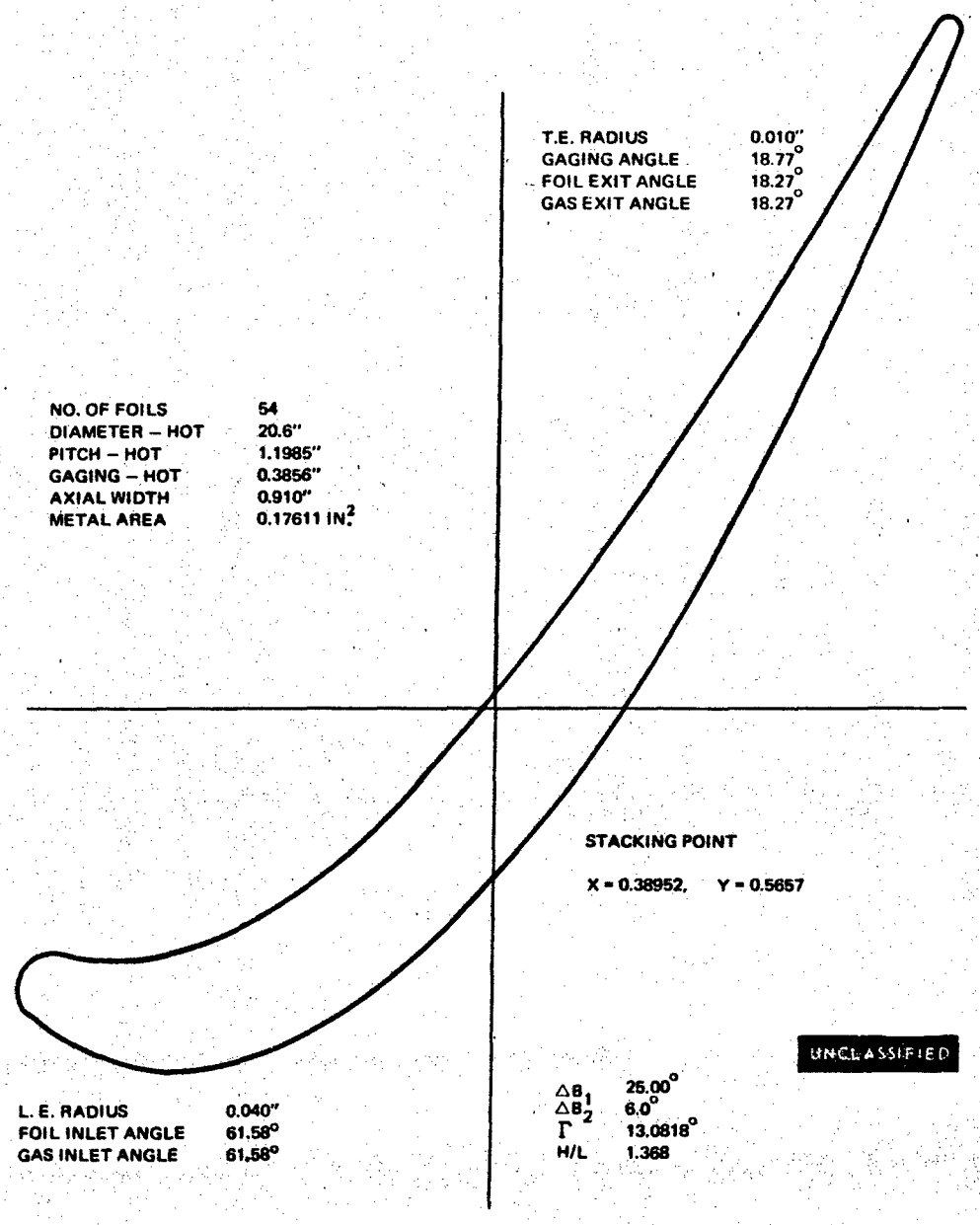

Figure 113 Medium Reaction, Medium Solidity, First Stage Vane, Tip (G-G) Section

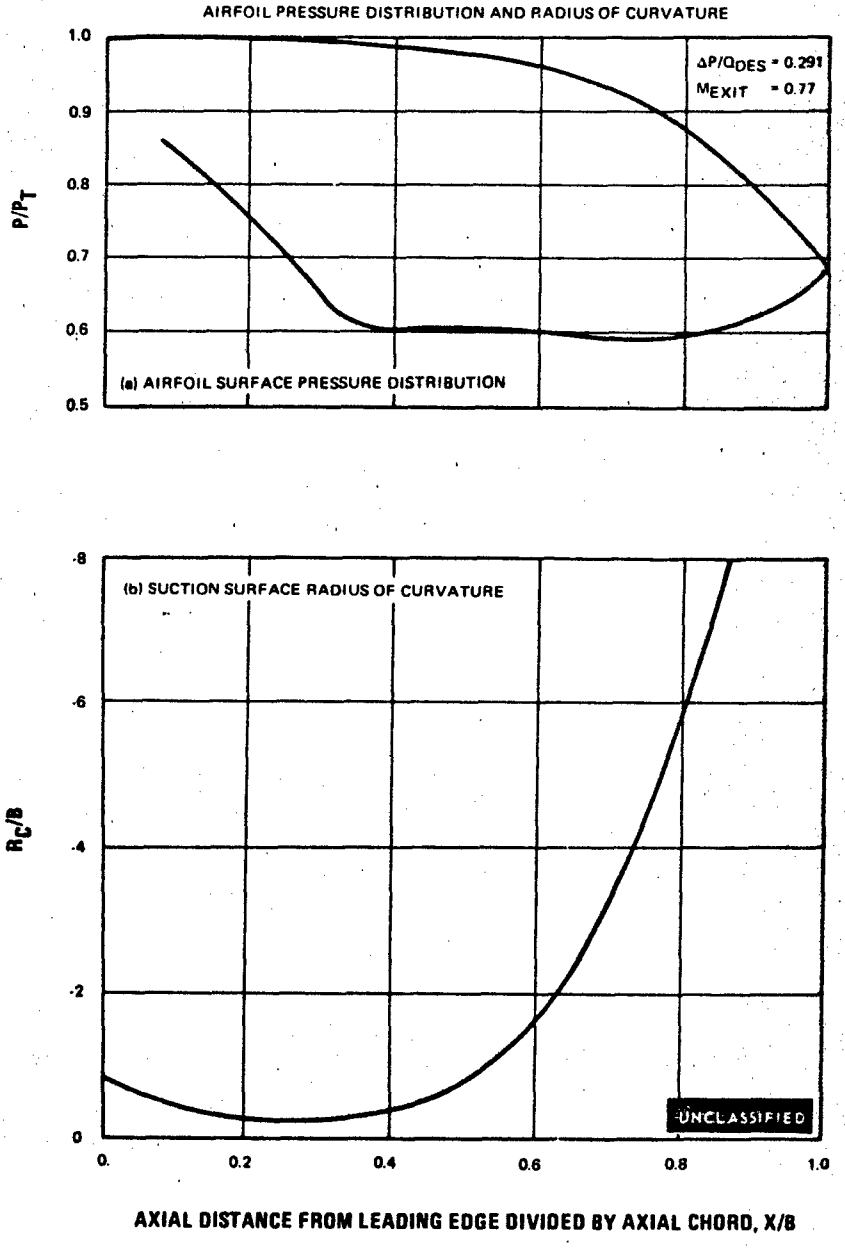

Figure 114 Medium Reaction, Medium Solidity, First Stage Vane, Tip Section

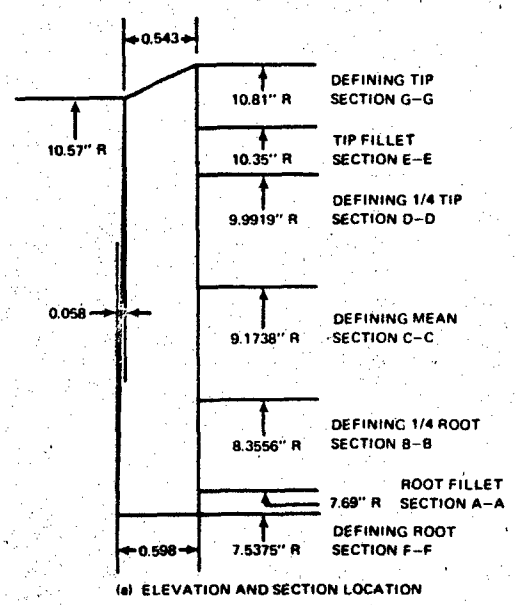

(a) ELEVATION AND SECTION LOCATION

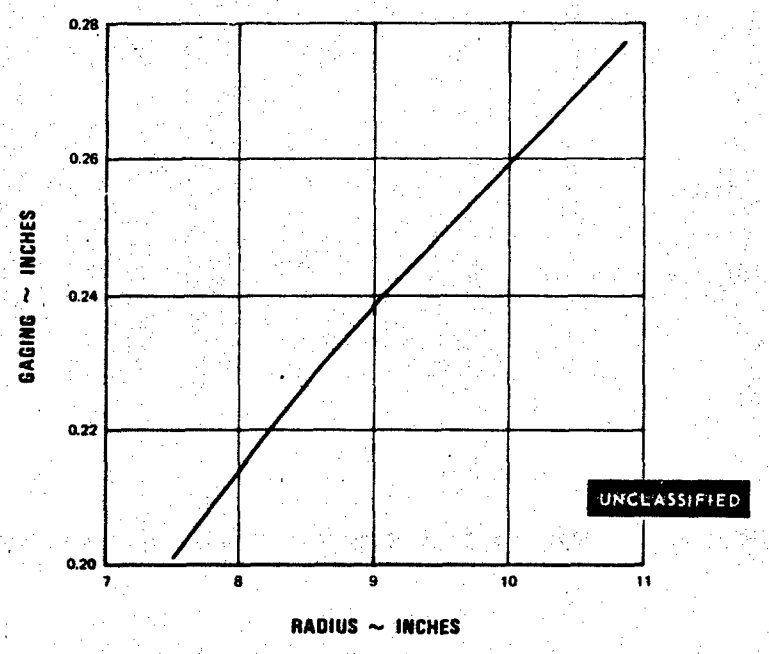

(b) GAGING DISTRIBUTION

Figure 115 Medium Reaction, Medium Solidity, First Stage Blade

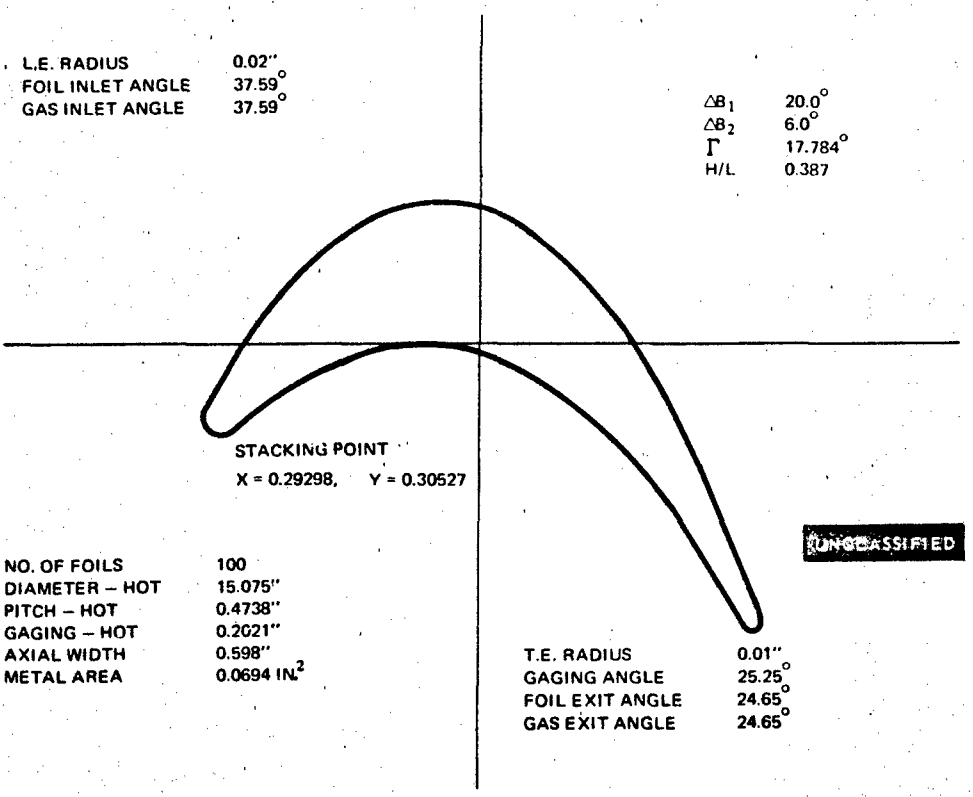

Figure 116 Medium Reaction, Medium Solidity, First Stage Blade Root (F-F) Section

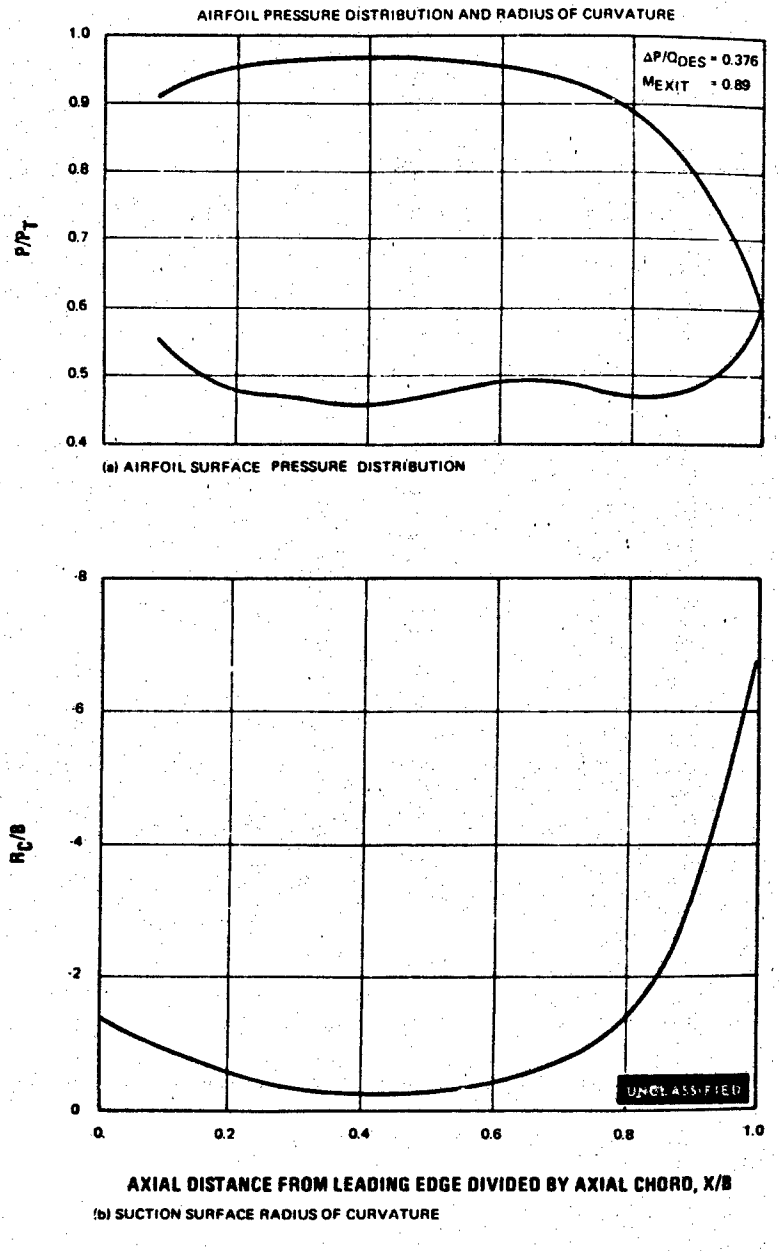

Figure 117 Medium Reaction, Medium Solidity, First Stage Blade, Root Section

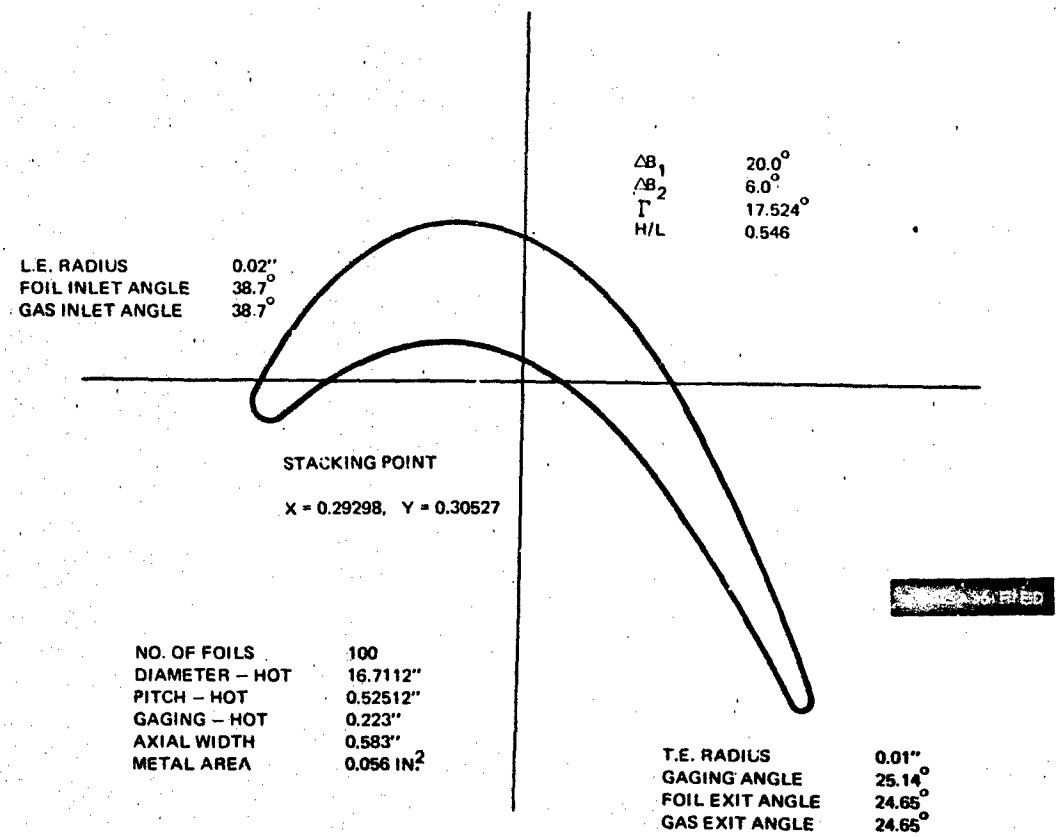

Figure 118 Medium Reaction, Medium Solidity, First Stage Blade, 1/4 Root (B-B) Section

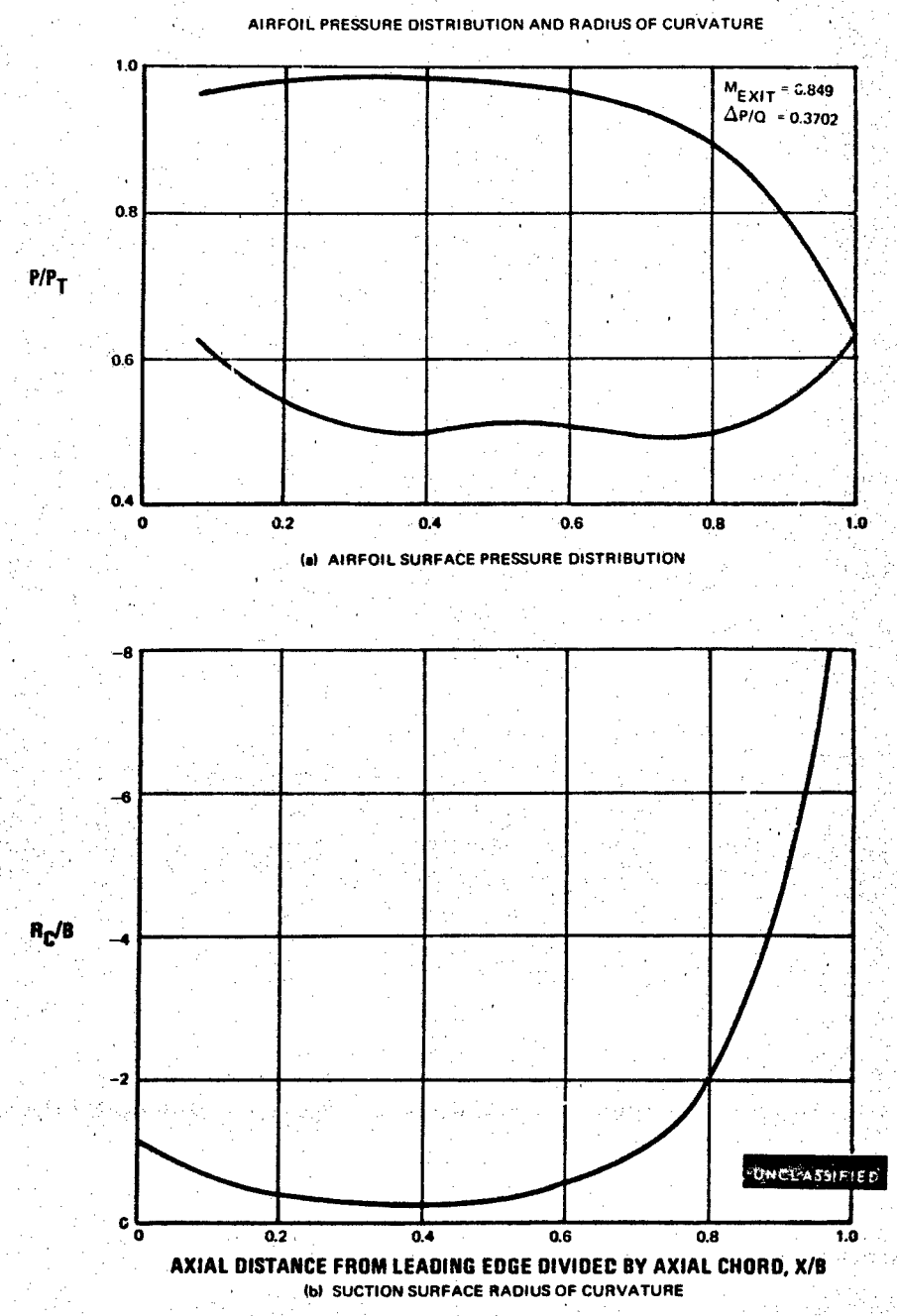

Figure 119 Medium Reaction, Medium Solidity, First Stage Blade, 1/4 Root Section

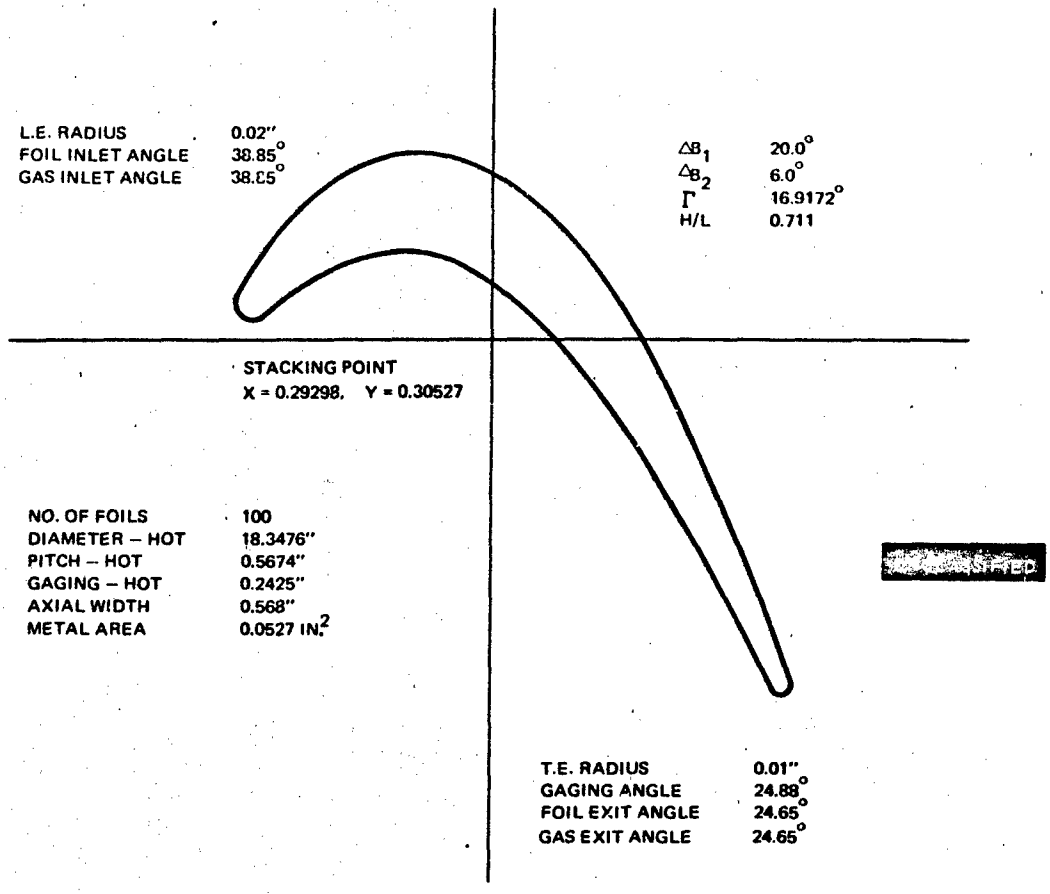

Figure 120 Medium Reaction, Medium Solidity, First Stage Blade, Mean (C-C) Section

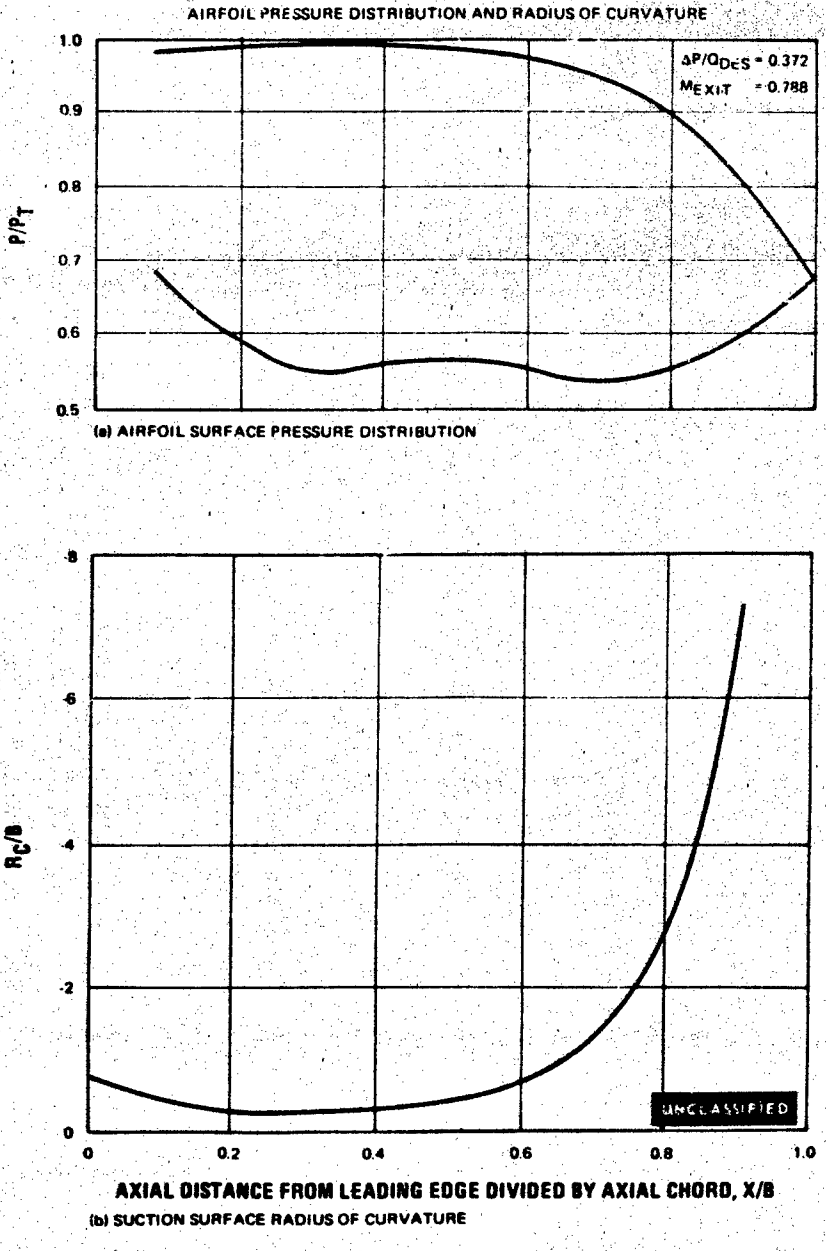

Figure 121 Medium Reaction, Medium Solidity, First Stage Blade, Mean Section

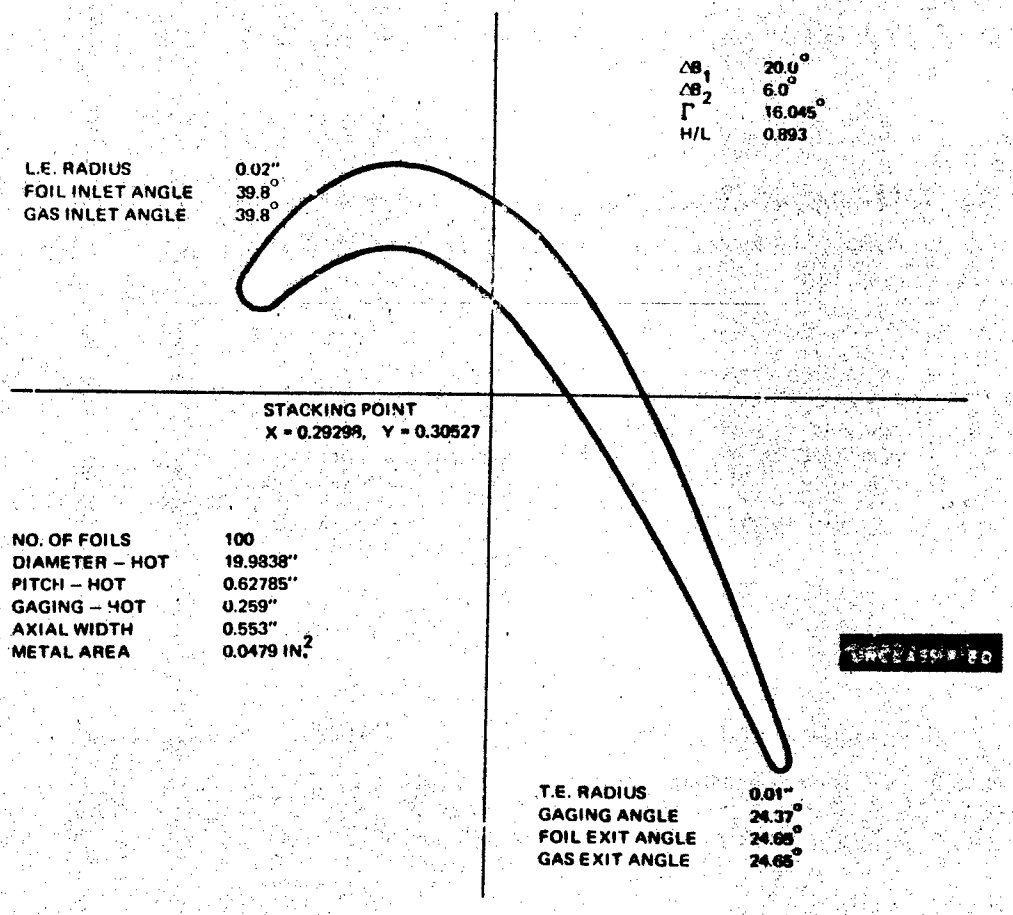

Figure 122 Medium Reaction, Medium Solidity, First Stage Blade, 1/4 Tip (D-D) Section

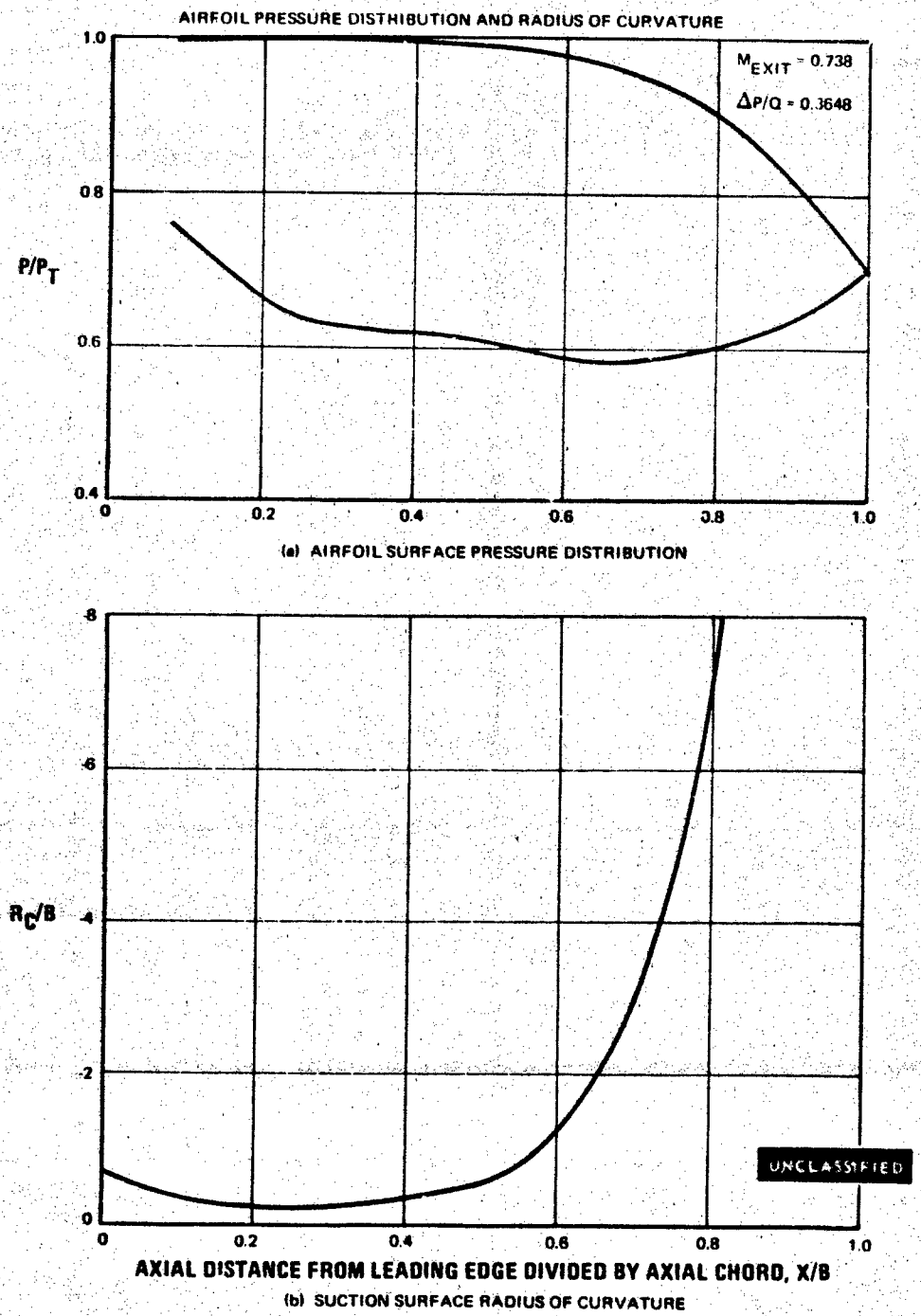

Figure 123 Medium Reaction, Medium Solidity, First Stage Blade, 1/4 Tip Section

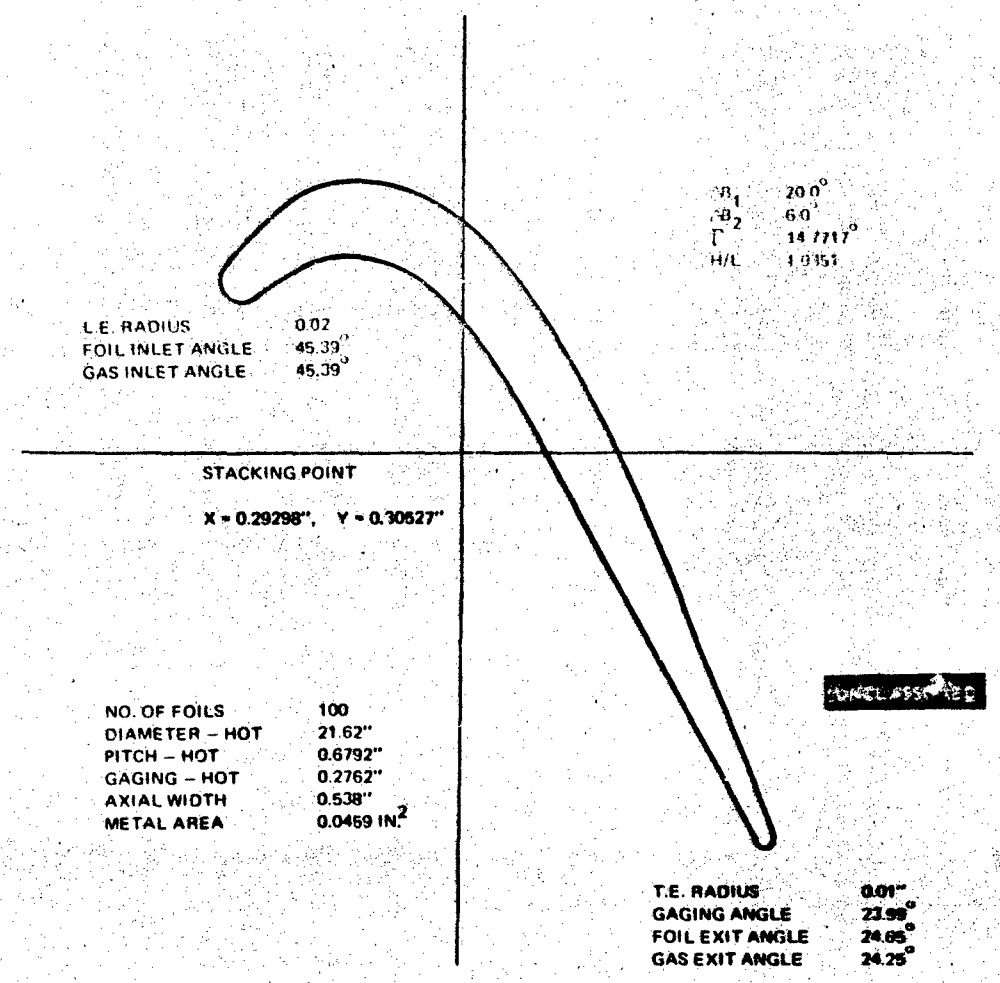

Figure 124 Medium Reaction, Medium Solidity, First Stage Blade, Tip (G-G) Section

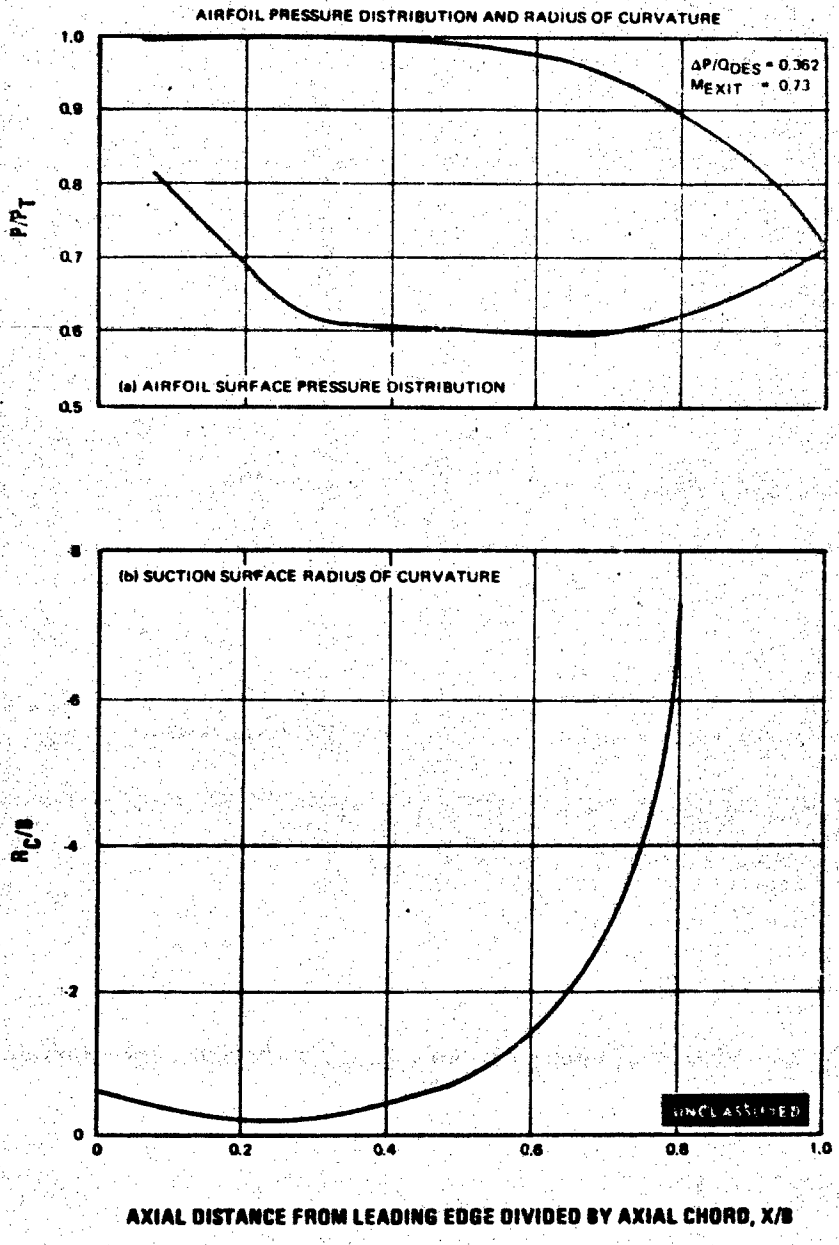

Figure 125 Medium Reaction, Medium Solidity, First Stage Blade, Tip Section

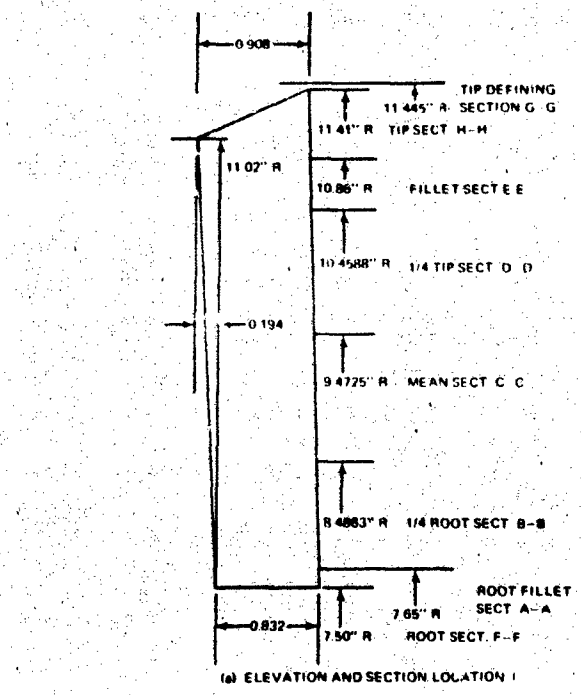

(a) ELEVATION AND SECTION LOCATION

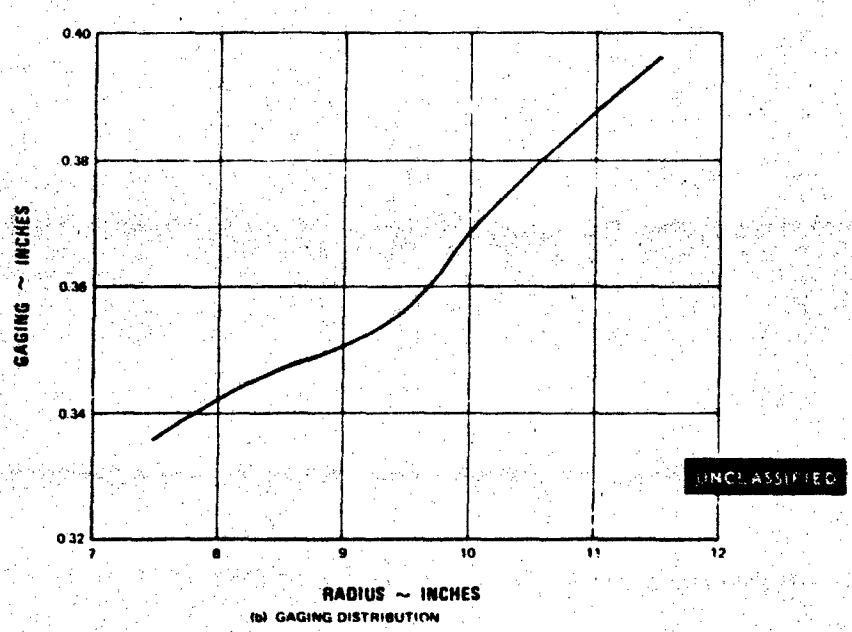

(b) GAGING DISTRIBUTION

Figure 126 Medium Reaction, Medium Solidity, Second Stage Vane

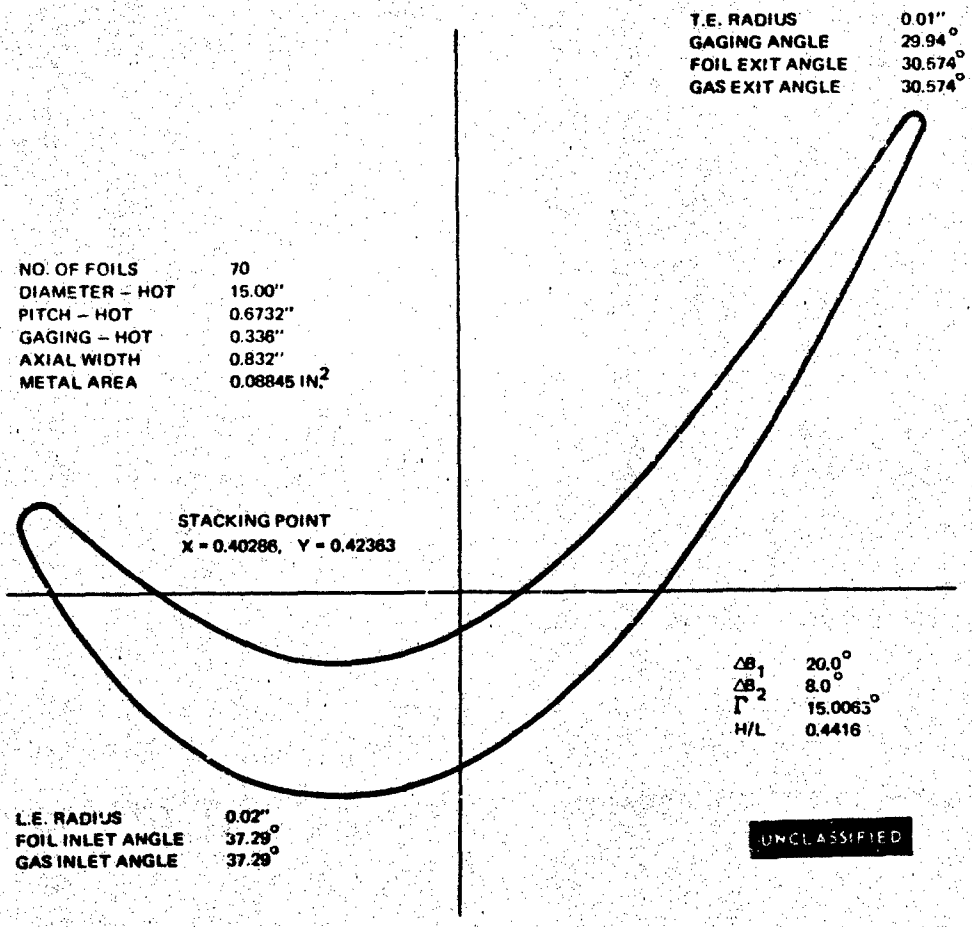

Figure 127 Medium Reaction, Medium Solidity, Second Stage Vane, Root (F-F) Section

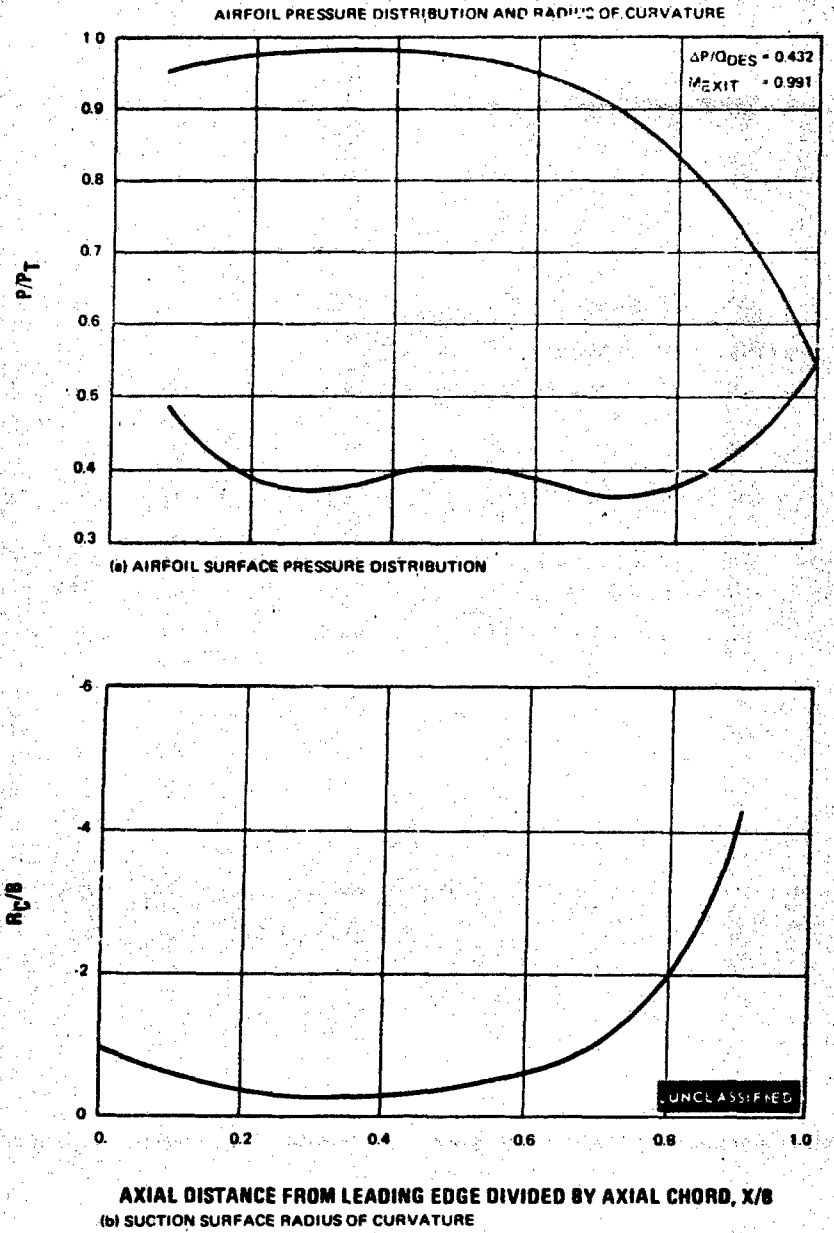

Figure 128 Medium Reaction, Medium Solidity, Second Stage Vane, Root Section

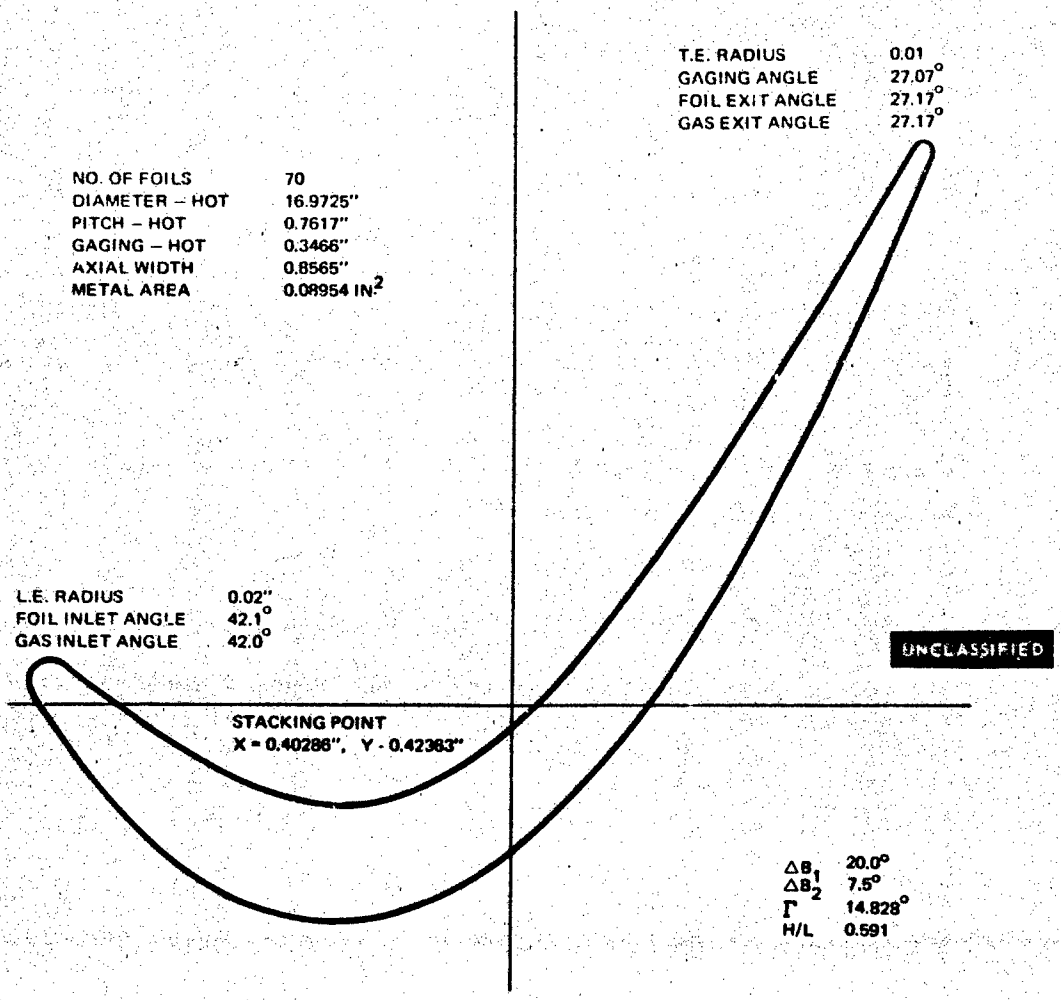

Figure 129 Medium Reaction, Medium Solidity, Second Stage Vane, 1/4 Root (B-B) Section

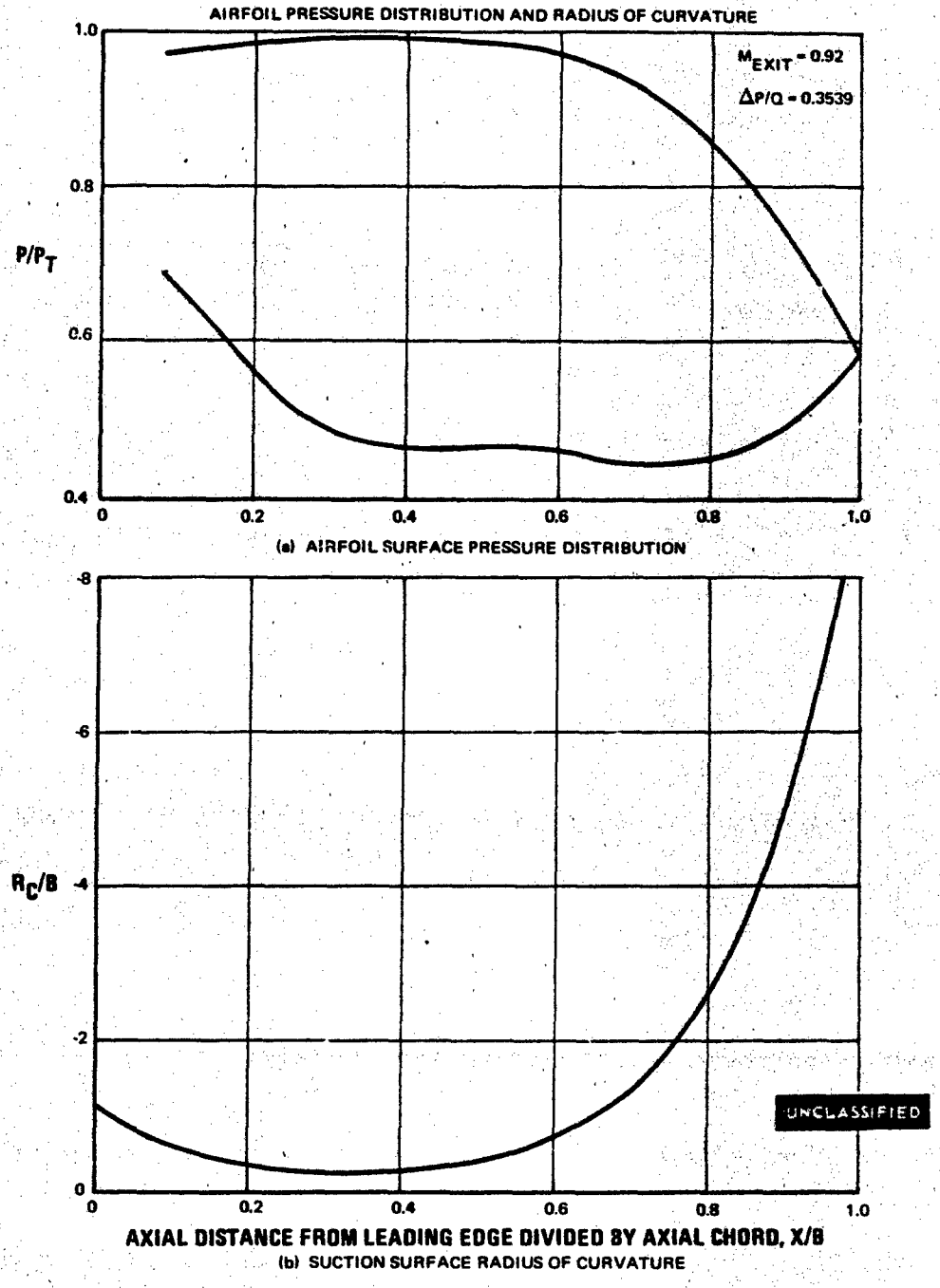

Figure 130 Medium Reaction, Medium Solidity, Second Stage Vane, 1/4 Root Section

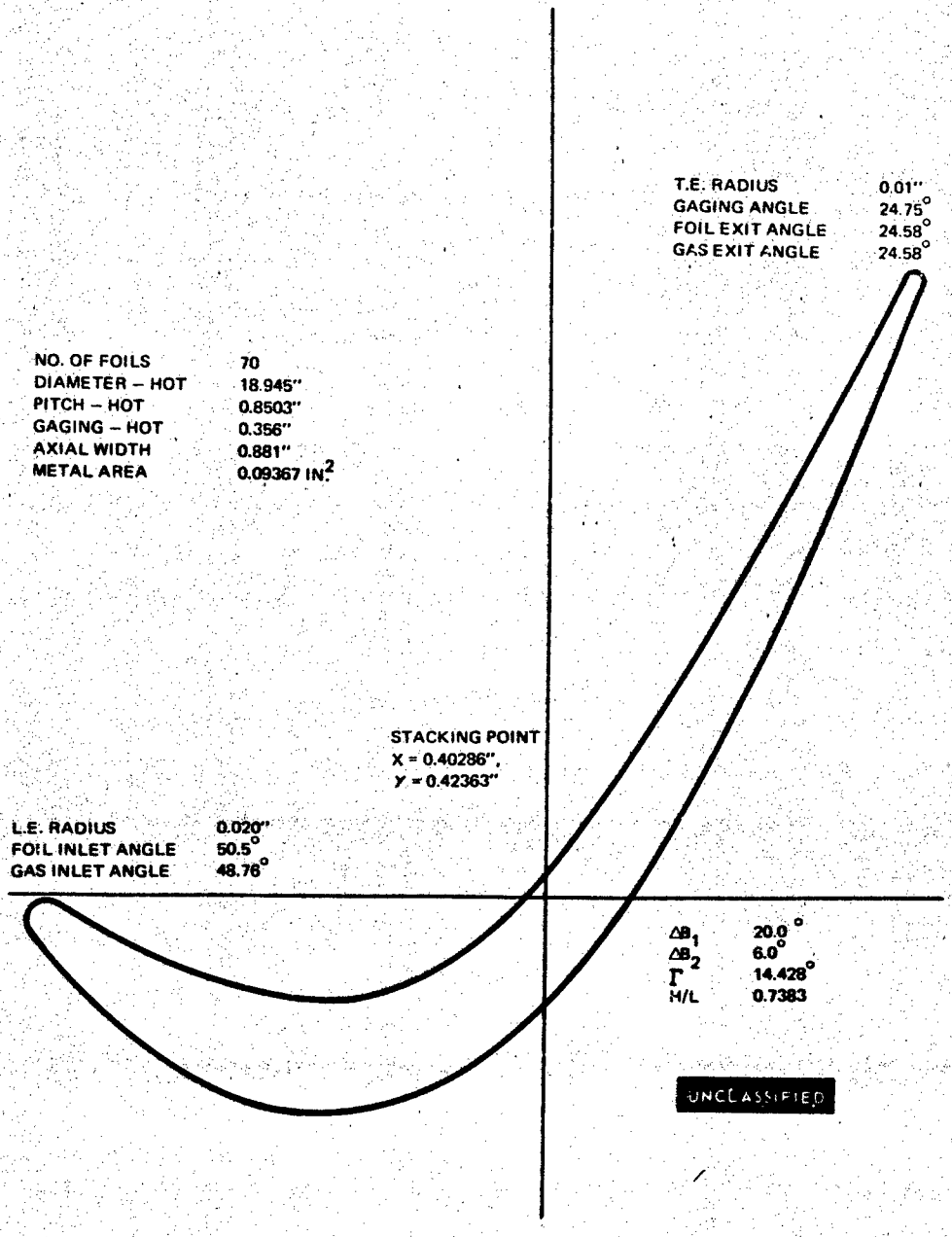

Figure 131 Medium Reaction, Medium Solidity, Second Stage Vane, Mean (C-C) Section

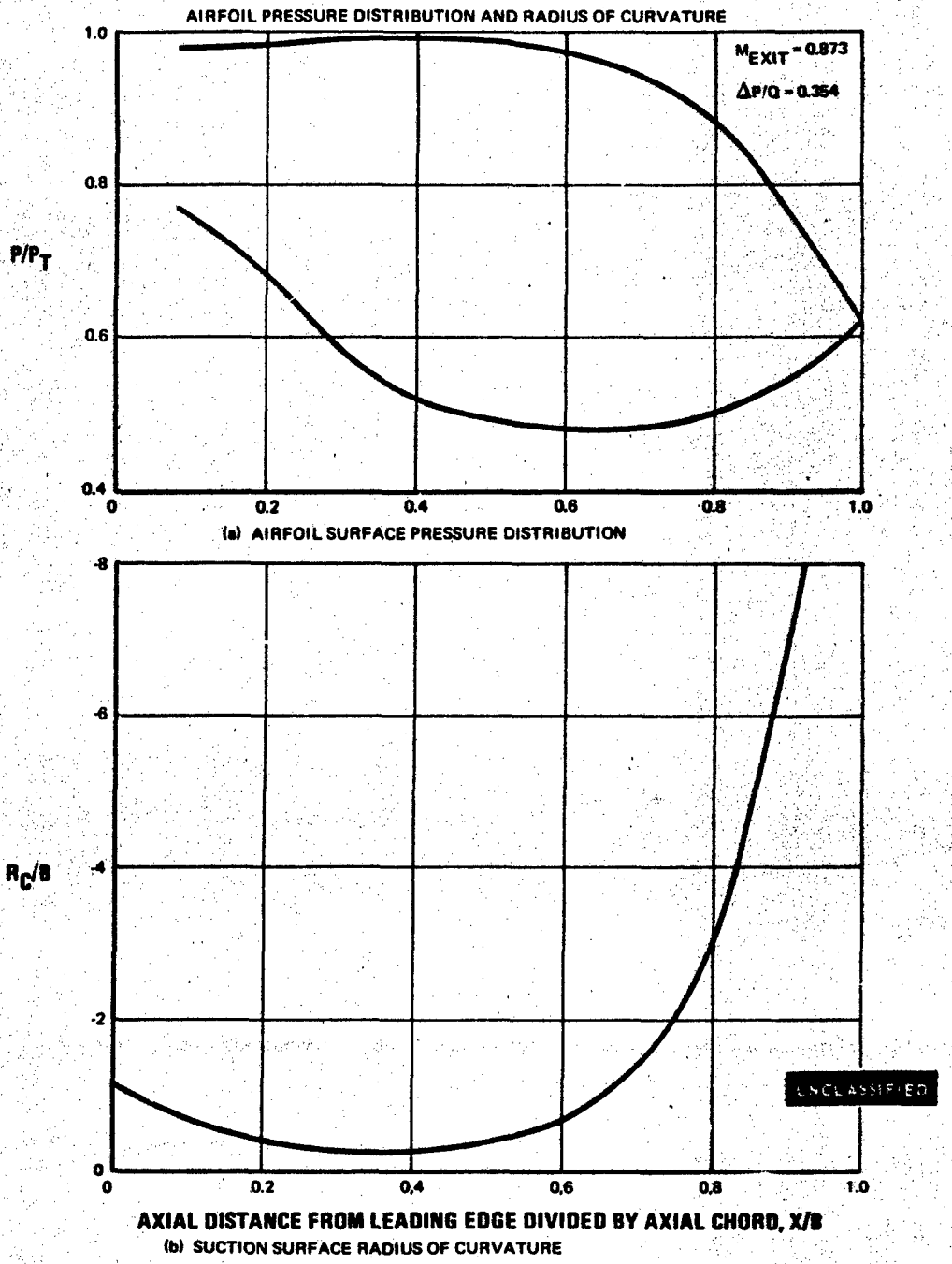

Figure 132 Medium Reaction, Medium Solidity, Second Stage Vane, Mean Section

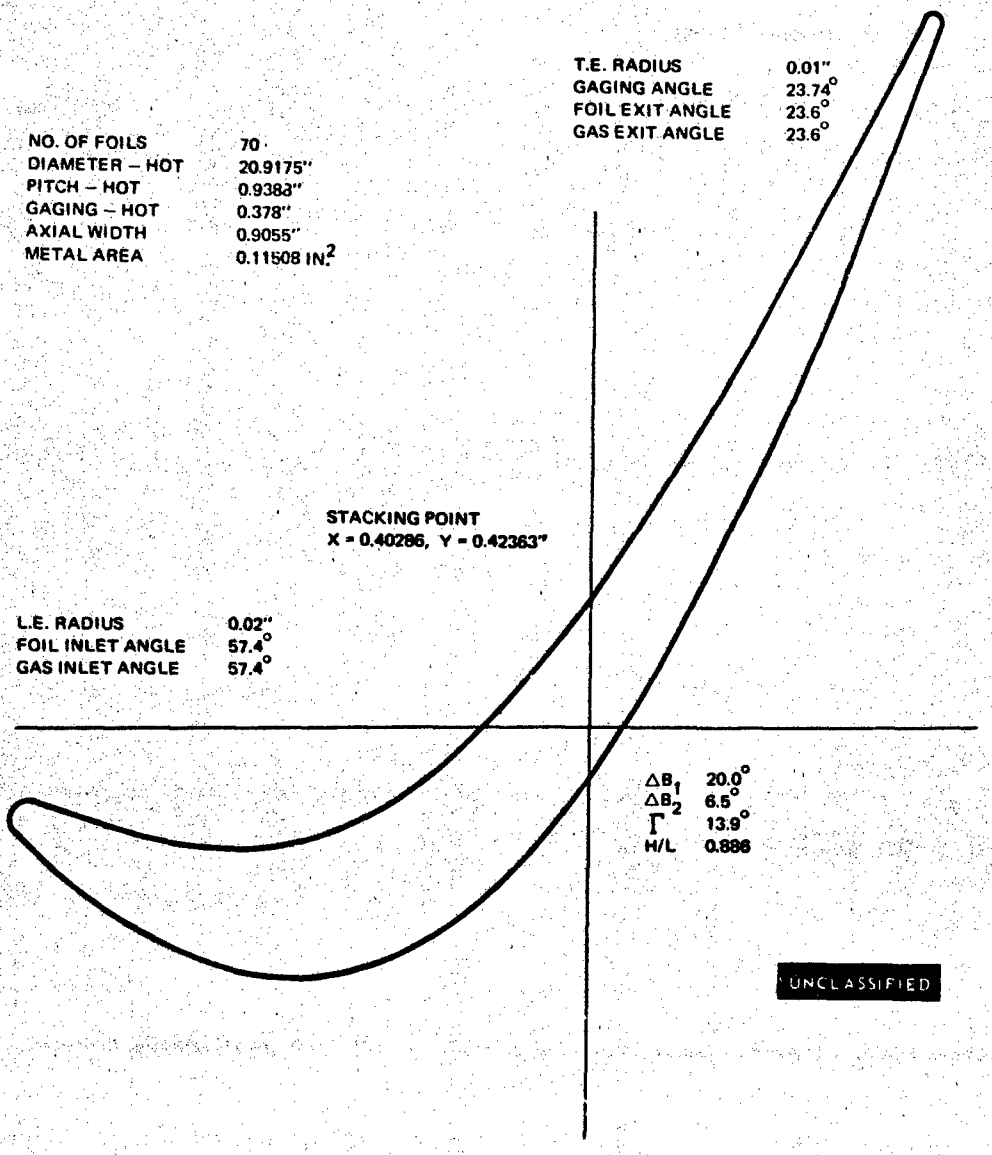

Figure 133 Medium Reaction, Medium Solidity, Second Stage Vane, 1/4 Tip (D-D) Section

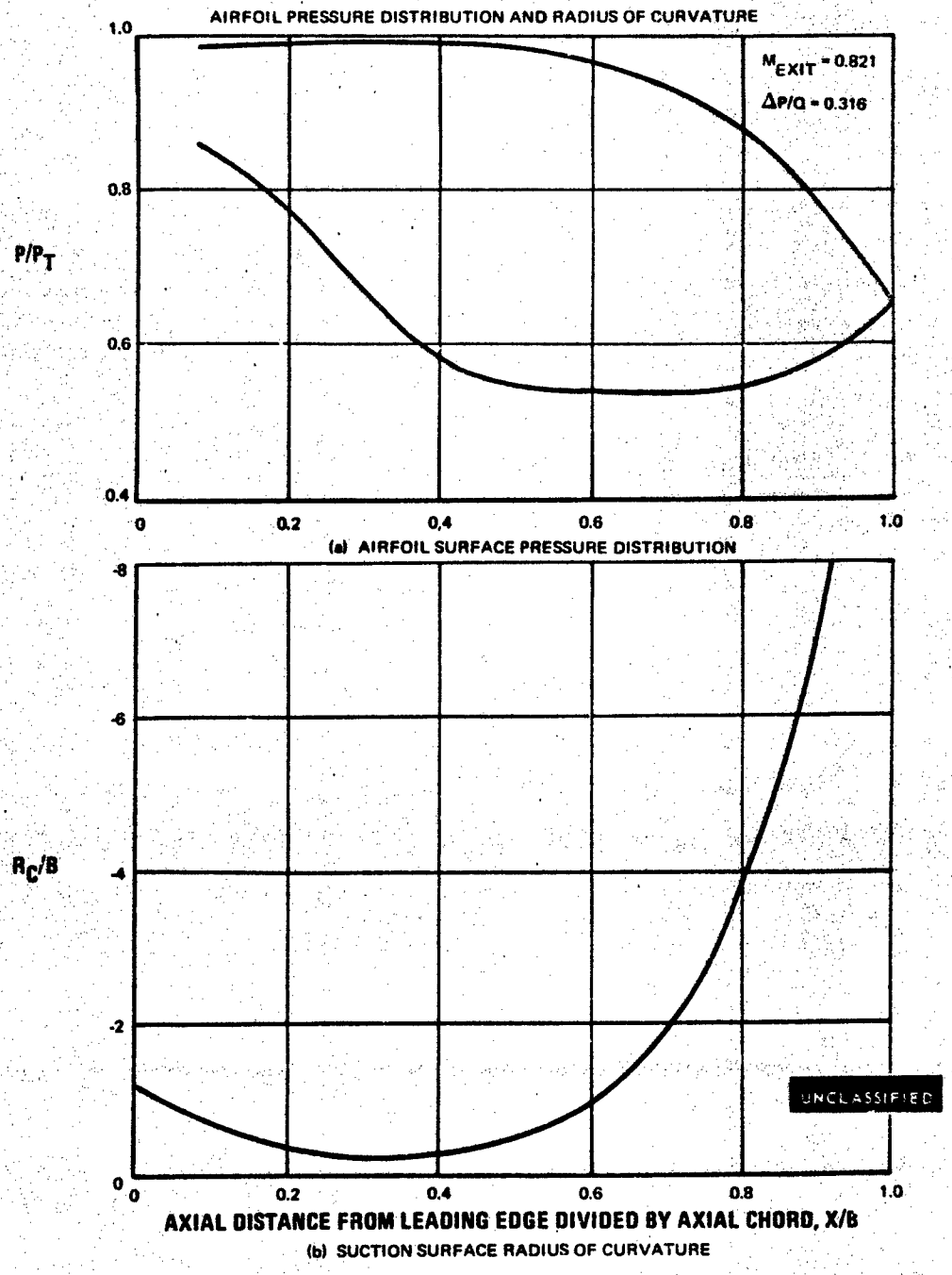

Figure 134 Medium Reaction, Medium Solidity, Second Stage Vane, 1/4 Tip Section

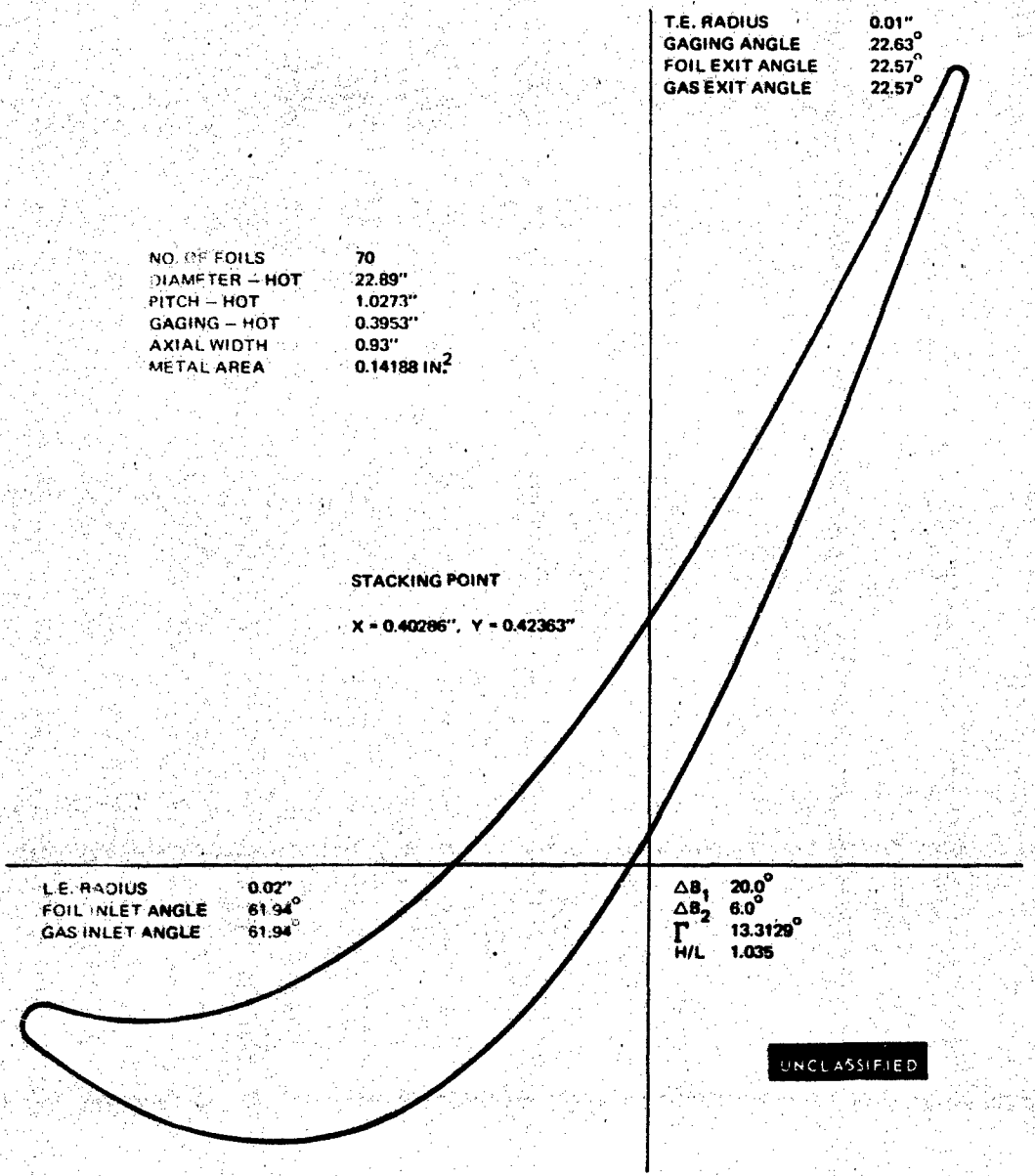

Figure 135 Medium Reaction, Medium Solidity, Second Stage Vane, Tip (H-H) Section

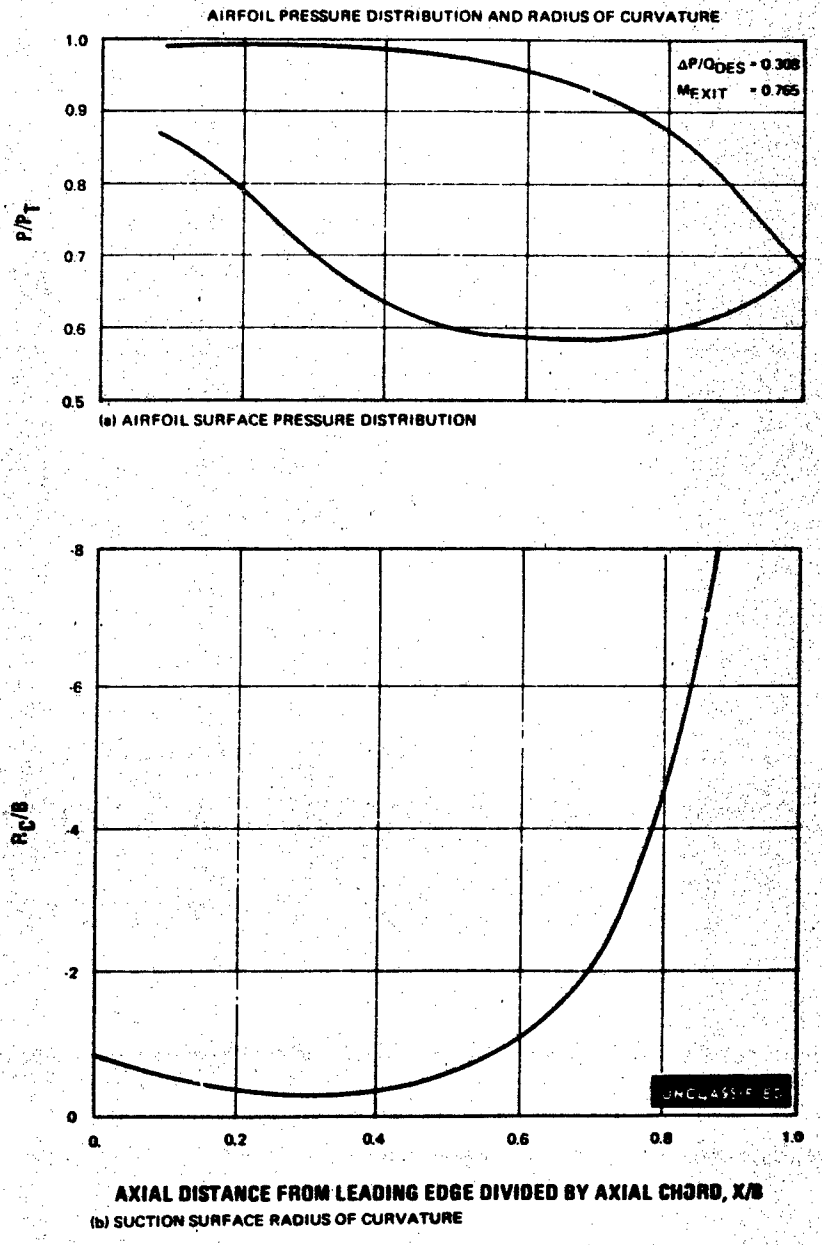

Figure 136 Medium Reaction, Medium Solidity, Second Stage Vane, Tip Section

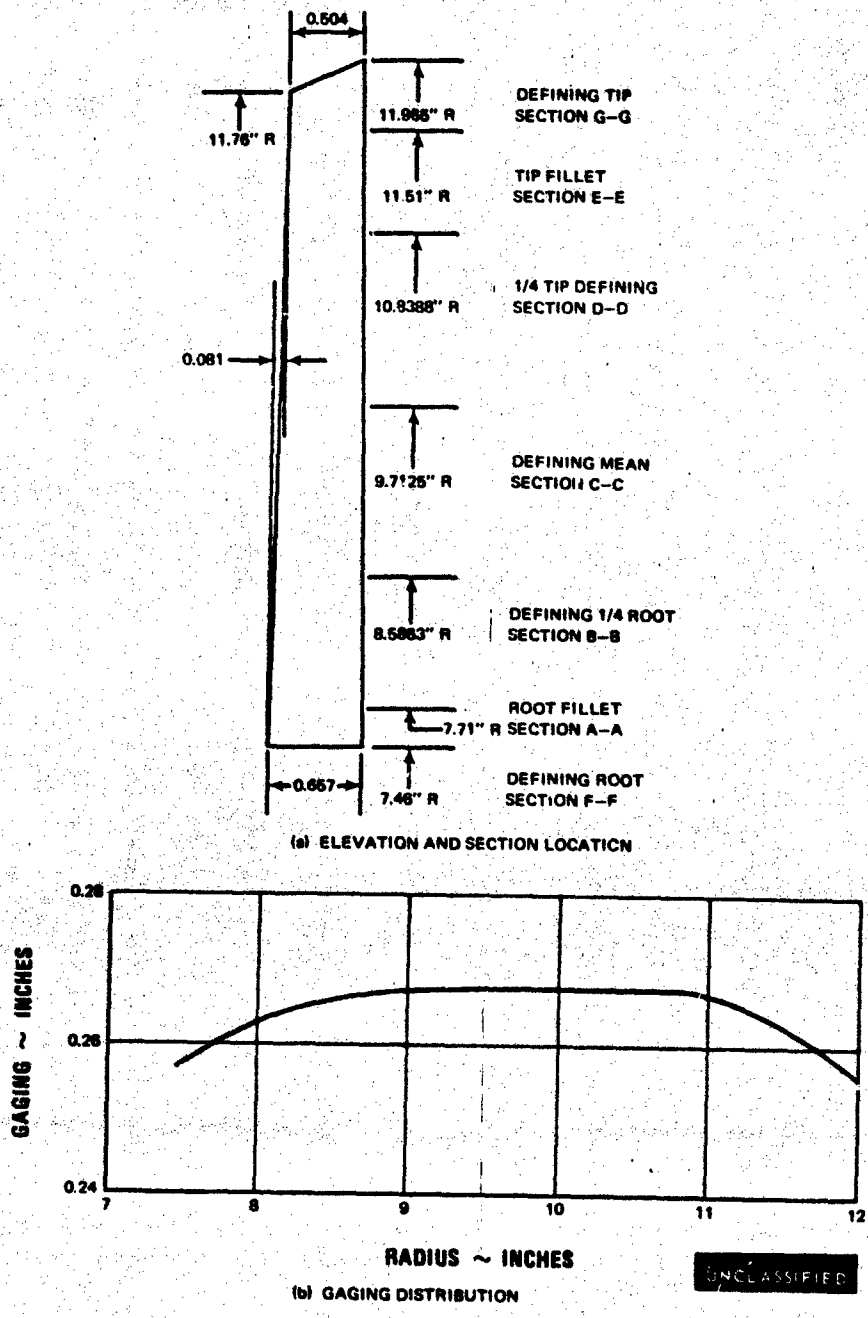

Figure 137 Medium Reaction, Medium Solidity, Second Stage Blade

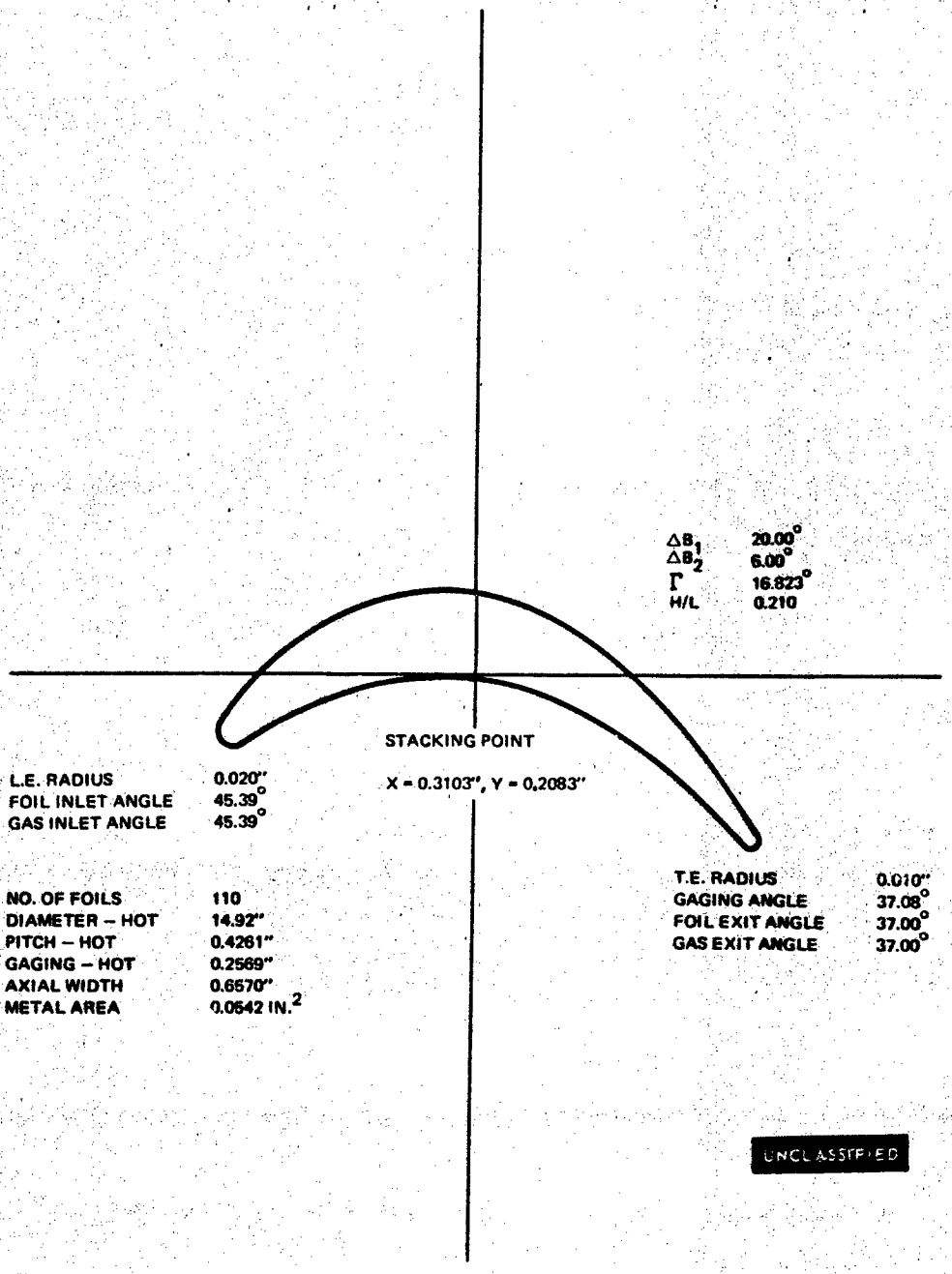

Figure 138 Medium Reaction, Medium Solidity, Second Stage Blade, Root (F-F) Section

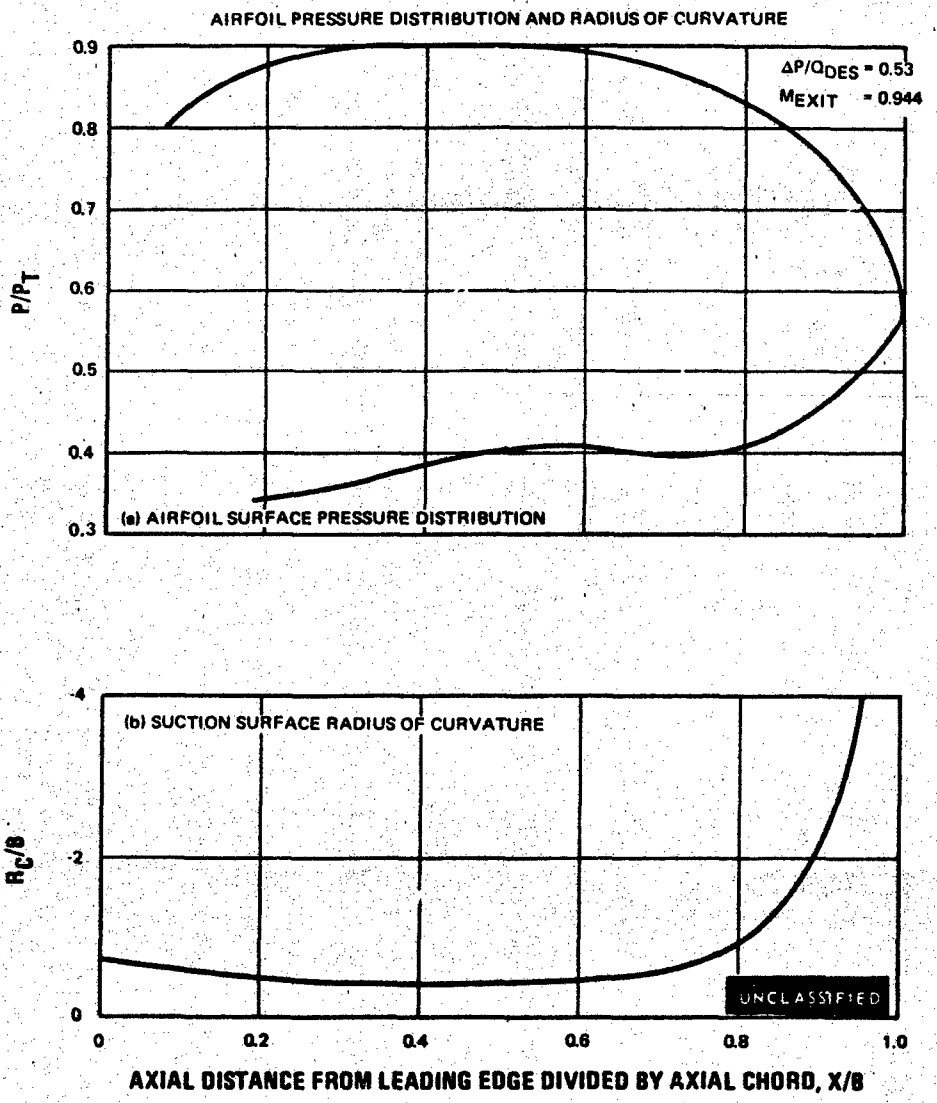

Figure 139 Medium Reaction, Medium Solidity, Second Stage Blade, Root Section

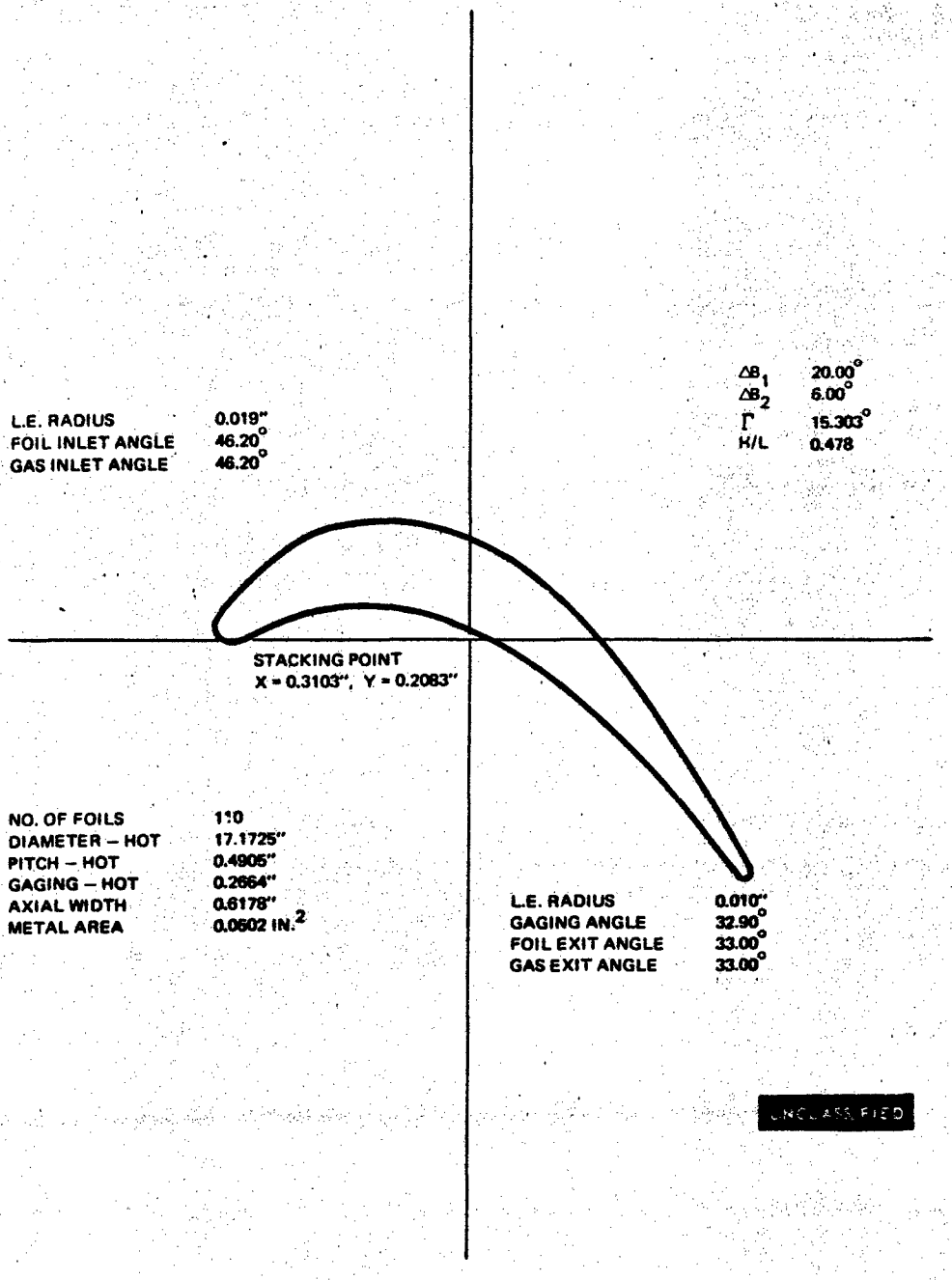

Figure 140 Medium Reaction, Medium Solidity, Second Stage Blade, 1/4 Root (B-B) Section

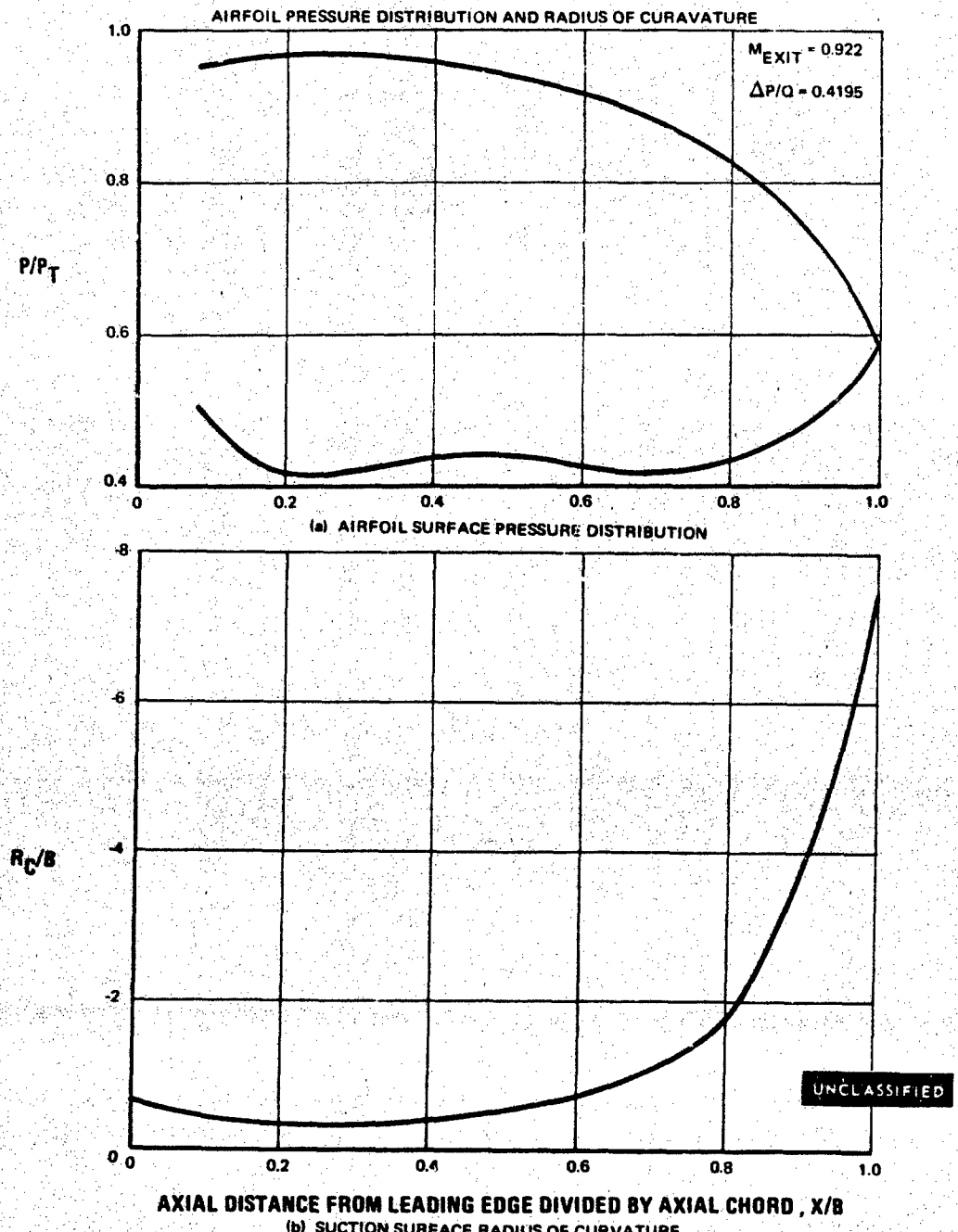

Figure 141 Medium Reaction, Medium Solidity, Second Stage Blade, 1/4 Root Section

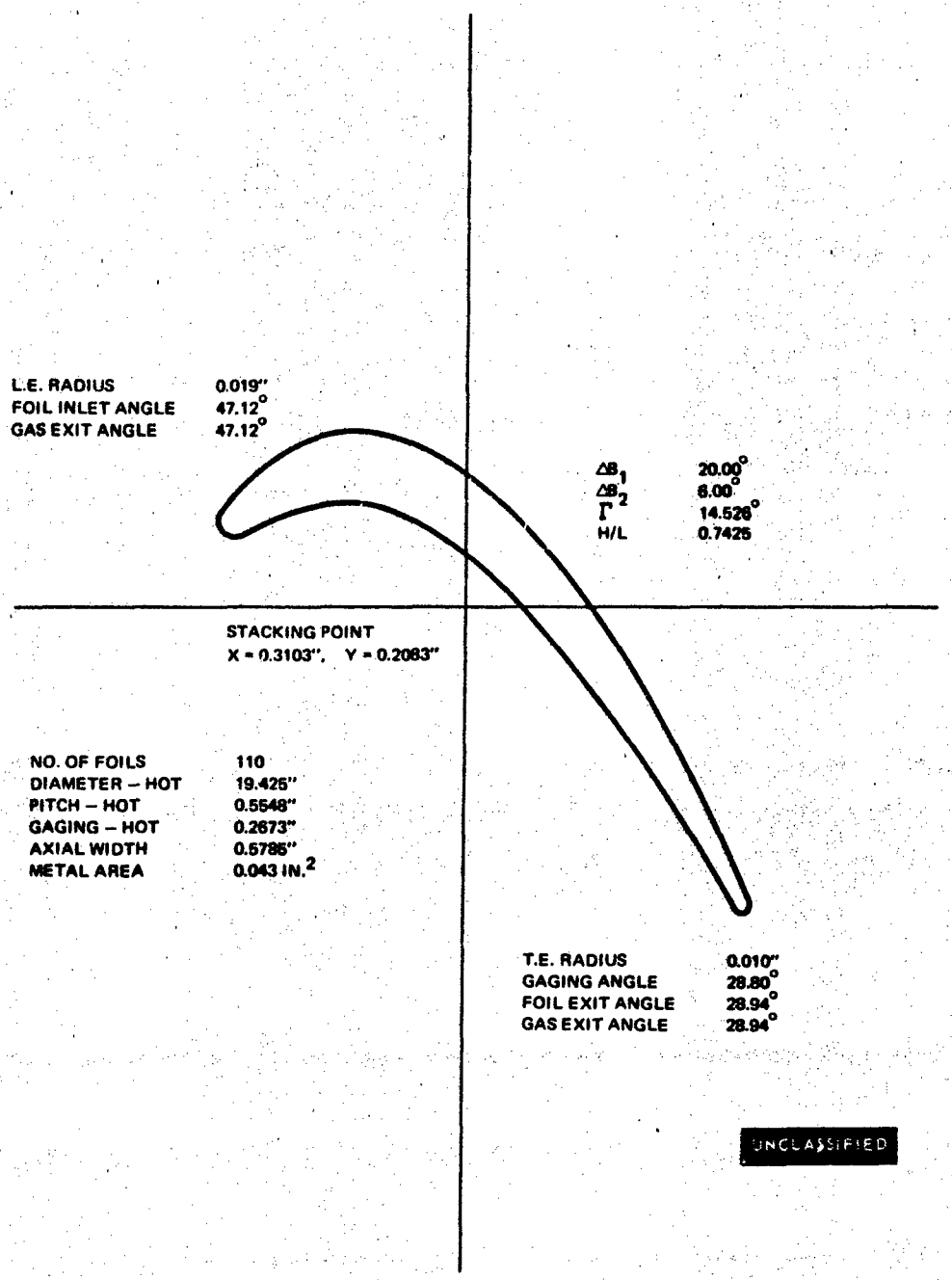

Figure 142 Medium Reaction, Medium Solidity, Second Stage Blade, Mean (C-C) Section

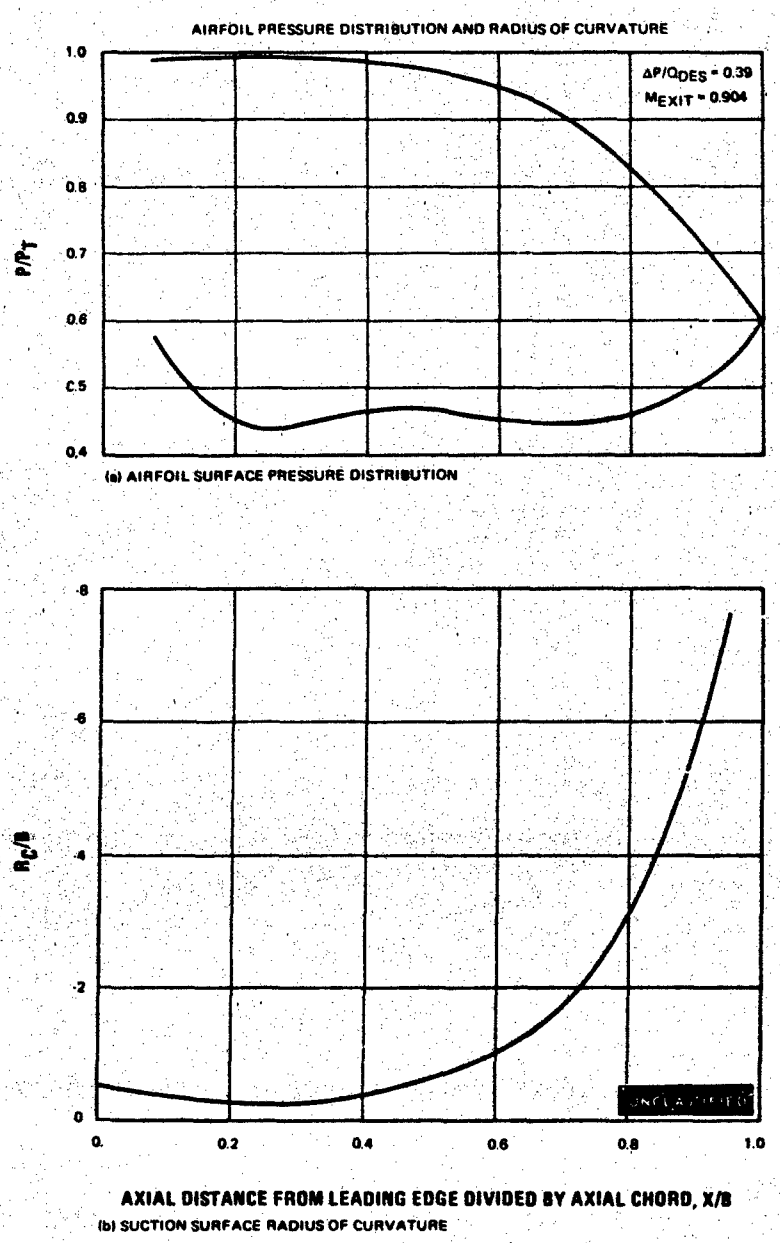

Figure 143 Medium Reaction, Medium Solidity, Second Stage Blade, Mean Section

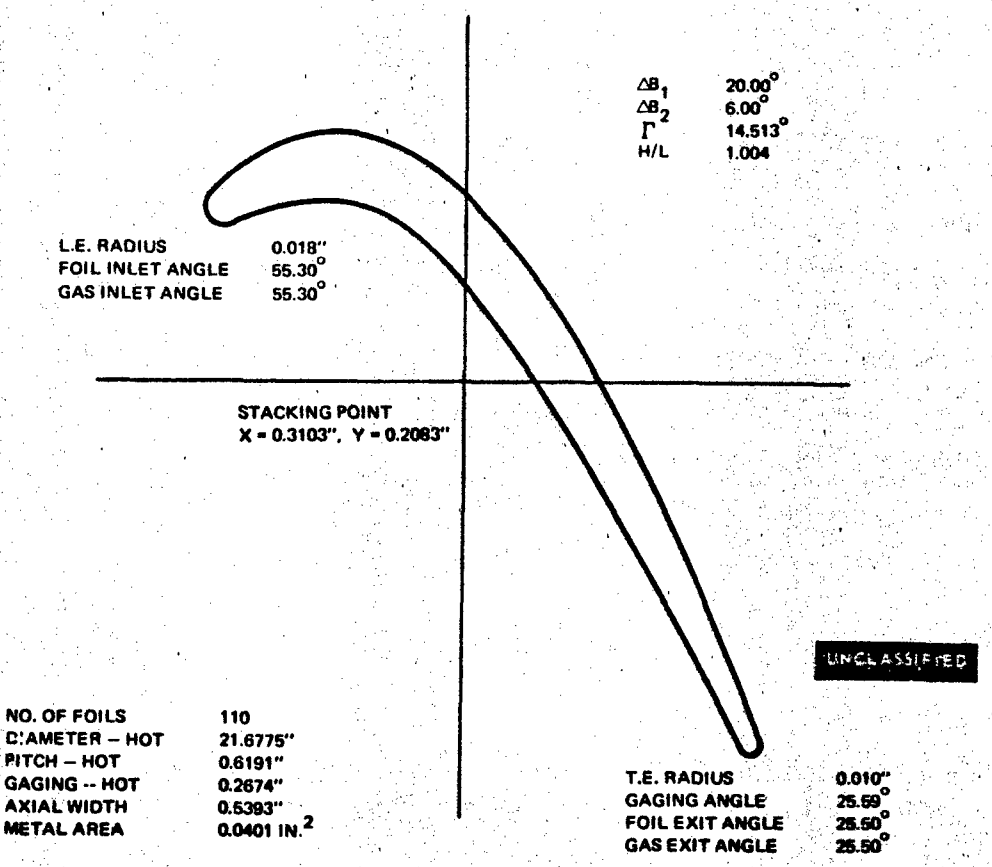

Figure 144 Medium Reaction, Medium Solidity, Second Stage Blade, 1/4 Tip (D-D) Section

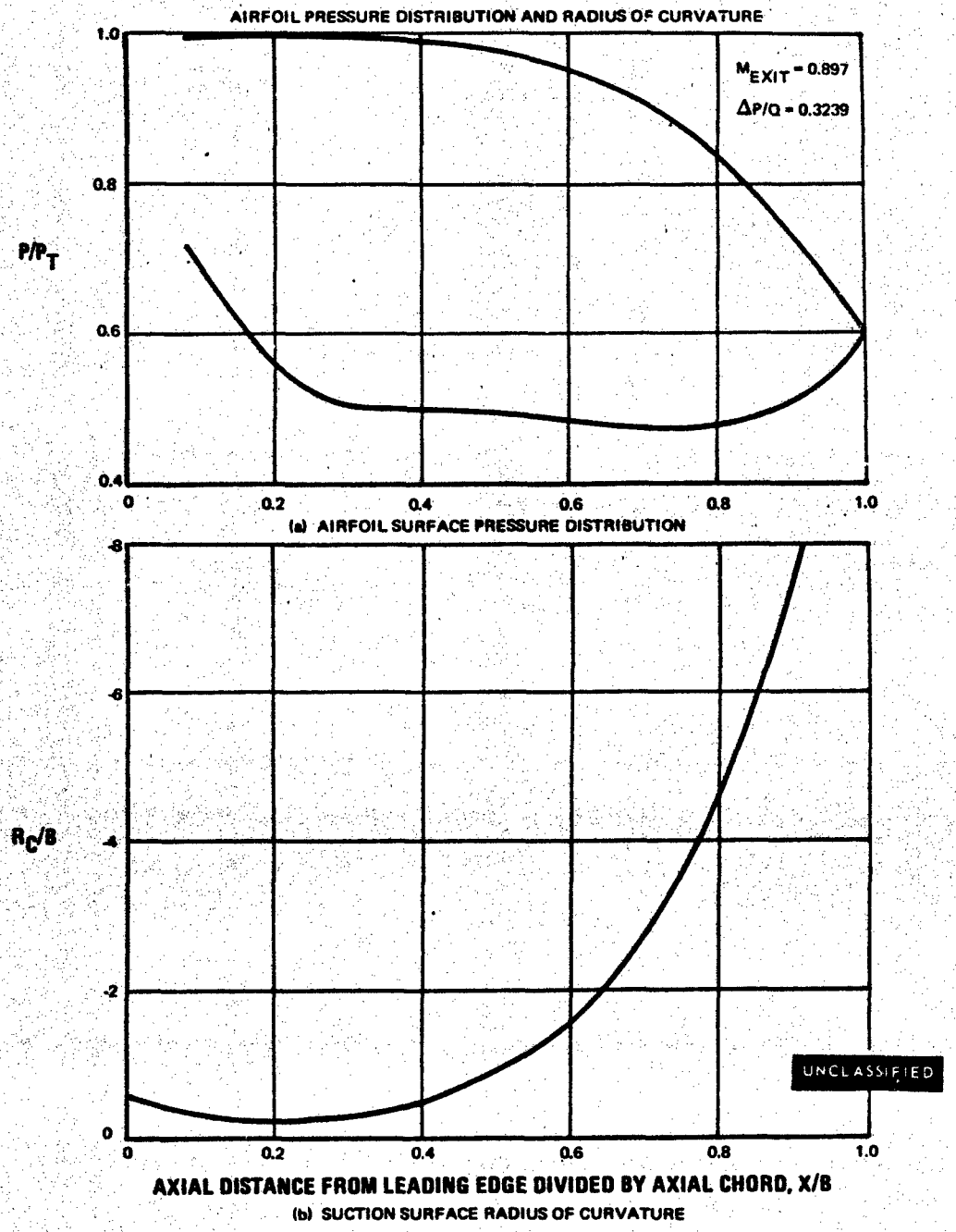

Figure 145 Medium Reaction, Medium Solidity, Second Stage Blade, 1/4 Tip Section

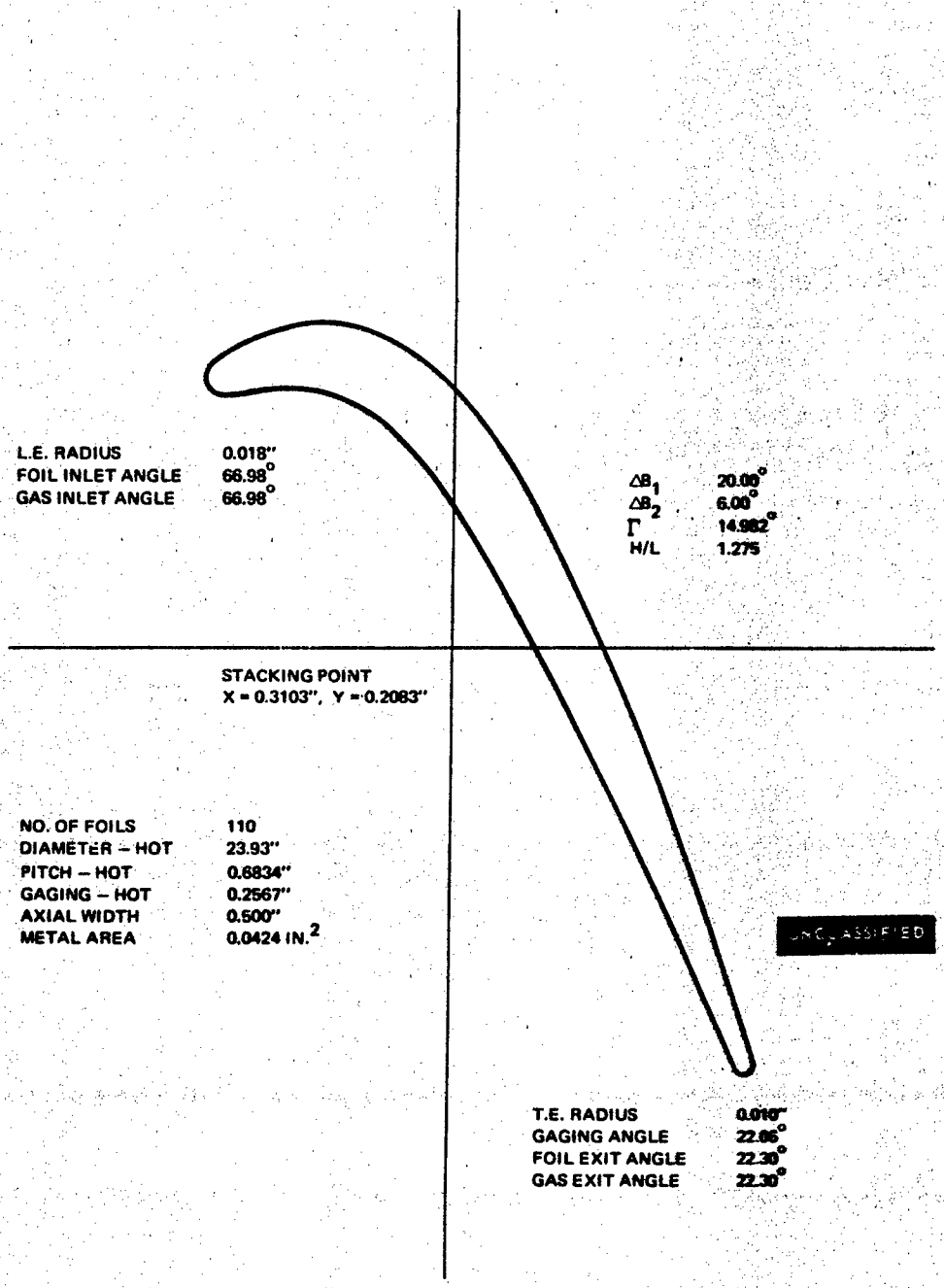

Figure 146 Medium Reaction, Medium Solidity, Second Stage Blade, Tip (G-G) Section

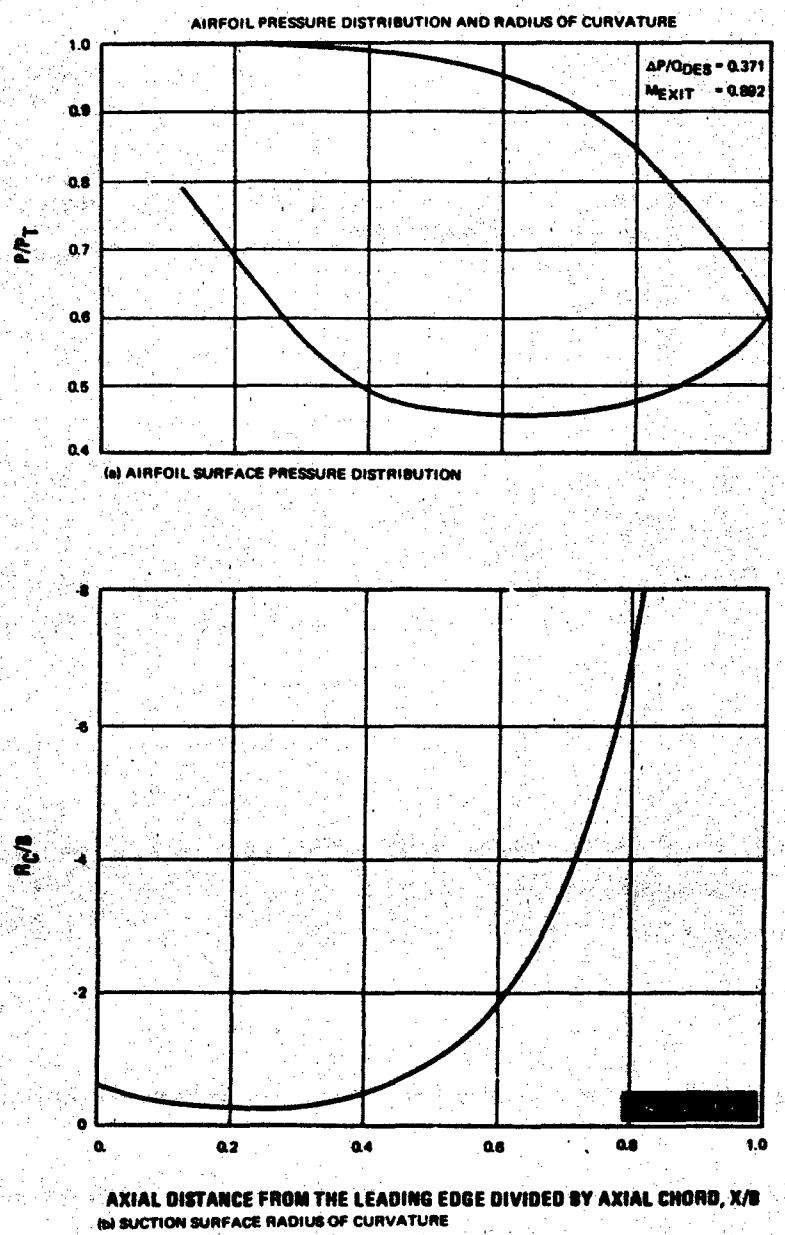

Figure 147 Medium Reaction, Medium Solidity, Second Stage Blade, Tip Section

TABLE VI
FIRST STAGE VANE

Section F-F AT R = 7.57500

Percent X	X	Y (Top)	(Circle)	Y (Bot)	(Circle)
.00	.00000	.81186	.79733	.75939	.79733
.01	.00765	.81793	.81734	.76121	.77732
.02	.01530	.82391		.76303	.77119
.03	.02295	.82949		.76485	.76818
.04	.03060	.83462		.76668	.76735
.05	.03825	.83929		.76847	
.10	.07650	.85634		.77338	
.15	.11475	.86375		.77034	
.20	.15300	.86251		.75946	
.25	.19125	.85339		.74110	
.30	.22950	.83701		.71582	
.35	.26775	.81386		.68431	
.40	.30600	.78434		.64731	
.45	.34425	.74875		.60553	
.50	.38250	.70738		.55966	
.55	.42075	.66042		.51028	
.60	.45900	.60805		.45793	
.65	.49725	.55039		.40306	
.70	.53550	.48759		.34603	
.75	.57375	.41983		.28717	
.80	.61200	.34725		.22675	
.85	.65025	.27000		.16497	
.90	.68850	.18827		.10204	
.95	.72675	.10222		.03809	
.98	.74970	.04850		-.00070	.00145
.99	.75735	.03022		-.01366	.00018
1.00	.76500	.01187	.00987	- 02663	.00987

LE Center	(.02998,	.79733)	R = .02998			
TE Center	(.75504,	.00987)	R = .00996			
Center of Gravity	(.38952,	.56570)				
Radial Reference	(.38952,	.56570)				
Gaging =	.39587					
Nose Point	(.00331,	.78363)				
Tail Point	(.75942,	.00092)				
LE Tangency Points	Top	(.01152,	.82095)	Bottom	(.03682,	.76813)
TE Tangency Points	Top	(.76423,	.01372)	Bottom	(.74646,	.00480)
Inlet Angle =	64.40788					
Exit Angle =	26.64093					
No. of Blades =	54					
Pitch =	.88139					
Tolerance =	-.00000					
Gaging =	.39587					
Uncovered Turning =	14.13973					
Gaging Angle =	26.68885					
Area =	.08700					
Axial Chord =	.76500					

UNCLASSIFIED

TABLE VII
FIRST STAGE VANE

Section A-A AT R = 7.72500

Percent X	X	Y (Top)	(Circle)	Y (Bot)	(Circle)
.00	-.01376	.81353	.79917	.75815	.79917
.01	-.00603	.81996	.81941	.76074	.77892
.02	.00170	.82614		.76318	.77270
.03	.00943	.83191		.76549	.76964
.04	.01716	.83724		.76766	.76879
.05	.02489	.84214		.76966	
.10	.06354	.86042		.77523	
.15	.10219	.86904		.77292	
.20	.14083	.86879		.76267	
.25	.17948	.86031		.74468	
.30	.21813	.84415		.71944	
.35	.25678	.82077		.68759	
.40	.29543	.79060		.64987	
.45	.33408	.75396		.60706	
.50	.37273	.71120		.55990	
.55	.41138	.66258		.50902	
.60	.45003	.60835		.45502	
.65	.48868	.54871		.39839	
.70	.52733	.48386		.33952	
.75	.56597	.41399		.27878	
.80	.60462	.33926		.21643	
.85	.64327	.25980		.15272	
.90	.68192	.17577		.08785	
.95	.72057	.08730		.02195	
.98	.74376	.03207		-.01800	-.01589
.99	.75149	.01328		-.03138	-.01727
1.00	.75922	-.00557	-.00755	-.04476	-.00755

LE Center	(.01662,	.79917)	R = .03039		
TE Center	(.74924,	-.00755)	R = .00998		
Center of Gravity	(.37914,	.56544)			
Radial Reference	(.38952,	.56570)			
Gaging =	.39764				
Nose Point	(-.00980,	.78416)			
Tail Point	(.75357,	-.01654)			
LE Tangency Points	Top	(-.00235,	.82290)	Bottom	(.02096, .76909)
TE Tangency Points	Top	(.75847,	-.00374)	Bottom	(.74060, -.01254)

Inlet Angle =	66.57798
Exit Angle =	26.21735
No. of Blades =	54
Pitch =	.89884
Tolerance =	-.00000
Gaging =	.39764
Uncovered Turning =	13.86707
Gaging Angle =	26.25680
Area =	.09002
Axial Chord =	.77298

UNCLASSIFIED

TABLE VIII
FIRST STAGE VANE

Section B-B AT R = 8.25650

Percent X	X	Y (Top)	(Circle)	Y (Bot)	(Circle)
.00	-.06252	.82125	.80674	.76006	.80674
.01	-.05451	.82853	.82809	.76362	.78538
.02	-.04650	.83541		.76691	.77874
.03	-.03849	.84188		.76993	.77538
.04	-.03047	.84794		.77267	.77427
.05	-.02246	.85360		.77513	
.10	.01760	.87586		.78294	
.15	.05767	.88827		.78278	
.20	.09773	.89113		.77421	
.25	.13779	.88476		.75710	
.30	.17786	.86953		.73171	
.35	.21792	.84581		.69858	
.40	.25798	.81398		.65847	
.45	.29805	.77446		.61226	
.50	.33811	.72763		.56080	
.55	.37817	.67391		.50491	
.60	.41824	.61367		.44530	
.65	.45830	.54729		.38257	
.70	.49836	.47507		.31725	
.75	.53842	.39728		.24976	
.80	.57849	.31414		.18044	
.85	.61855	.22585		.10958	
.90	.65861	.13255		.03742	
.95	.69868	.03438		-.03584	
.98	.72272	-.02687		-.08029	-.07838
.99	.73073	-.04766		-.09518	-.08020
1.00	.73874	-.06854	-.07040	-.11006	-.07040

LE Center	(-.03005,	.80674)	R = .03247			
TE Center	(.72874,	-.07040)	R = .01000			
Center of Gravity	(.34432,	.56408)				
Radial Reference	(.38952,	.56570)				
Gaging =	.40141					
Nose Point	(-.05742,	.78926)				
Tail Point	(.73284,	-.07952)				
LE Tangency Points	Top	(-.05120,	.83138)	Bottom	(-.02384,	.77486)
TE Tangency Points	Top	(.73807,	-.06680)	Bottom	(.71993,	-.07514)

Inlet Angle = 61.700°
Exit Angle = 24.600°

No. of Blades = 54
Pitch = .96066

Tolerance = .00000
Gaging = .40143

Uncovered Turning = 13.438°
Gaging Angle = 24.700°

Area = .10202 in^2
Axial Chord = .80125"

TABLE IX
FIRST STAGE VANE

Section C-C AT R = 8.93800

Percent X	X	Y (Top)	(Circle)	Y (Bot)	(Circle)
.00	-.12505	.83335	.81803	.76991	.81803
.01	-.11667	.84115	.84080	.77263	.79526
.02	-.10830	.84885		.77536	.78809
.03	-.09992	.85618		.77808	.78436
.04	-.09154	.86311		.78081	.78294
.05	-.08317	.86964		.78352	.78356
.10	-.04129	.89620		.79372	
.15	.00058	.91267		.79526	
.20	.04246	.91906		.78765	
.25	.08434	.91551		.77075	
.30	.12621	.90218		.74472	
.35	.16809	.87924		.71004	
.40	.20996	.84694		.66740	
.45	.25184	.80556		.61761	
.50	.29372	.75538		.56155	
.55	.33559	.69674		.50007	
.60	.37747	.62998		.43393	
.65	.41935	.55543		.36384	
.70	.46122	.47348		.29037	
.75	.50310	.38451		.21406	
.80	.54498	.28888		.13531	
.85	.58685	.18697		.05449	
.90	.62873	.07917		-.02811	
.95	.67060	-.03416		-.11222	
.98	.69573	-.10477		-.16335	-.16182
.99	.70411	-.12875		-.18045	-.16435
1.00	.71248	-.15280	-.15450	-.19756	-.15450

LE Center	(-.08992,	.81803)	R = .03513			
TE Center	(.70250,	-.15450)	R = .00998			
Center of Gravity	(.30185,	.56245)				
Radial Reference	(.38952,	.56570)				
Gaging =	.40062					
Nose Point	(-.11970,	.79941)				
Tail Point	(.70627,	-.16373)				
LE Tangency Points	Top	(-.11369,	.84390)	Bottom	(-.08160,	.78390)
TE Tangency Points	Top	(.71192,	-.15120)	Bottom	(.69354,	.15889)
Inlet Angle =	61.86554					
Exit Angle =	22.68680					
No. of Blades =	54					
Pitch =	1.03998					
Tolerance =	-.00000					
Gaging =	.40062					
Uncovered Turning =	12.97424					
Gaging Angle =	22.65705					
Area =	.12231					
Axial Chord =	.83753					

UNCLASSIFIED

TABLE X
FIRST STAGE VANE

Section D-D AT R = 9.61900

Percent X	X	Y (Top)	(Circle)	Y (Bot)	(Circle)
.00	-.18752	.84325	.82721	.76997	.82721
.01	-.17879	.85175	.85134	.77463	.80307
.02	-.17005	.85990		.77895	.79538
.03	-.16131	.86770		.78292	.79129
.04	-.15257	.87515		.78655	.78960
.05	-.14383	.88223		.78983	.78997
.10	-.10015	.91213		.80080	
.15	-.05646	.93257		.80250	
.20	-.01277	.94322		.79473	
.25	.03092	.94378		.77747	
.30	.07461	.93404		.75089	
.35	.11829	.91383		.71536	
.40	.16198	.88306		.67136	
.45	.20567	.84172		.61952	
.50	.24936	.78986		.56048	
.55	.29305	.72763		.49493	
.60	.33674	.65523		.42354	
.65	.38042	.57292		.34694	
.70	.42411	.48106		.26573	
.75	.46780	.38008		.18044	
.80	.51149	.27050		.09155	
.85	.55518	.15285		-.00051	
.90	.59886	.02770		-.09538	
.95	.64255	-.10438		-.19273	
.98	.66877	-.18679		-.25223	-.25104
.99	.67750	-.21477		-.27224	-.25430
1.00	.68624	-.24284	-.24437	-.29226	-.24437

LE Center	(-.14981,	.82721)	R = .03771
TE Center	(.67623,	-.24437)	R = .01001
Center of Gravity	(.26082,	.56082)	
Radial Reference	(.38952,	.56570)	
Gaging =	.39374		
Nose Point	(-.18068,	.80555)	
Tail Point	(.67966,	-.25377)	

LE Tangency Points	Top	(-.17554,	.85478)	Bottom	(-.14062,	.79063)
TE Tangency Points	Top	(.68578,	-.24138)	Bottom	(.66706,	-.24838)

Inlet Angle =	61.44217
Exit Angle =	20.48985
No. of Blades =	54
Pitch =	1.11922
Tolerance =	-.00000
Gaging =	.39374
Uncovered Turning =	12.82855
Gaging Angle =	20.59755
Area =	.14797
Axial Chord =	.87376

TABLE XI
FIRST STAGE VANE

Section E-E AT R = 9.72000

Percent X	X	Y (Top)	(Circle)	Y (Bot)	(Circle)
.00	-.19679	.84512	.82887	.77100	.82887
.01	-.18800	.85364	.85321	.77574	.80453
.02	-.17921	.86181		.78013	.79677
.03	-.17041	.86962		.78415	.79263
.04	-.16162	.87709		.78780	.79089
.05	-.15283	.88421		.79108	.79124
.10	-.10888	.91441		.80198	
.15	-.06492	.93532		.80356	
.20	-.02096	.94654		.79566	
.25	.02300	.94773		.77828	
.30	.06695	.93858		.75160	
.35	.11091	.91887		.71595	
.40	.15487	.88845		.67181	
.45	.19882	.84725		.61973	
.50	.24278	.79529		.56035	
.55	.28674	.73265		.49431	
.60	.33069	.65952		.42224	
.65	.37465	.57615		.34478	
.70	.41861	.48289		.26248	
.75	.46256	.38016		.17589	
.80	.50652	.26849		.08547	
.85	.55048	.14842		-.00833	
.90	.59443	.02054		-.10515	
.95	.63839	-.11458		-.20465	
.98	.66477	-.19895		-.26554	-.26440
.99	.67356	-.22760		-.28602	-.26779
1.00	.68235	-.25635	-.25786	-.30652	-.25786

LE Center	(-.15870,	.82887)	R = .03809			
TE Center	(.67234,	-.25786)	R = .01001			
Center of Gravity	(.25489,	.56057)				
Radial Reference	(.38952,	.56570)				
Gaging =	.39255					
Nose Point	(-.18990,	.80702)				
Tail Point	(.67571,	-.26728)				
LE Tangency Points	Top	(-.18462,	.85678)	Bottom	(-.14954,	.79190)
TE Tangency Points	Top	(.68191,	-.25492)	Bottom	(.66314,	-.26181)
Inlet Angle =	61.60248					
Exit Angle =	20.16631					
No. of Blades =	54					
Pitch =	1.13097					
Tolerance =	-.00000					
Gaging =	.39255					
Uncovered Turning =	12.82184					
Gaging Angle =	20.30941					
Area =	.15205					
Axial Chord =	.87914					

UNCLASSIFIED

TABLE XII
FIRST STAGE VANE

Section H-H AT R = 10.26000

Percent X	X	Y (Top)	(Circle)	Y (Bot)	(Circle)
.00	-.24633	.85867	.84050	.78677	.84050
.01	-.23725	.86664	.86590	.78966	.81511
.02	-.22817	.87454		.79249	.80696
.03	-.21909	.88218		.79528	.80255
.04	-.21002	.88954		.79802	.80062
.05	-.20094	.89660		.80069	.80081
.10	-.15554	.92731		.81025	
.15	-.11015	.94985		.81053	
.20	-.06476	.96356		.80144	
.25	-.01936	.96774		.78308	
.30	.02603	.96175		.75562	
.35	.07142	.94495		.71928	
.40	.11682	.91685		.67438	
.45	.16221	.87697		.62126	
.50	.20761	.82504		.56034	
.55	.25300	.76087		.49205	
.60	.29839	.68447		.41681	
.65	.34379	.59598		.33511	
.70	.38918	.49567		.24738	
.75	.43457	.38394		.15404	
.80	.47997	.26124		.05552	
.85	.52536	.12810		-.04778	
.90	.57075	-.01492		-.15549	
.95	.61615	-.16722		-.26726	
.98	.64338	-.26292		-.33611	-.33542
.99	.65246	-.29557		-.35925	-.33967
1.00	.66154	-.32838	-.32974	.38241	-.32974

LE Center	(-.20628,	.84050)	R = .04005			
TE Center	(.65157,	-.32974)	R = .00997			
Center of Gravity	(.22393,	.55929)				
Radial Reference	(.38952,	.56570)				
Gaging =	.38608					
Nose Point	(-.24080,	.82019)				
Tail Point	(.65466,	-.33922)				
LE Tangency Points	Top	(-.23257,	.87072)	Bottom	(-.19802,	.80131)
TE Tangency Points	Top	(.66118,	-.32707)	Bottom	(.64230,	-.33339)
Inlet Angle =	63.53871					
Exit Angle =	18.49922					
No. of Blades =	54					
Pitch =	1.19381					
Tolerance =	-.00000					
Gaging =	.38608					
Uncovered Turning =	12.92890					
Gaging Angle =	18.86906					
Area =	.17441					
Axial Chord =	.90787					

TABLE XIII
FIRST STAGE VANE

Section G-G AT R = 10.30000

Percent X	X	Y (Top)	(Circle)	Y (Bot)	(Circle)
.00	-.25000	.85991	.84155	.78862	.84155
.01	-.24090	.86780	.86702	.79122	.81608
.02	-.23180	.87566		.79381	.80790
.03	-.22270	.88327		.79641	.80348
.04	21360	.89060		.79901	.80153
.05	-.20450	.89764		.80160	.80170
.10	-.15900	.92831		.81100	
.15	-.11350	.95092		.81113	
.20	-.06800	.96477		.80192	
.25	-.02250	.96915		.78347	
.30	.02300	.96339		.75593	
.35	.06850	.94683		.71954	
.40	.11400	.91892		.67458	
.45	.15950	.87918		.62140	
.50	.20500	.82729		.56038	
.55	.25050	.76305		.49195	
.60	.29600	.68645		.41651	
.65	.34150	.59762		.33452	
.70	.38700	.49682		.24641	
.75	.43250	.38445		.15259	
.80	.47800	.26094		.05347	
.85	.52350	.12682		-.05054	
.90	.56900	-.01736		-.15909	
.95	.61450	-.17099		.27182	
.98	.64180	-.26759		- 34130	-.34065
.99	.65090	-.30057		-.36465	-.34498
1.00	.66000	-.33370	-.33505	-.38801	-.33505

LE Center	(-.20981,	.84155)	R = .04019
TE Center	(.65004,	-.33505)	R = .00996
Center of Gravity	(.22168,	.55921)	
Radial Reference	(.32952,	.56570)	

Gaging = .38560

Nose Point	(-.24468,	.82156)
Tail Point	(.65311,	-.34453)

LE Tangency Points	Top	(-.23608,	.87196)	Bottom	(-.20167,	.80218)
TE Tangency Points	Top	(.65964,	-.33240)	Bottom	(.64076,	-.33867)

Inlet Angle = 63.75445
Exit Angle = 18.38052

No. of Blades = 54
Pitch = 1.19846

Tolerance = .00000
Gaging = .38560

Uncovered Turning = 12.93508
Gaging Angle = 18.76835

Area = .17611
Axial Chord = .91000

UNCLASSIFIED

TABLE XIV
FIRST STAGE BLADE

Section F-F AT R = 7.53750

Percent X	X	Y (Top)	(Circle)	Y (Bot)	(Circle)
.00	-.00000	.23453	.22958	.18425	.22958
.01	.00598	.24592		.18970	.21528
.02	.01196	.25691		.19516	.21121
.03	.01794	.26749		.20062	.20961
.04	.02392	.27768		.20608	.20986
.05	.02990	.28752		.21154	.21206
.10	.05980	.33142		.23714	
.15	.08971	.36742		.25822	
.20	.11961	.39630		.27502	
.25	.14951	.41868		.28769	
.30	.17941	.43492		.29631	
.35	.20932	.44529		.30098	
.40	.23922	.44997		.30173	
.45	.26912	.44901		.29855	
.50	.29902	.44241		.29143	
.55	.32893	.43005		.28031	
.60	.35883	.41172		.26510	
.65	.38873	.38712		.24567	
.70	.41863	.35575		.22183	
.75	.44853	.31697		.19337	
.80	.47844	.27023		.16000	
.85	.50834	.21551		.12133	
.90	.53824	.15350		.07688	
.95	.56814	.08527		.02601	
.98	.58608	.04175		-.00761	.00024
.99	.59207	.02691		-.01909	.00090
1.00	.59805	.01202	.01007	-.03059	.01007

LE Center	(.02009,	.22958)	R = .02009			
TE Center	(.58803,	.01007)	R = .01002			
Center of Gravity	(.29297,	.30528)				
Radial Reference	(.29297,	.30528)				
Gaging =	.20198					
Nose Point	(.00845,	.21321)				
Tail Point	(.59220,	.00095)				
LE Tangency Points	Top	(.00230,	.23891)	Bottom	(.03315,	.21432)
TE Tangency Points	Top	(.59731,	.01383)	Bottom	(.57915,	.00541)
Inlet Angle =	38.56658					
Exit Angle =	24.88531					
No. of Blades =	100					
Pitch =	.47360					
Tolerance =	-.00000					
Gaging =	.20198					
Uncovered Turning =	17.41054					
Gaging Angle =	25.24408					
Area =	.06966					
Axial Chord =	.59805					

UNCLASSIFIED

TABLE XV
FIRST STAGE BLADE

Section F-F AT R = 7.54000

Percent X	X	Y (Top)	(Circle)	Y (Bot)	(Circle)
.00	.00005	.23469	.22974	.18439	.22974
.01	.00603	.24608		.18985	.21544
.02	.01201	.25706		.19531	.21137
.03	.01799	.26764		.20078	.20977
.04	.02397	.27783		.20624	.21002
.05	.02995	.28766		.21170	.21221
.10	.05985	.33155		.23729	
.15	.08975	.36753		.25837	
.20	.11965	.39640		.27517	
.25	.14955	.41876		.28783	
.30	.17945	.43498		.29645	
.35	.20935	.44534		.30111	
.40	.23925	.45000		.30185	
.45	.26915	.44903		.29866	
.50	.29905	.44242		.29152	
.55	.32895	.43004		.28039	
.60	.35885	.41170		.26515	
.65	.38875	.38708		.24570	
.70	.41865	.35570		.22184	
.75	.44855	.31691		.19335	
.80	.47845	.27015		.15995	
.85	.50835	.21542		.12126	
.90	.53825	.15341		.07679	
.95	.56815	.08518		.02592	
.98	.58609	.04166		-.00771	.00015
.99	.59207	.02682		-.01918	.00081
1.00	.59805	.01193	.00998	-.03069	.00998

LE Center (.02013, .22974) R = .02009
TE Center (.58803, .00998) R = .01002

Center of Gravity (.29300, .30531)
Radial Reference (.29297, .30528)

Gaging = .20204

Nose Point (.00849, .21337)
Tail Point (.59220, .00086)

LE Tangency Points	Top	(.00235,	.23908)	Bottom	(.03319,	.21448)
TE Tangency Points	Top	(.59731,	.01374)	Bottom	(.57915,	.00532)

Inlet Angle = 38.57090
Exit Angle = 24.88364

No. of Blades = 100
Pitch = .47375

Tolerance = -.00000
Gaging = .20204

Uncovered Turning = 17.51888
Gaging Angle = 25.24375

Area = .06963
Axial Chord = .59800

UNCLASSIFIED

TABLE XVI
FIRST STAGE BLADE

Section A-A AT R = 7.69000

Percent X	X	Y (Top)	(Circle)		Y (Bot)	(Circle)
.00	.00289	.24446	.23946		.19331	.23946
.01	.00884	.25568			.19905	.22519
.02	.01479	.26647			.20472	.22112
.03	.02075	.27686			.21033	.21950
.04	.02670	.28686			.21587	.21973
.05	.03265	.29650			.22134	.22187
.10	.06241	.33942			.24660	
.15	.09218	.37443			.26745	
.20	.12194	.40234			.28405	
.25	.15170	.42374			.29647	
.30	.18146	.43902			.30478	
.35	.21123	.44846			.30900	
.40	.24099	.45222			.30915	
.45	.27075	.45037			.30520	
.50	.30051	.44290			.29712	
.55	.33028	.42967			.28487	
.60	.36004	.41049			.26836	
.65	.38980	.38503			.24748	
.70	.41957	.35280			.22211	
.75	.44933	.31315			.19207	
.80	.47909	.26560			.15718	
.85	.50885	.21027			.11718	
.90	.53862	.14793			.07173	
.95	.56838	.07966			.02043	
.98	.58624	.03624			-.01321	-.00518
.99	.59219	.02146			-.02472	-.00449
1.00	.59814	.00663	.00467		-.03626	.00467

LE Center	(.02297,	.23946)	R = .02008			
TE Center	(.58811,	.00467)	R = .01003			
Center of Gravity	(.29496,	.30714)				
Radial Reference	(.29297,	.30528)				
Gaging =	.20592					
Nose Point	(.01134,	.22309)				
Tail Point	(.59227,	-.00445)				
LE Tangency Points	Top	(.00523,	.24888)	Bottom	(.03597,	.22415)
TE Tangency Points	Top	(.59741,	.00844)	Bottom	(.57922,	.00004)
Inlet Angle =	38.81996					
Exit Angle =	24.79333					
No. of Blades =	100					
Pitch =	.48318					
Tolerance =	-.00000					
Gaging =	.20592					
Uncovered Turning =	17.41889					
Gaging Angle =	25.22598					
Area =	.06759					
Axial Chord =	.59525					

UNCLASSIFIED

TABLE XVII
FIRST STAGE BLADE

Section B-B AT R = 8.35560

Percent X	X	Y (Top)	(Circle)	Y (Bot)	(Circle)
.00	.01550	.28989	.28474	.23798	.28474
.01	.02133	.30051		.24394	.27060
.02	.02716	.31067		.24975	.26652
.03	.03299	.32039		.25540	.26483
.04	.03882	.32969		.26088	.26493
.05	.04465	.33859		.26620	.26634
.10	.07380	.37755		.29030	
.15	.10295	.40827		.31012	
.20	.13211	.43175		.32553	
.25	.16126	.44866		.33640	
.30	.19041	.45948		.34262	
.35	.21956	.46451		.34410	
.40	.24871	.46395		.34080	
.45	.27787	.45788		.33267	
.50	.30702	.44628		.31971	
.55	.33617	.42903		.30196	
.60	.36532	.40592		.27945	
.65	.39447	.37658		.25226	
.70	.42362	.34049		.22050	
.75	.45278	.29709		.18429	
.80	.48193	.24630		.14376	
.85	.51108	.18867		.09906	
.90	.54023	.12518		.05037	
.95	.56938	.05694		-.00214	
.98	.58687	.01407		-.03551	-.02686
.99	.59270	-.00045		-.04688	-.02607
1.00	.59853	-.01502	-.01696	-.05830	-.01696

LE Center (.03558, .28474) R = .02008
TE Center (.58850, -.01696) R = .01003

Center of Gravity (.30418, .31518)
Radial Reference (.29297, .30528)

Gaging = .22296

Nose Point (.02383, .26846)
Tail Point (.59264, -.02610)

LE Tangency Points	Top	(.01798,	.29441)	Bottom	(.04837,	.26929)
TE Tangency Points	Top	(.59781,	-.01321)	Bottom	(.57958,	-.02156)

Inlet Angle = 39.60084
Exit Angle = 24.62404

No. of Blades = 100
Pitch = .52500

Tolerance = -.00000
Gaging = .22296

UNCLASSIFIED

Uncovered Turning = 17.34601
Gaging Angle = 25.13037

Area = .05987
Axial Chord = .58303

TABLE XVIII
FIRST STAGE BLADE

Section C-C AT R = 9.17380

Percent X	X	Y (Top)	(Circle)	Y (Bot)	(Circle)
.00	.03100	.34921	.34400	.30004	.34400
.01	.03668	.35943		.30500	.33001
.02	.04236	.36914		.30996	.32591
.03	.04804	.37831		.31493	.32415
.04	.05372	.38698		.31990	.32409
.05	.05940	.39518		.32485	.32572
.10	.08780	.42983		.34815	
.15	.11620	.45542		.36690	
.20	.14460	.47335		.38061	
.25	.17300	.48455		.38892	
.30	.20140	.48962		.39155	
.35	.22980	.48897		.38833	
.40	.25820	.48282		.37924	
.45	.28660	.47129		.36435	
.50	.31500	.45438		.34393	
.55	.34340	.43195		.31828	
.60	.37180	.40377		.28780	
.65	.40020	.36940		.25294	
.70	.42860	.32833		.21412	
.75	.45700	.28038		.17180	
.80	.48540	.22601		.12637	
.85	.51380	.16612		.07821	
.90	.54220	.10177		.02766	
.95	.57060	.03394		-.02499	
.98	.58764	-.00812		-.05741	-.04837
.99	.59332	-.02232		-.06828	-.04748
1.00	.59900	-.03652	-.03846	-.07914	-.03846

LE Center	(.05108,	.34400)	R = .02008		
TE Center	(.58899,	-.03846)	R = .01001		
Center of Gravity	(.31716,	.32509)			
Radial Reference	(.29297,	.30528)			
Gaging =	.24249				
Nose Point	(.03903,	.32794)			
Tail Point	(.59313,	-.04757)			
LE Tangency Points	Top	(.03353,	.35376)	Bottom	(.06382, .32847)
TE Tangency Points	Top	(.59828,	-.03473)	Bottom	(.58013, -.04310)
Inlet Angle =	39.84886				
Exit Angle =	24.76137				
No. of Blades =	100				
Pitch =	.57641				
Tolerance =	-.00000				
Gaging =	.24249				
Uncovered Turning =	16.76368				
Gaging Angle =	24.87856				
Area =	.05300				
Axial Chord =	.56800				

TABLE XIX
FIRST STAGE BLADE

Section D-D AT R = 9.99190

Percent X	X	Y (Top)	(Circle)	Y (Bot)	(Circle)
.00	.04650	.40862	.40327	.35790	.40327
.01	.05203	.41826		.36329	.38942
.02	.05756	.42728		.36855	.38532
.03	.06309	.43571		.37369	.38349
.04	.06862	.44361		.37871	.38328
.05	.07415	.45100		.38358	.38466
.10	.10180	.48127		.40575	
.15	.12945	.50223		.42355	
.20	.15710	.51546		.43607	
.25	.18475	.52198		.44237	
.30	.21240	.52242		.44168	
.35	.24005	.51720		.43354	
.40	.26770	.50653		.41798	
.45	.29536	.49050		.39546	
.50	.32301	.46906		.36678	
.55	.35066	.44200		.33286	
.60	.37831	.40898		.29464	
.65	.40596	.36946		.25294	
.70	.43361	.32321		.20845	
.75	.46126	.27070		.16173	
.80	.48891	.21294		.11321	
.85	.51656	.15106		.06325	
.90	.54421	.08608		.01210	
.95	.57186	.01879		-.04001	
.98	.58845	-.02247		-.07169	-.06207
.99	.59398	-.03633		-.08231	-.06107
1.00	.59951	-.05020	-.05212	-.09291	-.05212

LE Center	(.06659,	.40327)	R = .02009			
TE Center	(.58951,	-.05212)	R = .01000			
Center of Gravity	(.33266,	.33498)				
Radial Reference	(.29297,	.30528)				
Gaging =	.25904					
Nose Point	(.05450,	.38723)				
Tail Point	(.59363,	-.06124)				
LE Tangency Points	Top	(.04916,	.41326)	Bottom	(.07915,	.38759)
TE Tangency Points	Top	(.59880,	-.04841)	Bottom	(.58064,	-.05675)
Inlet Angle =	40.55889					
Exit Angle =	24.67845					
No. of Blades =	100					
Pitch =	.62781					
Tolerance =	-.00000					
Gaging =	.25904					
Uncovered Turning =	16.03184					
Gaging Angle =	24.36881					
Area =	.04816					
Axial Chord =	.55301					

UNCLASSIFIED

TABLE XX
FIRST STAGE BLADE

Section E-E AT R = 10.35000

Percent X	X	Y (Top)	(Circle)	Y (Bot)	(Circle)
.00	.05328	.43534	.42970	.38594	.42970
.01	.05875	.44430		.39099	.41592
.02	.06421	.45270		.39592	.41181
.03	.06968	.46056		.40073	.40994
.04	.07514	.46791		.40541	.40967
.05	.08061	.47479		.40996	.41094
.10	.10793	.50290		.43061	
.15	.13525	.52203		.44718	
.20	.16257	.53357		.45851	
.25	.18990	.53840		.46339	
.30	.21722	.53710		.46074	
.35	.24454	.53004		.44996	
.40	.27186	.51740		.43115	
.45	.29919	.49927		.40510	
.50	.32651	.47559		.37293	
.55	.35383	.44617		.33585	
.60	.38115	.41068		.29494	
.65	.40847	.36873		.25107	
.70	.43580	.32036		.20494	
.75	.46312	.26628		.15709	
.80	.49044	.20757		.10789	
.85	.51776	.14531		.05766	
.90	.54509	.08041		.00660	
.95	.57241	.01358		-.04511	
.98	.58880	-.02729		-.07645	-.06658
.99	.59427	-.04098		-.08695	-.06553
1.00	.59973	-.05469	-.05662	-.09744	-.05662

LE Center	(.07338,	.42970)	R = .02010		
TE Center	(.58973,	-.05662)	R = .01000		
Center of Gravity	(.33880,	.33915)			
Radial Reference	(.29297,	.30528)			
Gaging =	.26645				
Nose Point	(.06083,	.41400)			
Tail Point	(.59385,	-.06573)			
LE Tangency Points	Top	(.05622,	.44016)	Bottom	(.08550, .41368)
TE Tangency Points	Top	(.59902,	-.05291)	Bottom	(.58086, -.06124)
Inlet Angle =	42.14633				
Exit Angle =	24.65757				
No. of Blades =	100				
Pitch =	.65031				
Tolerance	-.00000				
Gaging =	.26645				
Uncovered Turning =	15.59672				
Gaging Angle =	24.18738				
Area =	.04689				
Axial Chord =	.54645				

TABLE XXI
FIRST STAGE BLADE

Section G-G AT R = 10.81000

Percent X	X	Y (Top)	(Circle)	Y (Bot)	(Circle)
.00	.06200	.47068	.46428	.42622	.46428
.01	.06738	.47825		.42993	.45061
.02	.07276	.48549		.43365	.44650
.03	.07814	.49232		.43736	.44460
.04	.08352	.49877		.44107	.44427
.05	.08890	.50483		.44478	.44541
.10	.11580	.52986		.46229	
.15	.14270	.54683		.47620	
.20	.16960	.55651		.48510	
.25	.19650	.55949		.48737	
.30	.22340	.55614		.48148	
.35	.25030	.54673		.46665	
.40	.27720	.53142		.44320	
.45	.30410	.51028		.41246	
.50	.33100	.48327		.37606	
.55	.35790	.45029		.33550	
.60	.38480	.41114		.29194	
.65	.41170	.36586		.24621	
.70	.43860	.31499		.19888	
.75	.46550	.25944		.15037	
.80	.49240	.20015		.10097	
.85	.51930	.13800		.05088	
.90	.54620	.07366		.00025	
.95	.57310	.00767		-.05081	
.98	.58924	-.03258		-.08163	-.07147
.99	.59462	-.04607		-.09191	-.07036
1.00	.60000	-.05957	-.06149	-.10219	-.06149

LE Center	(.08207,	.46428)	R = .02007			
TE Center	(.58999,	-.06149)	R = .01001			
Center of Gravity	(.34537,	.34488)				
Radial Reference	(.29297,	30528)				
Gaging =	.27615					
Nose Point	(.06820,	.44978)				
Tail Point	(.59412,	-.07060)				
LE Tangency Points	Top	(.06571,	.47590)	Bottom	(.09301,	.44746)
TE Tangency Points	Top	(.59929,	-.05778)	Bottom	(.58113,	-.06613)
Inlet Angle =	46.17006					
Exit Angle =	24.69860					
No. of Blades =	100					
Pitch =	.67921					
Tolerance =	-.00000					
Gaging =	27615					
Uncovered Turning =	14.79202					
Gaging Angle =	23.98998					
Area =	.04619					
Axial Chord =	.53800					

UNCLASSIFIED

TABLE XXII
SECOND STAGE VANE

Section F-F AT R = 7.50000

Percent X	X	Y (Top)	(Circle)	Y (Bot)	(Circle)
.00	.00000	.36904	.36411	.31838	.36411
.01	.00832	.38490		.32606	.34786
.02	.01664	.40000		.33374	.34437
.03	.02496	.41433		.34142	.34471
.04	.03328	.42792		.34910	.34911
.05	.04160	.44083		.35680	
.10	.08320	.49604		.39249	
.15	.12480	.53796		.42366	
.20	.16640	.56868		.44950	
.25	.20800	.58964		.46911	
.30	.24960	.60182		.48166	
.35	.29120	.60591		.48643	
.40	.33280	.60239		.48301	
.45	.37440	.59160		.47132	
.50	.41600	.57371		.45166	
.55	.45760	.54881		.42461	
.60	.49920	.51686		.39099	
.65	.54080	.47771		.35168	
.70	.58240	.43110		.30752	
.75	.62400	.37677		.25931	
.80	.66560	.31497		.20772	
.85	.70720	.24653		.15334	
.90	.74880	.17255		.09663	
.95	.79040	.09416		.03799	
.98	.81536	.04538		.00203	.00250
.99	.82368	.02687		-.01004	.00009
1.00	.83200	.01230	.00993	-.02211	.00993

LE Center	(.02002,	.36411)	R = .02002		
TE Center	(.82202,	.00993)	R = .00998		
Center of Gravity	(.40292,	.42352)			
Radial Reference	(.40292,	.42352)			
Gaging =	.33598				
Nose Point =	(.00846,	.34776)			
Tail Point =	.82704,	.00130)			
LE Tangency Points	Top	(.00229,	.37341)	Bottom	(.03362, .34941)
TE Tangency Points	Top	(.83093,	.01442)	Bottom	(.81381, .00426)
Inlet Angle =	37.44870				
Exit Angle =	30.68017				
No. of Blades =	70				
Pitch =	.67320				
Tolerance =	-.00000				
Gaging =	.33598				
Uncovered Turning =	14.89425				
Gaging Angle =	29.93924				
Area =	.08845				
Axial Chord =	.83200				

UNCLASSIFIED

TABLE XXIII
SECOND STAGE VANE

Section A-A AT R = 7.65000

Percent X	X	Y (Top)	(Circle)	Y (Bot)	(Circle)
.00	-.00826	.37386	.36884	.32354	.36884
.01	.00009	.38947		.33119	.35259
.02	.00845	.40438		.33883	.34912
.03	.01681	.41856		.34645	.34951
.04	.02516	.43205		.35404	.35404
.05	.03352	.44489		.36163	
.10	.07531	.50013		.39707	
.15	.11709	.54237		.42830	
.20	.15888	.57342		.45447	
.25	.20067	.59455		.47459	
.30	.24245	.60666		.48763	
.35	.28424	.61040		.49266	
.40	.32603	.60623		.48901	
.45	.36781	.59451		.47642	
.50	.40960	.57543		.45523	
.55	.45138	.54913		.42618	
.60	.49317	.51561		.39031	
.65	.53496	.47480		.34867	
.70	.57674	.42655		.30224	
.75	.61853	.37065		.25188	
.80	.66032	.30735		.19830	
.85	.70210	.23736		.14209	
.90	.74389	.16163		.08371	
.95	.78568	.08119		.02355	
.98	.81075	.03100		-.0.1326	-.01279
.99	.81910	01399		-.02562	-.01526
1.00	.82746	-.00309	-.00541	-.03797	-.00541

LE Center (.01173, .36884) R = .01999
TE Center (.81748, -.00541) R = .00999

Center of Gravity (.39838, .42175)
Radial Reference (.40292, .42352)

Gaging = .33811

Nose Point (.00006, .35261)
Tail Point (.82242, -.01409

LE Tangency Points Top (-.00590 .37827) Bottom (.02517, .35405)
TE Tangency Points Top (.82644, -.00100) Bottom (.80921, -.01101)

Inlet Angle = 37.94162
Exit Angle = 30.14094

No. of Blades = 70
Pitch = .68666

Tolerance = -.00000
Gaging = .33811

Uncovered Turning = 14.92332
Gaging Angle = 29.49865

Area = .08870
Axial Chord = .83573

UNCLASSIFIED

TABLE XXIV
SECOND STAGE VANE

Section B-B AT R = 8.48630

Percent X	X	Y (Top)	(Circle)	Y (Bot)	(Circle)
.00	-.05434	.40599	.40022	.35882	.40022
.01	-.04578	.41957		.36572	.38382
.02	-.03721	.43267		.37256	.38044
.03	-.02865	.44529		.37933	.38107
.04	-.02008	.45744		.38602	
.05	-.01152	.46912		.39263	
.10	.03131	.52078		.42428	
.15	.07413	.56170		.45312	
.20	.11696	.59245		.47823	
.25	.15978	.61351		.49843	
.30	.20261	.62527		.51221	
.35	.24543	.62801		.51782	
.40	.28826	.62199		.51358	
.45	.33108	.60738		.49834	
.50	.37391	.58431		.47192	
.55	.41673	.55285		.43522	
.60	.45956	.51302		.38982	
.65	.50238	.46481		.33748	
.70	.54521	.40816		.27982	
.75	.58803	.34313		.21810	
.80	.63086	.27010		.15332	
.85	.67368	.18977		.08621	
.90	.71651	.10302		.01729	
.95	.75933	.01076		-.05302	
.98	.78503	-.04692		-.09578	-.09525
.99	.79359	-.06650		-.11010	-.09813
1.00	.80216	-.08613	-.08823	-.12445	-.08823

LE Center (-.03436, .40022) R = .01998
TE Center (.79216, -.08823) R = .01000

Center of Gravity (.37378, .41107)
Radial Reference (.40292, .42352)

Gaging = .34663

Nose Point (-.04721, .38492)
Tail Point (.79667, -.09715)

LE Tangency Points	Top	(-.05126,	.41087)	Bottom	(-.02207,	.38447)
TE Tangency Points	Top	(.80132,	-.08421)	Bottom	(.78357,	-.09336)

Inlet Angle = 42.12211
Exit Angle = 27.26789

No. of Blades = 70
Pitch = .76173

Tolerance = -.00000
Gaging = .34663

UNCLASSIFIED

Uncovered Turning = 14.62011
Gaging Angle = 27.06821

Area = .08954
Axial Chord = .85650

TABLE XXV
SECOND STAGE VANE

Section C-C AT R = 9.47250

Percent X	X	Y (Top)	(Circle)	Y (Bot)	(Circle)
.00	-.10868	.45643	.44906	.41445	.44906
.01	-.09987	.46676		.41961	.43249
.02	-.09106	.47681		.42471	.42921
.03	-.08225	.48658		.42974	.43014
.04	-.07344	.49606		.43472	
.05	-.06463	.50527		.43963	
.10	-.02058	.54698		.46308	
.15	.02347	.58131		.48428	
.20	.06752	.60801		.50250	
.25	.11157	.62683		.51677	
.30	.15562	.63748		.52577	
.35	.19967	.63971		.52786	
.40	.24372	.63320		.52111	
.45	.28777	.61768		.50375	
.50	.33182	.59282		.47464	
.55	.37587	.55832		.43382	
.60	.41992	.51384		.38246	
.65	.46397	.45906		.32235	
.70	.50802	.39365		.25541	
.75	.55207	.31773		.18328	
.80	.59612	.23220		.10725	
.85	.64017	.13846		.02828	
.90	.68422	.03806		-.05291	
.95	.72827	-.06758		-.13581	
.98	.75470	-.13303		-.18623	-.18571
.99	.76351	-.15514		-.20314	-.18915
1.00	.77232	-.17730	-.17922	-.22005	-.17922

LE Center (-.08869, .44906) R = .01999
TE Center (.76231, -.17922) R = .01001

Center of Gravity (.34591, .39862)
Radial Reference (.40292, .42352)

Gaging = .35594

Nose Point (-.10374, .43590)
Tail Point (.76644, -.18834)

LE Tangency Points	Top	(-.10390,	.46203)	Bottom	(-.07886,	.43166)
TE Tangency Points	Top	(.77161,	-.17551)	Bottom	(.75344,	-.18385)

Inlet Angle = 50.49834
Exit Angle = 24.64338

No. of Blades = 70
Pitch = .85025

Tolerance = -.00000
Gaging = .35594

Uncovered Turning = 14.33407
Gaging Angle = 24.74842

Area = .09367
Axial Chord = .88100

UNCLASSIFIED

TABLE XXVI
SECOND STAGE VANE

Section D-D AT R = 10.45880

Percent X	X	Y (Top)	(Circle)	Y (Bot)	(Circle)
.00	-.16302	.52165	.51290	.48242	.51290
.01	-.15397	.53002		.48646	.49617
.02	-.14491	.53819		.49040	.49300
.03	-.13586	.54615		.49424	.49424
.04	-.12680	.55392		.49795	
.05	-.11775	.56147		.50155	
.10	-.07247	.59589		.51761	
.15	-.02720	.62429		.52987	
.20	.01808	.64600		.53752	
.25	.06335	.66035		.53957	
.30	.10863	.66661		.53497	
.35	.15390	.66411		.52264	
.40	.19918	.65220		.50167	
.45	.24445	.63033		.47150	
.50	.28973	.59806		.43201	
.55	.33500	.55512		.38356	
.60	.38028	.50140		.32696	
.65	.42555	.43700		.26320	
.70	.47083	.36218		.19337	
.75	.51610	.27754		.11849	
.80	.56138	.18389		.03947	
.85	.60665	.08222		-.04294	
.90	.65193	-.02646		-.12811	
.95	.69720	-.14116		-.21553	
.98	.72437	-.21255		-.26893	-.26868
.99	.73342	-.23674		-.28686	-.27277
1.00	.74248	-.26099	-.26280	-.30482	-.26280

LE Center (-.14303, .51290) R = .01999
TE Center (.73247, -.26280) R = .01001

Center of Gravity (.31292, .38617)
Radial Reference (.40292, .42352)

Gaging = .37791

Nose Point (-.15957, .50167)
Tail Point (.73643, -.27200)

LE Tangency Points	Top	(-.15660,	.52758)	Bottom	(-.13544,	.49441)
TE Tangency Points	Top	(.74184,	-.25929)	Bottom	(.72353,	-.26732)

Inlet Angle = 57.46778
Exit Angle = 23.67498

No. of Blades = 70
Pitch .93878

Tolerance = -.00000
Gaging = .37791

UNCLASSIFIED

Uncovered Turning = 13.76426
Gaging Angle = 23.73784

Area = .11508
Axial Chord = .90550

TABLE XXVII
SECOND STAGE VANE

Section E-E AT R = 10.86000

Percent X	X	Y (Top)	(Circle)	Y (Bot)	(Circle)
.00	-.18513	.54979	.54061	.51138	.54061
.01	-.17597	.55766		.51503	.52381
.02	-.16682	.56533		.51859	.52069
.03	-.15766	.57281		.52206	
.04	-.14851	.58008		.52538	
.05	-.13935	.58713		.52853	
.10	-.09358	.61909		.54154	
.15	-.04781	.64502		.54953	
.20	-.00203	.66426		.55185	
.25	.04374	.67606		.54777	
.30	.08951	.67970		.53654	
.35	.13529	.67447		.51753	
.40	.18106	.65971		.49028	
.45	.22683	.63484		.45469	
.50	.27261	.59942		.41097	
.55	.31838	.55315		.35958	
.60	.36415	.49595		.30114	
.65	.40993	.42792		.23633	
.70	.45570	.34941		.16586	
.75	.50147	.26110		.09046	
.80	.54725	.16383		.01077	
.85	.59302	.05857		-.07261	
.90	.63879	-.05371		-.15916	
.95	.68457	-.17208		-.24844	
.98	.71203	-.24573		-.30319	-.30305
.99	.72119	-.27067		-.32158	-.30745
1.00	.73034	-.29570	-.29748	-.34001	-.29748

LE Center (-.16513, .54061) R = .01999
TE Center (.72034, -.29748) R = .01000

Center of Gravity (.29726, .38087)
Radial Reference (.40292, .42352)

Gaging = .38604

Nose Point (-.18209, .53002)
Tail Poine (.72423, -.30669)

LE Tangency Points	Top	(-.17817,	.55577)	Bottom	(-.15806,	.52191
TE Tangency Points	Top	(.72973,	-.29403)	Bottom	(.71139,	-.30194)

Inlet Angle = 59.28881
Exit Angle = 23.31652

No. of Blades = 70
Pitch = .97479

Tolerance = -.00000
Gaging = .38604

Uncovered Turning = 13.46908
Gaging Angle = 23.32981

Area = .12584
Axial Chord = .91547

UNCLASSIFIED

TABLE XXVIII
SECOND STAGE VANE

Section H-H AT R = 11.41000

Percent X	X	Y (Top)	(Circle)	Y (Bot)	(Circle)
.00	-.21543	.58879	.57913	.55151	.57913
.01	-.20614	.59616		.55458	.56225
.02	-.19685	.60332		.55764	.55919
.03	-.18756	.61025		.56067	
.04	-.17827	.61696		.56353	
.05	-.16898	.62343		.56611	
.10	-.12252	.65213		.57466	
.15	-.07606	.67437		.57596	
.20	-.02961	.68959		.56994	
.25	.01685	.69717		.55658	
.30	.06331	.69656		.53595	
.35	.10976	.68715		.50810	
.40	.15622	.66837		.47320	
.45	.20268	.63969		.43148	
.50	.24913	.60065		.38319	
.55	.29559	.55083		.32863	
.60	.34205	.48996		.26814	
.65	.38850	.41787		.20202	
.70	.43496	.33461		.13061	
.75	.48142	.24080		.05425	
.80	.52787	.13749		-.02675	
.85	.57433	.02599		-.11205	
.90	.62079	-.09237		-.20137	
.95	.66724	-.21637		-.29440	
.98	.69512	-.29310		-.35189	-.35185
.99	.70441	-.31904		-.37122	-.35675
1.00	.71370	-.34506	-.34680	-.39058	-.34680

LE Center	(-.19544,	.57913)	R = .01999			
TE Center	(.70372,	-.34680)	R = .00998			
Center of Gravity	(.27418,	.37412)				
Radial Reference	(.40292,	.42352)				
Gaging =	.39479					
Nose Point	(-.21287,	.56935)				
Tail Point	(.70751,	-.35603)				
LE Tangency Points	Top	(-.20787,	.59479)	Bottom	(-.18923,	.56013)
TE Tangency Points	Top	(.71311,	-.34343)	Bottom	(.69473,	-.35112)
Inlet Angle =	61.73699					
Exit Angle =	22.69943					
No. of Blades =	70					
Pitch =	1.02416					
Tolerance =	-.00000					
Gaging =	.39479					
Uncovered Turning =	13.24489					
Gaging Angle =	22.67323					
Area =	.14091					
Axial Chord	.92913					

UNCLASSIFIED

TABLE XXIX
SECOND STAGE VANE

Section G-G AT R = 11.44500

Percent X	X	Y (Top)	(Circle)	Y (Bot)	(Circle)
.00	-.21736	.59129	.58161	.55408	.58161
.01	-.20806	.59864		.55711	.56471
.02	-.19876	.60577		.56014	.56166
.03	-.18946	.61267		.56315	
.04	-.18016	.61935		.56598	
.05	-.17086	.62578		.56852	
.10	-.12436	.65428		.57678	
.15	-.07786	.67627		.57762	
.20	-.03136	.69121		.57103	
.25	.01514	.69850		.55705	
.30	.06164	.69759		.53580	
.35	.10814	.68790		.50741	
.40	.15464	.66886		.47206	
.45	.20114	.63995		.43000	
.50	.24764	.60070		.38146	
.55	.29414	.55070		.32674	
.60	.34064	.48964		.26613	
.65	.38714	.41733		.19994	
.70	.43364	.33378		.12846	
.75	.48014	.23960		.05203	
.80	.52664	.13586		-.02906	
.85	.57314	.02391		-.11451	
.90	.61964	-.09488		-.20404	
.95	.66614	-.21926		-.29736	
.98	.69404	-.29619		-.35506	-.35502
.99	.70334	-.32219		-.37446	-.35996
1.00	.71264	-.34827	-.35000	-.39389	-.35000

LE Center	(-.19737,	.58161)	R = .01999
TE Center	(.70266,	-.35000)	R = .00998
Center of Gravity	(.27265,	.37372)	
Radial Reference	(.40292,	.42352)	
Gaging =	.39526		
Nose Point	(-.21483,	.57187)	
Tail Point	(.70645,	-.35923)	

LE Tangency Points	Top	(-.20976,	.59729)	Bottom	(-.19121,	.56258)
TE Tangency Points	Top	(.71206,	-.34664)	Bottom	(.69367,	-.35432)

Inlet Angle =	61.87273
Exit Angle =	22.65588
No. of Blades =	70
Pitch =	1.02730
Tolerance =	-.00000
Gaging =	.39526
Uncovered Turning =	13.23072
Gaging Angle =	22.62846
Area =	.14188
Axial Chord =	.93000

UNCLASSIFIED

TABLE XXX
SECOND STAGE BLADE

Section F-F AT R = 7.46000

Percent	X	Y (Top)	(Circle)	Y (Bot)	(Circle)
.00	.00000	.14809	.14166	.10353	.14166
.01	.00657	.15726		.10806	.12684
.02	.01314	.16610		.11260	.12287
.03	.01971	.17455		.11713	.12166
.04	.02628	.18261		.12167	.12267
.05	.03285	.19031		.12623	
.10	.06570	.22402		.14700	
.15	.09855	.25084		.16440	
.20	.13140	.27186		.17857	
.25	.16425	.28780		.18961	
.30	.19710	.29913		.19762	
.35	.22995	.30620		.20266	
.40	.26280	.30921		.20474	
.45	.29565	.30828		.20390	
50	.32850	.30345		.20012	
.55	.36135	.29471		.19338	
.60	.39420	.28194		.18363	
.65	.42705	.26495		.17080	
.70	.45990	.24345		.15479	
.75	.49275	.21698		.13547	
.80	.52560	.18509		.11268	
.85	.55845	.14787		.08622	
.90	.59130	.10610		.05582	
.95	.62415	.06084		.02116	
.98	.64386	.03238		-.00174	.00043
.99	.65043	.02275		-.00960	.00056
1.00	.65700	.01308	.00997	-.01749	.00997

LE Center	(.02000,	.14166)	R = .02000			
TE Center	(.64697,	.00997)	R = .01003			
Center of Gravity	(.31032,	.20826)				
Radial Reference	(.31032,	.20826)				
Gaging =	.25684					
Nose Point	(.00616,	.12722)				
Tail Point	(.65302,	.00197)				
LE Tangency Points	Top	(.00374,	.15331)	Bottom	(.03141,	.12523)
TE Tangency Points	Top	(.65525,	.01564)	Bottom	(.63930,	.00351)
Inlet Angle =	45.42861					
Exit Angle =	37.26776					
No. of Blades =	110					
Pitch =	.42611					
Tolerance =	-.00000					
Gaging =	.25684					
Uncovered Turning =	16.50482					
Gaging Angle =	37.06764					
Area =	.05424					
Axial Chord =	.65700					

UNCLASSIFIED

TABLE XXXI
SECOND STAGE BLADE

Section A-A AT R = 7.71000

Percent X	X	Y (Top)	(Circle)	Y (Bot)	(Circle)
.00	.00469	.16699	.16059	.12156	.16059
.01	.01118	.17600		.12652	.14591
.02	.01766	.18461		.13136	.14197
.03	.02414	.19283		.13606	.14074
.04	.03063	.20066		.14065	.14168
.05	.03711	.20811		.14513	
.10	.06952	.24052		.16491	
.15	.10194	.26589		.18068	
.20	.13435	.28533		.19282	
.25	.16677	.29957		.20159	
.30	.19918	.30908		.20721	
.35	.23160	.31423		.20981	
.40	.26401	.31522		.20946	
.45	.29642	.31220		.20623	
.50	.32884	.30521		.20013	
.55	.36125	.29425		.19114	
.60	.39367	.27923		.17922	
.65	.42608	.25997		.16431	
.70	.45850	.23621		.14632	
.75	.49091	.20755		.12512	
.80	.52332	.17369		.10060	
.85	.55574	.13487		.07256	
.90	.58815	.09183		.04080	
.95	.62057	.04551		.00506	
.98	.64002	.01647		-.01839	-.01584
.99	.64650	.00664		-.02646	-.01563
1.00	.65298	-.00321	.00624	-.03455	-.00624

LE Center	(.02455,	.16059)	R = .01986		
TE Center	(.64294,	-.00624)	R = .01004		
Center of Gravity	(.31245,	.21036)			
Radial Reference	(.31032,	.20826)			
Gaging =	.26008				
Nose Point	(.01092,	.14615)			
Tail Point	(.64886,	-.01435)			
LE Tangency Points	Top	(.00844,	.17219)	Bottom	(.03584, .14425)
TE Tangency Points	Top	(.65131,	-.00069	Bottom	(.63514, -.01256)

Inlet Angle = 45.55790
Exit Angle = 36.28733

No. of Blades = 110
Pitch = .44039

Tolerance = -.00000
Gaging = .26008

Uncovered Turning = 16.14393
Gaging Angle 36.19715

Area = .05388
Axial Chord = .64829

UNCLASSIFIED

TABLE XXXII
SECOND STAGE BLADE

Section B-B AT R = 8.58630

Percent X	X	Y (Top)	(Circle)	Y (Bot)	(Circle)
.00	.02115	.22968	.22338	.18418	.22338
.01	.02733	.23817		.18942	.20921
.02	.03351	.24620		.19440	.20534
.03	.03968	.25378		.19913	.20405
.04	.04586	.26095		.20360	.20479
.05	.05204	.26772		.20782	
.10	.08293	.29629		.22552	
.15	.11381	.31723		.23796	
.20	.14470	.33173		.24569	
.25	.17559	.34059		.24912	
.30	.20648	.34435		.24859	
.35	.23736	.34339		.24437	
.40	.26825	.33798		.23666	
.45	.29914	.32829		.22565	
.50	.33003	.31441		.21148	
.55	.36091	.29636		.19426	
.60	.39180	.27410		.17408	
.65	.42269	.24751		.15102	
.70	.45357	.21639		.12511	
.75	.48446	.18058		.09640	
.80	.51535	.14024		.06491	
.85	.54624	.09585		.03064	
.90	.57712	.04806		-.00643	
.95	.60801	-.00247		-.04633	
.98	.62654	-.03389		-.07171	-.06763
.99	.63272	-.04451		-.08038	-.06713
1.00	.63890	-.05514	-.05786	-.08909	-.05786

LE Center	(.04050,	.22338)	R = .01935		
TE Center	(.62885,	-.05786)	R = .01005		
Center Gravity	(.32080,	.21886)			
Radial Reference	(.31032,	.20826)			
Gaging =	.26629				
Nose Point	(.02730,	.20924)			
Tail Point	(.63429,	-.06630)			
LE Tangency Points	Top	(.02485,	.23477)	Bottom	(.05143, .20741)
TE Tangency Points	Top	(.63753,	-.05279)	Bottom	(.62069, -.06371)
Inlet Angle =	45.82385				
Exit Angle =	32.97753				
No. of Blades =	110				
Pitch =	.49045				
Tolerance =	-.00000				
Gaging =	.26629				
Uncovered Turning =	15.12040				
Gaging Angle =	32.88514				
Area =	.05038				
Axial Chord =	.61775				

UNCLASSIFIED

TABLE XXXIII
SECOND STAGE BLADE

Section C-C AT R = 9.71250

Percent X	X	Y (Top)	(Circle)	Y (Bot)	(Circle)	
.00	.04230	.30512	.29882	.26436	.29882	
.01	.04809	.31274		.26809	.28528	
.02	.05387	.31999		.27184	.28152	
.03	.05966	.32679		.27557	.28015	
.04	.06544	.33317		.27932	.28062	
.05	.07123	.33915		.28308		
.10	.10015	.36351		.29942		
.15	.12907	.37983		.31081		
.20	.15800	.38927		.31695		
.25	.18693	.39262		.31769		
.30	.21585	.39044		.31302		
.35	.24477	.38316		.30304		
.40	.27370	.37105		.28802		
.45	.30262	.35434		.26831		
.50	.33155	.33313		.24431		
.55	.36047	.30749		.21651		
.60	.38940	.27744		.18529		
.65	.41832	.24290		.15110		
.70	.44725	.20385		.11432		
.75	.47617	.16044		.07528		
.80	.50510	.11302		.03429		
.85	.53402	.06206		-.00840		
.90	.56295	.00807		-.05255		
.95	.59187	-.04845		-.09798		
.98	.60923	-.08343		-.12574	-.11924	
.99	.61501	-.09523		-.13505	-.11843	
1.00	.62080	-.10702	-.10935	-.14434	-.10935	
LE Center	(.06102,	.29882)	R = .01872			
TE Center	(.61079,	-.10935	R = .01001			
Center of Gravity	(.33442,	.22945)				
Radial Reference	(.31032,	.20826)				
Gaging =	.26726					
Nose Point		.28568)				
Tail Point		-.11812)				
LE Tangency Point	Top	(.04611,	.31013)	Bottom	(.07023,	.28252)
TE Tangency Points	Top	(.61977,	-.10493)	Bottom	(.60230,	-.11465)

Inlet Angle = 48.86158
Exit Angle = 29.06888

No. of Blades = 110
Pitch = .55478

Tolerance = -.00000
Gaging = .26726

UNCLASSIFIED

Uncovered Turning = 14.31738
Gaging Angle = 28.79904

Area = .04304
Axial Chord = .57850

TABLE XXXIV
SECOND STAGE BLADE

Section D-D AT R = 10.83880

Percent X	X	Y (Top)	(Circle)		Y (Bot)	(Circle)
.00	.06345	.38275	.37532		.?4575	.37532
.01	.06884	.38822			.34870	.36242
.02	.07424	.39342			.35155	.35874
.03	.07963	.39835			.35429	.35730
.04	.08502	.40300			.35692	.35752
.05	.09041	.40739			.35943	
.10	.11738	.42541			.37003	
.15	.14434	.43709			.37681	
.20	.17130	.44268			.37894	
.25	.19826	.44241			.37565	
.30	.22523	.43651			.33635	
.35	.25219	.42515			.35079	
.40	.27915	.40853			.32916	
.45	.30611	.38681			.30199	
.50	.33308	.36013			.27004	
.55	.36004	.32865			.23413	
.60	.38700	.29249			.19502	
.65	.41396	.25181			.15335	
.70	.44092	.20681			.10965	
.75	.46789	.15778			.06434	
.80	.49485	.10506			.01773	
.85	.52181	.04900			-.02991	
.90	.54877	-.01006			-.07841	
.95	.57574	-.07179			-.12759	
.98	.59191	-.11002			-.15740	-.14784
.99	.59731	-.12294			-.16738	-.14675
1.00	.60270	-.13586	-.13787		-.17735	-.13787

LE Center	(.08158,	.37532)	R = .01813			
TE Center	(.59270,	-.13787)	R = .01000			
Center of Gravity	(.34840,	.24005)				
Radial Reference	(.31032,	.20826)				
Gaging =	.26740					
Nose Point	(.06716,	.36433)				
Tail Point	(.59697,	-.14691)				
LE Tangency Points	Top	(.06867,	.38804)	Bottom	(.08924,	.35889)
TE Tangency Points	Top	(.60192,	-.13401)	Bottom	(.58391,	-.14263)
Inlet Angle =	54.79284					
Exit Angle =	25.58786					
No. of Blades =	110					
Pitch =	.61911					
Tolerance =	-.00000					
Gaging =	.26740					
Uncovered Turning =	14.31656					
Gaging Angle =	25.58860					
Area =	.04022					
Axial Chord =	.53925					

UNCLASSIFIED

TABLE XXXV
SECOND STAGE BLADE

Section E-E AT R = 11.51000

Percent X	X	Y (Top)	(Circle)	Y (Bot)	(Circle)
.00	.07606	.42473	.41614	.39068	.41614
.01	.08121	.42884	.42865	.39277	.40364
.02	.08637	.43282		.39475	.40004
.03	.09153	.43661		.39665	.39856
.04	.09669	.44023		.39845	.39865
.05	.10185	.44364		.40012	
.10	.12764	.45785		.40689	
.15	.15343	.46705		.41050	
.20	.17923	.47106		.40999	
.25	.20502	.46975		.40431	
.30	.23081	.46306		.39250	
.35	.25661	.45090		.37401	
.40	.28240	.43328		.34889	
.45	.30819	.41017		.31781	
.50	.33398	.38164		.28177	
.55	.35978	.34777		.24182	
.60	.38557	.30867		.19888	
.65	.41136	.26458		.15367	
.70	.43716	.21586		.10675	
.75	.46295	.16292		.05851	
.80	.48874	.10621		.00926	
.85	.51453	.04617		-.04079	
.90	.54033	-.01679		-.09148	
.95	.56612	-.08231		-.14269	
.98	.58160	-.12280		-.17364	-.16194
.99	.58675	-.13646		-.18399	-.16070
1.00	.59191	-.15013	-.15196	-.19432	-.15196

LE Center	(.09379,	.41614)	R = .01773		
TE Center	(.58193,	-.15196)	R = .00999		
Center of Gravity	(.35566,	.24620)			
Radial Reference	(.31032,	.20826)			
Gaging =	.26246				
Nose Point	(.07845,	.40724)			
Tail Point	(.58588,	.16113)			
LE Tangency Points	Top	(.08296,	.43018)	Bottom	(.09925, .39927)
TE Tangency Points	Top	(.59126,	-.14842)	Bottom	(.57299, -.15642)

Inlet Angle =	62.20556
Exit Angle =	23.64532
No. of Blades =	110
Pitch =	.65745
Tolerance =	-.00000
Gaging =	.26246
Uncovered Turning =	14.59695
Gaging Angle =	23.52839
Area =	.04097
Axial Chord =	.51586

UNCLASSIFIED

TABLE XXXVI
SECOND STAGE BLADE

Section G-G AT R = 11.96500

Percent X	X	Y (Top)	(Circle)		Y (Bot)	(Circle)
.00	.08460	.45041	.44093		.41896	.44093
.01	.08960	.45366	.45317		.42012	.42869
.02	.09460	.45693			.42127	.42513
.03	.09960	.46005			.42243	.42363
.04	.10460	.46303			.42359	.42364
.05	.10960	.46585			.42470	
.10	.13460	.47766			.42908	
.15	.15960	.48537			.43070	
.20	.18460	.48863			.42856	
.25	.20960	.48713			.42147	
.30	.23460	.48055			.40823	
.35	.25960	.46862			.38802	
.40	.28460	.45112			.36079	
.45	.30960	.42785			.32729	
.50	.33460	.39874			.28870	
.55	.35960	.36375			.24623	
.60	.38460	.32294			.20090	
.65	.40960	.27656			.15347	
.70	.43460	.22506			.10450	
.75	.45960	.16899			.05436	
.80	.48460	.10896			.00336	
.85	.50960	.04557			-.04832	
.90	.53460	-.02065			-.10053	
.95	.55960	-.08923			-.15316	
.98	.57460	-.13145			-.18487	-.17158
.99	.57960	-.14568			-.19544	-.17025
1.00	.58460	-.15990	-.16161		-.20598	-.16161
LE Center	(.10208,	.44093)	R = .01748			
TE Center	(.57463,	-.16161)	R = .00997			
Center of Gravity	(.35973,	.25066)				
Radial Reference	(.31032,	.20826)				
Gaging =	.25667					
Nose Point	(.08609,	.43388)				
Tail Point	(.57837,	-.17085)				
LE Tangency Points	Top	(.09251,	.45556)	Bottom	(.10587,	.42387)
TE Tangency Points	Top	(.58403,	-.15829)	Bottom	(.56561,	-.16588)
Inlet Angle =	67.14932					
Exit Angle =	22.38053					
No. of Blades =	110					
Pitch =	.68344					
Tolerance =	-.00000					
Gaging =	.25667					
Uncovered Turning =	14.97379					
Gaging Angle =	22.05843					
Area =	.04233					
Axial Chord =	.50000					

UNCLASSIFIED

REFERENCES

1. H. Welna, D. E. Dahlberg and W. H. Heiser; (Unclassified) Investigation of a Highly Loaded Two-Stage Fan-Drive Turbine; Interim Technical Status Report; Pratt & Whitney Aircraft Division of United Aircraft Corporation; 28 June 1968; Confidential.

2. H. Welna, D. E. Dahlberg and W. H. Heiser; (Unclassified) Investigation of a Highly Loaded Two-Stage Fan-Drive Turbine, Phase II, Part I. Preliminary Experimental Evaluation; Interim Technical Status Report; Pratt & Whitney Aircraft Division of United Aircraft Corporation; December 1968; Confidential.

Unclassified

Security Classification

DOCUMENT CONTROL DATA - R & D

(Security classification of title, body of abstract and indexing annotation must be entered when the overall report is classified)

1. ORIGINATING ACTIVITY (Corporate author)	2a. REPORT SECURITY CLASSIFICATION
Pratt & Whitney Aircraft Division United Aircraft Corporation East Hartford, Connecticut 06108	Confidential 2b. GROUP 4

3. REPORT TITLE

(U) Investigation of a highly loaded two-stage fan-drive turbine
Volume III. Phase II, Part 2, Experimental Baseline Evaluation.

4. DESCRIPTIVE NOTES (Type of report and inclusive dates)

Technical Report (Jan. 1, 1969 – June 30, 1969)

5. AUTHOR(S) (First name, middle initial, last name)

Welna, Henry; Dahlberg, Donald E.; Heiser, William H.

6. REPORT DATE	7a. TOTAL NO. OF PAGES	7b. NO. OF REFS
December 1969	189	2

8a. CONTRACT OR GRANT NO.	9a. ORIGINATOR'S REPORT NUMBER(S)
F33615-68-C-1208 b. PROJECT NO. 3066 c. Task No. 306606 d.	PWA 3717 9b. OTHER REPORT NO(S) (Any other numbers that may be assigned this report) AFAPL-TR-69-92, Volume III

10. DISTRIBUTION STATEMENT

11. SUPPLEMENTARY NOTES	12. SPONSORING MILITARY ACTIVITY
	Air Force Aero Propulsion Laboratory Wright-Patterson AFB, Ohio 45433

13. ABSTRACT

(U) An extensive, four-phase, three-year program is in progress to investigate methods of improving the performance of fan-drive turbines. The goals of this program are to develop turbine design procedures and aerodynamic techniques for high work, efficient, low-pressure turbines. The first phase effort defining the preliminary turbine design has been completed, and the results were reported. The second phase consists of an experimental evaluation which includes establishment of both two-dimensional loss levels and three-dimensional flow behavior for the baseline airfoils and for airfoils utilizing boundary layer control devices. The design of the cascade hardware and baseline airfoils was previously reported. The test results of baseline airfoil performance in the annular cascade and the status of the other tasks are presented in this report.

Distribution of this abstract is unlimited.

DD FORM 1 NOV 68 1473 REPLACES DD FORM 1473, 1 JAN 64, WHICH IS OBSOLETE FOR ARMY USE.

Unclassified

Security Classification

14. KEY WORDS	LINK A		LINK B		LINK C	
	ROLE	WT	ROLE	WT	ROLE	WT
Turbine Aerodynamic Design						
Boundary Layer Control Survey						